Solid-State Chemistry of Drugs

Second Edition

Stephen R. Byrn
Ralph R. Pfeiffer
Joseph G. Stowell

SSCI, Inc. • West Lafayette, Indiana
www.ssci-inc.com

SSCI, Inc., 3065 Kent Avenue, West Lafayette, Indiana 47906-1076
www.ssci-inc.com

Printed in the United States of America
Printing History: 03 02 01 00 99 5 4 3 2 1

Library of Congress Cataloging-in-Publication Data

Byrn, Stephen R.
Solid-State Chemistry of Drugs / Stephen R. Byrn, Ralph R. Pfeiffer, Joseph G. Stowell—2nd ed.
xvii, 576 p. :ill.; 24 cm.
Includes bibliographical references and index.
ISBN 0-967-06710-3
ISBN 0-967-06711-1 (paperback student edition only)
1. Pharmaceutical Chemistry. 2. Solid state chemistry. 3. Chemistry, Pharmaceutical. I. Title.
QV744.B995s 1999
615'.19

The publisher offers a discount paperback edition of this book to registered students only. Quantity discounts on the hardover edition are also vailable.

Printed on acid-free paper.

Cover illustration: The figures are space-filling representations of prednisolone 21-*tert*-butylacetate crystal packing diagrams. On the top is Form IV illustrating the densely packed crystal lattice. On the bottom is Form V showing the oxygen-accessible tunnels produced by desolvation.

In memory of Peggy Etter

1

Drugs as Molecular Solids

This chapter provides a general overview of solid-state chemistry of drugs. Specifically, it treats the impact on pharmaceuticals of solid-state chemistry, the crystalline state, amorphous solids, moisture uptake, patents, and physical as well as chemical transformations. In many cases, a subject is introduced in this chapter and addressed in depth in a later chapter. It is hoped that the reader will gain an appreciation of what this discipline encompasses by reading this chapter.

1.1 Role of Solid-State Technology in the Pharmaceutical Industry

Figure 1.1 depicts the central role that solid-state research plays in the pharmaceutical industry. Reflection on the part of anyone even slightly familiar with the industry will confirm many of the connections shown in Figure 1.1, but some specific examples will further point out how important these connections can be in given cases.

Solid pharmaceuticals exist as **polymorphs**, **solvates**, or in **amorphous** forms, collectively described as **solid forms**. Figure 1.2 shows the solubility behavior of two polymorphs with time. It is clear that the solubility of each of the solid forms is decreasing because of the crystallization of a more stable crystal form (Carless *et al.*, 1968). Thus, this figure illustrates the effect of polymorphic change on **suspension** stability. Obviously these changes reflect on the stability of the product as well as

Figure 1.1 A diagram of the role of solid-state studies in the pharmaceutical industry.

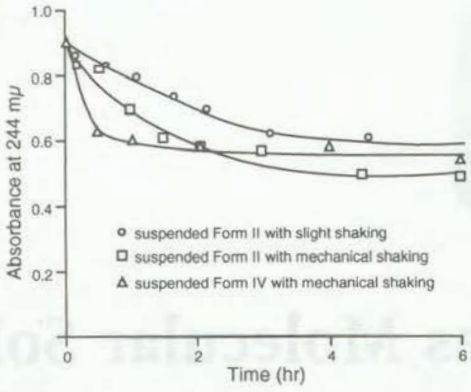

Figure 1.2 Decrease in absorbance of a cortisone acetate Form II solution in the presence of suspended Form II or Form IV as a function of time (Carless *et al.*, 1968).

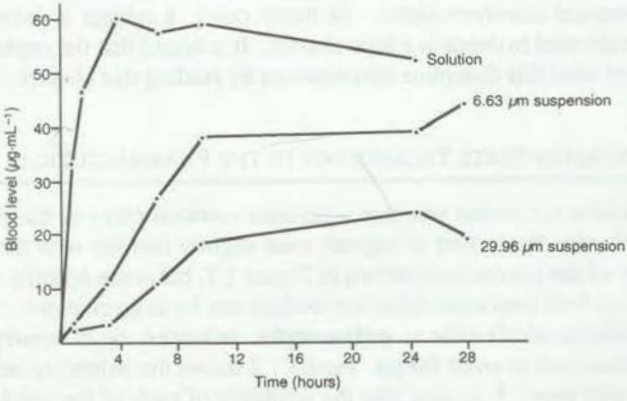

Figure 1.3 Blood levels of phenobarbitone versus time after intramuscular injection of two preparations with different particle sizes (redrawn from Miller and Fincher 1971).

regulatory issues, quality control, **formulation**, and drug bioavailability. Figure 1.3 depicts the effect of particle size on the **dissolution rate** of phenobarbitone and illustrates the role of solid-state technology in the formulation and **drug delivery**, quality control, and regulatory areas.

Studies of hydrocortisone *tert*-butylacetate and prednisolone *tert*-butylacetate (Byrn *et al.*, 1988; Lin *et al.*, 1982) and dihydrophenylalanine (Ressler, 1972) show that different crystal forms of these substances have different chemical reactivity. For example, the hexagonal crystal form of both hydrocortisone *tert*-butylacetate and prednisolone *tert*-butylacetate oxidizes in the solid state whereas the other crystal forms of these two pharmaceuticals are chemically stable.

The shape and particle size of the solid drug substance can have an important effect on the **flowability**, **syringeability**, **filterability**, **tableting behavior**, and **bulk density** of the drug. For example a suspension of plate-shaped crystals may be in-

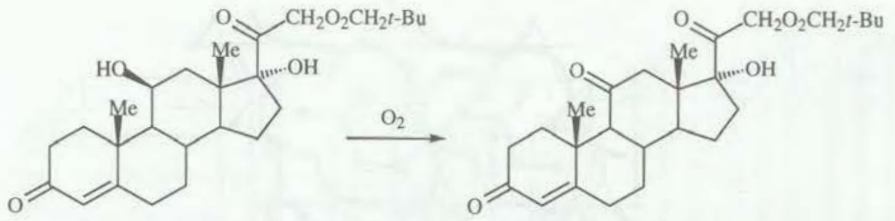

hydrocortisone 21-*tert*-butylacetate **cortisone 21-*tert*-butylacetate**

jected through a small needle with greater ease than one of needle-shaped crystals. Similarly, the tableting behavior of plate-shaped crystals would differ from that of needle-shaped crystals. Furthermore, the shape and size of the particles is generally related to the internal crystal structure of the solid. Thus, the internal structure of the solid material can dramatically influence the bulk properties of the drug. These properties in turn relate to formulation, manufacturing, patents, quality control, regulatory, and possibly other areas indicated in Figure 1.1.

1.2 The Crystalline State: Basic Concepts

An understanding of the solid-state chemistry of drugs begins with a statement of several general points:

- most drugs are used in a crystalline form
- crystals are held together by molecular forces
- the arrangement of molecules in a crystal determine its physical properties
- the physical properties of a drug can affect its performance

We can then proceed to learn how an understanding of the crystalline state leads to understanding of drug properties. (A treatment of non-crystalline, or amorphous, solids is given in Chapter 12.)

To accommodate the general reader in following this discussion of the crystalline state, brief definitions of some terms are listed in a glossary at the end of the book. Many of the terms may require further explanations which will be given when appropriate.

A. Packing and Symmetry

One definition of a crystal is that of a solid in which the component molecules are arranged, or "packed," in a highly ordered fashion. When the specific local order, defined by the **unit cell**, is rigorously preserved without interruption throughout the boundaries of a given particle, that particle is called a **single crystal**. This ordered packing leads to a structure with very little **void space**, which explains why most substances are more dense in their solid state than in their liquid state. By way of illustration, Figure 1.4 shows a projection of a unit cell and also shows how tightly the molecules are packed in a typical crystalline substance such as glycine.

Looking at this example and contemplating the enormous number of crystalline compounds known to modern science, not to mention those to be discovered, it be-

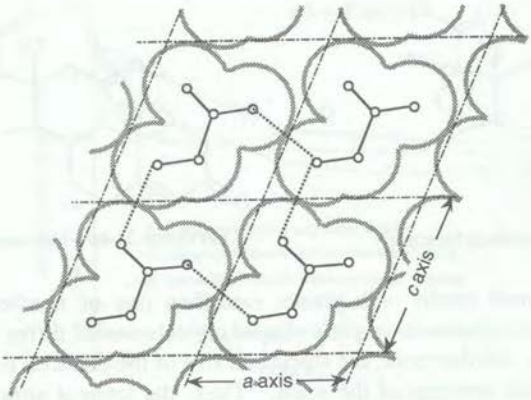

Figure 1.4 A close packed layer of glycine molecules in a crystal projected on the *ac* plane. The heavy gray lines show the van der Waals radii of the atoms (the hydrogens have been omitted for clarity).

comes obvious there must be a remarkable variety of structures found in different crystals. What factors, then, determine the crystal structure of a given compound?

When the question "In how many different ways can varied-shaped molecules be packed?" is put on a mathematical basis, it has been shown that certain **symmetry elements** (or, **symmetry operations**) are involved and that all possible combinations of these can be summarized in exactly 230 ways, called **space groups**. The symmetry operations are listed in Table 1.1. Formal representations of the 230 space groups, which encompass all seven **crystal systems** and all possible combinations of symmetry operations, are found in the *International Tables for Crystallography* (1987).

To understand how the packing of a crystal structure is described by the symmetry operations of the space group it may be helpful to regard the following example (see Figure 1.5). Figure 1.5 shows a diagram of the symmetry elements in space group *Pmm*2. The *P* means that the space group is **primitive** rather than **body-centered** or **face-centered**. The *mm*2 means that the cell contains **mirror planes** (*m*) perpen-

Table 1.1 The Symmetry Elements of Crystal Packing[a]

Symmetry Element	Description
rotation axis	When a rotation of 360°/*n* results in the same structure, then the crystal contains an *n*-fold rotation axis. For crystals, *n* is restricted to 1, 2, 3, 4, and 6.
screw axis	An *n*-fold screw axis exists when a rotation of 360°/*n* followed by a translation parallel to the axis of rotation brings the structure into coincidence.
rotatory-inversion axis	An *n*-fold rotatory-inversion axis exists when a rotation of 360°/*n* followed by inversion results in the same structure.
mirror plane	A mirror plane exists when a reflection through that plane results in the same structure.
glide plane	A glide plane exists when reflection through a mirror plane followed by translation brings the structure into coincidence.

a Note that a crystal containing only one enantiomer of a chiral compound cannot fall into a space group containing any one of the last three symmetry elements in Table 1.1.

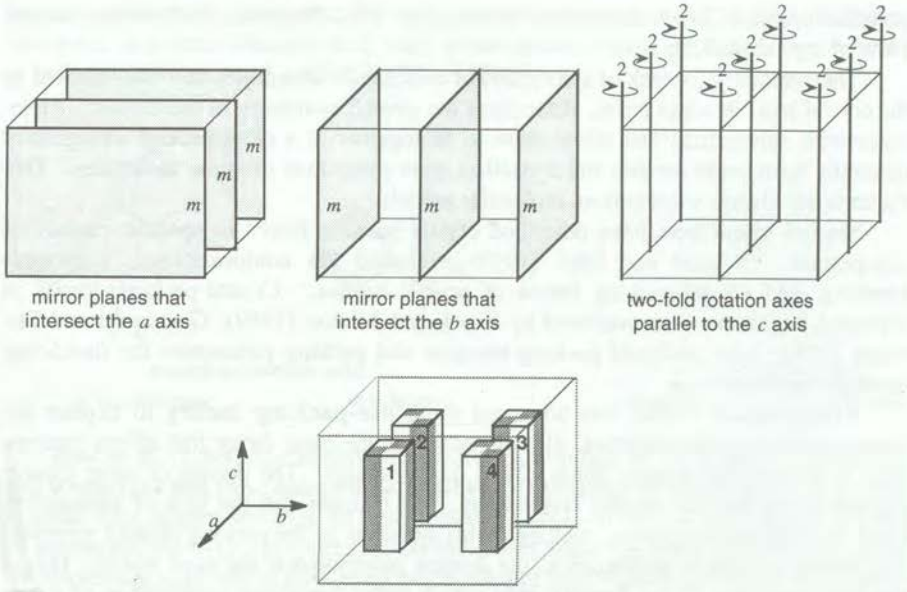

Figure 1.5 Symmetry elements for space group *Pmm*2.

dicular to both the *a* and *b* axes and a **two-fold rotation axis** along the *c* axis.

Taking block 1 at position (x,y,z) and reflecting it across the mirror that intersects the *a* axis at ½*a*, block 2 is obtained. Reflecting block 2 across the mirror that intersects the *b* axis at ½*b* generates block 3, and block 4 results from block 3 being reflected across the mirror at ½*a*. [In actual cases, of course, these blocks are molecules, but the operations are the same and thus the *x*, *y*, *z* coordinates of each atom in molecule 1 are translated to the corresponding $(1-x,y,z)$ in the first step, to $(1-x,1-y,z)$ in the next step, and $(x,1-y,z)$ in the last step.] Note that this combination of mirror planes necessarily creates the two-fold rotation axes parallel to the *c* axis. These steps, in any order, are continued into the neighboring unit cells. In this exercise we are, in a sense, mimicking actual crystal growth.

B. Forces Responsible for Crystal Packing

At this point, it is appropriate to consider the forces responsible for holding crystals together. **Ionic crystals** are held together by **ionic bonds** while **organic crystals** are held together largely by **non-covalent interactions**. These non-covalent interactions are either hydrogen-bonding or **non-covalent attractive forces**. Both hydrogen-bonding and non-covalent attractive interactions result in the formation of a regular arrangement of molecules in the crystal. **Non-covalent attractive interactions**, which are sometimes called **non-bonded interactions**, depend on the dipole moments, polarizability, and electronic distribution of the molecules. Hydrogen bonding, of course, requires donor and acceptor functional groups. Another important factor is the symmetry of the molecules. Kitaigorodskii (1961) provided a review of the forces holding crystals together in his classic book *Organic Chemical Crystallography*. The two-

volume *Structure Correlations* (Bürgi and Dunitz, 1994) describes in detail the modern view of crystal packing.

The symmetry (or lack of symmetry) of a molecule determines how it is packed in the crystal and, in some cases, determines the overall symmetry of the crystal. Molecules with symmetries that allow them to fit together in a close-packed arrangement generally form better crystals and crystallize more easily than irregular molecules. This factor is not always evident from molecular models.

Several researchers have described crystal packing forces in specific classes of compounds. Reutzel and Etter (1992) evaluated the conformational, hydrogen-bonding, and crystal-packing forces of acyclic imides. Crystal-packing forces in biphenyl fragments were evaluated by Brock and Minton (1989); Gavezzotti and Desiraju (1988) have analyzed packing energies and packing parameters for fused-ring aromatic hydrocarbons.

Kitaigorodskii (1961) has advanced the **close-packing theory** to explain the forces holding crystals together. He suggested that the basic factor that affects free energy is the packing density which affects ΔH, enthalpy. The denser or more closely packed crystal has the smaller free energy. This means that the heat of sublimation (and, to a first approximation, melting point) increases as the packing density increases and, that in a series of polymorphs, the densest polymorph is the most stable. This is the molecular basis of the **density rule** which states that if one modification of a molecular crystal has a lower density than the other, it may be assumed to be less stable at absolute zero (Burger and Ramberger, 1979a). However, it is important to note that there are exceptions to this rule. Some exceptions probably arise because strong hydrogen bonds can negate less dense packing (*e.g.*, ice) thereby causing the less dense polymorph to be more thermodynamically more stable (Burger and Ramberger, 1979a–b). Brock *et al.*(1991) studied the validity of **Wallach's rule**, which states that the racemic crystals of a pair of enantiomers are denser and thus more stable than crystals of the individual enantiomers, and showed that, for the 65 chiral/racemic pairs investigated, the racemic crystals are only ~1% more dense than the corresponding chiral crystals (yet the racemates are less dense for many individual pairs).

Kitaigorodskii (1961) also pointed out the importance of symmetry which affects ΔS, entropy. The free energy of a crystal undoubtedly increases as the number of crytallographically **independent molecules** in the crystal increases. Thus high symmetry, which reduces the number of independent molecules in a crystal, *increases* the free energy of the crystal and conflicts with the *reduction* in free energy gained from close packing. The magnitude of these opposing effects varies from structure to structure.

C. Hydrogen Bonding

Of the various forces that hold organic molecules in the solid, hydrogen bonding is perhaps the most important. Etter (1990) has reviewed the extent and types of hydrogen bonding that can exist in solids and pointed out that polar organic molecules in solution tend to form hydrogen-bonded aggregates. These aggregates are precursors to the crystals which form when the solution is supersaturated. This concept helps to explain the many different hydrogen-bonding motifs seen in different solids.

Several different types of carboxylic acids have been studied. For example, in *o*-alkoxybenzoic acids, the presence of dimers or the formation of intramolecular hydrogen bonds depends on the state of the sample. In *o*-anisic acid, dimers are observed in

the solid state while intramolecular hydrogen bonds are observed in dilute solution. However, in *o*-ethoxybenzoic acid, only intramolecular hydrogen bonds are observed in both the solid state and in solution (Etter, 1990).

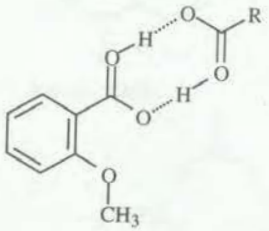

o-methoxybenzoic acid
in the solid state

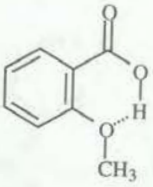

in solution

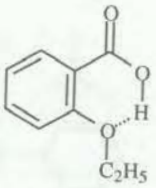

o-ethoxybenzoic acid
in solution and in the solid state

Etter *et al.* (1988) also studied the hydrogen bonding in salicylamide derivatives and pointed out that two types of hydrogen bonding patterns are possible in these compounds. One pattern involves an intramolecular —N—H···OH— hydrogen bond and an intermolecular —O—H···O=C hydrogen bond while the other pattern involves an intermolecular —N—H···OH— hydrogen bond and an intramolecular —O—H···O=C hydrogen bond.

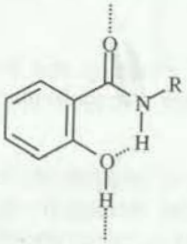

Intra: NH···OH
Inter: C=O···HO

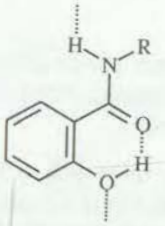

Intra: C=O···HO
Inter: NH···OH

Etter and co-workers (1990a) defined a system which uses a graph set to classify and symbolically represent the different types of hydrogen bonds that can be formed. A short representation of the different graph sets is shown in Figure 1.6. A graph set motif designator (C for intermolecular chains or **catemers**, R for intermolecular rings, D for discrete or other finite sets, and S for intramolecular hydrogen bonds) is assigned by identifying the size or degree of the hydrogen-bond pattern G, the number of acceptors a, the number of donors d, and the total number of atoms n in that pattern. This designation takes the form: $G_d^a(n)$.

Etter (1990b) also developed rules governing hydrogen bonding in solid organic compounds. Hydrogen-bond donors and acceptors in solids are classified either as "reliable" or "occasional" donors and acceptors and are listed in Table 1.2. Using these classifications, three rules were devised:

1. All reliable proton donors and acceptors are used in hydrogen bonding.
2. Six-membered ring *intra*molecular hydrogen bonds form in preference to *inter*molecular hydrogen bonds.

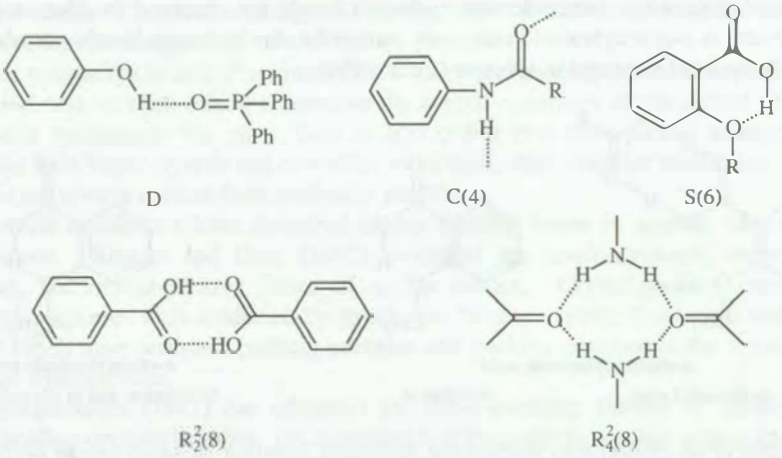

Figure 1.6 Etter graph sets describing different hydrogen bond motifs where D designates a discrete or other finite set, C a chain or catemer, S an intramolecular ring, and R designates an intermolecular ring. The number of hydrogen-bond acceptors in rings is superscripted, the number of hydrogen-bond donors is subscripted, and the total number of atoms in the hydrogen-bond pattern is in parentheses (Etter, 1990; Bernstein *et al.*, 1995).

3. The best proton donors and acceptors remaining after intramolecular hydrogen bond formation will form intermolecular hydrogen bonds.

These rules apply quite well to hydrogen bonding of small molecules. However, in some larger molecules (*e.g.*, erythromycins), factors dictated by the geometry of the molecule as well as the large number of donors and acceptors present may make it impossible to satisfy all these rules.

It has been demonstrated that the systematic study of **cocrystals** (crystals which contain an ordered arrangement of two different neutral molecules that are not solvent molecules) can lead to insight concerning the factors influencing hydrogen bonding in crystals (Etter and Baures, 1988; Etter *et al.*, 1990a–b, Etter and Adsmond, 1990; Etter and Reutzel, 1991). An important aspect of this research into hydrogen bonding is the realization that cocrystals can form and crystallize from certain solutions that contain more than one molecular species. Cocrystals are often formed between hydrogen-bond donor molecules and hydrogen-bond acceptor molecules. The geometry and nature of hydrogen bonding in cocrystals can be described using the above rules. Among the cocrystals studied by Etter's group were cocrystals involving ureas with ketones, carboxylic acids with 2-aminopyridine (see Figure 1.7), as well as adenine or cytosine with many acidic organic compounds including carboxylic and *N*-acyl-amino acids. The urea cocrystals are especially interesting because so many can be studied. Other cocrystal systems investigated by Etter's group include:

Table 1.2 Reliable and Occasional Hydrogen Bond Donors and Acceptors

Type	Functional Group Involved
Reliable Donor	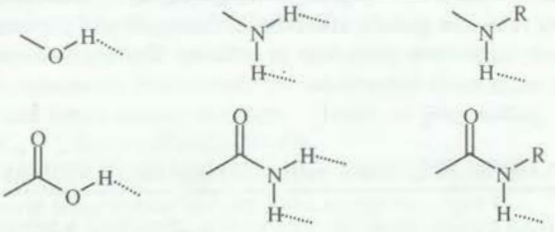
Occasional Donor	
Reliable Acceptors	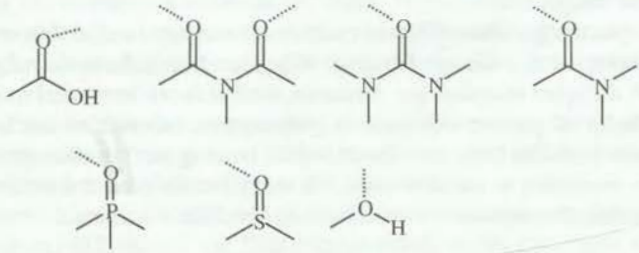
Occasional Acceptors	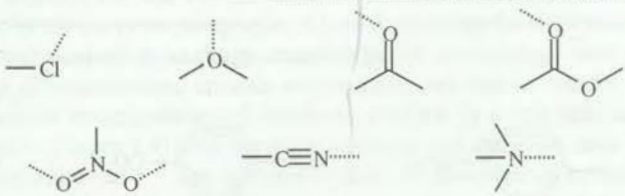

Etter, 1990; Bernstein *et al.*, 1995

pyrimidines, pyridines ..... carboxylic acids
pyridine-*N*-oxides ..... acids, alcohols, amines
triphenylphosphine oxides ..... acids, amides, alcohols, ureas, sulfonamides, amines, water
carboxylic acids ..... other carboxylic acids, amides
m-dinitrophenylureas ..... acids, ethers, phosphine oxides, sulfoxides, nitroanilines
imides ..... other imides, amides

The formation of cocrystals may also be important in explaining certain drug-excipient interactions.

Panunto *et al.* (1987) have reviewed hydrogen bond formation in crystalline nitroanilines. They showed that hydrogen bonding occurred between the amino group and the nitro group even though the nitro group is only an occasional acceptor. In general, they found that the donor hydrogen from the amino group is placed equidistant

between the acceptor oxygens of the nitro group. The geometry of this interaction appears to be controlled by the lone pair directionality of the nitro groups.

This elegant work by Etter on graph set definitions and qualitative hydrogen-bonding rules can greatly assist the understanding of the interaction of molecules in the solid state and presumably also in solution. Further discussion of hydrogen bonding in salts is included in Chapter 5.

1.3 A Given Substance can Crystallize in Different Ways

Apart from exhibiting differences in size, crystals of a substance from different sources can vary greatly in their shape. Typical particles in different samples may resemble, for example, needles, rods, plates, prisms, etc. Such differences in shape are collectively referred to as differences in **morphology**. This term merely acknowledges the fact of different shapes: it does not distinguish among the many possible reasons for the different shapes.

Naturally, when different compounds are involved, different crystal shapes would be expected as a matter of course. When batches of the *same substance* display crystals with different morphology, however, further work is needed to determine whether the different shapes are indicative of polymorphs, solvates or just **habits**. Because these distinctions can have a profound impact on drug performance, their careful definition is very important to our discourse. At this time, only brief definitions are presented, but an exhaustive treatment of each will be given later.

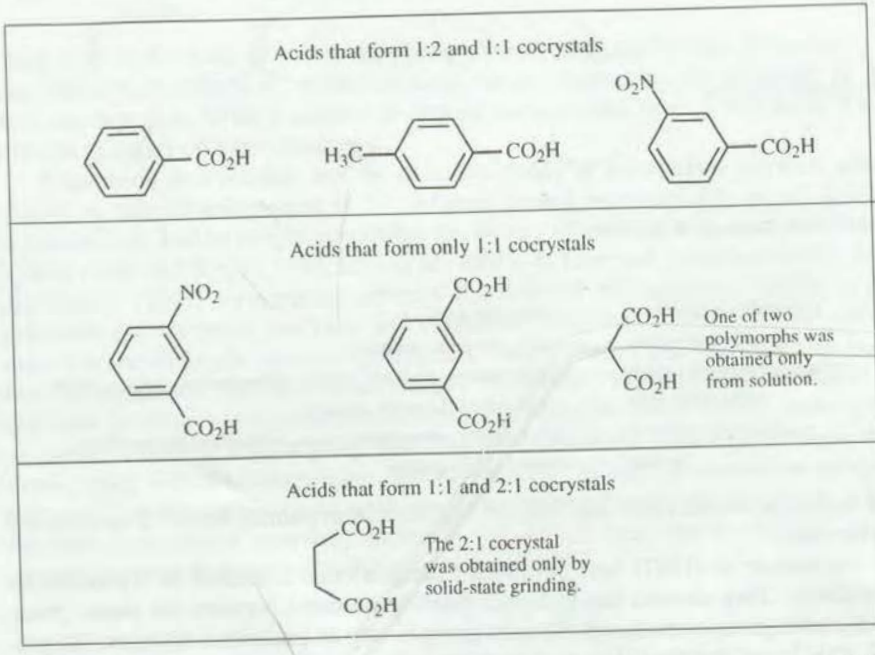

Figure 1.7 Observed stoichiometries of cocrystals of 2-aminopyridine with the compounds listed here (Etter and Adsmond, 1990).

Polymorphs — When two crystals have the *same chemical composition* but *different internal structure* (molecular packing) they are polymorphic modifications, or polymorphs. (Think of the three forms of carbon: diamond, graphite, and fullerenes.)

Solvates — These crystal forms, in addition to containing molecules of the same given substance, also contain *molecules of solvent* regularly incorporated into a unique structure. (Think of wet, setting plaster: $CaSO_4 + 2\ H_2O \rightarrow CaSO_4{\cdot}2H_2O$)

Habits — Crystals are said to have different habits when samples have the *same* chemical composition and the *same* crystal structure (*i.e.*, the same polymorph and unit cell) but display different shapes. (Think of snowflakes.)

Together, these solid-state modifications of a compound are referred to as **crystalline forms**. When differences between early batches of a substance are found by microscopic examination, for example, a reference to "form" is particularly useful in the absence of information that allows the more accurate description of a given variant batch (*i.e.*, polymorph, solvate, habit, or amorphous material). The term **pseudopolymorphism** is applied frequently to designate solvates.

To put these important definitions into a practical context, let us look at two cases in which a drug was crystallized from several different solvents and different-shaped crystals resulted in each experiment. (See Figures 1.8 and 1.9.)

Although sometimes dramatically different shapes were obtained upon changing solvents for the various crystallizations, the final interpretations in the two cases were significantly different. Figures 1.8 and 1.9 can be used to illustrate the application of the terminology defined in the previous paragraphs. Upon first seeing these pictures, it might be asked: "Although each of these drugs shows different *morphology* with different treatment, are the different-shaped crystals *polymorphs*, *solvates* or merely different *habits*?" After various investigations (*cf.* Methods, Chapter 2) it was concluded that all *forms* of the aspirin (Figure 1.8) have the same *structure* and therefore each is a different *habit* of the aspirin crystal. The various crystals of β-estradiol, however, were found to exist as a number of *solvate* forms (two *unsolvated* forms are also known but not shown in Figure 1.9). At this point we are aware that: a given structure can form crystals of quite different shapes; and a given drug may exist in more than one crystal structure or crystal form (*i.e.*, polymorph or solvate).

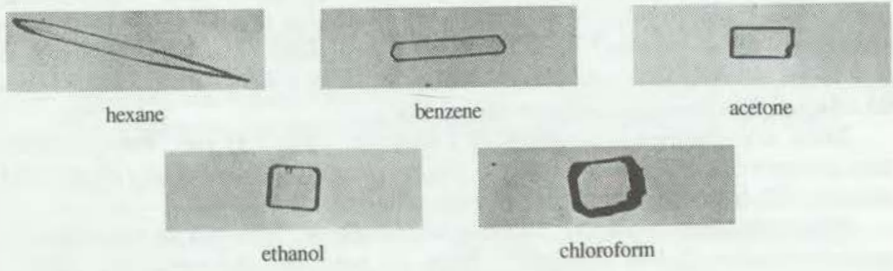

Figure 1.8 Aspirin crystals grown from different solvents.

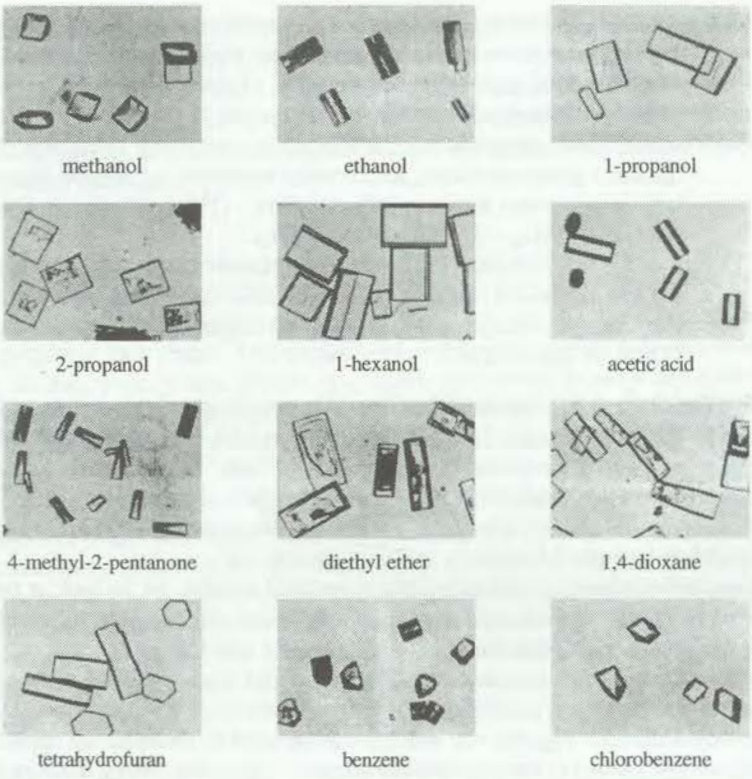

Figure 1.9 β-Estradiol pseudopolymorph crystals (solvate and crystallizing solvent are indicated, Kuhnert-Brandstätter, 1971).

1.4 Properties that Affect Pharmaceutical Behavior

The familiar example of pure carbon in its three forms—diamond (tetrahedral lattice), graphite (polyaromatic sheets), and fullerenes (polyaromatic spheres)—dramatizes the profound effect that differences in crystal structure can have on the properties of a solid. Similar effects can apply to other solid compounds, including drugs. The complex nature of manufacturing operations and regulatory requirements peculiar to the pharmaceutical industry thus demands an even closer look at how the properties of a given drug can vary with each of its solid-state forms. Given the endless chemical variety of modern drug molecules it becomes obvious why solid-state studies are vital to the thorough characterization of pharmaceuticals.

Many physicochemical properties of a drug (see Table 1.3) vary when the solid-state *structure* of the substance is altered. The *practical significance* of any of these differences will, of course, vary from case to case.

Other properties of drug crystals that are of concern primarily in pharmaceutical *operations* also need to be addressed. These are properties that vary even when the crystal structure is fixed and are directly or indirectly related to surface relationships and thus largely controlled by **crystal habit** and **size distribution** (see Table 1.4). These

Table 1.3 Properties of a Compound that Depend on Structure Differences

Density	Water Uptake	Solid-State Reactivity
Hardness	Optical Properties	Physical Stability
Cleavage	Electrical Properties	Chemical Stability
Solubility	Thermoanalytical Behavior	

Table 1.4 Some Areas Where Control of Solid Form and Size Distribution are Important

Yield	Milling	Dissolution
Filtration	Mixing	Suspension Formulation
Washing	Tableting	Lyophilization
Drying	Flowability	

variables determine how particles behave with respect to neighboring particles (and upon exposure to solvent or solvent vapor) and thus the physical properties of powders.

At this point, the concept that these crystal properties are directional is introduced. In discussing symmetry and space groups (see Sec. 1.2A), it is important to convey the notion that unit cells contain different symmetry elements along their axes. A necessary consequence of this fact is that *most drug crystals have different properties in different directions*, or alternatively stated, *the chemistry on the different faces of a drug crystal may be quite different*. Both the structure and the properties, in short, are **anisotropic**. For example, one face of a crystal may be studded with carboxyl groups whereas another face might be entirely occupied by phenyl moieties, thus giving rise to some relatively hydrophilic surfaces and some hydrophobic surfaces, to mention only one consequence. Furthermore, with a change in crystal habit, the relative areas, hence the relative chemical importance of these two kinds of faces would be altered. If we now consider additional crystal forms of the same compound, the anisotropic chemical variability must be regarded anew for each polymorph and solvate.

Although it is by now obvious that control of crystal formation is of extreme importance, this control is not always easy to achieve. What general principles dictate the formation of crystals?

1.5 How Crystals Form

In this section we discuss how crystals form and the factors that influence crystallization. Table 1.5 lists the common crystallization methods employed for pharmaceuticals. Most of the methods covered in Table 1.5 depend on reducing the **solubility** of the compound by one means or another. It is therefore necessary to carefully define the solubility-related terms that will be used repeatedly in the discussions that follow.

A. Solubility

The solubility of a solid substance is the concentration at which the solution phase is *in equilibrium with a given solid phase at a stated temperature and pressure*. Under these conditions the solid is neither dissolving nor continuing to crystallize. Note that the definition implies the presence of a specific solid phase. Once determined under the

Table 1.5 Common Methods for the Production of Solids in the Pharmaceutical Industry

Evaporation (including spray drying and slurry fill)
Cooling a solution
Seeding a supersaturated solution with crystals of the desired form
Freeze drying (including from mixed solvents)
Addition of antisolvents
Salting out
Changing pH
Addition of reagent to produce a salt or new compound
Deliberate phase transitions during slurry, washing or drying steps
Simultaneous addition of two solutions

stated conditions, however, we can talk about the "solubility" of a given phase (*e.g.*, a specific polymorph or pseudopolymorph) as a quantity, even in the absence of that solid phase.

Use of the term "equilibrium" in connection with crystallizing systems requires clarification. When a substance exists in more than one crystal form, that is, when other polymorphs are possible, only the *least soluble* of these at a *given* temperature is considered the most physically stable form at that temperature, all others are considered to be **metastable forms**. In given cases, a solution of a substance may be in apparent equilibrium with one of these metastable phases for a long time, in which case, the system is in metastable equilibrium and is expressing the thermodynamic solubility of *that* solid form.

It is important to stress the difference between polymorphs and solvates (pseudopolymorphs) at this point. If a pseudopolymorph exists, it is always (with few exceptions) the most stable form in the solvent that produces the pseudopolymorph.

Undersaturation pertains to solutions at a lower concentration than the saturation value (*i.e.*, diluted solutions). *Crystals will dissolve in undersaturated solutions.*

Saturation is the state of a system where *the solid is in equilibrium with the solution*, or in other words, *the solution will neither dissolve crystals nor let them grow* (*i.e.*, the concentration of the solution represents the solubility value for that crystalline phase).

Supersaturation pertains to solutions that, for one reason or another (*e.g.*, rapid cooling of a saturated solution without forming crystals) are at a higher concentration than the saturation value. *Supersaturation is required for crystals to grow.*

B. Nucleation

Supersaturated solutions can sometimes remain in that condition for long periods without forming crystals. For example, the reader may have heard of slowly cooling very clean water to well below its freezing point of 0 °C without the formation of ice crystals taking place. The first step in forming crystals from a supersaturated solution requires the assembly of a critical number of ordered molecules (unit cells) into viable **nuclei**. This process is termed **primary nucleation**. Assemblies below the critical number tend to dissolve while those above the critical number persist and grow into recognizable crystals. This behavior is based on the simple fact that the surface area of a spherical body increases with the square of its radius but the volume increases with the cube

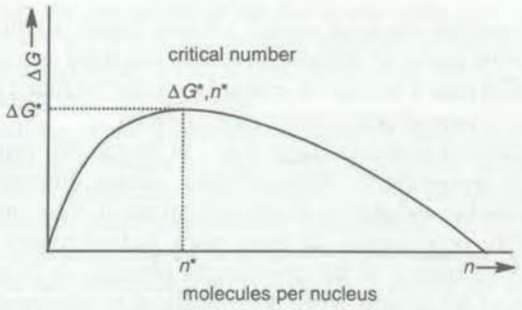

Figure 1.10 Free energy changes (ΔG) which occur during nucleation. Molecules assemble and disassemble until a nucleus of a critical number with an energy ΔG^* is achieved; then crystallization ensues as the size of the nucleus increases (Lieser, 1969).

of the radius. In other words, as an assembly becomes larger, the internal bonds holding it together become relatively more significant than the surface forces (solvent-solute interactions) acting to pull the particle apart. A more formal explanation of this phenomenon is given in Figure 1.10.

Despite various tidy theoretical analyses of nucleus formation that have been derived, nucleation in the laboratory or industrial setting remains very difficult to control in perhaps the majority of cases, due to the many disparate factors that are observed to affect nucleation (Table 1.6). In addition to primary nucleation, there is a phenomenon known as **secondary nucleation** which involves further crystallization after initial crystals are formed (either from deliberate seeding or primary nucleation). Among the factors which affect secondary nucleation are: agitation (including the design and type of crystallization vessel and agitator); temperature and concentration gradients; friable (breakable) crystal form or habit; and crystal irregularities caused by impurities. Secondary nucleation sometimes has undesirable consequences since it tends to produce excessive numbers of very small particles. Furthermore, once crystallization begins, factors like concentration, supersaturation, and many of the parameters in Table 1.6 may change, producing a dynamic environment that makes continued control of the process exceedingly difficult.

The most important lesson in this discussion is that *the number of particles and the crystal form resulting from a crystallization procedure are determined by nucleation*

Table 1.6 Factors that may Initiate Nucleation

Pre-existing nuclei on equipment or in air
Foreign particles of a suitable nature
Deliberate seeding with desired phase
Local hypersaturation by soluble metastable phase
Separation of a liquid phase during processing (*e.g.*, a temperature change or addition of antisolvent)
Local hypersaturation at an immiscible solvent interface
Ultrasonic or shock waves
Scratched surfaces
Local temperature irregularities
Local concentration gradients (*e.g.*, created by surface evaporation or reagent addition)

events. Thus: "one nucleus, one large crystal; a billion nuclei, a billion tiny crystals." In polymorphic systems nuclei of different structures can form and coexist in a given crystallization, in which case a mixture of crystal forms may be found in the final product when kinetic factors prevent achievement of equilibrium.

Consider the situations shown in Figure 1.11. In the top two panels, a crystallization procedure, using apparently the same protocol, affords different polymorphs on separate occasions (needles and plates). In the bottom panel, the "same procedure" results in a mixture of the polymorphs. In these cases, lack of control of the nucleation process leads to lack of control of the polymorphs present. It is therefore common practice to add nuclei of the desired phase deliberately at an appropriate stage in an industrial crystallization. This process is called **seeding**, and is one of many measures used to control the outcome of crystallizations.

C. Transitions Between Crystal Forms

When different crystal forms are possible for a substance each form has a solubility value under a fixed set of conditions: solvent composition; temperature; and pressure. Even if crystals of two forms have been produced, however, the system will always

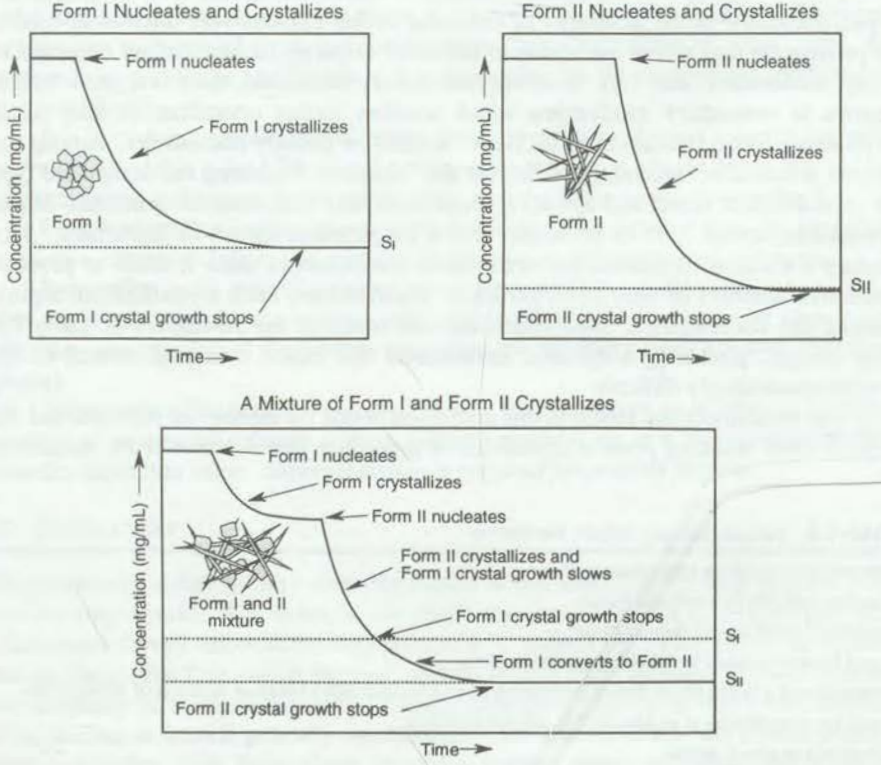

Figure 1.11 Uncontrolled crystallization in a polymorphic system showing the different polymorphs (top panels) or the mixture of polymorphs (bottom panel) which can result. (SI and SII are the solubility limits for Forms I and II, respectively.)

tend to produce only the less soluble of two forms eventually (see Figure 1.11). To be sure, the time it takes to express this tendency depends on kinetic factors and may be quite variable; but in any event, a less soluble form never converts to the more soluble form under rigorously defined conditions.

A few illustrations of the dissolution behavior of some polymorphic drugs may help to review these relationships as they apply to solutions at constant temperature. Figure 1.12 shows concentration versus time plots for furosemide and Figure 1.13 shows the concentration versus time plots for theophylline. In Figure 1.12 there is no conversion to the most stable crystal form during the experiment. In contrast, in Figure 1.13 the less stable anhydrate converts to the hydrate during the experiment providing unequivocal proof that the hydrate is more stable (less soluble) than the anhydrate. In these examples it is obvious which form of theophylline is the less soluble. Under

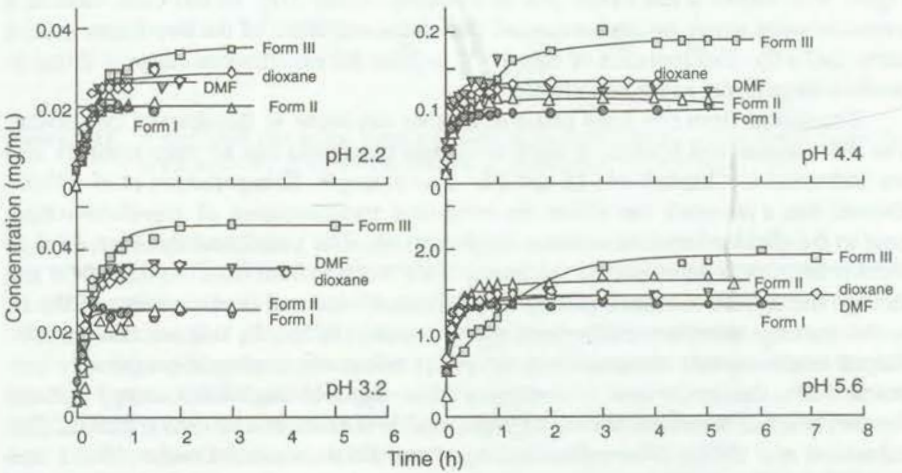

Figure 1.12 Dissolution profiles of the different crystal forms of furosemide in buffer solution at various pH values at 37° C (Matsuda and Tatsumi, 1990).

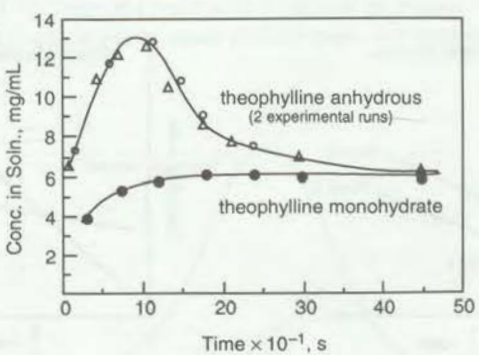

Figure 1.13 Concentration versus time curves for anhydrous and hydrated crystal forms of theophylline in water at 25 °C (Shefter and Higuchi, 1963).

these conditions, this form will never convert to the other, and can therefore also be referred to as the thermodynamically more **stable form**.

When temperature is introduced as a variable, however, further distinctions concerning the relative stability of alternative forms need to be made. The thermodynamic activity (usually observed as solubility) of each form may change quite differently as a function of temperature. **Monotropic** systems are defined as systems where a single form is always more stable regardless of the temperature. **Enantiotropic** systems are defined as systems where the relative stability of the two forms inverts at some transition temperature. These relationships are evident in graphic form (see Figure 1.14).

In actual practice, it is customary to plot log solubility versus $1/T$ for each solid phase (*i.e.*, as a so-called **van't Hoff plot**). These plots give, in most cases, the data in a linear form that lends itself to extrapolation, so that transition points can be determined even when complete data for a given solid phase are unreliable or unavailable. Figure 1.15 shows a van't Hoff plot of solubility versus $1/T$. In this case, there is a transition point where the lines cross and the relative stabilities of the two forms are the same ($\Delta G = 0$). Extrapolation of data 10 K beyond the experimental range is prone to produce large errors and is not reliable.

Transitions from one solid phase to another can occur in the absence of solvent. The mechanisms and kinetics of such solid-state transitions can be very complex and are addressed in Chapters 14, 15 and 20. For example, Kitaigorodskii *et al.* (1965) showed that a pin-prick can initiate the solid-state transformation of α-*p*-dichlorobenzene to β-*p*-dichlorobenzene within a single crystal. The transformation of α- to β-*p*-dichlorobenzene is delineated by the spread of the reaction front from the nucleation site through the crystal. A related process is the thermally-induced rearrangement of the α- to β form of *p*-nitrophenol (Coppens and Schmidt, 1965). In this reaction, needle-shaped single crystals rearrange with the phase boundary moving approximately perpendicular to the needle axis. Grinding or other input of mechanical energy induces the polymorphic transformation of chlorpropamide (Otsuka *et al.*, 1989), fostedil (Takahashi *et al.*, 1985), chloramphenicol palmitate (Kaneniwa and Otsuka, 1985), and several other drugs (Chan and Doelker, 1985).

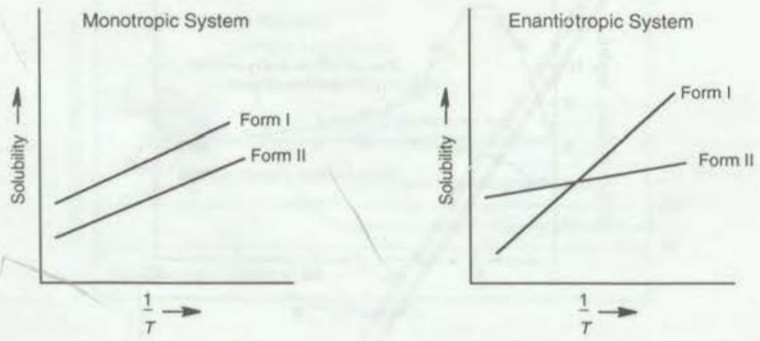

Figure 1.14 Schematic graphs of concentration versus temperature for a monotropic system and an enantiotropic system.

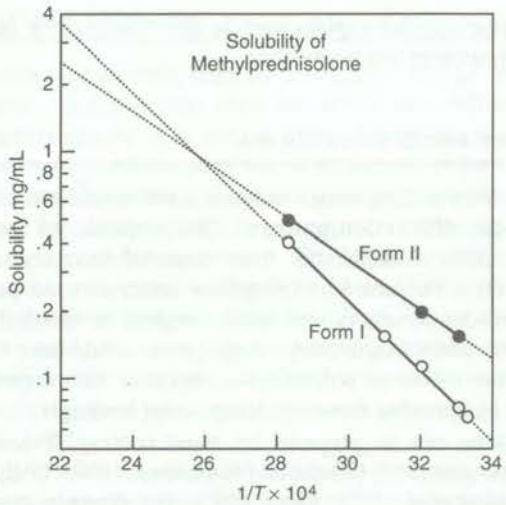

Figure 1.15 A van't Hoff plot of the water solubility of two methylprednisolone crystal forms (log of the solubility as an inverse function of temperature, Higuchi *et al.*, 1963).

D. Other Spontaneous Changes in the Solid State

In addition to the crystal-to-crystal transitions treated above, we should mention another change that can affect properties of drugs: **crystal ripening**. Crystal ripening occurs when the crystal size increases as the solid remains in contact with solution. In this process, larger crystals grow (or ripen) at the expense of smaller crystals. In practice, newly formed crystals contain many "high-energy sites" from the inclusion of impurities, disordered areas (due to rapid growth), and other causes. Crystals less than about one micrometer in size also have excess free energy because of their high surface curvature. These "high-energy" crystals tend to dissolve and then contribute to the ripening process when the material is redeposited on a larger crystal, that is, on a lower free energy site. This process is called "**Ostwald ripening**," after its discoverer (Ostwald, 1896). The effect of ripening on crystal size is shown in Figure 1.16. Control of this process is important in cases where small particle sizes are needed (*e.g.*, aerosol prod-

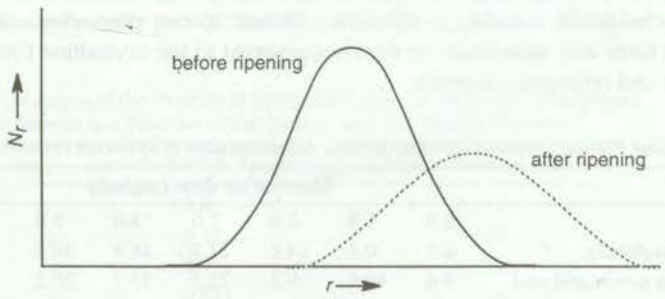

Figure 1.16 Change in crystal size distribution as a result of ripening (Lieser, 1969).

ucts). In addition, ripening can explain particle size changes that take place in suspension during crystallization or wet granulation.

1.6 PROPERTIES OF AMORPHOUS SOLIDS

Amorphous solids have no long-range order, are not crystalline, and therefore do not give a definitive **X-ray diffraction pattern**. The properties of these solids are of interest because they differ considerably from those of their crystalline counterparts. Amorphous solids do not exhibit **birefringence** under crossed polars on the microscope. The most profoundly amorphous solid is a glass in which the atoms and molecules exist in a totally non-uniform array. Amorphous solids have no faces and cannot be identified as either habits or polymorphs. Because the properties of amorphous solids are *direction independent* these solids are called **isotropic**.

Amorphous forms can be prepared by rapid cooling (Fukuoka *et al.*, 1991), grinding (Kitamura *et al.*, 1989; Otsuka and Kaneniwa, 1990), or by lyophilization and spray drying (Haleblian *et al.*, 1971; Pikal, 1990). For example, rapid cooling gives an amorphous form of chloramphenicol palmitate (Kimura and Hashimoto, 1960), as did over 20 other pharmaceuticals (Fukuoka *et al.*, 1991 and references therein). Lyophilization gave amorphous forms of fluprednisolone (Haleblian *et al.*, 1971), antibiotics (Pikal *et al.*, 1977), and proteins (Pikal, 1990).

An amorphous solid is characterized by a unique **glass transition temperature** T_g, the temperature at which it changes from a **glass** to a **rubber**. When T rises above T_g, the rigid solid can flow and the corresponding increase in molecular mobility can result in crystallization or increased chemical reactivity of the solid.

Although amorphous solids often have desirable pharmaceutical properties, such as rapid dissolution rates (Fukuoka *et al.*, 1987), they are not usually marketed because of their lower chemical stability (Pikal *et al.*, 1977) and their tendency to crystallize (Fukuoka *et al.*, 1991), thus overriding any adventitious properties. Nevertheless, in some cases, amorphous forms are used as products. An excellent example is novobiocin (Mullins and Macek, 1960) which exists in a crystalline and an amorphous form. The crystalline form is poorly absorbed and does not provide therapeutic blood levels; in contrast, the amorphous form is readily absorbed and is therapeutically active. Further studies show that the solubility rate of the amorphous form is 70 times greater than the crystalline form in 0.1 *N* HCl at 25 °C when particles <10 μm are used. Table 1.7 (Haleblian, 1975) shows data for the plasma levels of novobiocin's amorphous and crystalline forms and for sodium novobiocin, which also gives detectable plasma levels, but is chemically unstable in solution. Unless special precautions are taken, an amorphous form will sometimes be slowly converted to the crystalline form (Fukuoka *et al.*, 1991 and references therein).

Table 1.7 Dog Plasma Levels of Novobiocin after Administration of Different Novobiocin Forms

	Hours after dose (mg/mL)						
Form	0.5	1.0	2.0	3.0	4.0	5.0	6.0
Sodium novobiocin	0.5	0.5	14.6	22.2	16.9	10.4	6.4
Amorphous novobiocin acid	5.0	40.6	29.3	22.3	23.7	20.2	17.5
Crystalline novobiocin acid	Not detectable at any time						

Haleblian, 1975.

1.7 MOISTURE UPTAKE BY SOLIDS

Some crystalline solids take up water from the atmosphere and are termed **hygroscopic solids** in the literature. Unfortunately, there can be no clear definition of hygroscopic solids because **hygroscopicity** is a relative term. Hygroscopicity is determined by both a kinetic and a thermodynamic term and is a function of the atmospheric relative humidity. In high relative humidities, many solids are hygroscopic. In atmospheres of low humidity, only a few solids will be hygroscopic. Another factor influencing hygroscopicity is surface area and thus porosity. The larger the surface area of the solid, the more rapid the uptake of moisture. This is because solids with larger surface areas have more sites for adsorption of water molecules. Zografi *et al.* (1991) suggested that hydroscopicity not be used and that the relative humidity at which a water-soluble solid **deliquesces** (RH_0) should be used instead. This is a scientific term that can be clearly defined and will not vary from investigator to investigator but is only applicable for highly water soluble solids.

Zografi *et al.* (1991) also described guidelines for the establishment of pharmaceutical compendium water specifications and processes by which water is adsorbed by solids. They suggested that surface water generally does not amount to more than 1 to 3 molecular layers. Since the cross-sectional area of a water molecule is about 0.125 nm^2, 1 to 3 molecular layers would amount to only negligible percentages of water. Table 1.8 shows the calculated layers of water on the surface of a solid as a function of surface area and particle diameter. It is clear from this table that even for the smallest particles, 0.1% water will form a monolayer on the surface. Hence, three layers would only account for about 0.3% water. Obviously, claims for large increases in weight because of surface moisture are not consistent with this observation.

When solids that are not solvates contain large amounts of water, it has been hypothesized that water must be taken up into the solid by disordered or high-energy regions such as defects and amorphous sites. They further suggested that such effects might be exaggerated by manufacturing processes that reduce particle size, such as micronization, milling, or related processes known to increase the number of high energy sites. Of course, some solids can take up so much water during these processes that they become damp or even liquefy at RH_0 (Zografi *et al.*, 1991). This tendency is usually easily detected by microscopic observation. The mass of water necessary for the solid to change from a glass to a more fluid-like system is designated W_g.

The formation of crystal hydrates, of course, is another way for water to be incorporated into a solid. In these cases the water molecules generally occupy a specific crystallographic site in the solid. This site can be determined by X-ray crystallography which thus unequivocally proves the existence and composition of the hydrate. How-

Table 1.8 Calculation of the Number of Molecular Layers of Water on Solid Spheres of Sucrose as a Function of the Surface Area and Particle Diameter.[a]

Number of Layers	Specific Surface Area (m^2/g)	Particle diameter (microns)
1.1	3.8	1
11	0.38	10
42	0.10	38
110	0.038	100

a Density = 1.59 g/cm^3 at 0.1% water content.

ever, many hydrates exist in which the water is located in tunnels within the crystal. The water can be located accurately only by determination of the crystal structure at low temperatures (if even then). In these cases, the water content may change rather easily with changes in relative humidity.

Plots of vapor pressure versus relative humidity are an excellent way to determine the nature of a solid with respect to water sorption (see Figure 1.17). The different kinds of behavior that these plots may be expected to show include:

1. Virtually no water uptake
2. Gradual water uptake, characteristic of an amorphous material or a **nonstoichiometric hydrate** (a hydrate without a simple ratio of water to host molecule)
3. "Stair-step" water uptake, characteristic of a stoichiometric hydrate

Figure 1.18 shows the behavior of two stoichiometric hydrates (a monohydrate and a sesquihydrate) as well as a nonstoichiometric hydrate of sodium cefazolin. In addition, amorphous sodium cefazolin also exists and takes up and loses water in a more or less gradual fashion as described below.

Sorption of water into amorphous solids or regions of a solid involves dispersion or dissolution of the water molecules within a solid. The more polar a solid, the greater the amount of water taken up. Obviously, in such systems the water content depends upon relative humidity. In addition, the amount of water absorbed may not reach equilibrium for several months (Zografi *et al.*, 1991).

In summary, Zografi *et al.* (1991) made the following recommendations with regard to water specifications:

1. A complete profile of relative humidity versus water content (weight) should be reported for all reference standards.
2. For amorphous solids, both T_g and W_g should be reported.
3. For deliquescent solids, the RH_0 and an appropriate warning on the label should be provided.
4. For stoichiometric hydrates, the water specifications should reflect the stoichiometry.
5. Attention should be paid to materials which do not form well-defined hydrates and can take up or lose water as the humidity is

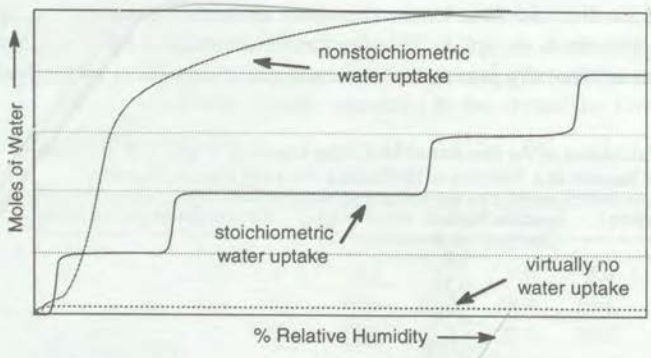

Figure 1.17 Idealized vapor pressure versus relative humidity plot.

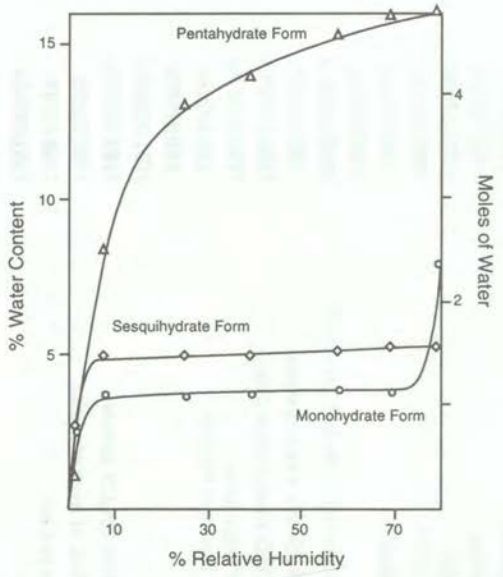

Figure 1.18 Vapor pressure versus relative humidity diagrams for three hydrates of sodium cefazolin. The sesquihydrate and monohydrate behave normally and the "pentahydrate" is actually a nonstoichiometric hydrate (Osawa *et al.*, 1988; Pfeiffer, 1988).

varied. Any structural changes that accompany changes in water content should be noted. (Some hydrates can lose water without changing crystal structure. This is due to the formation of an extremely stable crystal packing network by the host molecule.)

1.8 Lyophilized Powders

Many antibiotics, proteins, and other drugs are marketed as lyophilized powders. The process of freezing a solution of the drug and then removing the ice by sublimation yields a product that is low in moisture and high in specific surface area. Although the solid may crystallize during the freeze drying process, the usual product is an amorphous powder. If the solid crystallizes during storage, a slower dissolution rate would be expected.

1.9 Patents on Various Crystal Forms

A review of the patent literature indicates that crystal forms and processes involving crystal forms are patentable. Of the approximately 41,000 patents in the *Pharmaceuticals* section of *Chemical Abstracts* (listed prior to August 28, 1991), 122 use the keyword "crystal," 10 use the keyword "polymorph," 27 use the keyword "solvate," and 191 use the keyword "hydrate," or keywords involving higher hydrates. In addition, 79 use the keyword "crystallization." Many of the most interesting patents which were retrieved in this search are listed in Table 1.9. It is important to note that this search is

Table 1.9 Selected Patents on Various Crystal Forms Listed in Chemical Abstracts

Substance	Crystal Form	Utility	Abstract No.
Sodium Acetylsalicylate	crystalline	stable	**108**:44030*n*
Amoxicillin	anhydrous sodium salt	nonhygroscopic and stable	**102**:172646*f*
Amoxicillin	pyrrolidone solvate	injectable	**96**:74631*k*
Amphotericin B	crystals	purification process	**112**:240473*f*
Azetidine Sulfonic Acid	crystalline anhydrous form	improved stability	**99**:10852*n*
Azithromycin	dihydrate	nonhygroscopic	**111**:45265*s*
Beclomethasone	chlorofluorocarbon solvate	stability	**94**:52972*d*
Beclomethasone	solvates	aerosol formulation	**96**:91650*h*
Beclomethasone Dipropionate	Freon® solvate	aerosols	**113**:29296*p*
Beclomethasone Diproprionate	alkane solvates	formulation	**102**:209431*k*
Beclomethasone Diproprionate	new crystal form	does not form solvates with propellants	**94**:162747*s*
Benzimidazole Derivative	crystalline	thermostable with small particle size	**108**:137876*h*
Buspirone·HCl	interconversion	preparation of either form	**111**:239476*g*
Catechin	monohydrate and anhydrate	formulations	**103**:59298*b*
Cefadroxyl	anhydrate	preparation	**111**:239478*j*
Cefadroxyl Monohydrate	monohydrate	preparation	**111**:239477*h*
Cefahydroxyl Monohydrate	crystalline	preparation from CH_3CN solvate	**103**:166151*v*
Cefamandole Derivative	γ-form	stability and lack of hygroscopicity	**86**:78672*r*
Sodium Cefazolin	monohydrate	crystallization process	**90**:61247*r*
Ceftazidime	anhydrous crystal modification	stability	**102**:67395*a*
Ceftazidime Intermediate	crystalline $HCl·H_2O$	purification	**102**:191162*m*
Ceftazidime·$5H_2O$	pentahydrate	increased activity	**105**:30045*x*
Cefuroxime	crystalline sodium salt	crystallization	**102**:32299*v*
Cephalexin	crystalline	formulation	**84**:184895*j*
Cephalexin	monohydrate	stability	**74**:6404*j*
Cephalexin	*t*-type monohydrate	novel	**89**:169093*f*

Table 1.9 (continued) Selected Patents on Various Crystal Forms Listed in Chemical Abstracts

Substance	Crystal Form	Utility	Abstract No.
Cephalexin·HCl	monohydrate	immediate release	**103**:129047*v*
Cephalosporin Antibiotic	heptahydrate sodium salt	improved stability	**100**:73975*q*
Sodium Cephalothin	crystallization	improved filtration properties	**87**:141273*z*
A Cephem Carboxylic Acid	hydrates	stability	**110**:29096*m*
Sodium Cephem-carboxylate	crystals	formulation	**103**:129069*d*
Cephradine	hydrate	stability	**115**:35741*n*
Cimetidine	Form A	formulation	**100**:12669*w*
Cimetidine	Form B	formulation	**109**:237026*v*
Cimetidine	Form B	preparation	**109**:176349*d*
Cimetidine	Form Z	formulation	**99**:10848*r*
Corticosteroids	chlorofluorocarbon solvates	lack of crystal growth in aerosols	**85**:51743*g*
Cyclosporin	orthorhombic form	sustained release	**112**:145575*g*
DDI, DDT	monohydrate	high water solubility	**115**:35706*e*
Deoxycholic Acid	unsolvated crystals	improved formulations	**94**:162743*n*
Deoxyspergalin	crystalline	improved hygroscopicity, stability, handling	**115**:15582*h*
Dianemycin glycon	crystalline anhydrous form		**106**:23267*p*
Dibenzopyrone	polycrystalline form	improved blood levels	**86**:95990*k*
Famotidine	morphologically homogeneous	homogeneous forms	**108**:192770*u*
Famotidine	separation of crystal forms	increased activity	**111**:180678*u*
Flunisolide	crystal form	aerosols	**93**:138020*h*
Flunisolide	crystal form	aerosols	**94**:214609*v*
Gabapentin Monohydrate	monohydrate	novel crystal form	**113**:138572w
Gabexate Mesylate	lyophilized crystals	high stability	**111**:63927*p*
Ibuprofen	crystalline	improved flow properties	**102**:50901*q*
Inotropic Agent	hydrates	administration	**112**:204687*v*
Insulin	crystalline suspension	improved release	**94**:214619*y*

Table 1.9 (continued) Selected Patents on Various Crystal Forms Listed in Chemical Abstracts

Substance	Crystal Form	Utility	Abstract No.
Isoglutamine Derivative	monohydrate	more stable, less hygroscopic	**106**:125878*f*
Josamycin	solvent-free crystals	formulation	**87**:90714*j*
LY163892	dihydrate and trihydrate	preparation and formulation	**114**:88656*z*
LY163892	solvates	intermediates	**114**:88639*w*
LY163892 (antibiotic)	monohydrate	formulation	**111**:201646*z*
Meclophenoxate·HCl	type I crystals	more stable, less hygroscopic	**107**:64843*n*
Mefloquine·HCl	polymorph	improved solubility and bioavailability	**103**:129044*s*
Methylbutylamine·HCl Derivative	monohydrate	not hygroscopic	**107**:223314*j*
Methyldopa Salts	crystalline solvates	crystalline	**107**:242598*w*
Milrinone	3 crystal modifications	formulations	**110**:63770*m*
Naphthyridine Carboxylic Acid	sesquihydrate	stability	**98**:59888*x*
Necromodil Na	Form B	stability	**108**:226832*h*
4-Oxo-2-azetidinyl Derivative	crystals	crystalline	**108**:137873*e*
Penicillin Derivative	hemisolvate	stability	**85**:130523*p*
Phenylpropiophenone	spherical crystals	sustained release	**115**:15598*t*
A piperazine·HCl	new crystal form	increased solubility	**105**:158806*p*
Piroxicam	β-form	improved flow properties	**111**:140479*y*
Prazosin·HCl	α-form	preparation	**99**:10849*s*
Pyran-9-one Derivative	polymorphs	particle size	**83**:152334*p*
N-Pyridylcarboxyamide	polymorphic monoethanolamine salt	increased stability	**105**:66460*t*
Quinolone Carboxylate	anhydrate	stability and preparation	**112**:185779*h*
Sorbitol	γ-form	improved tableting	**95**:30396*n*
Steroid	monoclinic or triclinic forms	preparation and formulation	**114**:214521*s*
Sulfametrole Hemihydrate	hemihydrate	no sediment upon storage	**107**:223316*m*
(*S*)-Timolol	hemihydrate	preparation	**114**:49576*d*

by no means comprehensive since several of the most important patents on crystal forms, including those on ranitidine hydrochloride and cefuroxime axetil, did not show up as "hits."

It is clear from Table 1.9 that patents based on solid-state properties have been issued for a wide range of drugs crystallizing in many different crystal forms and having many different uses. The types of drugs included in Table 1.9 range from antibiotics, to antiulcer drugs, to antitumor and antiviral agents, to anti-inflammatory agents. Proteins and various salts are also included. Polymorphs, solvates, hydrates of various types, and lyophilized crystals are among the crystal forms claimed. As might be expected, a wide range of uses is cited. Among the most frequent uses cited are improved formulation, handling, and stability. In addition, there are several patents on crystal forms with reduced hygroscopicity and improved solubility and bioavailability. Patents will no doubt continue to be issued on crystal forms. In fact, it is likely that the number of crystal forms patented will greatly increase since our ability to characterize and understand the crystal forms has greatly improved.

1.10 Solid-State Reactions of Drugs

The scientific discipline of solid-state chemistry of drugs emphasizes studies of the chemical and physical properties of the various solid forms just discussed. These studies include solid-state phase transformations (polymorphic transformations), reactions in which solvent of crystallization is lost or gained, and a broad range of solid-state chemical reactions.

It is necessary to establish criteria for solid-state reactions in order to focus on true solid-state reactions. This will avoid a liquid-state reaction being identified as a solid-state reaction. Morawetz (1966) suggested four criteria for determining whether a reaction is a true solid-state reaction and a fifth and very important criterion can be added from Paul and Curtin (1973):

1. A reaction occurs in the solid when the liquid reaction does not occur or is much slower.
2. A reaction occurs in the solid when pronounced differences are found in the reactivity of closely related compounds.
3. A reaction occurs in the solid when different reaction products are formed in the liquid state.
4. A reaction occurs in the solid if the same reagent in different crystalline modifications has different reactivity or leads to different reaction products.
5. A reaction occurs in the solid phase if it occurs at a temperature below the eutectic point of a mixture of the starting material and products.

Once it has been established that the reaction is occurring in the solid state, the reaction can be understood in terms of a four-step process (Paul and Curtin, 1973):

1. loosening of the molecules at the reaction site
2. molecular change
3. solid solution formation
4. separation of the product phase

Table 1.10 Solid-State Chemical Reactions of Drugs

Solid-State Oxidations (Chapter 18)

Dialuric Acid (Clay *et al.*, 1982)

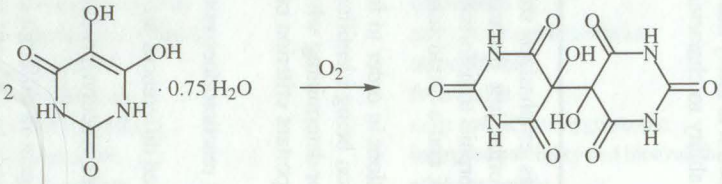

Dihydrophenylalanine (Ressler, 1972)

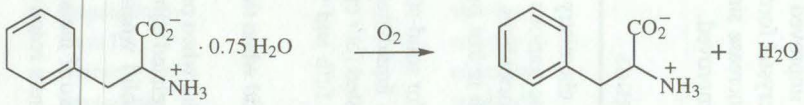

Phorbol Esters (Schmidt and Hecker, 1975)

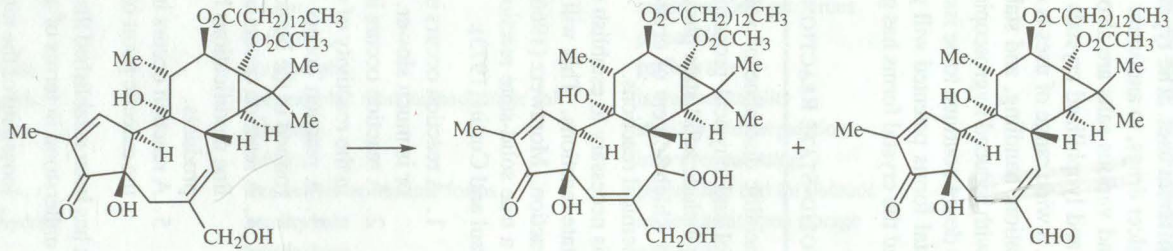

Table 1.10 (continued) Solid-State Chemical Reactions of Drugs

Vitamin C (Rubin *et al.*, 1976)

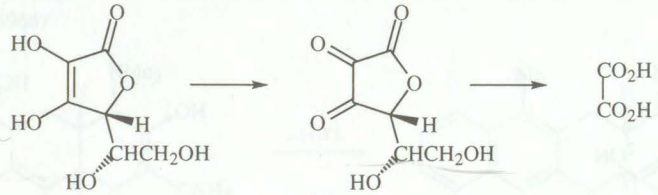

Hydrocortisone *tert*-Butylacetate (Brenner *et al.*, 1969)

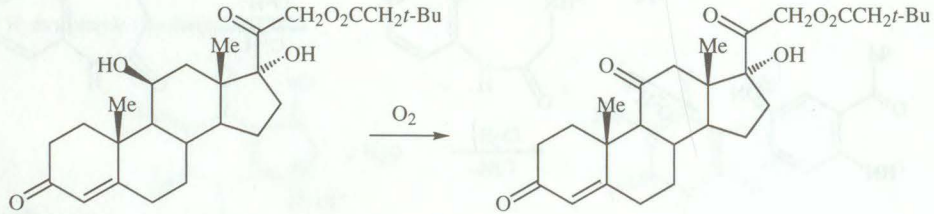

Vitamin D_2 (Kanzawa and Kotaku, 1953)

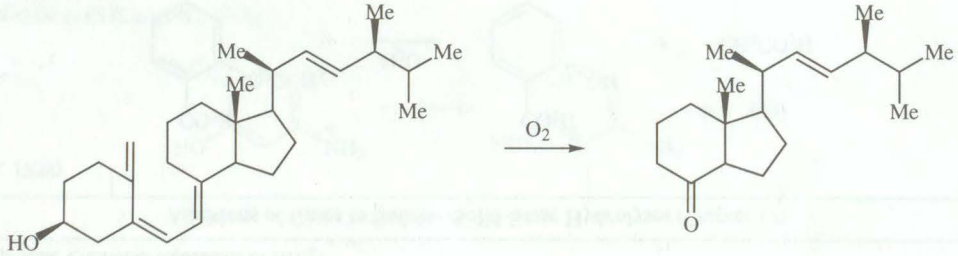

Table 1.10 (continued) Solid-State Chemical Reactions of Drugs

Additions of Gases to Solids—Solid-State Hydrolyses (Chapter 19)

Aspirin (Leeson and Mattocks, 1958)

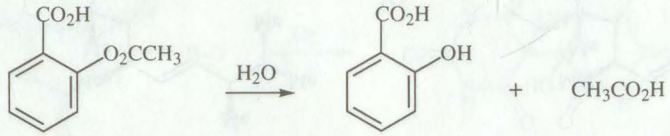

Nitrazepam (Genton and Kesselring, 1977)

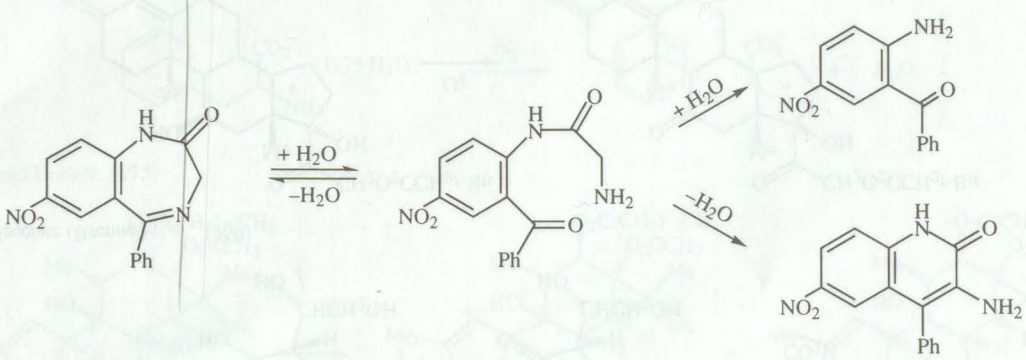

Table 1.10 (continued) Solid-State Chemical Reactions of Drugs

Solid-State Decomposition Reactions: A (solid) → B (solid) + C (gas) (Chapter 20)

Dehydration of Tetracyclines (Simmons *et al.*, 1966)

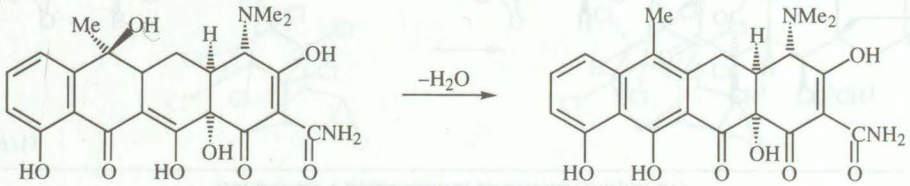

Dehydrochlorination of Caffeine Hydrochloride (Biedermann, 1883)

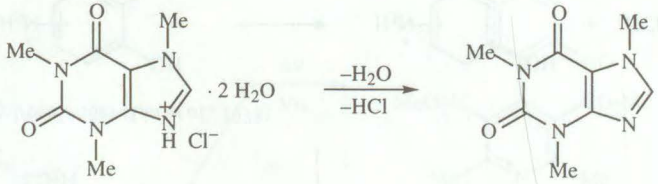

Decarboxylation of *p*-Aminosalicylic Acid (Lin *et al.*, 1978)

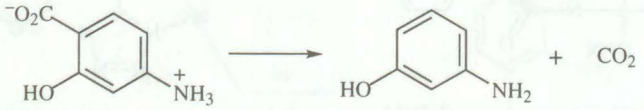

Table 1.10 (continued) Solid-State Chemical Reactions of Drugs

Solid-State Decomposition Reactions: A (solid) → B (solid) + C (gas) (continued)

Decarboxylation of Moxalactam (Pikal and Dellerman, 1989)

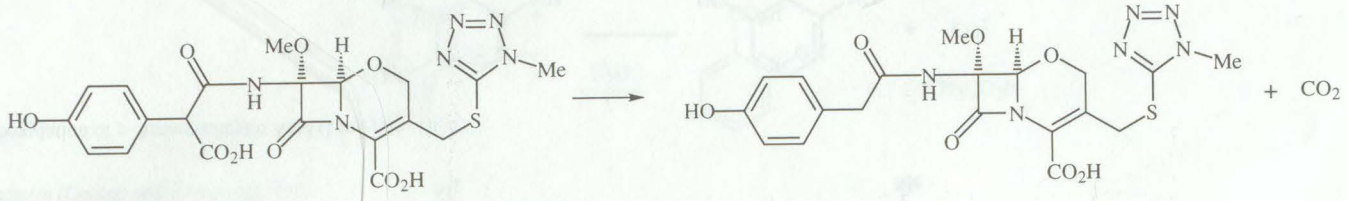

Dehydrochlorination of Aminosalicylic Acid Hydrochlorides (Lin *et al.*, 1978)

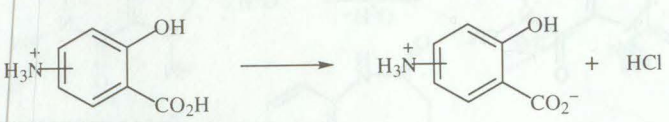

Solid-State Photochemical Reactions (Chapter 21)

Gibberellins (Adam and Voigt, 1971)

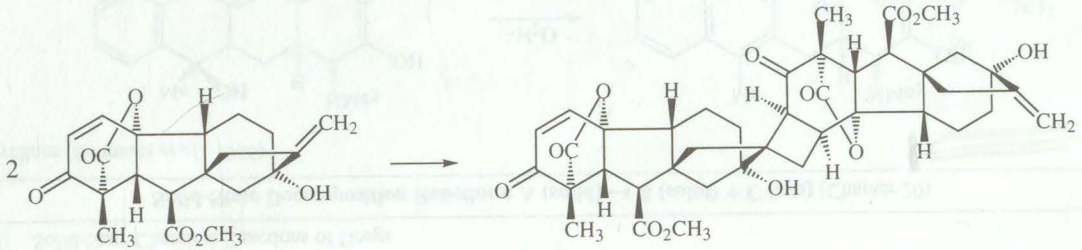

Table 1.10 (continued) Solid-State Chemical Reactions of Drugs

Dieldrin (Benson, 1971)

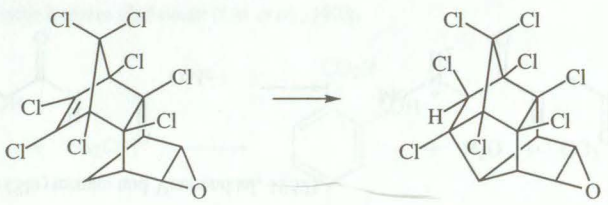

Nifedipine (Hayase *et al.*, 1994)

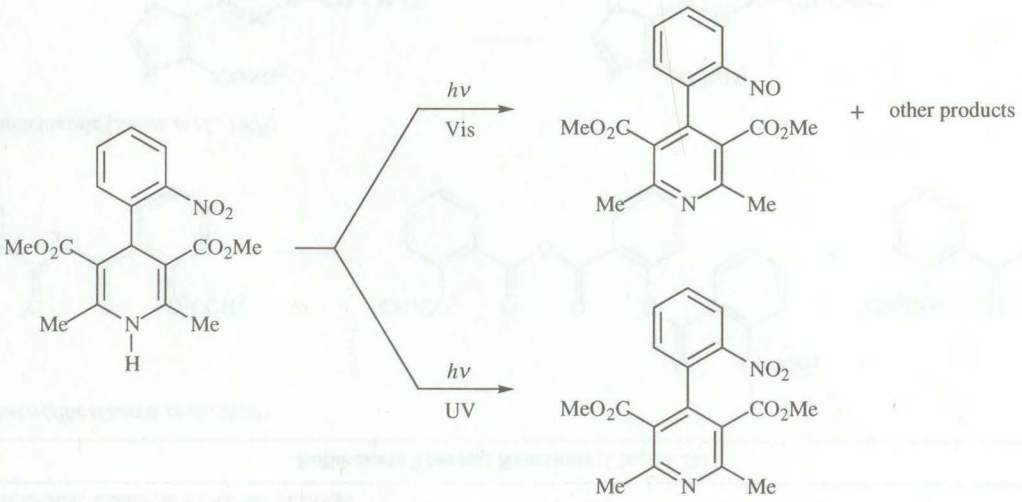

Table 1.16 (continued) Solid-State Chemical Reactions of Drugs

Solid-State Thermal Reactions (Chapter 22)

Rearrangement of Aspirin Anhydride (Garrett *et al.*, 1959)

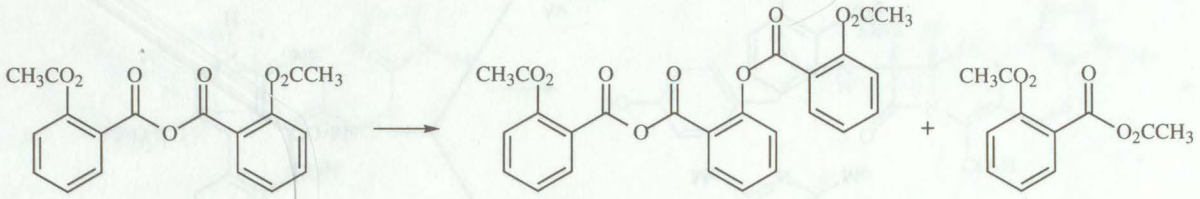

Rearrangement of a Triazenoimidazole (James *et al.*, 1969)

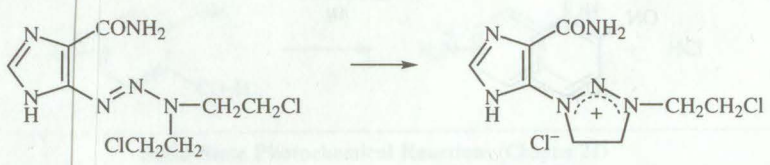

Rearrangement of the Methyl Ester of Tetraglycine (Sluyterman and Veenendaal, 1952)

Table 1.10 (continued) Solid-State Chemical Reactions of Drugs

Solid–Solid Reactions (Chapter 24)

Reaction of *p*-Aminosalicylic Acid Hydrochloride with Sodium Carbonate (Lin *et al.*, 1978)

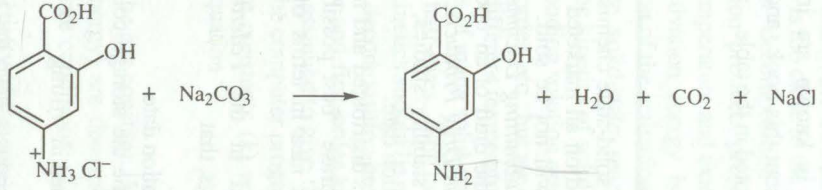

These four steps are discussed in more detail in Part 5 of this book.

It is important to realize that many solid-state reactions of drugs involve drug degradations which have been studied mostly on the macroscopic level. In fact, few studies aimed at determining the molecular aspects of the solid-state chemistry of drugs have been published. These reactions are of interest because of a desire to prevent such degradation. Even for such common drugs as vitamin D_2 and vitamin A, the structures of only a few of the solid-state degradation products have been published. Therefore, in many respects, the solid-state chemistry of drugs is synonymous with drug degradation.

Table 1.10 summarizes some of the solid-state chemical reactions of drugs and is arranged according to the type of chemical reaction involved. Only solid-state reactions in which the chemical structure of the product(s) is known are included. The classification scheme used in this table is used throughout this book, and each class of reaction is treated in a separate chapter or chapters as noted in the table.

1.11 STABILITY TESTING

One of the practical areas encompassed by the field of solid-state chemistry of drugs is the area of stability testing. Stability tests are conducted on all marketed drugs in order to determine an expiration date after which the drug will not be sold. The FDA has issued guidelines for stability testing (*Guideline for Submitting Documentation for the Stability of Human Drugs and Biologics*, 1987) and the draft of an update (*Guidance for Industry: Stability Testing of Drug Substances and Drug Products*, 1998). These guidelines describe the design and interpretation of stability studies, the content of stability reports, and methods for computing an expiration date.

Manufacturers are required to ensure that the drugs distributed and marketed are of the best possible quality. However, because the phrase "best possible quality'' is vague, the government has attempted to define this idea in terms of current good manufacturing practices (cGMP).

Good manufacturing practices were published in the *Federal Register* on September 29, 1978. They require, among other things, that

1. essentially all products must bear an expiration date
2. all products bearing this date must describe the storage conditions under which this date applies
3. the stability-testing program must be defined in writing

An expiration date is required to assure that drug products have the identity, purity, structure, and quality described on the label and package insert during their period of use under the storage conditions described. If the product is subjected to higher temperatures than those described, then the actual expiration date will be sooner than the expiration date on the label.

Generally, stability studies and expiration dates should be determined under conditions approximating normal storage conditions rather than under accelerated conditions. One of the reasons is that elevated temperatures used in accelerated stability tests may be above the eutectic of the reactant or product and may result in misleading

information (see Figure 1.18). Nevertheless, a series of accelerated stability tests can be used to determine the best storage conditions.

For **accelerated stability tests**, each crystalline form and habit of the pure solid as well as solid-solid mixtures of the pure solid with **excipients** and **adjuncts** (additives used to prepare the pharmaceutical product) should be maintained at elevated temperature (different companies use different temperatures) in vials or ampoules. In addition, accelerated studies in which samples are deliberately exposed to light are often carried out. One ampoule or vial should be assayed each day using the most sensitive method available. The experiment should be run for at least two weeks, and the data should be used to determine the rate of decomposition. The rate is conveniently determined using the computer program described in Chapter 23. If the elevated temperature is too close to the melting point of the solid, liquid could form after only a few percent decomposition through the lowering of the melting point by the decomposition products present. Under these circumstances, it is probably best to lower the temperature and extend the study.

The activation energy is also of interest in predicting product stability. For determination of the activation energy, the kinetics (percentage of decomposition versus time) of the solid-state reactions are determined at three or more temperatures. However, the kinetics of solid-state reactions are often much more complicated than in the corresponding solution reactions. Solid-state reactions are usually not clearly zero-order, first-order, etc., but are often of fractional orders. Thus determination of the rate constant at different temperatures is difficult, if not impossible. In addition, because of the slowness of many solid-state reactions, rate studies are usually only carried through one or two half-lives. For this reason, Carstensen (1974) suggests that first-order or zero-order kinetics should be assumed for determination of the activation energy. Thus the rates of decomposition are measured at several temperatures and plotted according to zero-order and first-order kinetics. The equation that gives the best fit by statistical tests is then assumed to give the best rate constants. An attractive alternative approach is to apply the computer program discussed in Chapter 3 to the data.

The rate constants (k) are then plotted versus temperature (T) according to the Arrhenius equation

$$k = Ae^{-E_a/RT} \tag{1.1}$$

where R is the gas constant. From this plot, A (the pre-exponential factor) and E_a (the activation energy) are determined and used to determine the rate constant (k) at the labeled storage conditions. This rate constant is then used to estimate the expiration date.

The reactivity of the compound in solution at elevated temperatures should also be determined to give information about the "intrinsic reactivity" of the drug.

The stability of the drug in light is also usually determined. Each crystalline form and habit of the pure solid and mixtures with adjuncts and excipients is exposed in a suitable light cabinet under the following conditions: inert atmosphere, exposure to air, and exposure to increased humidity humidity. These latter studies can conveniently be performed using a glove bag. Samples are assayed each day using the most sensitive method available.

The container in which the drug has the greatest stability is selected. The best container is determined by measuring the rate of degradation of the drug in various

containers under various storage conditions. Obviously, the container and storage conditions in which the rate of decomposition is slowest should be chosen.

1.12 SUMMARY

This chapter summarizes the scope of the area of solid-state chemistry of drugs. It is clear that this is a broad, relatively unexplored area involving an understanding of crystallization, the properties of crystals, the forces holding crystals together, the properties of other solids (*i.e.*, amorphous solids), the chemical or physical reactions involved, the criteria for solid-state reactions, the kinetics of solid-state reactions, and the broad field of stability testing.

There is a need to develop an understanding of solid-state reactions of drugs in terms of the molecular details of the reactions. Of particular interest is the determination of the molecular parameters that can lead to retardation of the solid-state reactions of drugs and thus render drugs more stable.

It is the aim of the rest of this book to further illustrate the importance and value of molecular understanding of solid-state reactions.

REFERENCES

Adam, G. and B. Voigt (1971) "Solid state photoaromatization of 3-keto-gibberellin A_3" *Tetrahedron Lett.* **1971** 4601–4604.

Benson, Walter R. (1971) "Photolysis of solid and dissolved dieldrin" *J. Agr. Food Chem.* **19** 66–72.

Bernstein, Joel, Raymond E. Davis, Liat Shimoni, and Ning-Leh Chang (1995) "Patterns in hydrogen bonding: functionality and graph set analysis in crystals" *Angew. Chem. Int. Ed. Engl.* **34** 1555–1573.

Biedermann, H. (1883) "Concerning caffeine and its salts" *Arch. Pharm.* **221** 175–186.

Brenner, G., F. E. Roberts, A. Hoinowski, J. Budavari, B. Powell, D. Hinkley, and E. Schoenewaldt (1969) "Effect of crystalline form on the air-oxidation of steroidal 11β-ols to 11-ones" *Angew. Chem. Int. Ed.* **8** 975–976.

Brock, Carolyn Pratt and Robin P. Minton (1989) "Systematic effects of crystal-packing forces: biphenyl fragments with hydrogen atoms in all four ortho positions" *J. Am. Chem. Soc.* **111** 4586–4593.

Brock, Carolyn Pratt, W. Bernd Schweizer, and Jack D. Dunitz (1991) "On the validity of Wallach's rule: on the density and stability of racemic crystals compared with their chiral counterparts" *J. Am. Chem. Soc.* **113** 9811–9820.

Burger, A. and R. Ramberger (1979a) "On the polymorphism of pharmaceuticals and other molecular crystals. I. Theory and thermodynamic rules" *Mikrochim. Acta* **2** 259–271.

Burger, A. and R. Ramberger (1979b) "On the polymorphism of pharmaceuticals and other molecular crystals. II. Applicability of thermodynamic rules" *Mikrochim. Acta* **2** 273–316.

Bürgi, Hans-Beat and Jack D. Dunitz, Eds. (1994) *Structure Correlation*; VCH: New York, NY; Vols. 1 and 2.

Byrn, Stephen R., Paul A. Sutton, Brian Tobias, James Frye, and Peter Main (1988) "The crystal structure, solid-state NMR spectra, and oxygen reactivity of five crystal forms of prednisolone *tert*-butylacetate" *J. Am. Chem. Soc.* **110** 1609-1614.

Carless, J. E., M. A. Moustafa, and H. D. C. Rapson (1968) "Dissolution and crystal growth in aqueous suspensions of cortisone acetate" *J. Pharm. Pharmacol.* **20** 630–638.

Carstensen, J. T. (1974) "Stability of solids and solid dosage forms" *J. Pharm. Sci.* **63** 1–14.

Chan, H. K. and E. Doelker (1985) "Polymorphic transformation of some drugs under compression" *Drug. Dev. Ind. Pharm.* **11** 315–332.

Clay, Ronald J., Adelbert M. Knevel, and Stephen R. Byrn (1982) "The desolvation and oxidation of crystals of dialuric acid monohydrate" *J. Pharm. Sci.* **71** 1289–1291.

Coppens, Phillip and G. M. J. Schmidt (1965) "The crystal structure of the metastable (β) modification of *p*-nitrophenol" *Acta Cryst.* **18** 654–663.

Dargel, Erwin and Jobst B. Mielck (1989) "Chemical stability of drugs in solid dispersion: accelerated tests of reserpine disperesed in Kollidon® 25 and in Eudragit® E" *Acta Pharm. Technol.* **35** 197–209.

Etter, Margaret C., and Paul W. Baures (1988) "Triphenylphosphine oxide as a crystallization aid" *J. Am. Chem. Soc.* **110** 639–640.

Etter, Margaret C., Zofia Urbańczyk-Lipkowska, Touradj M. Ameli, and Thomas W. Panunto (1988) "Intra- versus intermolecular hydrogen bonds in salicylamide derivatives" *J. Crystallogr. Spectrosc. Res.* **18** 491–507.

Etter, Margaret C. (1990) "Encoding and decoding hydrogen-bond patterns of organic compounds" *Acc. Chem. Res.* **23** 120–126.

Etter, Margaret C. and Daniel A. Adsmond (1990) "The use of cocrystallization as a method of studying hydrogen bond preferences of 2-aminopyridine" *J. Chem. Soc., Chem. Commun.* **1990** 589–591.

Etter, Margaret C., John C. MacDonald, and Joel Bernstein (1990a) "Graph-set analysis of hydrogen-bond patterns in organic crystals" *Acta Crystallogr., Sect. B, Struct. Sci.* **B46** 256–262.

Etter, Margaret C., Zofia Urbańczyk-Lipkowska, Mohammad Zia-Ebrahimi, and Thomas W. Panunto (1990b) "Hydrogen bond directed cocrystallizaton and molecular recognition properties of diarylureas" *J. Am. Chem. Soc.* **112** 8415–8426.

Etter, Margaret C. and Susan M. Reutzel, (1991) "Hydrogen bond directed cocrystallization and molecular recognition properties of acyclic imides" *J. Am. Chem. Soc.* **113** 2586–2598.

Fukuoka, Eihei, Midori Makita, and Shigeo Yamamura (1987) "Glassy state of pharmaceuticals. II. Bioinequivalence of glassy and crystalline indomethacin" *Chem. Pharm. Bull.* **35** 2943–2948.

Fukuoka, Eihei, Midori Makita, and Yasuo Nakamura (1991) "Glassy state of pharmaceuticals. V. Relaxation during cooling and heating of glass by differential scanning calorimetry" *Chem. Pharm. Bull.* **39** 2087–2090.

Garrett, Edward R., Edward L. Schumann, and Marvin F. Grostic (1959) "Prediction of stability in pharmaceutical preparations. VI. Stability, products, and mechanism in the pyrolytic degradation of aspirin anhydrate" *J. Am. Pharm. Assoc. Sci. Ed.* **68** 684–691.

Gavezzotti, A. and Gautam R. Desiraju (1988) "A systematic analysis of packing energies and other packing parameters for fused-ring aromatic hydrocarbons" *Acta Crystallogr., Sect. B, Struct. Sci.* **B44** 427–434.

Genton, D., and U. W. Kesselring (1977) "Effect of temperature and relative humidity on nitrazepam stability in solid state" *J. Pharm. Sci.* **66** 676–680.

Guideline for Submitting Documentation for the Stability of Human Drugs and Biologics (1987) Food and Drug Administration, Center for Drugs and Biology, Office of Drug Research and Review; Rockville, MD, USA.

Guidance for Industry: Stability Testing of Drug Substances and Drug Products (1998) Kenneth Furnkranz, Ed.; U.S. Department of Health and Human Services, Food and Drug Administration, Center for Drug Evaluation and Research (CDER), Center for Biologics Evaluation and Research (CBER); Rockville, MD, USA.

Haleblian, John K., Robert T. Koda, and John A. Biles (1971) "Isolation and characterization of some solid phases of fluprednisolone" *J. Pharm. Sci.* **60** 1485–1488.

Haleblian, John K. (1975) "Characterization of habits and crystalline modifications of solids and their pharmaceutical applications" *J. Pharm. Sci.* **64** 1269–1288.

Hayase, Nobumasa, Yu-Ichi Itagaki, Satoshi Ogawa, Shigetaka Akutsu, Shun-Ichi Inagaki, and Yasushi Abiko (1994) "Newly discovered photodegradation products of nifedipine in hospital prescriptions" *J. Pharm. Sci.* **83** 532–538.

Higuchi, W. I., P. K. Lau, T. Higuchi, and J. W. Shell (1963) "Polymorphism and drug availability. Solubility relations in the methylprednisolone system" *J. Pharm. Sci.* **52** 150-153.

International Tables for Crystallography (1987) Theo Hahn, Ed.; International Union of Crystallography; D. Reidel: Boston, MA, USA.

James, Ruby H., Paul D. Sternglanz, and Y. Fulmer Shealy (1969) "5(or 4)-[3, 3-Bis(2-chloroethyl)-1-triazeno]imidazole-4(or 5)-carboxamide: a titrametric determination of its υ-triazolinium transformation product and studies of its stability" *J. Pharm. Sci.* **58** 1193–1195.

Kaneniwa, Nobuyoshi and Makoto Otsuka (1985) "Effects of grinding on the transformation of polymorphs of chloramphenicol palmitate" *Chem. Pharm. Bull.* **33** 1660–1668.

Kanzawa, Tokunosuke and Saburo Kotaku (1953) "Stability of Vitamin D" *J. Pharm. Soc. Japan* **73** 1357-1360.

Kimura, Takeshi and Shuzo Hashimoto (1960) "Amorphous chloramphenicol palmitate" Japan Patent 5798, Sankyo Co., Ltd., May 25, 1960, *Chem. Abstr.* **55** 5878f.

Kitaigorodskii, A. I. (1961) *Organic Chemical Crystallography*, Consultants Bureau: New York, NY.

Kitaigorodskii, A. I., Yu. V. Mnyukh, and Yu. G. Asadov (1965) "Relations for single-crystal growth during polymorphic transformation" *J. Phys. Chem. Solids* **26** 463–472.

Kitamura, Satoshi, Akira Miyamae, Shigetaka Koda, and Yukiyoshi Morimoto (1989) "Effect of grinding on the solid-state stability of cefixime trihydrate" *Int. J. Pharm.* **56** 125–134.

Kuhnert-Brandstätter, M. (1971) *Thermomicroscopy in the Analysis of Pharmaceuticals*; Pergamon: New York, NY.

Leeson, Lewis J. and Albert M. Mattocks (1958) "Decomposition of aspirin in the solid state" *J. Am. Pharm. Assoc. Sci. Ed.* **67** 329–333.

Lieser, Karl H. (1969) "Steps in precipitation reactions" *Angew. Chem., Int. Engl.* **8** 188–202.

Lin, Chung-Tang, Pik-Yen Siew, and Stephen R. Byrn (1978) "Solid-state dehydrochlorination and decarboxylation reactions. I. Reactions of *p*-aminosalicylic acid hydrochloride and *p*-aminosalicylic acid, revised crystal structure of *p*-aminosalicylic acid" *J. Chem. Soc. Perkin Trans. 2* **1978** 975–962.

Lin, Chung-Tang, Phillipe Perrier, Gail Gibson Clay, Paul A. Sutton, and Stephen R. Byrn (1982) "Solid-state photooxidation of 21-cortisol *tert*-butylacetate to 21-cortisone *tert*-butylacetate" *J. Org. Chem.* **47** 2978–2981.

Matsuda, Yoshihisa and Etsuko Tatsumi (1990) "Physiochemical characterization of furosemide modifications" *Int. J. Pharm.* **60** 11-26.

Miller, L. G. and J. H. Fincher (1971) "Influence of drug particle size after intramuscular dosage of phenobarbital to dogs" *J. Pharm. Sci.* **60** 1733–1736.

Morawetz, H. (1966) "Reactivity of organic crystals" *Science* **152** 705–711.

Mullins, John D. and Thomas J. Macek (1960) "Some pharmaceutical properties of novobiocin" *J. Am. Pharm. Assoc., Sci. Ed.* **49** 245–248.

Osawa, Takashi, Madhav S. Kamat, and Patrick P. DeLuca (1988) "Hygroscopicity of cefazolin sodium: application to evaluate the crystallinity of freezer-dried products" *Pharm. Res.* **7** 421–425.

Ostwald, W. (1896) "Studies concerning the formation and transformation of solid bodies. I. Discussion: supersaturation and supercooling" *Z. Phys. Chem., Stoechiom. Verwandtschaftsl.* **22** 289–330.

Otsuka, Makoto, Takahiro Matsumoto, and Nobuyoshi Kaneniwa (1989) "Effects of the mechanical energy of multi-tableting compression on the polymorphic transformations of chlorpropamide" *J. Pharm. Pharmacol.* **41** 665–669.

Otsuka, Makoto and Nobuyoshi Kaneniwa (1990) "Effect of grinding on the crystallinity and chemical stability in the solid state of cephalothin sodium" *Int. J. Pharm.* **62** 65–73.

Panunto, Thomas W., Zofia Urbańczyk-Lipkowska, Ruth Johnson, and Margaret C. Etter (1987) "Hydrogen-bond formation in nitroanilines: the first step in designing acentric materials" *J. Am. Chem. Soc.* **109** 7786–7797.

Paul, Iain C. and David Y. Curtin (1973) "Thermally induced organic reactions in the solid state" *Acc. Chem. Res.* **6** 217–225.

Pfeiffer, Ralph R. (1988) Personal communication.

Pikal, M. J., A. L. Lukes, and J. E. Lang (1977) "Thermal decomposition of amorphous β-lactam antibacterials" *J. Pharm. Sci.* **66** 1312–1316.

Pikal, Michael J. and Karen M. Dellerman (1989) "Stability testing of pharmaceuticals by high-sensitivity isothermal calorimetry at 25 °C: cephalosporins in the solid and aqueous solution states" *Int. J. Pharm.* **50** 233–52.

Pikal, Michael J. (1990) "Freeze-drying of proteins. Part I: process design" *BioPharm.* **3** 18–28.

Ressler, Charlotte (1972) "Solid-state dehydrogenation of L-1,4-cyclohexadiene-1-alanine hydrate to L-phenylalanine" *J. Org. Chem.* **37** 2933–2936.

Reutzel, Susan M. and Margaret C. Etter (1992) "Evaluation of the conformational, hydrogen bonding, and crystal packing preferences of acyclic imides" *J. Phys. Org. Chem.* **5** 44–54.

Rubin, S. H., E. DeRitter, and J. B. Johnson (1976) "Stability of vitamin C (ascorbic acid) in tablets" *J. Pharm. Sci.* **65** 963–968.

Schmidt, Rainer and Erich Hecker (1975) "Autooxidation of phorbol esters under normal storage conditions" *Cancer Res.* **35** 1375–1377.

Shefter, Eli and Takeru Higuchi (1963) "Dissolution behavior of crystalline solvated and nonsolvated forms of pharmaceuticals" *J. Pharm. Sci.* **52** 781-791.

Simmons, D. L., H. S. L. Woo, C. M. Koorengevel, and P. Seers (1966) "Quantitative determination by thin-layer chromatography of anhydrous tetracycline in degraded tetracycline tablets" *J. Pharm. Sci.* **55** 1313–1315.

Sluyterman, L. A. Æ. and H. J. Veenendaal, (1952) "Reactions of polypeptide esters in the solid state. I. Migration of methyl groups" *Recl. Trav. Chim. Pays-Bas.* **71** 137–152.

Takahashi, Yoshiteru, Kazuko Nakashima, Toshihiro Ishihara, Hiroshi Nakagawa, and Isao Sugimoto (1985) "Polymorphism of fostedil: characterization and polymorphic change by mechanical treatments" *Drug. Dev. Ind. Pharm.* **11** 1543–1563.

Zografi, George, R. Gary Hollenbeck, Sharon M. Laughlin, Michael J. Pikal, Joseph P. Schwartz, and Lynn Van Campen (1991) "Report of the advisory panel on moisture specifications" *Pharmacopeial Forum* **17** 1459–1474.

3

The X-Ray Powder Diffraction Method

X-Ray powder diffraction, like the single crystal method discussed in the previous section, is an effective method of distinguishing solid phases having different internal structure. The X-ray powder method is experimentally simple and does not require large single crystals, but instead can readily be applied to any powdered sample. While the powder method is much simpler, it gives data about only a relatively few *hkl* planes of a substance, *i.e.*, only the most strongly diffracting planes. Nevertheless, this information is quite adequate to distinguish among any solid phases present.

3.1 Instruments for Powder Diffraction Measurements

Instruments used in the X-ray powder diffraction method fall into two categories: diffractometers and cameras. Figure 3.1 shows a schematic drawing of a modern powder diffractometer and Figure 3.2 shows a photograph of a powder X-ray camera. All instrumentation for X-ray powder diffraction yields the same information about the diffraction characteristics of the sample, namely the intensities of the maxima and the angles at which they occur. The raw data are recorded either on film (which takes about

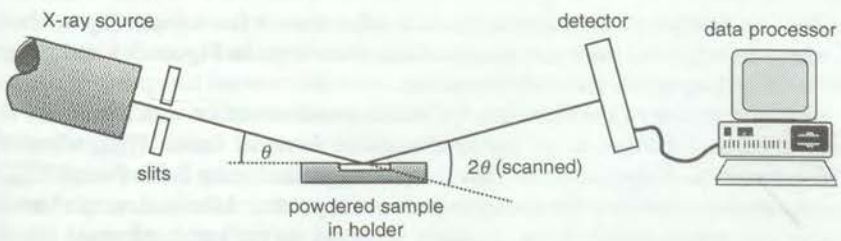

Figure 3.1 Schematic drawing of a modern 2θ powder X-ray diffractometer

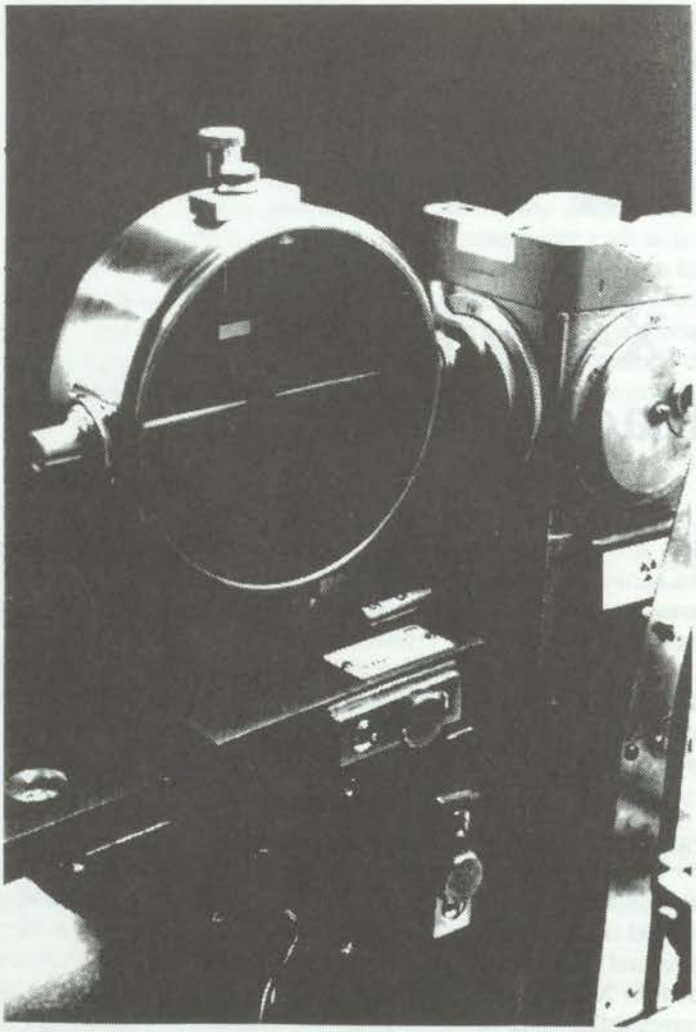

Figure 3.2 A Debye-Scherrer powder camera.

two hours) or on a plotter or strip chart (which takes from a few minutes up to about a half hour). Examples of these data presentations are shown in Figure 3.3 and either is suitable for making direct visual comparisons.

Further treatment of the film data, by visual measurement or with automated densitometer, reduces the data to the universal standard form: d verses I/I_{max} where d is the "d-spacing" (in Ångstroms) obtained from Bragg's law ($n\lambda = 2d\sin\theta$) and I/I_{max} is the peak intensity relative to the strongest peak in the pattern. Likewise, strip chart data is readily converted, usually by a computer program, to the same universal standard form. Modern instruments with computerized data handling features can express the data in any desired format.

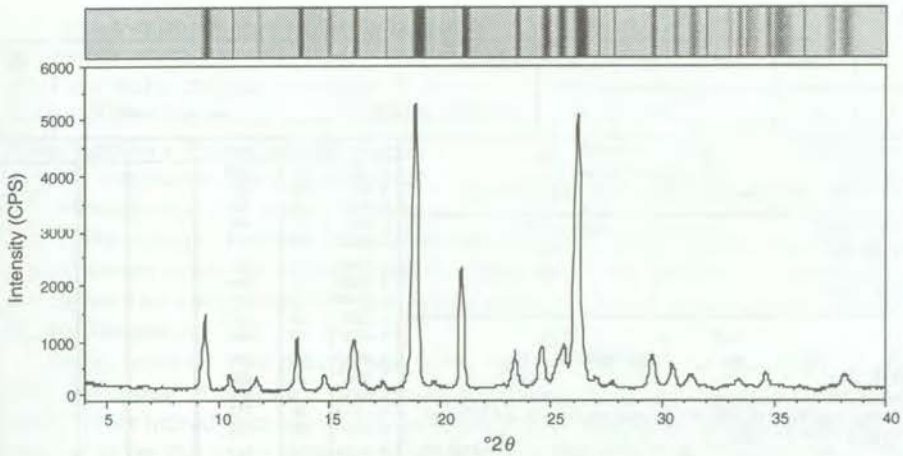

Figure 3.3 Two forms of powder diffractogram data presentation for the same material. The top bar represents the film diffractogram obtained by a powder camera and corresponds to the diffractogram below it obtained by a computer controlled diffractometer.

3.2 Powder Diffraction Using Synchrotron Radiation

In recent years, major advances have been made in applying synchrotron X-radiation to powder diffraction problems. The high intensity and nearly monochromatic radiation obtained from a synchrotron allow measurement of high resolution diffraction patterns. In favorable cases, synchrotron radiation has been used to obtain enough diffraction data to solve crystal structures of small organic molecules including cimetidine (Cernik *et al.*, 1991) and 6,13-dichlorotriphendioxazine (Fagan *et al.*, 1995). In the future, high speed computers and better computational methods are expected to allow more complicated structures to be determined. Even in cases where the structure cannot be determined, synchrotron powder diffraction allows accurate determination of the unit cell parameters and space group. This information is especially important for detecting extraneous phases.

3.3 The Hanawalt System

Hanawalt *et al.* (1938) devised a system for cataloging the X-ray powder data for any substance. The system requires the data to be in the universal standard form: d versus $I/I_{max.}$ In this form, wavelength and instrument constants are eliminated, and therefore data can be compared between laboratories that may be using different conditions.

A central file is maintained by the ICDD (International Centre for Diffraction Data, 1998) [formerly called the Joint Commission on Powder Diffraction Specifications (JCPDS)] in printed and electronically retrievable forms. Updates are made available periodically and, of course, the system is suited to customized additions by any user.

An example of the file data for a typical entry is given in Figure 3.4 All diffraction peaks for the compound are listed in decreasing order of d value along with the corresponding relative intensity. Other useful crystallographic data, including optical data, are also included when available.

10-310

d	2.49	2.92	1.46	2.92
I/I_0	100	60	45	60

$MnAl_2O_4$ ★

MANGANESE ALUMINATE (GALAXITE)

Rad. $CuK\alpha_1$ λ 1.5405 Filter Ni
Cut off I/I_0 DIFFRACTOMETER
Ref. NAT. BUR. STANDARDS (U.S.) CIRC. 539 9 (1959)

Sys. CUBIC S.G. O7,H - FD3M (227)
a_0 8.258 b_0 c_0 A C
α β γ Z 8 D_x 4.077
Ref. IBID.

εα nωβ εγ Sign
2V D mp Color BROWN
Ref. IBID.

SAMPLE PREPARED BY NBS BY HEATING $MnCO_3$ AND $Al(OH)_3$ TO 1300°C. FOR 24 HOURS.
SPECT. ANAL. SHOWED:< 1.0% Co, NA;< 0.1% SI;< 0.01% CR, Cu, FE, MG.
SPINEL-TYPE STRUCTURE.
PATERN MADE AT 25°C

d Å	I/I_0	hkl	d Å	I/I_0	hkl
2.921	60	220			
2.492	100	311			
2.383	10	222			
2.065	25	400			
1.6862	20	422			
1.5896	40	511			
1.4600	45	440			
1.3060	8	620			
1.2596	12	533			
1.1037	10	642			
1.0749	25	731			
1.0322	14	800			
0.9732	8	822			
0.9534	20	751			
0.8656	16	931			
0.8429	30	844			
0.8097	12	10.2.0			
0.7983	18	951			

10-310 JCPDS-ICDD Copyright (c) 1989 Quality: i DELETED

MnAl O
2 4

Manganese Aluminum Oxide

Galaxite, syn

Rad: Cu Lambda: 1.54056 Filter: d-sp:
Cutoff: Int: I/Icor:
Ref: See comments box for primary powder pattern reference.

Sys: Cubic S.G.: Fd3m (227)
a: 8.258 b: c: A: C:
A: B: C: Z: 8 mp:
Ref: Ibid.

Dx: 4.08 Dm: SS/FOM: F18=12(.045,33)

ea: nwB: ey: Sign: 2v:
Ref:

PSC: cF56. Deleted by 29-880. INVALID reference: For original reference see PDF card set prior to 1980.. Mwt: 172.90. Volume(CD): 563.15.

d A	Int.	h k l
2.921	60	2 2 0
2.492	100	3 1 1
2.383	10	2 2 2
2.065	25	4 0 0
1.6862	20	4 2 2
1.5896	40	5 1 1
1.4600	45	4 4 0
1.3060	8	6 2 0
1.2596	12	5 3 3
1.1037	10	6 4 2
1.0749	25	7 3 1
1.0322	14	8 0 0
0.9732	8	6 6 0
0.9534	20	7 5 1
0.8656	16	9 3 1
0.8429	30	8 4 4
0.8097	12	10 2 0
0.7983	18	9 5 1

Figure 3.4 Examples of powder diffraction data from the Powder Diffraction File (PDF): (top) a card entry and (bottom) an entry from the CD-ROM (International Centre for Diffraction Data, 1998).

Note that retrieval is based on the *d* values of the four most intense peaks (boxes at upper left). While this system is generally adequate for retrieving close matches, some flexibility in applying it does need to be exercised in view of the possible unknown effects of **preferred orientation** on the intensities (see Sect. 3.4). A group of, say, three or four close matches can then usually be reduced or eliminated on the basis of other available information.

3.4 Comparing X-Ray Powder Data

The most useful method to compare X-ray powder diffraction data obtained from different samples and on the same instrumentation is to overlay and align the respective films or plots. When plots are available, a tracing of each previously characterized form on transparent film is very helpful. The ensuing comparisons of peak positions and intensities may fall anywhere between complete agreement to complete disagreement of the patterns. In either of these extreme cases, the respective conclusions are, of course, unequivocal: the structures are the same or they are different. An alternative method involves comparing 2θ values versus intensities of the various forms and noting any differences.

Often, however, two patterns may show many differences but also have several peaks that appear to coincide. A judgment must be made as to whether the coincident peaks: 1) are indeed, just a few coincidences and the samples do have different structures; or 2) are due to the presence of a common component implying the sample is a mixture of structures. The patterns of highly unequal mixtures will contain only the stronger peaks of the minor component at greatly reduced intensity, but all of the peaks of the major component. With experience, the pattern recognition capabilities of the human mind will play an important role in these comparisons.

Let us turn to some factors that affect the quality of the X-ray powder diffraction data, (*i.e.*, factors that affect the accuracy of peak locations and intensities). Most errors in peak locations are usually minor and arise from either film shrinkage in the camera method or sample misalignment in the diffractometer method. In both situations, these errors can be detected and corrected by mixing an internal standard with the powder.

The observed intensities of one or more peaks, however, can vary considerably among different samples of the same substance. This variability is most often the result of preferred orientation of the crystals that comprise the powder. For an individual single crystal, a given *hkl* plane gives a single diffraction spot when the crystal is at a fixed orientation to the X-ray beam and detector. A powder, containing many crystals randomly oriented with respect to the X-ray beam and detector, produces a uniform cone of diffracted radiation for each *hkl* plane. This uniform cone results in a uniform intensity measurement regardless of the geometry of the diffraction equipment. Preferred orientation is most likely to arise when the powder consists of needle-like or plate-like crystals (*i.e.*, shapes that are prone to align in a non-random or *preferred orientation*). For example, if several handful of soda straws are thrown into a shoe box, the straws will mostly align parallel to each other. Similarly, scatter a deck of cards on a table and all of the cards lay flat on the table. For needle- and plate-like crystals, the preferred orientation effects can be minimized by reducing the size of the crystals (usually by grinding) before the sample is placed onto the sample holder. However, care must be taken to guard against grinding to an extent that phase transitions to other crystal forms or an amorphous form are induced. Where amorphous material is produced, the incoherent scattered radiation from the amorphous fraction of the sample adds to the general background of the powder pattern (a diffuse halo on films, a broad hump of higher background scatter on diffractometer tracings). Therefore, when the pattern of a substance is found to gradually become weaker as the material is milled or ground, it may be taken as strong evidence that the structure is being destroyed by the process. If these changes occur, serious consideration must be given to how particle-size reduction

is achieved. In addition, observations of this kind are useful indications of what kind of solid-state changes might occur during processing of the drug product.

Another situation in which fixed peaks may vary in intensity arises when a solvated crystal loses solvent but does not lose its crystal structure. (See Chapter 16 on Solvates and Desolvated Crystals.) In this case, the loss of solvent may affect the intensity of certain planes more than others. It is therefore good practice to obtain reference patterns of solvated crystals using powders damp with the appropriate solvent. The effect of solvent loss on peak intensities will then be easier to interpret.

3.5 Variable Temperature and Atmosphere Studies

Modern diffractometers can be fitted with an environmental chamber that allows control of the atmosphere as well as the temperature. This method has been quite useful in the study of interconversions of crystal forms under different conditions as well as for the study of desolvations and other processes. If changes in the X-ray powder diffraction pattern are observed upon heating, additional studies are needed to determine whether desolvation, degradation, or a polymorphic transformation is occurring. The method is also useful in conjunction with **differential scanning calorimetry** (DSC) and other thermal methods (see Chapter 5).

3.6 Quantitative Analysis of Mixtures

X-Ray powder diffraction has also been used to quantify the percentages of a crystal form in a mixture of forms. Quantification usually requires extensive calibration using known mixtures of the two components, but the effort can provide a powerful method for pharmaceutical analysis and assurance of a consistant product.

Matsuda) *et al.* (1984) have shown that X-ray powder diffraction can be used to analyze mixtures of α- with δ- and β- with δ-phenylbutazone as shown in Figures 3.5 and 3.6. In these cases, Matsuda and co-workers made known mixtures of α- with δ- and β- with δ-phenylbutazone and obtained the powder diffraction patterns shown in Figure 3.5. Figure 3.6 shows the calibration curves obtained by taking the intensity ratios of the peaks indicated by the arrows in Figure 3.5. They were able to use these calibration curves to determine the rate of interconversion of α- to δ- and β- to δ-phenylbutazone. It is important to note that some calibration curves are nearly horizontal, meaning that large errors can result. However, in other cases, the calibration curves have a relatively large slope and can give more accurate results. Because the intensity ratio of the α–δ mixture at 6.6° and 7.1° approached infinity at low concentrations, the reciprocal ratio was also used to establish the calibration curve. Thus for the α–δ mixtures, Figure 3.6 shows two curves (diamonds and filled circles) for the peaks at 6.6° and 7.1° where the lower portions of the curves (bolded) were used for the calibration.

Suryanarayanan (1989) has used powder diffraction extensively to study the different polymorphs and hydrates of carbamazepine determining the relative amounts of α- and β-carbamazepine in mixtures. In this case, the integrated intensities of the 10.1 Å line (unique to α-carbamazepine) in the mixtures were measured. Plots of the integrated intensity of this line versus the weight fraction of the α form gave a good straight-line calibration curve with coefficients of variation of up to 10% and a mini-

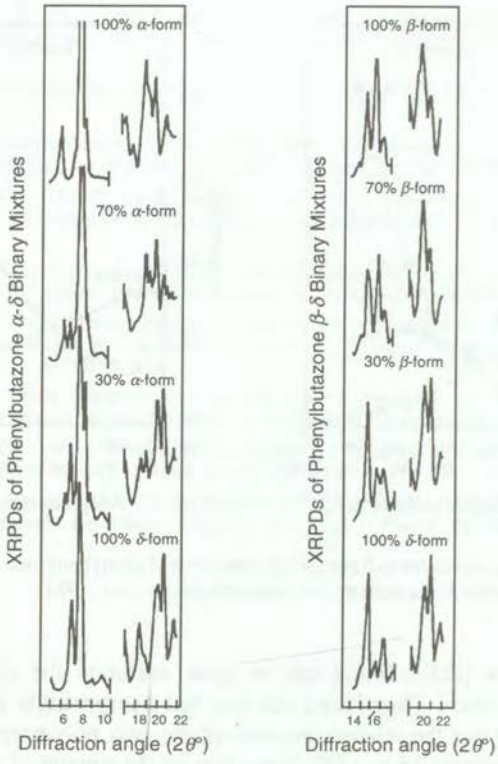

Figure 3.5 X-Ray diffraction patterns of α- mixed with δ-phenylbutazone and β- mixed with δ-phenylbutazone binary mixtures in various ratios (Matsuda) *et al.*, 1984).

mum detectable limit of less than 5%. Furthermore, Suryanarayanan stated that preferred orientation can have a major effect on quantification of powder mixtures and that it is thus important to grind the samples in quantitative studies.

Suryanarayanan (1990) also used powder diffraction to determine the ratios of anhydrous carbamazepine and carbamazepine dihydrate in mixtures. In these studies he measured the ratios between the 6.78 and 9.93 Å lines. The 6.78 Å line was used to analyze for anhydrous carbamazepine and the 9.93 Å line to analyze for carbamazepine dihydrate. Interestingly, he found that if he analyzed loosely packed powders, a rather large coefficient of variation resulted. When he compressed the samples, the coefficients of variation were greatly reduced.

Suryanarayanan and Herman (1991) also used powder diffraction to quantify the amount and form of carbamazepine in tablets that also contained microcrystalline cellulose, starch, and stearic acid. In this study, the tablets were ground in a **ball mill** and the powder was mixed with LiF (as an internal standard) in a 20% w/w mixture. These studies allowed the determination of the carbamazepine content of unknown tablets with a coefficient of variation of between 0.28–2.1%. This study was very successful in part because carbamazepine was the major ingredient in the tablet.

Recently, profile-fitting approaches, rather than single-line measurement, have been used to quantitate X-ray powder diffraction (Tanninen and Yliruusi, 1992). These

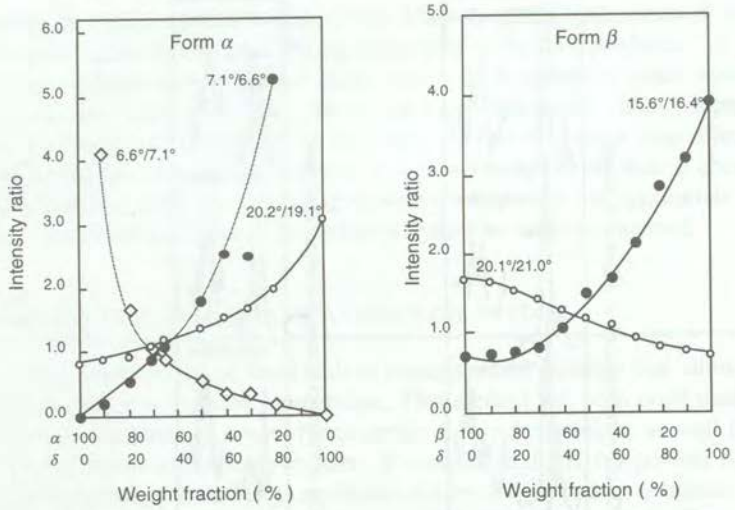

Figure 3.6 Calibration curves for α-δ phenylbutazone and β-δ phenylbutazone binary mixtures using intensity ratios at the indicate 2θ values (Matsuda) *et al.*, 1984).

workers showed that profile-fitting can be quite useful in the study of α- and δ-prazosin hydrochlorideα-. They found that they had a surprisingly good detection sensitivity of 0.5% and that the relative amounts of the two polymorphs could be determined with an accuracy of 0.5 to 1.0% depending on the amount of peak overlap. The use of peak-profile fitting, which has also been used to quantitate mixtures by FT-IR spectroscopy, appears to have significant potential for improving the accuracy of X-ray powder diffraction analysis of mixtures.

Mixtures of crystalline and amorphous materials have also been studied using powder diffraction. In early studies, Pikal *et al.* (1977) determined the percentages of amorphous and crystalline forms in antibiotics but found the errors using this procedure were large. Ryan (1986) has shown that X-ray powder diffraction can be used to determine the crystallinity of imipenem:cilastatin sodium mixtures using the peak intensity of the crystalline component. Crocker and McCauley (1995) measured the X-ray diffraction intensity of amorphous imipenem at a diffraction angle where crystalline imipenem peaks did not occur.

REFERENCES

Cernik, R. J., A. K. Cheetham, C. K. Prout, D. J. Watkin, A. P. Wilkinson, and B. T. M. Willis (1991) "The structure of cimetidine ($C_{10}H_{16}N_6S$) solved from synchrotron-radiation X-ray-powder diffraction data" *J. Appl. Crystallogr.* **24** 222–224.

Crocker, Louis S. and James A. McCauley (1995) "Comparison of the crystallinity of imipenem samples by X-ray diffraction of amorphous material, *J. Pharm. Sci.*, **84**, 226–227.

Fagan, Paul G., Robert B. Hammond, Kevin J. Roberts, Robert Docherty, Alan P. Chorlton, William Jones, and Graham D. Potts (1995) "An *ab initio* approach to crystal structure determination using high-resolution powder diffraction and computational chemistry techniques: application to 6,13-dichlorotriphendioxazine" *Chem. Mater.* **7** 2322-2326.

Hanawalt, J. D., H. W. Rinn, and L. K. Frevel (1938) "Chemical analysis by X-ray diffraction—classification and use of X-ray diffraction patterns" *Ind. Eng. Chem., Anal. Ed.* **10**, 457–512.

International Centre for Diffraction Data (1998) 12 Campus Boulevard, Newtown Square, PA 19073-3273 USA.

Matsuda, Yoshihisa, Etsuko Tatsumi, Etsuko Chiba, and Yukie Miwa (1984) "Kinetic study of the polymorphic transformations of phenylbutazone" *J. Pharm. Sci.* **73**, 1453–1460.

Pikal, M. J., A. L. Lukes, John E. Lang, and K. Gaines (1977) "Quantitative crystallinity determinations for β-lactam antibiotics by solution calorimetry: correlations with stability" *J. Pharm. Sci.* **67**, 767–773.

Ryan, James Arthur (1986) "Compressed pellet X-ray diffraction monitoring for optimization of crystallinity in lyophilized solids: imipenem:cilastatin sodium case" *J. Pharm. Sci.* **75**, 805–807.

Suryanarayanan, Raj (1989) "Determination of the relative amounts of anhydrous carbamazepine ($C_{15}H_{12}N_2O$) and carbamazepine dihydrate ($C_{15}H_{12}N_2O{\cdot}2H_2O$) in a mixture by powder X-ray diffractometry" *Pharm. Res.* **6**, 1017–1024.

Suryanarayanan, Raj (1990) "Determination of the relative amounts of α-carbamazepine and β-carbamazepine in a mixture by powder X-ray diffractometry" *Powder Diffr.* **5**, 155–159.

Suryanarayanan, Raj, and Craig S. Herman (1991) "Quantitative analysis of the active tablet ingredient by powder X-ray diffractometry" *Pharm. Res.* **8**, 393–399.

Tanninen, V. P. and J. Yliruusi (1992) "X-ray powder diffraction profile fitting in quantitative determination of two polymorphs from their powder mixture" *Int. J. Pharm.* **81**, 169–177.

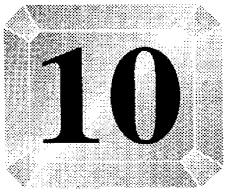

Polymorphs

As discussed in Chapter 1, polymorphs exist when two crystals have the same chemical composition but different internal structure, including different unit cell dimensions and different crystal packing. Compounds that crystallize as polymorphs can show a wide range of different physical and chemical properties, including different melting points and spectral properties. Polymorphs can also differ in their solubility, density, hardness, and crystal shape. While some compounds may exist in only two polymorphs, others may exist in many polymorphs (*e.g.*, progesterone has five polymorphs and water has nine polymorphs). Control of polymorphism is particularly important for pharmaceuticals where changing the polymorph can alter the bulk properties, dissolution rate, bioavailability, chemical stability, or physical stability of a drug. The clearest indication of the existence of polymorphs comes from the X-ray crystallographic examination of single crystals of the various samples that are known to have the same composition. Often, however, X-ray powder diffraction is sufficient to establish the existence of polymorphs.

There is, unfortunately, no standard numbering system for polymorphs. In the literature, the various polymorphs have been designated by Roman numerals (preceded by the word "Form," *e.g.*, Form I), Greek letters (with the suffix "-form," *e.g.*, α-form), or in some cases, capital letters (similar to the Roman numeral system). To add to the confusion, some of numbering schemes of polymorphs also include solvates (*e.g.*, the α- and γ-forms of indomethacin are anhydrates, yet the β-form is the benzene solvate). Furthermore, some polymorphs have been identified only by their crystallographic classification (*e.g.*, the two polymorphs of (±)-β-promedol are designated the monoclinic form and the rhombohedral form). It has been suggested that polymorphs be numbered consecutively in the order of their stability at room temperature or by their melting point. This of course would lead to confusion upon the discovery of a new polymorph having intermediate stability or melting point and thus requiring renumbering of the existing polymorph system. It has also been suggested that polymorphs be numbered consecutively in the order of discovery, but this requires knowledge of their history and a timely access to that information. Whatever the numbering system, it is imperative that it be consistent. Thus, when a new polymorph is discovered and characterized, the designation of the new polymorph should be the next increment in the

previous system. However, this is not always practical when more than one laboratory is involved in the development process at the same time.

10.1 CLASSIC EXAMPLES OF POLYMORPHISM

This section summarizes several classic examples of polymorphism which have appeared in the chemical literature.

A. 4-CHLOROPHENOL

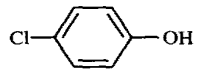

4-chlorophenol

The crystal structure of both the thermodynamically stable (α) and unstable (β) forms of 4-chlorophenol have been determined (Perrin and Michel, 1973a–b). Both forms belong to the same space group ($P2_1/c$); they both have the same number of molecules per unit cell ($Z = 8$) and nearly identical densities, yet they have different cell parameters (see Table 10.1). The crystal structure of the β-form projected on the (100) plane is shown in Figure 10.1. The packing consists of tetramers of molecules connected by hydrogen bonding. The crystal packing of the α-form (shown in Figure 10.2) also consists of tetramers connected by hydrogen bonds, but the arrangement of the rings is slightly different than that of the β-form. Although the β-form converts to the α-form, no detailed studies of this transformation have been reported.

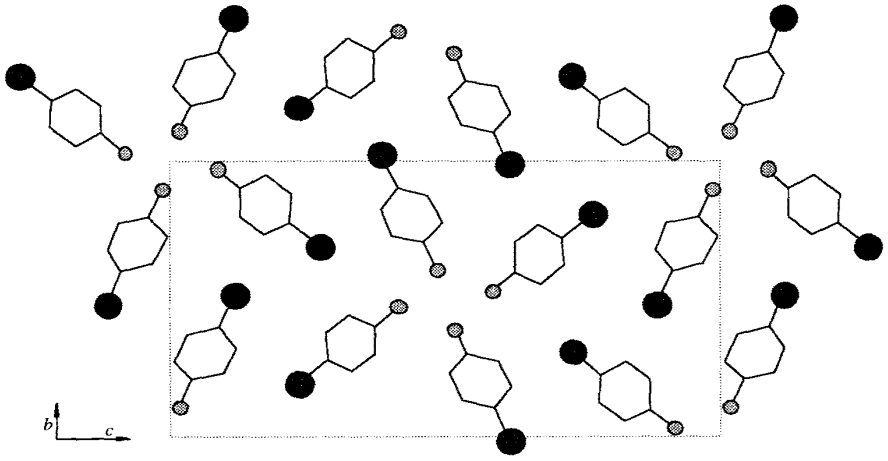

Figure 10.1 Projection of the crystal structure of the β-form of 4-chlorophenol (● chlorine atom, ◎ hydroxyl group) (Perrin and Michel, 1973b).

Table 10.1 Crystallograp
4-Chlorophen

Parameter	α-
Space Group	
a (Å)	
b (Å)	
c (Å)	
β	9
Z	
ρ_{calc} (g cm^{-3})	
V (Å^3)	122

a Perrin and Michel, 1973a.

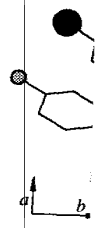

Figure 10.2 Projection of t
◎ hydroxyl gr

B. DIBENZ[*a*,*h*]ANTHRA

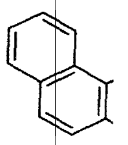

In an early study of polyr
[*a*,*h*]anthracene (1,2:5,6-
1947; 1956). Although th
groups (Table 10.2) and

Table 10.1 Crystallographic Parameters for Two 4-Chlorophenol Polymorphs

Parameter	α-Form[a]	β-Form[b]
Space Group	$P2_1/c$	$P2_1/c$
a (Å)	8.84	4.14
b (Å)	15.726	12.85
c (Å)	8.790	23.20
β	92.61°	93.00°
Z	8	8
ρ_{calc} (g cm^{-3})	1.40	1.38
V (Å^3)	1220.7	1232.5

a Perrin and Michel, 1973a. *b* Perrin and Michel, 1973b.

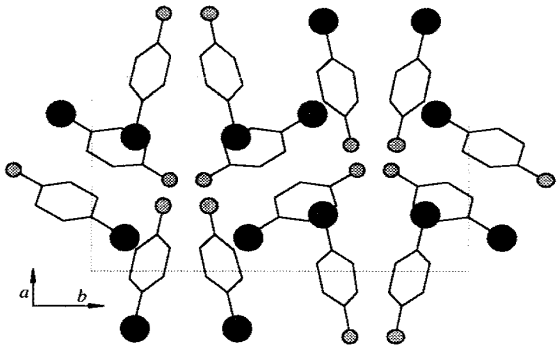

Figure 10.2 Projection of the crystal structure of the α-form of 4-chlorophenol (● chlorine atom, ◍ hydroxyl group) (Perrin and Michel, 1973a).

B. Dibenz[*a*,*h*]anthracene

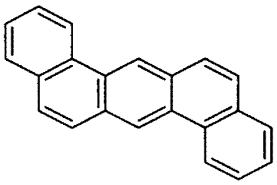

dibenz[*a*,*h*]anthracene
(1,2:5,6-dibenzanthracene)

In an early study of polymorphism, the crystal structures of Forms I and II of dibenz-[*a*,*h*]anthracene (1,2:5,6-dibenzanthracene) were determined (Robertson and White, 1947; 1956). Although the forms have the same density, they belong to different space groups (Table 10.2) and have quite different packing. The crystal packing of Form I

(orthorhombic form) is shown in Figure 10.3 and the crystal packing of Form II (monoclinic form) is shown in Figure 10.4.

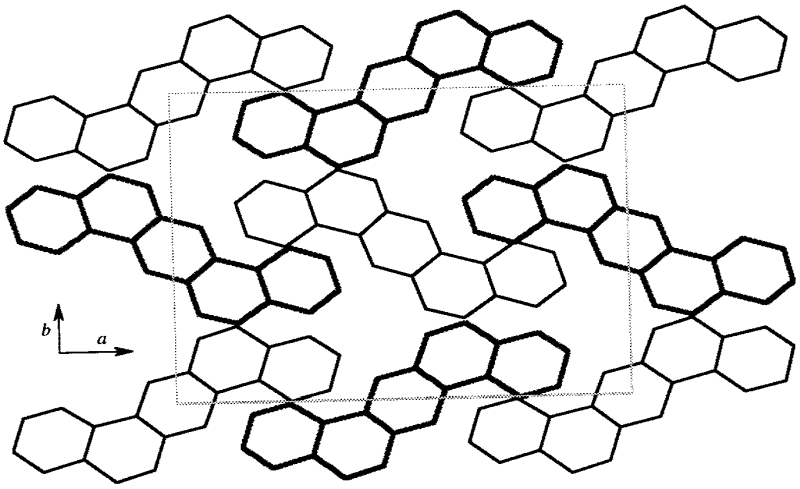

Figure 10.3 Crystal packing of Form I (orthorhombic form) of dibenz[*a*,*h*]anthracene (Robertson and White, 1947).

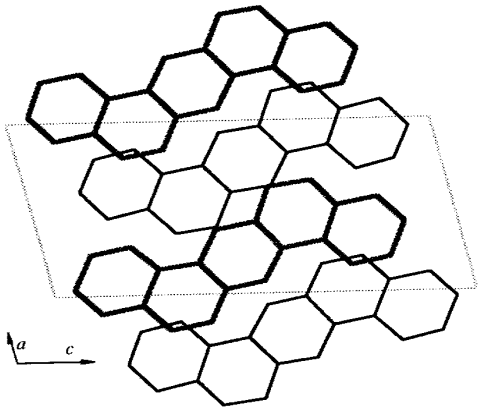

Figure 10.4 Crystal packing drawing of Form II (monoclinic form) of dibenz[*a*,*h*]anthracene (Robertson and White, 1956).

Table 10.2 Crystallographic
Dibenz[*a*,*h*]anthra

Parameter	Fo
Space group	
a (Å)	
b (Å)	1
c (Å)	1
β	9
Z	
ρ_{calc} (g cm^{-3})	
V (Å^3)	141
V/molecule	35

Robertson and White, 1947; R

C. Acridine

Acridine crystallizes in fi
Schmidt, 1955). The crys
and are shown in Figures
forms appear to be quite si

Table 10.3 Crystal Parameter

Parameter	α-For
Space group	$P2_1/c$
a (Å)	16.18
b (Å)	18.88
c (Å)	6.08
β	95.67°
Z	8
ρ_{calc} (g cm^{-3})	1.27
V (Å^3)	1848.2
V/*Z* (Å^3)	231.0
Habit	Needle

Herbstein and Schmidt, 1955

Table 10.2 Crystallographic Parameters for Two Dibenz[*a*,*h*]anthracene Polymorphs

Parameter	Form I	Form II
Space group	*Pcab*	$P2_1$
a (Å)	8.22	6.59
b (Å)	11.39	7.84
c (Å)	15.14	14.17
β	90.0°	103.5°
Z	4	2
ρ_{calc} (g cm^{-3})	1.29	1.29
V (Å^3)	1417.5	711.9
V/molecule	354.4	355.9

Robertson and White, 1947; Robertson and White, 1956.

C. Acridine

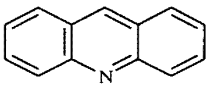

acridine

Acridine crystallizes in five polymorphs as shown in Table 10.3 (Herbstein and Schmidt, 1955). The crystal structures of the α- and γ-forms have been determined and are shown in Figures 10.5 and 10.6, respectively. The crystal packing of these forms appear to be quite similar although the cell parameters are obviously different.

Table 10.3 Crystal Parameters of the Various Polymorphs of Acridine

Parameter	α-Form	β-Form	γ-Form	δ-Form	ε-Form
Space group	$P2_1/a$	*Aa*	*Pnab*	$P2_12_12_1$	$P2_1/n$
a (Å)	16.18	16.37	17.45	15.61	11.37
b (Å)	18.88	5.95	8.89	6.22	5.98
c (Å)	6.08	30.01	26.37	29.34	13.64
β	95.67°	141.33°	90.00°	90.00°	98.67°
Z	8	8	16	12	4
ρ_{calc} (g cm^{-3})	1.27	1.29	1.15	1.24	1.29
V (Å^3)	1848.2	1826.3	4090.8	2848.7	918.2
V/*Z* (Å^3)	231.0	228.3	255.7	237.4	229.5
Habit	Needles	Plates	Laths	Laths	Prisms

Herbstein and Schmidt, 1955

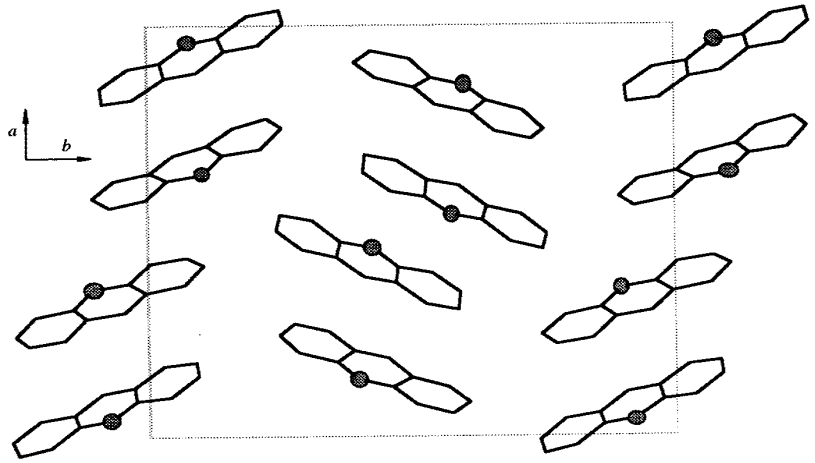

Figure 10.5 Crystal packing of acridine α-form with ● representing the nitrogen atom of the acridine ring (Phillips, 1956).

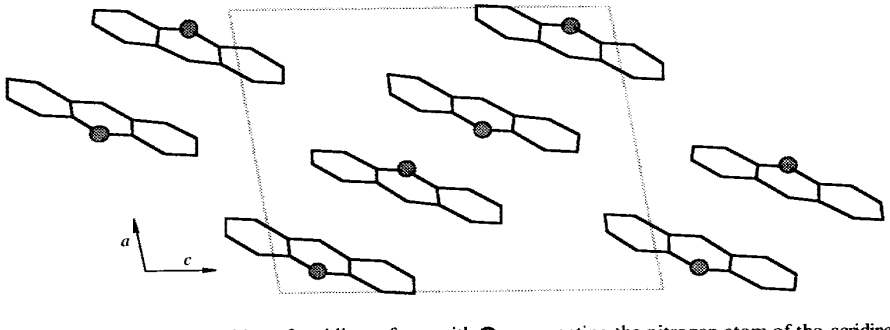

Figure 10.6 Crystal packing of acridine γ-form with ● representing the nitrogen atom of the acridine ring (Phillips *et al.*, 1960).

10.2 Conformational and Configurational Polymorphism

In this section, two special types of polymorphism will be discussed. *Conformational polymorphism* occurs when a molecule adopts a significantly different conformation in different crystal polymorphs (Bernstein, 1987). (The term "significantly different" is open to interpretation.) This term does not adequately describe cases where different types of isomers crystallize in different forms. Thus an additional term—*configurational polymorphism*—is defined. Configurational polymorphism exists when different

configurations (*i.e.*, *cis*,
forms.

Crystallization of *ci*
occurs whenever the pu
forms in separate crystal
The crystallization of equ
cantly more interest. W
phism can be used to is
crystalline form.

A. Tri-α-Naphthylb

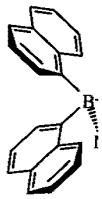

tri-α-naphth
For

Brown and Sujishi (1948
with the following observ

1. Two crystalli
2. The metastab
   room tempera
3. The dissociat
   stable form.
4. Removal of N
   naphthylboro

Based on these results,
above. In these forms, th
that the NH_3 is connected
and the less hindered side
ence in dissociation press
the same conformer of tri-
being the most sterically h

Unfortunately, while
formational polymorphism
The example, neverthele
polymorph formation.

configurations (*i.e.*, *cis*,*trans* isomers or tautomers) crystallize in separate crystalline forms.

Crystallization of *cis*,*trans* isomers in different crystalline forms is well known and occurs whenever the pure isomer is crystallized. Crystallization of pure tautomeric forms in separate crystals leads to what may be called *tautomerizational polymorphism*. The crystallization of equilibrating isomers in configurational polymorphs is of significantly more interest. When this occurs, the phenomenon of configurational polymorphism can be used to isolate and study the individual isomers provided they exist in crystalline form.

A. Tri-α-Naphthylboronamine

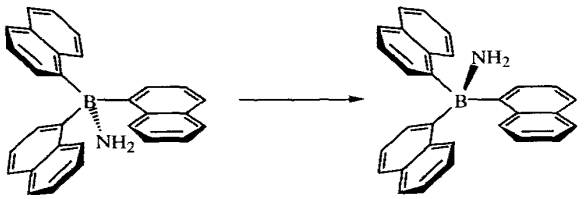

tri-α-naphthylboronamine
Form A

tri-α-naphthylboronamine
Form B

Brown and Sujishi (1948) reported an early example of conformational polymorphism with the following observations:

1. Two crystalline forms of tri-α-naphthylboronamine are found.
2. The metastable Form A is converted to the stable Form B slowly at room temperature and rapidly above 100 °C.
3. The dissociation pressure of the metastable form is higher than the stable form.
4. Removal of NH_3 from either form gives identical samples of tri-α-naphthylboron.

Based on these results, the two forms were suggested to have structures depicted above. In these forms, the conformation of the tri-α-naphthylboron is the same except that the NH_3 is connected to the boron on the more hindered side for the unstable form and the less hindered side for the stable form. Thus these structures explain the difference in dissociation pressures of the two forms and the fact that removal of NH_3 gives the same conformer of tri-α-naphthylboron. They also explain why the unstable form, being the most sterically hindered, can be converted to the stable form.

Unfortunately, while tri-α-naphthylboron was one of the first suggestions of conformational polymorphism, it was never confirmed by X-ray crystallographic analysis. The example, nevertheless, points out some of the molecular factors that influence polymorph formation.

B. Ethyl 2-[(phenylmethyl)amino]-2-butenoate

ethyl *Z*-2-[(phenylmethyl)-amino]-2-butenoate

ethyl *E*-2-[(phenylmethyl)-amino]-2-butenoate

Infrared studies (Dabrowski, 1963) and NMR studies (Dudek and Volpp, 1963) indicate that the Schiff base ethyl 2-[(phenylmethyl)amino]-2-butenoate (ethyl β-benzylaminocrotonate) exists in configurational polymorphs; the low-melting form (mp 23 °C) has the *cis*- or *Z*-conformation and the high-melting form (mp 75–80 °C) has the *trans*- or *E*-conformation. These conformers equilibrate in solution, but upon crystallization, the configurations shown are "frozen" out in their respective polymorphic structures.

The crystal structure of the *E*-isomer has been determined in our laboratory (Shieh *et al.*, 1983). Crystals of the *E*-isomer belong to space group $P2_12_12_1$ with a = 19.655 Å, b = 5.778 Å, and c = 10.632 Å. Figure 10.7 shows the structure of this isomer, and indeed it has the structure of the *E*-isomer suggested by spectroscopic evidence (Dudek and Volpp, 1963).

The NMR and IR spectra of ethyl 2-[(phenylmethyl)amino]-2-butenoate are completely consistent with this assignment. A solution-NMR spectrum of the low-melting form (prepared by dissolving crystals at low temperature) indicates that it is indeed the *Z*-isomer (Dudek and Volpp, 1963). In this experiment the isomer present in the solid state predominates in solution because of the low temperature. In our laboratory we have studied the isomerization rate of the *Z*-isomer to the *E*-isomer at ambient temperature in DMSO where it is relatively rapid. Measurement of the rate of this reaction at various temperatures gives an activation energy of 56.9 kJ/mol.

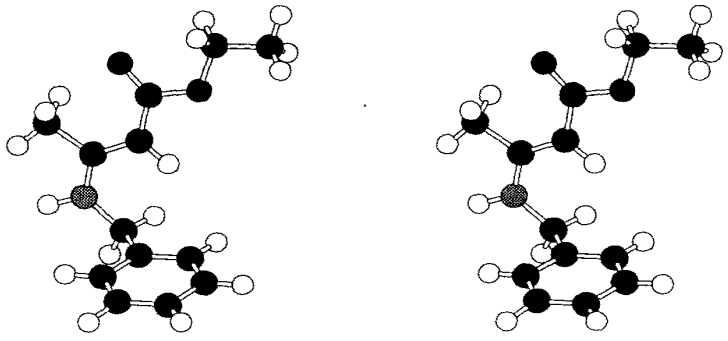

Figure 10.7 Stereoview of ethyl 2-[(phenylmethyl)amino]-2-butenoate in the high-melting *E*-isomer: H ○, C ●, N ◎, O ● (Shieh*et al.*, 1983).

The energies in kJ/mol for a number of rotamers of the *E*- and *Z*-isomers have been calculated using the *CAMSEQ* program (Weintraub and Hopfinger, 1975) which employs semiempirical potential and electrostatic functions to calculate the energies of each rotamer. These calculations indicate that the conformation of the *E*-isomer as determined by X-ray crystallography is one of the lowest energy conformations, although the *E*- and *Z*-isomers have nearly the same energy in a vacuum.

C. 4-(*N*-Chlorobenzylidene)-4-chloroaniline

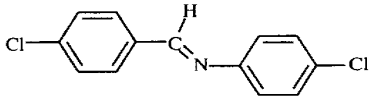

4-(*N*-chlorobenzylidene)-4-chloroaniline

The Schiff base 4-(*N*-chlorobenzylidene)-4-chloroaniline crystallizes in two polymorphs (Bernstein and Hagler, 1978). Although the structures of both polymorphs are disordered, it can be seen that the conformation of the molecule is strikingly different in the two polymorphs. Hence, these forms are termed conformational polymorphs. Conformational polymorphism of drugs is discussed in more detail later in Section 10.11. In the stable (triclinic) form, the molecules are planar, whereas in the unstable (orthorhombic) form the phenyl rings are rotated by equal but opposite amounts (24.8°) with respect to the H—C=N least-squares plane of the imine. The crystal packings of these two forms is shown in Figures 10.8 and 10.9.

Molecular orbital and lattice energy calculations were used to analyze the reasons for conformational polymorphism of 4-(*N*-chlorobenzylidene)-4-chloroaniline (Bernstein and Hagler, 1978). Quantum-mechanical calculations for a single molecule

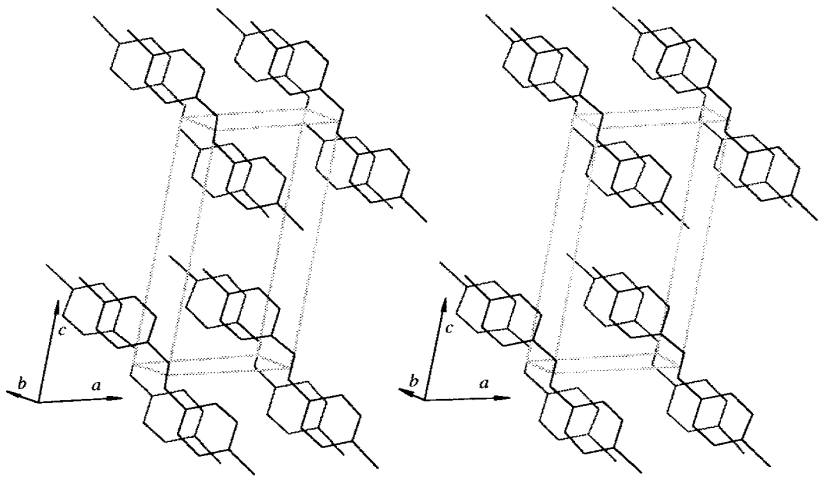

Figure 10.8 Stereoview of 4-(*N*-chlorobenzylidene)-4-chloroaniline triclinic polymorph (Bernstein and Hagler, 1978).

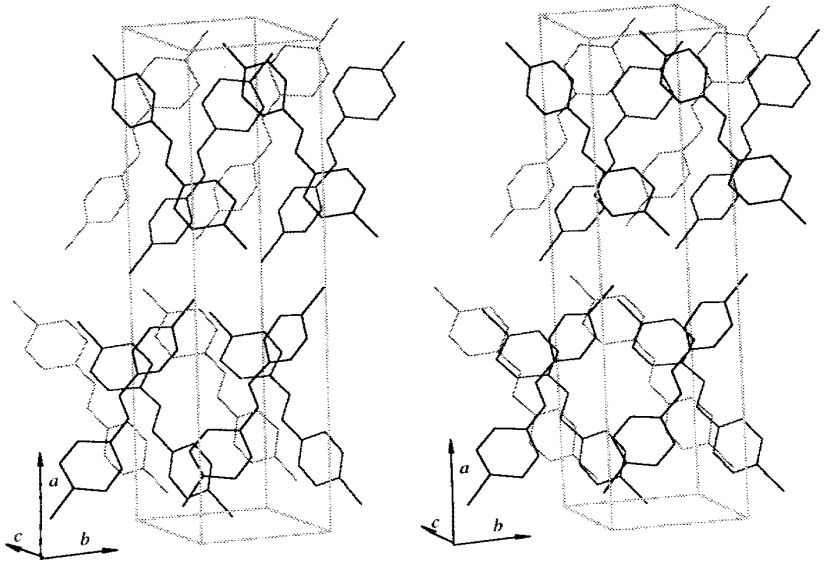

Figure 10.9 Crystal packing stereoview of 4-(*N*-chlorobenzylidene)-4-chloroaniline orthorhombic form. (Bernstein and Hagler, 1978).

showed that the nonplanar conformation was energetically favored by perhaps 2.09–6.28 kJ/mol but the lattice-energy calculations, using semiempirical potential functions, showed that the planar structure (triclinic form) gave a lower lattice energy by about 4.19 kJ/mol. These calculations explain why the triclinic polymorph is the stable crystalline polymorph even though it contains the less stable (planar) conformer.

Programs that calculate the packing energy are now available, for example, *Cerius*[2] (Molecular Simulations, Inc., 1997). These programs alone or in combination with structure elucidations based on powder diffraction data will provide new approaches to the structure analysis of materials when suitable single crystals are not available.

D. 3-Oxo-3*H*-2,1-benzoxiodol-1-yl 3-Chlorobenzoate

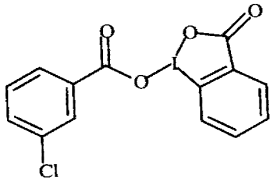

3-oxo-3*H*-2,1-benzoxiodol-1-yl 3-chlorobenzoate

As part of their extensive study of the crystal chemistry of iodoperoxides, Gougoutas and Lessinger (1974) determined the crystal structure of two polymorphs of 3-oxo-3*H*-2,1-benzoxiodol-1-yl 3-chlorobenzoate. This compound crystallizes in α- and β-forms that both belong to the monoclinic crystal system (Table 10.4).

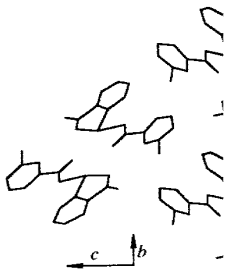

Figure 10.10 The crystal pa
(Gougoutas and

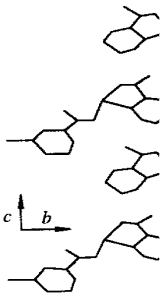

Figure 10.11 The crystal
(Gougoutas and

Table 10.4 Crystallographic
2,1-benzoxiodol-

Parameter
Space Group
a (Å)
b (Å)
c (Å)
β
Z
ρ_{calc} (g cm^{-3})
V (Å^3)

Gougoutas and Lessinger, 19

The α-form is essent
rings make an angle of a
two forms is also quite

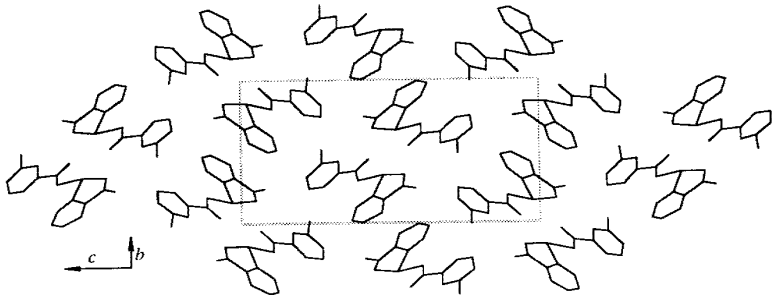

Figure 10.10 The crystal packing of 3-oxo-3*H*-2,1-benzoxiodol-1-yl 3-chlorobenzoate α-form (Gougoutas and Lessinger, 1974).

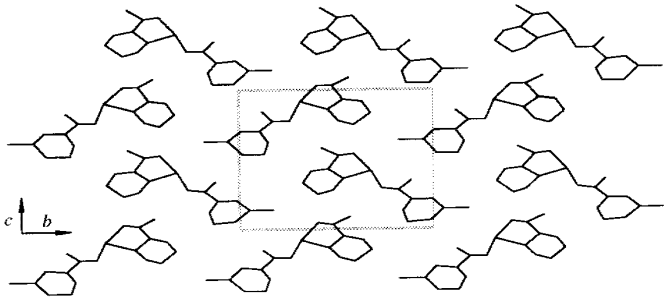

Figure 10.11 The crystal packing of 3-oxo-3*H*-2,1-benzoxiodol-1-yl 3-chlorobenzoate β-form (Gougoutas and Lessinger, 1974).

Table 10.4 Crystallographic Unit Cell Parameters for 3-Oxo-3*H*-2,1-benzoxiodol-1-yl 3-Chlorobenzoate

Parameter	α-Form	β-Form
Space Group	$P2_1/n$	Pc
a (Å)	6.376	5.057
b (Å)	10.547	13.035
c (Å)	20.066	10.339
β	92.0°	99.5°
Z	4	2
ρ_{calc} (g cm^{-3})	1.984	2.009
V (Å^3)	1348.6	672.2

Gougoutas and Lessinger, 1974.

The α-form is essentially planar in the crystal while in the β-form the two phenyl rings make an angle of approximately 55° with each other. The crystal packing of the two forms is also quite different as shown in Figures 10.10 and 10.11. These two

forms have different solid-state infrared spectra (see Figure 10.12), as expected since the molecule is in different conformation in the two crystal forms.

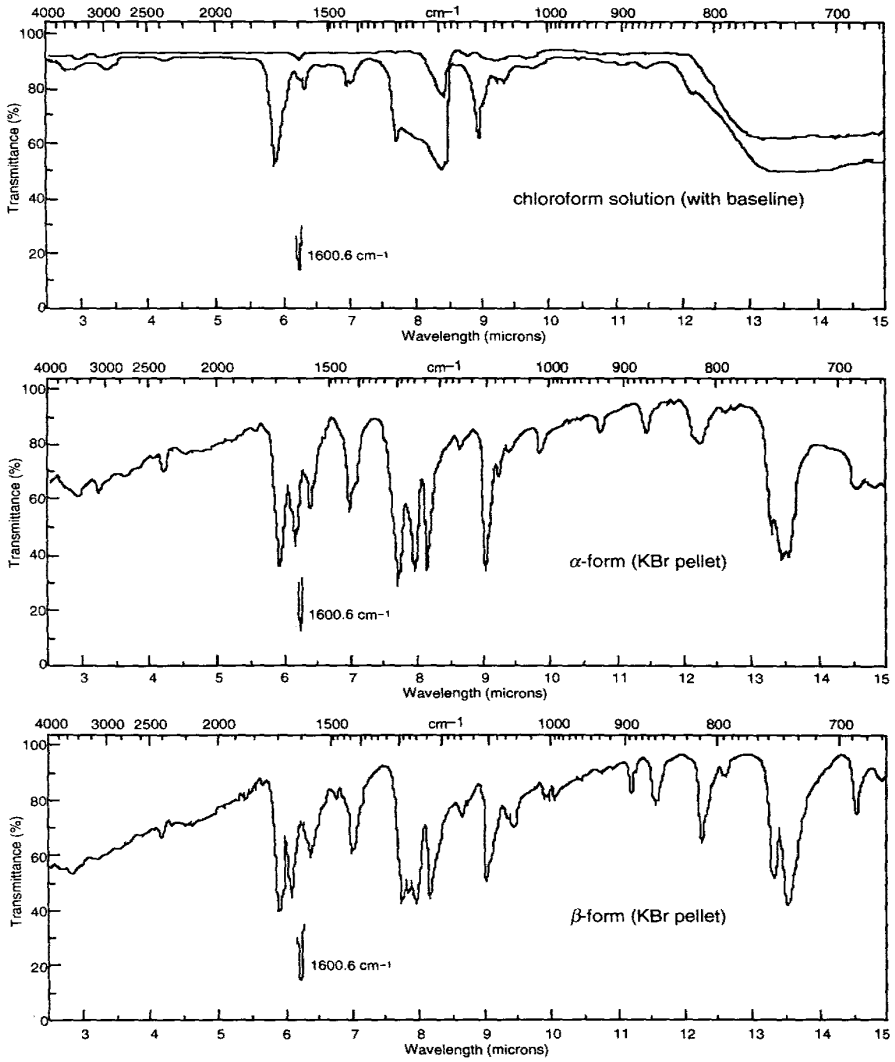

Figure 10.12 Infrared spectra of 3-oxo-3*H*-2,1-benzoxiodol-1-yl 3-chlorobenzoate (Gougoutas and Lessinger, 1974).

E. Tautomerizational Polymorphism

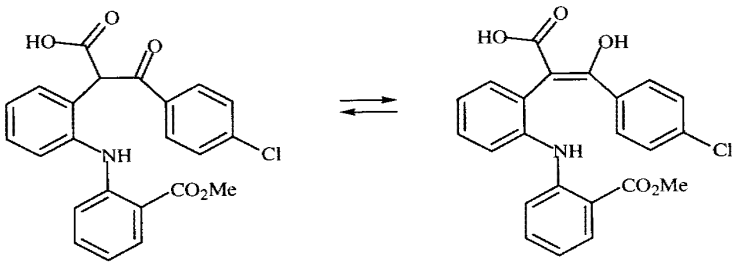

keto form
3-(4-chlorophenyl)-2-[2-(2-(methoxycarboxyphenyl)-amino)phenyl]-3-oxopropanoic acid

enol form
3-(4-chlorophenyl)-3-hydroxy-2-[2-(2-(methoxycarboxyphenyl)-amino)phenyl]propenoic acid

Schulenberg (1968) has reported that 3-(4-chlorophenyl)-2-[2-(2-(methoxycarboxyphenyl)amino)phenyl]-3-oxopropanoic acid crystallizes in two tautomeric forms. One form has a melting point of 93–99 °C that upon dissolution in $CDCl_3$ gave NMR spectra consistent with the keto form, 3-(4-chlorophenyl-2-[2-(2-(methoxycarboxyphenyl)amino)phenyl]-3-oxopropanoic acid. The other form had a melting point of 110–122 °C and upon dissolution gave NMR spectra consistent with the enol form, 3-(4-chlorophenyl)-3-hydroxy-2-[2-(2-(methoxycarboxyphenyl)amino)phenyl]propenoic acid. Addition of triethylamine to either solution gave an equilibrium mixture containing 70% of the keto form and 30% of the enol form.

Although the crystal structures of the keto and enol forms have not been determined, this study illustrates a case in which two different crystalline forms exist, each containing an individual tautomer. This situation is termed tautomerizational polymorphism (*cf.* p. 143).

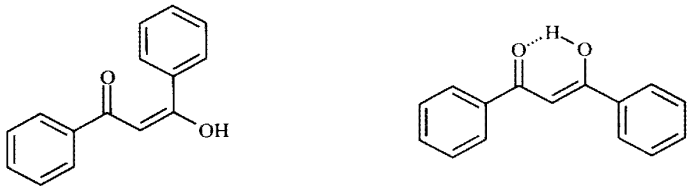

E-conformer of the enolate of
1,3-diphenylpropane-1,3-dione

Z-conformer of the enolate of
1,3-diphenylpropane-1,3-dione

Several other cases of tautomerizational polymorphism exist. For example, the enol of 1,3-diphenylpropane-1,3-dione crystallizes in two forms. One form contains the *E*-isomer and the other contains the *Z*-isomer (Eistert *et al.*, 1952). In addition, there are numerous examples of the crystallization process freezing one configurational isomer or tautomer out of solution. These cases are reviewed by Curtin and Engelmann (1972).

F. Polychromism

One of the most striking differences in physical properties among polymorphs is **polychromism** (*i.e.*, different colors). Polychromism has been reported for only a limited number of cases. Dimethyl 3,6-dichloro-2,5-dihydroxyterephthalate, for example, crystallizes in yellow, light-yellow, and white polymorphs (Byrn *et al.*, 1972; Fletton *et al.*, 1986; Yang *et al.*, 1989; Richardson *et al.*, 1990). The colors of these three polymorphs are attributed to differences in orientation of the carboxylate group with respect to the aromatic ring (see also Sections 10.7E and 20.1A).

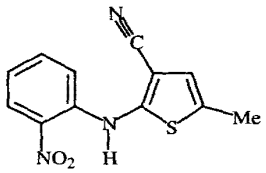

5-methyl-2-[(2-nitrophenyl)amino]-3-thiophenecarbonitrile
(ROY)

5-Methyl-2-[(2-nitrophenyl)amino]-3-thiophenecarbonitrile is a dramatic example of polychromism. Crystallization of this compound from ethanol yields a mixture of yellow and red prisms, whereas crystallization from methanol yields orange needles; hence the alias ROY for the red, orange, and yellow forms (Borchardt, 1997). Crystals of the red form also appear to be **pleochroic**, displaying both red and orange colors under polarized illumination.

The three polymorphs are free of solvent and stable at room temperature. The red, orange, and yellow forms are similar in energy with melting points of 106.2, 114.8, and 109.8 °C, respectively (Yu, 1998). The red and orange forms undergo solution-mediated transformation to the yellow form at room temperature, indicating the latter is the most stable at room temperature. The yellow and orange forms are related enantiotropically, with yellow being more stable at low temperature. Between room temperature and the melting point, the red form is always less stable than the yellow form. The heats of melting, as measured by DSC, confirmed these stability relationships. Solid-state phase transitions from red to yellow and from red to orange have been observed between 70—90 °C in a solvent free environment. The transition from red to yellow (at temperatures greater than 90 °C) results in a dramatic change in color but no apparent change in crystal morphology, whereas the transition from red to orange leads to the growth of orange needles from the initial red crystals.

The crystal structures of red, orange, and yellow forms have been determined by single-crystal X-ray diffraction and show that the molecule adopts a dramatically different conformation in each of the forms. Subsequent studies show that these different conformations are the reasons for the different colors. Hydrogen bonding in the polymorphs is exclusively intramolecular—between the adjacent amine and nitro substituents. The heteroatom-to-heteroatom distances of the hydrogen bond in red, orange, and yellow are 2.636(2), 2.607(3), and 2.625(3) Å, respectively. The conformations of the molecule in the three polymorphs are significantly different (Figure 10.13). In the yellow and orange forms, the nitro group is essentially co-planar with the phenyl ring, whereas in the red form it is twisted out-of-plane by 18°. The color of the polymorphs may be related to the degree of electron delocalization, which is related to the angle between the planes of the phenyl and the thiophene moieties (red 46°,

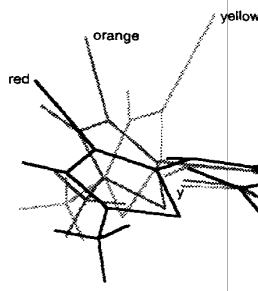

Figure 10.13 Conformations
crystalline form

orange 54°, and yellow 1(
order of the expected w
Section 8.1). Studies ha
direct result of the differe
1998; Yu, 1998). The ol
those calculated from the
^{13}C CP/MAS solid-st
tinguish the polymorphs.
reported for polymorphic
shifts of C3 (the carbon in
97.9, 105.2, and 109.3
covering a range of 11
104.41 ppm in solution.)
red form with respect to t
conjugation effect. Smitl
(total suppression of spir
shift anisotropy (CSA) o
increases in magnitude by
ric as the coplanar angle
electrons between the tw
site.

This parallels the re
quency are 2211, 2223,
tively (see Section 8.1).
the red form from a highe
vations confirm the signi
pronounced color change

A number of deriva
nitrile were synthesized
nitrophenylaminothiophe
Me) crystallized in three
the gold form were un
polymorph" class. How

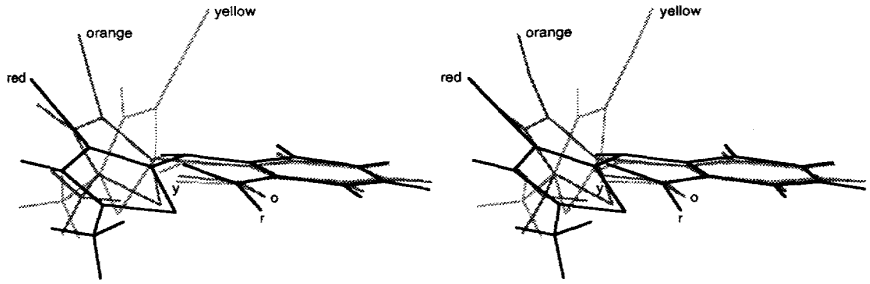

Figure 10.13 Conformations of 5-methyl-2-[(2-nitrophenyl)amino]-3-thiophenecarbonitrile in three crystalline forms.

orange 54°, and yellow 106°). The order of these angles appears to correlate with the order of the expected wavelengths of absorption by the colored polymorphs (see Section 8.1). Studies have shown that the different colors of the polymorphs are a direct result of the difference in molecular conformation (Borchardt, 1997; Smith *et al.*, 1998; Yu, 1998). The observed XRPD patterns of the three polymorphs agree with those calculated from the single-crystal structures.

^{13}C CP/MAS solid-state NMR, solid-state FT-IR, and XRPD can be used to distinguish the polymorphs. The observed spectral differences are among the largest reported for polymorphic organic compounds. For example, the ^{13}C NMR chemical shifts of C3 (the carbon in the thiophene ring to which the nitrile group is attached) are 97.9, 105.2, and 109.3 ppm for the red, orange, and yellow forms, respectively, covering a range of 11.4 ppm. (For comparison, the chemical shift of C3 is 104.41 ppm in solution.) This indicates an increase in the electron density of C3 in the red form with respect to the yellow and orange forms, possibly a result of an increased conjugation effect. Smith and coworkers (1998) have used a two-dimensional TOSS (total suppression of spinning sidebands) pulse sequence to investigate the chemical-shift anisotropy (CSA) of C3. These studies show that the extent of the CSA for C3 increases in magnitude by 30 ppm and the line shape appears to become more asymmetric as the coplanar angle increases. This was taken to reflect a greater transfer of π electrons between the two ring systems and hence a greater electron density at the C3 site.

This parallels the results from IR spectroscopy in which the nitrile stretching frequency are 2211, 2223, and 2231 cm^{-1}, for the red, orange, and yellow forms, respectively (see Section 8.1). This shift is indicative of the decreased nitrile bond strength in the red form from a higher degree of conjugation with the aromatic ring. These observations confirm the significant changes in the electronic structure, as demonstrated by pronounced color changes among different polymorphs.

A number of derivatives of 5-methyl-2-[(2-nitrophenyl)amino]-3-thiophenecarbonitrile were synthesized in order to determine the extent of the color polymorphism of nitrophenylaminothiophenes. 2-[(2-Nitrophenyl)amino]-3-thiophenecarbonitrile (NorMe) crystallized in three forms: red, orange, and gold. Numerous attempts to obtain the gold form were unsuccessful thus placing the gold from in the "disappearing polymorph" class. However, crystallization of a newly synthesized lot of NorMe gave

the gold form once again only to disappear when the material was subjected to further crystallization and handling. As with other disappearing polymorphs, this behavior is due to the presence of impurities and the fact that the gold polymorph is unstable in the presence of seeds of the other forms (Dunitz and Bernstein, 1995).

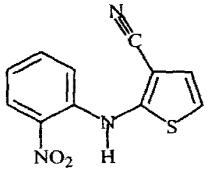

2-[(2-nitrophenyl)amino]-3-thiophenecarbonitrile (NorMe)

The XRPD patterns of the three forms of NorMe are different from the parent compound. The crystal structure of the red form NorMe was determined (Borchardt, 1997). The red form is nearly coplanar further substantiating the concept that the red color is associated with planarity. The IR spectra of the NorMe polymorphs are quite similar to ROY. The red form has a nitrile stretching absorption at 2210 cm^{-1}, the orange is a 2222 cm^{-1}, and the yellow at 2230 cm^{-1}.

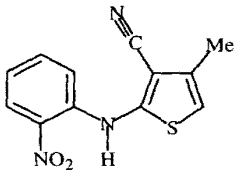

4-methyl-2-[(2-nitrophenyl)amino]-3-thiophenecarbonitrile (4-Me)

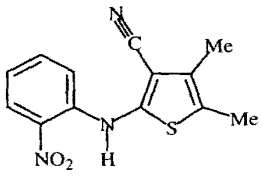

4,5-dimethyl-2-[(2-nitrophenyl)amino]-3-thiophenecarbonitrile (4,5-DiMe)

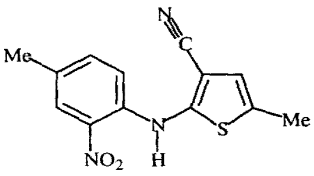

5-methyl-2-[(4-methyl-2-nitrophenyl)amino]-3-thiophenecarbonitrile (4'-Me)

The conformation of the red form of 4-methyl-2-[(2-nitrophenyl)amino]-3-thiophenecarbonitrile (4-Me) is the most coplanar of the structures determined (see Figure 10.14). 4,5-Dimethyl-2-[(2-nitrophenyl)amino]-3-thiophenecarbonitrile (4,5-DiMe) crystallized in two polymorphs: red and orange. As with the previous derivatives, the conformation of the red form as determined by single-crystal X-ray methods is rather coplanar (see Figure 10.14). 5-Methyl-2-[4-methyl-2-nitrophenyl)amino]-3-thiophenecarbonitrile (4'-Me) was crystallized in red, dark red, light red, and orange forms. Only the red form gave crystals suitable for structure determination. As with the previous derivatives, this red form has a nearly coplanar conformation. Figure 10.14 compares the conformation of the various red forms in this nitrophenylaminothiophene series. In all cases, the red form has the most coplanar conformation of the polymorphs. This further supports the conclusion that the conformation of the nitrophenylaminothiophene determines the color of the polymorph.

Griesser and He (1998) have carried out a preliminary study of the solubilities and interconversions of the four forms of 4'-Me and found that all four forms are within 4 kJ/mol or less of each other in energy. These studies allowed the development of the energy–temperature diagram (see Section 5.2) shown in Figure 10.15. Such diagrams

are extremely usefu
polymorphs.

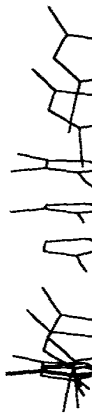

Figure 10.14 Stereovie
the thiop
Hydroger

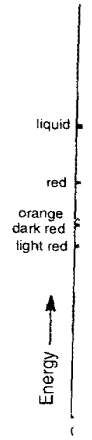

Figure 10.15 Energy–t
phenyl)a

are extremely useful in visualizing the energy–temperature relationships between polymorphs.

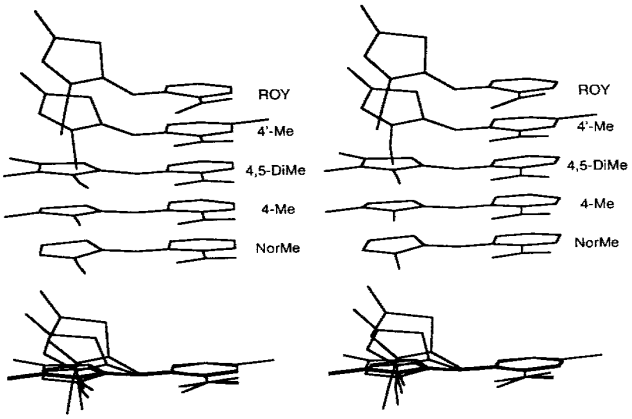

Figure 10.14 Stereoview showing a comparison (both stacked and overlayed) of the conformations of the thiophene and phenyl rings in the nitrophenylaminothiophene series red forms. Hydrogens were omitted for clarity.

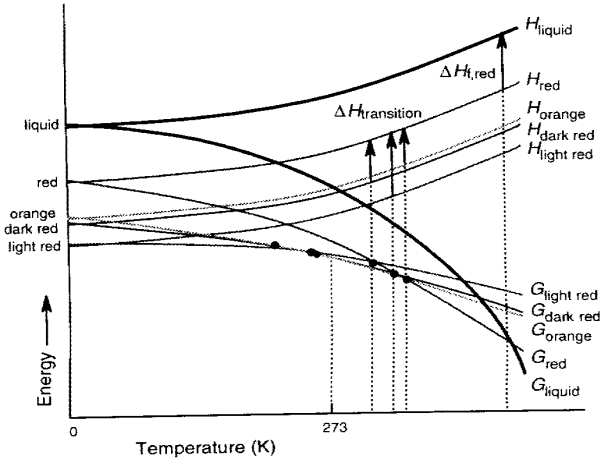

Figure 10.15 Energy–temperature diagram for the four forms of 5-methyl-2-[4-methyl-2-nitrophenyl)amino]-3-thiophenecarbonitrile (Griesser and He, 1998).

10.3 SULFONAMIDES

The polymorphism of sulfonamides has been investigated and reviewed by Kuhnert-Brandstätter (1971). These studies were carried out using microscopy on a Kohfler hot stage (see Section 4.4). Sulfonamides exhibited behavior expected of polymorphs, including successive melting points as the temperature is raised and changes in color under crossed Nicol gratings (crossed polarizers). Table 10.5 summarizes the results of Kuhnert-Brandstätter's (1971) studies on these compounds.

Although all of these studies have not been confirmed by crystallographic data, the crystal structures of several polymorphs of sulfonamides have been determined and will

Table 10.5 Polymorphism of Sulfonamides and Related Compounds[a]

Compound	Melting Point of Form (°C)						
	I	II	III	IV	V	VI	VII
Acetazolamide	258-260	248-250					
Acetyl Sulfisoxazole	190-195	176-177	173-174				
Chlorthalidone	212-224	188-189					
Clofenamide	210-215	203-207	183-185	168-170			
Diphenylmethane-4,4'-disulfonamide	185-187	172-174					
Mafenide HCl	250-260	235-240	220-225	210-212			
4'-(Methylsulfamoyl)-sulfanilanilide	148-151	144-146					
Phthalylsulfathiazole	260-274	230					
Sulfachlorpyridazine	196-197	178-181					
Sulfadicramide	176-180	174-176					
Sulfadimethoxine	194-198	176-177	156-158				
Sulfaethidole	188	181	149				
Sulfaguanidine	187-191	174-176	143-145				
Sulfameline	210-212	197-199	181-183	179-181	176-177	155	
Sulfamerazine	235-238	228					
Sulfamethazine	206-208	199	178	~175			
Sulfamethizole	209	193					
Sulfamethoxazole	169	168	166				
Sulfamethoxypyridazine	180-182	158-159	153-154				
Sulfamidochrysoidine	224-228	217-219	212				
Sulfamoxole	200-204	188-195	177-180				
Sulfanilamide	165	156	153				
N-Sulfanilyl-3,4-xylamide	215-218	208	203	196			
Sulfapyridine	192	185	179	176	174	167	149
Sulfathiazole	202	175	162	158			
Sulfathiourea	178-180	168-171					
Sulfatriazine	158-166	132-135					
Sulfazamet	182-185	176-178					
Sulfisoxazole	190-195	131-133					
Tolbutamide	127	117	106				

[a] Kuhnert-Brandstätter (1971).

be discussed next. In gen
polymorphs. Thus, in th
ble for polymorphism.

A. SULFANILAMIDE

NH

Sulfanilamide exists in th
ters shown in Table 10.6
(O'Conner and Maslen,
phenyl rings. In each sta
···amino···sulfonamide··
substituent in each stack.

The crystal packing
the α-form (Alleaume an
but the order of the s
···amino···sulfonamide··
stack.

The crystal packing
10.18 appears, in genera
sulfonamide amino grou
successive rings in a sta
which resembles that of t

The density of the
(see Table 10.6). The p
sulfanilamide have been
diagram constructed. It i
group is similar in all for
plane of the phenyl ring
relationships between th
depicted in Figures 10.1
10.19.

Table 10.6 Crystallographi

Parameter	
Space group	
a (Å)	
b (Å)	
c (Å)	
β	
Z	
ρ_{calc} (g cm^{-3})	
V (Å^3)	

O'Conner and Maslen, 1965

be discussed next. In general, the conformations of the drug are similar in the different polymorphs. Thus, in these cases, differences in crystal packing are mainly responsible for polymorphism.

A. Sulfanilamide

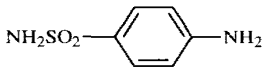

sulfanilamide

Sulfanilamide exists in three crystalline forms which have the crystallographic parameters shown in Table 10.6. The α-form has the crystal packing shown in Figure 10.16 (O'Conner and Maslen, 1965). The crystal packing of this form contains layers of phenyl rings. In each stack, the order of the substituent groups on successive rings is ···amino···sulfonamide···sulfonamide···amino···, etc., resulting in alternating pairs of substituent in each stack.

The crystal packing of the β-form shown in Figure 10.17 is quite different from the α-form (Alleaume and Decap, 1965). There are, again, columns of phenyl rings but the order of the substituent groups on successive rings is ···sulfonamide··· ···amino···sulfonamide···amino···, etc., resulting in alternating substituents in the stack.

The crystal packing of the γ-form (Alleaume and Decap, 1966) shown in Figure 10.18 appears, in general, to be similar to the α-form with layers of phenyl rings and sulfonamide amino groups. In these columns, the order of substituent groups on successive rings in a stack is ···amino···sulfonamide···amino···sulfonamide···, etc., which resembles that of the β-form.

The density of the β-form (the most thermodynamically stable form) is greatest (see Table 10.6). The polymorphic interconversions and thermodynamic properties of sulfanilamide have been investigated by Burger (1973a–b) and an energy-temperature diagram constructed. It is interesting to note that the conformation of the sulfanilamide group is similar in all forms, with the nitrogen atom being the atom furthest out of the plane of the phenyl ring. A comparison of the α-, β-, and γ-forms showing the relationships between the arrangement of the substituents in successive molecules depicted in Figures 10.16, 10.17, and 10.18 is illustrated in a stereoview in Figure 10.19.

Table 10.6 Crystallographic Data for the Polymorphs of Sulfanilamide

Parameter	Form α	Form β	Form γ
Space group	*Pbca*	$P2_1/c$	$P2_1/c$
a (Å)	5.65	8.98	7.95
b (Å)	18.51	9.01	12.95
c (Å)	14.79	10.04	7.79
β	90.00°	111.43°	106.50°
Z	8	4	4
ρ_{calc} (g cm^{-3})	1.47	1.51	1.49
V (Å^3)	1547.1	755.2	768.7

O'Conner and Maslen, 1965

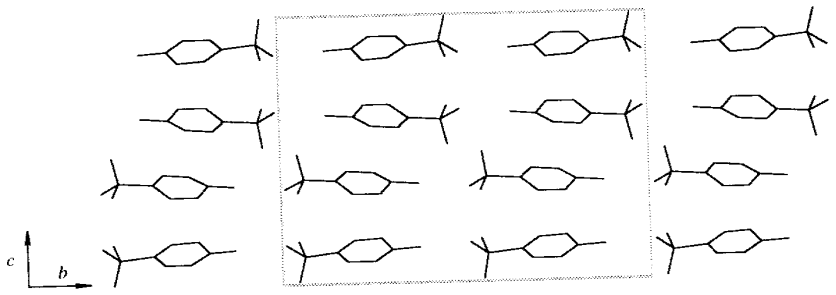

Figure 10.16 Molecular packing of the α-form of sulfanilamide (O'Conner and Maslen, 1965).

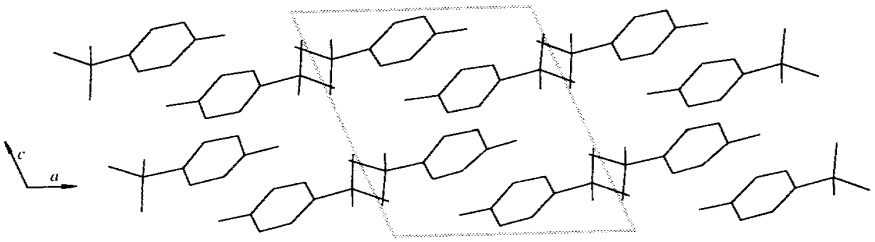

Figure 10.17 The crystal packing of the β-form of sulfanilamide (Alleaume and Decap, 1965).

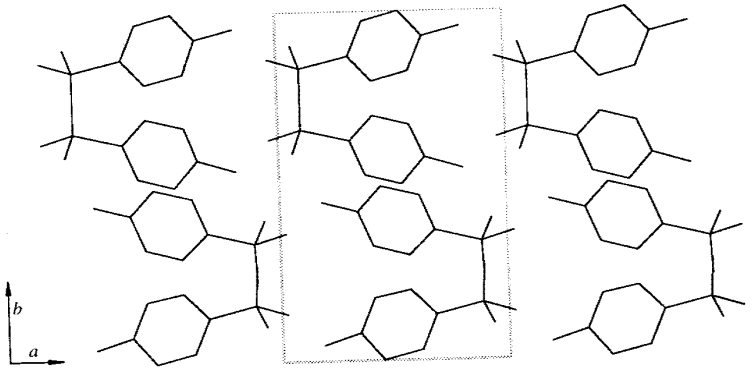

Figure 10.18 Crystal packing of the γ-form of sulfanilamide (Alleaume and Decap, 1966).

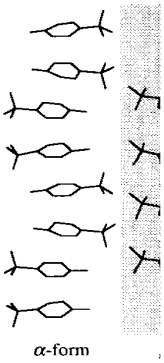

Figure 10.19 Stereovie
α-, β-, ar

B. SULFATHIAZOLE

NH_2

Table 10.7 indicates
(1983) have studied
the four polymorphs.
dynamically stable at
of all three polymorp
mide group is the at
This is in marked si
molecule in all three
between these forms

Table 10.7 Crystallogr

Parameter
Space Group
a (Å)
b (Å)
c (Å)
β
Z
ρ_{meas} (g cm^{-3})
V (Å^3)
Habit
Melting point
Transition point

a Kruger and Gafner, 19

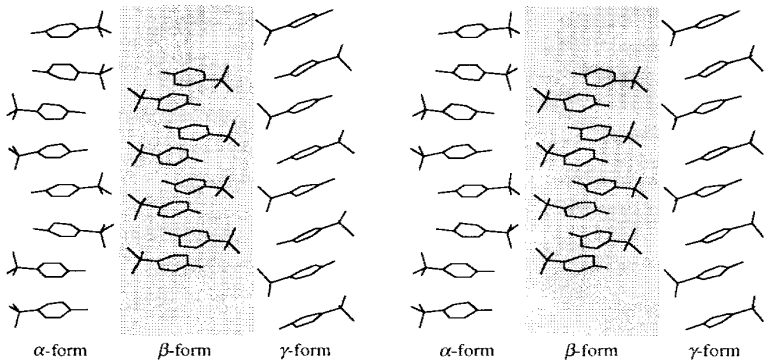

Figure 10.19 Stereoview showing the molecular arrangement of sulfanilamide columns in the α-, β-, and γ-forms.

B. Sulfathiazole

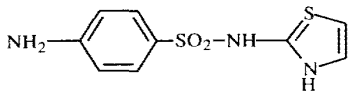

sulfathiazole

Table 10.7 indicates that sulfathiazole exists in four polymorphs. Burger and Dialer (1983) have studied this system and have produced an energy-temperature diagram of the four polymorphs. Form I is the least stable of the four forms; Form III is thermodynamically stable at room temperature. Figures 10.20–10.22 show packing drawings of all three polymorphs of sulfathiazole. It is obvious that the nitrogen of the sulfonamide group is the atom that is the greatest distance from the plane of the phenyl ring. This is in marked similarity to sulfanilamide. In addition, the conformation of the molecule in all three forms is very similar. The major crystallographic difference between these forms is the nature and type of hydrogen bonds.

Table 10.7 Crystallographic Parameters for the Polymorphs of Sulfathiazole

Parameter	Form I[a]	Form II[b]	Form III[a]
Space Group	$P2_1/c$	$P2_1/c$	$P2_1/c$
a (Å)	10.554	8.235	17.570
b (Å)	13.220	8.550	8.574
c (Å)	17.050	15.558	15.583
β	108.06°	93.67°	112.93°
Z	8	4	8
ρ_{meas} (g cm^{-3})	1.50	1.55	1.57
V (Å^3)	2261.7	1093.2	2162.0
Habit	Rods	Hexagonal prisms	Hexagonal plates
Melting point	200-202	200-202	173-175 (or 200-202)
Transition point	...	173-175	173-175

a Kruger and Gafner, 1971a. *b* Kruger and Gafner, 1971b.

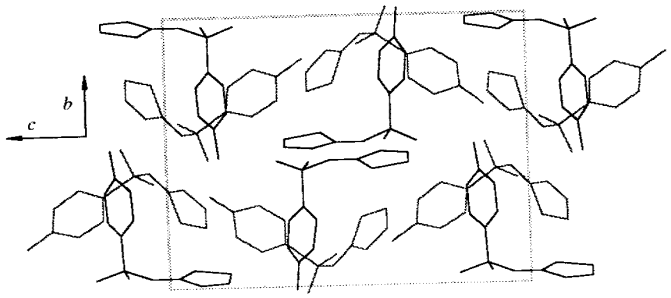

Figure 10.20 Crystal packing of sulfathiazole Form I (Kruger and Gafner, 1971a).

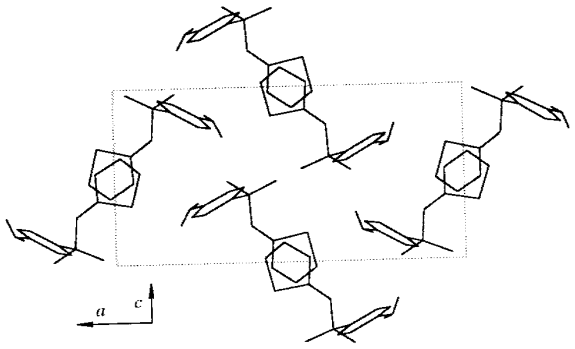

Figure 10.21 Crystal packing of sulfathiazole Form II (Kruger and Gafner, 1971b).

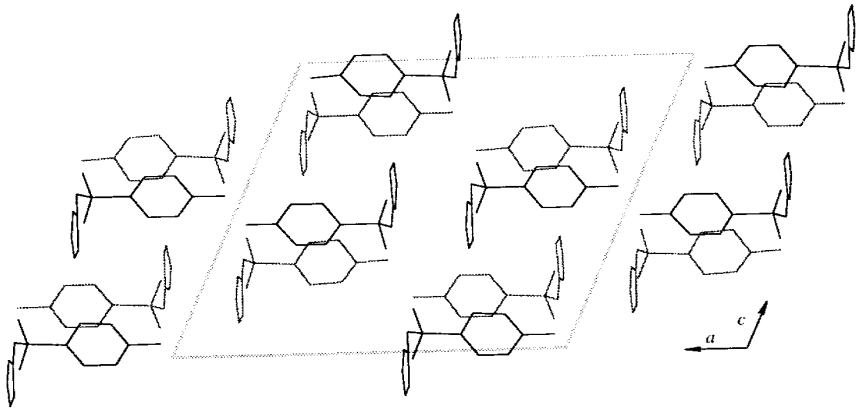

Figure 10.22 Crystal packing of sulfathiazole Form III (Kruger and Gafner, 1971a).

Table 10.8 Dissolution Rate

Temperature (°C)	Form (mg cm^{-2}
59.1	0.18
48.8	0.10
39.4	0.05
29.6	0.03
24.1	0.02
20.4	0.02

Milosovich, 1964.

The crystallographic
morphs of sulfathiazole; I
polymorphism of this dru
Kuhnert-Brandstätter rep
stage microscopy. In the
lory (1967), and Higuchi
Shenouda (1970) also in
Mesley (1971) using IR,
of three polymorphs. He
with mixtures of the three
these findings and charac
microscopy, solubility, a

To avoid prolonged
involve separation of hal
each habit. X-ray powd
crystal X-ray data and
approach would make su

The physical propert
and Eisen, 1971; Miloso
the dissolution rate under
results in Table 10.8 sho
solubility than Form I. T
II should have a slower d

C. Succinylsulfathi

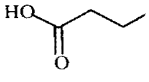

In early studies of succi
and Higuchi, 1963) a lar

Table 10.8 Dissolution Rate and Solubility of Forms I and II of Sulfathiazole

Temperature (°C)	Dissolution Rate		Solubility	
	Form I (mg cm^{-2} sec^{-1})	Form II (mg cm^{-2} sec^{-1})	Form I (g/1000 gm)	Form II (g/1000 gm)
59.1	0.185	0.239	31.5	40.7
48.8	0.102	0.145	19.8	28.1
39.4	0.0598	0.0913	14.0	21.4
29.6	0.0355	0.0597	9.93	16.7
24.1	0.0237	0.0413	8.15	14.2
20.4	0.0201	0.0371	7.10	13.1

Milosovich, 1964.

The crystallographic data clearly established the existence of at least four polymorphs of sulfathiazole; however, at this point, it is worthwhile to review studies of the polymorphism of this drug using other techniques. As reported earlier in this section, Kuhnert-Brandstätter reported that sulfathiazole has four polymorphs based on hot stage microscopy. In the 1960's, three groups of workers [Milosovich (1964), Guillory (1967), and Higuchi *et al.* (1967)] reported only two polymorphs. DSC work by Shenouda (1970) also indicated the existence of only two polymorphs. Studies by Mesley (1971) using IR, DSC, and X-ray powder diffractometry showed the existance of three polymorphs. He suggested that most of the earlier workers had been dealing with mixtures of the three polymorphic forms. Burger and Dialer (1983) reinvestigated these findings and characterized four polymorphs by IR-spectroscopy, DSC, thermomicroscopy, solubility, and density.

To avoid prolonged confusion of this sort, studies of unfamiliar systems should involve separation of habits under a microscope and then crystallographic studies of each habit. X-ray powder diffraction patterns should be calculated from the single crystal X-ray data and compared with the experimentally observed XRPDs. This approach would make sure that mixtures of polymorphs are not involved.

The physical properties of sulfathiazole Forms I and II have been studied (Sunwoo and Eisen, 1971; Milosovich, 1964). These studies, which used a flow cell, measured the dissolution rate under conditions where Form II did not transform to Form I. The results in Table 10.8 show that Form II has a significantly higher dissolution rate and solubility than Form I. This is not consistent with the densities which predict that Form II should have a slower dissolution rate and be less soluble than Form I.

C. Succinylsulfathiazole

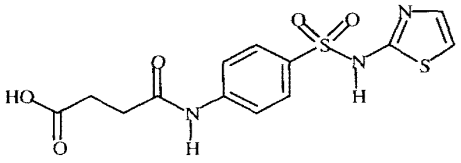

succinylsulfathiazole

In early studies of succinylsulfathiazole (Armour Research Foundation, 1949; Shefter and Higuchi, 1963) a large number of different crystal forms were found. The studies

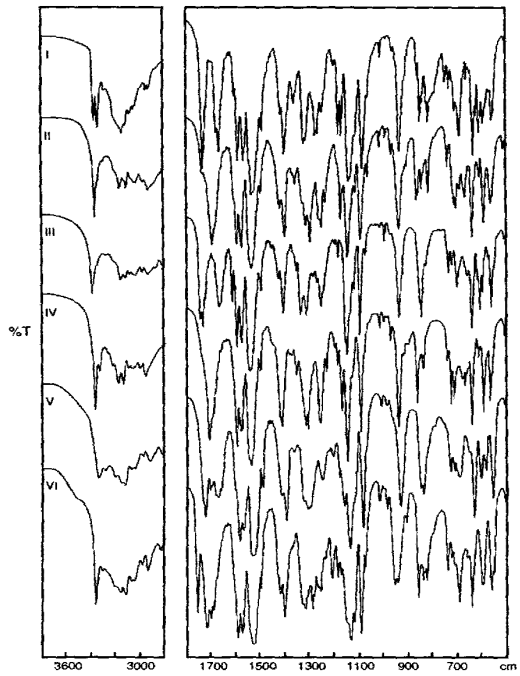

Figure 10.23 IR spectra (KBr pellets) of the unsolvated crystal forms of succinylsulfathiazole (Burger and Griesser, 1989).

by Burger and Griesser (1989; 1991) provide the most complete summary of the solid-state behavior of this compound. As summarized in Table 10.9, they found that succinylsulfathiazole crystallized in six anhydrous crystal forms, three polymorphic monohydrates, as well as an acetone solvate and an *n*-butanol solvate. These different crystal forms were prepared by a variety of methods involving crystallization from different solvents and by drying the different solvates. For example, Form IV was prepared by drying the acetone solvate at 150 °C. Form VI was prepared by dehydration of one of the monohydrates in vacuum at 100 °C. The three monohydrates are termed "polymorphic" because they contain the same chemical composition (compound and solvent) but exist in different crystal structures. The IR spectra of all eleven crystal forms were measured in KBr pellets. The polymorphs and solvates were also characterized by thermal microscopy and DSC. Figure 10.23 shows the IR spectra of the six unsolvated crystal forms and Figure 10.24 shows the DSC thermograms of these polymorphs. The IR spectra of the different crystal forms are different and indicate that these are different polymorphs. The DSC thermograms of Forms I through V show destinctive differences in melting points. The DSC thermogram of Form VI shows an incongruent melting process. However, IR appears to be better than DSC for distinguishing these forms. Figure 10.25 shows the X-ray powder diffraction patterns of the six crystal forms which are all different and confirm the IR results.

Table 10.9 Comparison of Succinyls

Form	Stability (20 °C)	
I	Stable[a]	Suspens solv
II	< I	Evapora EtO
III	< II	Dehydra °C
IV	< III	Suspens EtO
V	< IV	Annealii 160
VI	< V	Dehydra
H_I	Stable	Suspens water
H_{II}	< H_I	Crystalli
H_{III}	< H_{II}	Suspensi for 1

a in the absence of water. water at 20 °C. (Burger a

Figure 10.24 DSC therm Griesser, 1

Table 10.9 Comparison of the Physical Properties of the Polymorphic Anhydrates and Monohydrates of Succinylsulfathiazole

Form	Stability (20 °C)	Preparation	MP[b] (°C)	MP[c] (°C)	1st Peak in IR (cm^{-1})	Density (g cm^{-3})	Solubility[d] Ratio to H_I
I	Stable[a]	Suspension of acetone solvate in EtOAC	204	205	3361	1.592	3.24
II	< I	Evaporation of absolute EtOH solution	195-199	195	3360	1.535	5.69
III	< II	Dehydration of H_I at 100 °C	189-194	188-191	3372	1.571	6.15
IV	< III	Suspension of V or VI in EtOAC	187-191	189	3338	1.518	9.26
V	< IV	Annealing of I at 160 °C	182-185	182-187	3330	1.488	~12.7
VI	< V	Dehydration of H_{II}	139-143	135-138	3350	1.463	—
H_I	Stable	Suspension of any form in water	123-125		3480 (OH) 3320 (NH)	1.527	1.00
H_{II}	< H_I	Crystallization from water	~110		3500 (OH) 3350 (NH)	1.520	1.81
H_{III}	< H_{II}	Suspension of III in water for 15 min	105		3450 (OH) 3335 (NH)		

a in the absence of water. *b* by thermomicroscopy. *c* by differential scanning calorimetry (DSC). *d* in water at 20 °C. (Burger and Griesser, 1991)

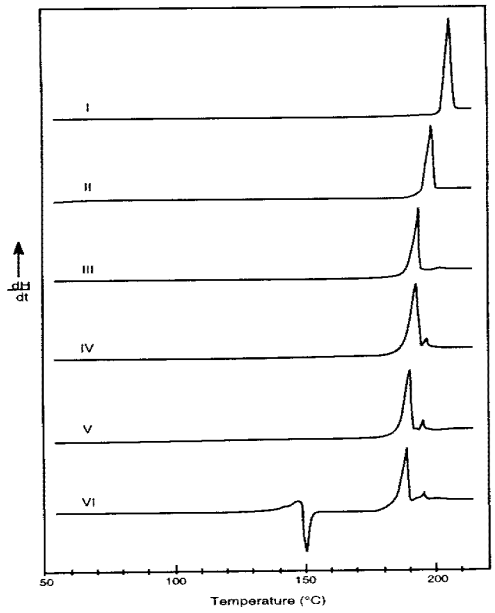

Figure 10.24 DSC thermograms of the unsolvated crystal forms of succinylsulfathiazole (Burger and Griesser, 1989).

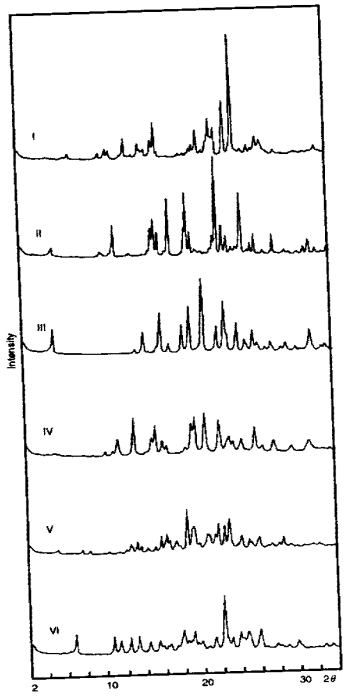

Figure 10.25 X-ray powder diffraction patterns of the six unsolvated crystal forms of succinylsulfathiazole (Burger and Griesser, 1989).

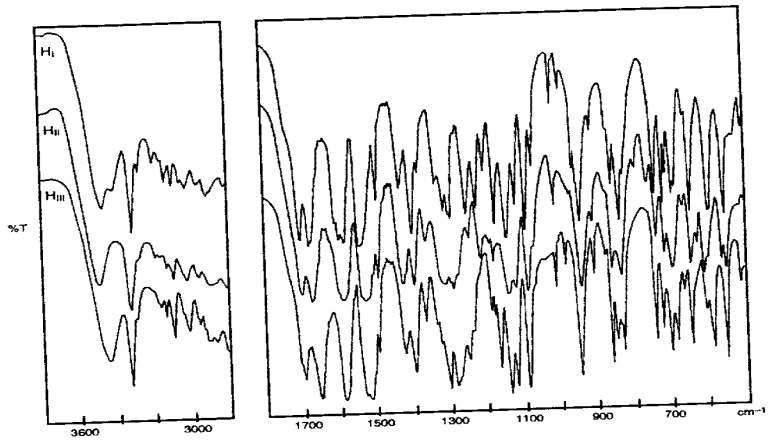

Figure 10.26 IR spectra of the polymorphic monohydrates of succinylsulfathiazole (Burger and Griesser, 1989).

Figure 10.26 shows
sulfathiazole. The IR sp
are different polymorph
tion patterns shown in F

The physical stabili
of succinylsulfathiazole
Figure 10.28. The mo
variety of methods used
crystal forms have diff
high humidity. The solu

Figure 10.27 X-ray powde
(Burger and

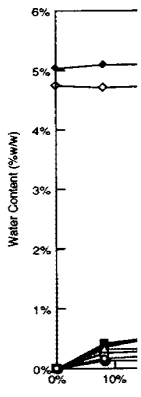

Figure 10.28 Water vapor
(Burger and

Figure 10.26 shows the IR spectra of the polymorphic monohydrates of succinylsulfathiazole. The IR spectra of these materials are also different establishing that these are different polymorphs. This conclusion is confirmed by the X-ray powder diffraction patterns shown in Figure 10.27.

The physical stability, water sorption, and solubility of the different crystal forms of succinylsulfathiazole have also been studied and are summarized in Table 10.9 and Figure 10.28. The most stable forms are Form I and hydrate H_I. In addition, the variety of methods used to prepare the different crystal forms are noted. The different crystal forms have differences in hygroscopicity and interconvert in the presence of high humidity. The solubilities of the different forms are also different. Most notable

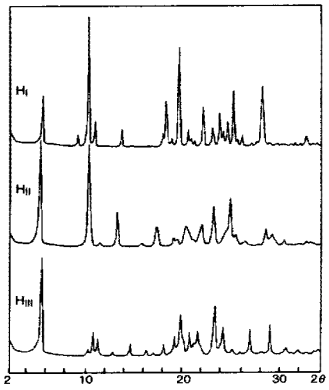

Figure 10.27 X-ray powder diffraction patterns of the three monohydrates of succinylsulfathiazole (Burger and Griesser, 1989).

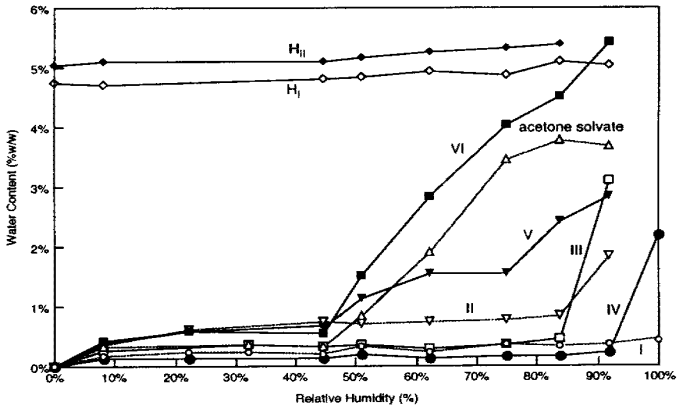

Figure 10.28 Water vapor sorption isotherms of the different crystal forms of succinylsulfathiazole (Burger and Griesser, 1991).

is that the differences in solubility among the anhydrate crystal forms is as large as a factor of 4 and that differences in solubility between anhydrate and hydrate crystal forms are as large as a factor of 12. This is one of many cases where anhydrate crystal forms have significantly higher solubilities than the hydrate.

Figure 10.28 shows the water vapor sorption isotherms for the different succinylsulfathiazole crystal forms. It is clear that some of the anhydrate forms absorb water relatively easily; furthermore, this data shows that the metastable forms are more hygroscopic.

Figure 10.29 shows the dissolution behavior of the different crystal forms of succinylsulfathiazole in buffer solution at pH 1.20 at 20 °C. It is clear that at equilibrium many of the anhydrates recrystallize and approach the solubility of the hydrates as might be expected. Figure 10.30 shows a van't Hoff plot for four of the crystal forms of succinylsulfathiazole. These curves do not cross in the temperature ranges studied and this indicates, in connection with the thermodynamic data, that all of the forms are monotropically related. Recall that monotropic forms retain the order of stability at all temperatures (see Section 5.2).

Figure 10.31 shows a scheme which illustrates the interconversion of the different crystal forms and methods to prepare each form. This figure illustrates how complicated interconversion of the different crystal forms can be. The van't Hoff plot clearly shows that the transformation of the more soluble form into the less soluble hydrate will occur at room temperature. This indicates the complications that can arise by relying on just one study and shows that several different approaches should be used to try to understand the interconversion of different crystal forms.

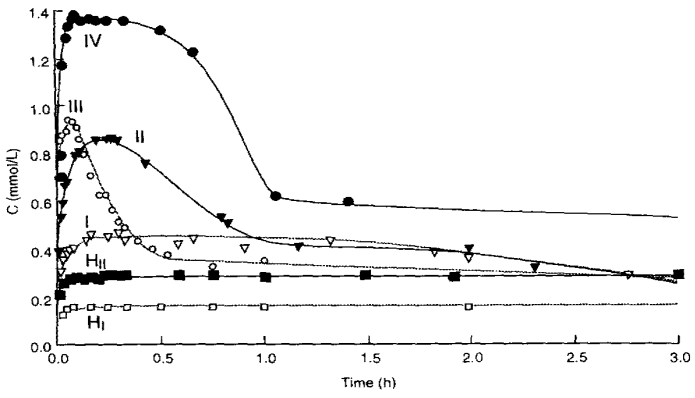

Figure 10.29 Dissolution behavior of the different crystal forms of succinylsulfathiazole in buffer solution, pH 1.3 at 20 °C (Burger and Griesser, 1991).

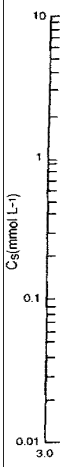

Figure 10.30 Van't Hoff pl
pH 1.3 (Burge

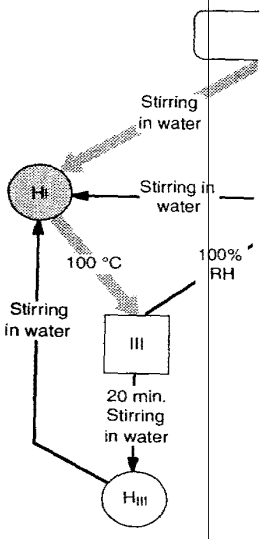

Figure 10.31 Diagram illu
produce the
mark paths w
most stable f

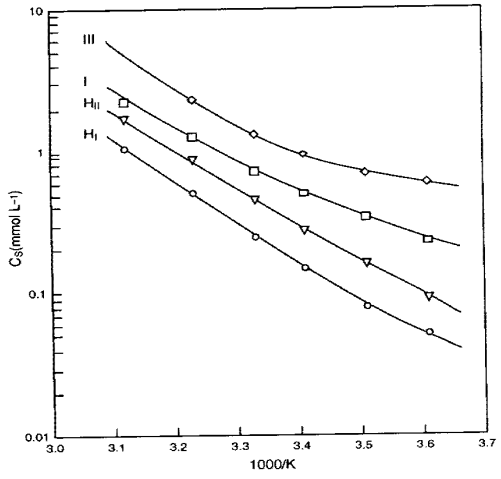

Figure 10.30 Van't Hoff plot of the solubility of four of the crystal forms of succinylsulfathiazole at pH 1.3 (Burger and Griesser, 1991).

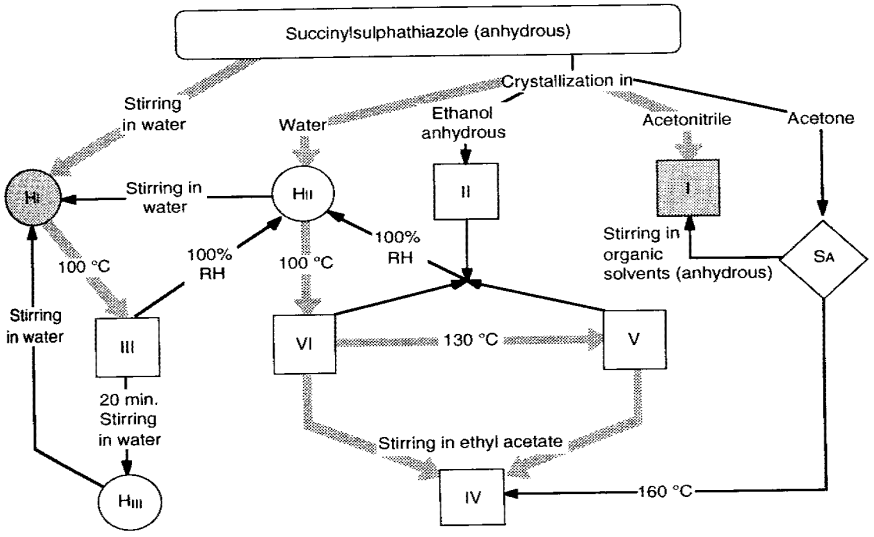

Figure 10.31 Diagram illustrating the most important transformation paths and production ways to produce the different crystal forms of succinylsulfathiazole. The thick, gray arrows mark paths whereby the different crystal forms can be produced in gram quantities. The most stable forms, Forms I and H_I, are shaded (Burger and Griesser, 1991).

D. SULFAMETER

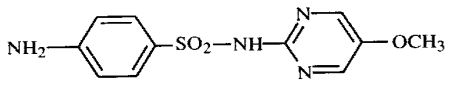

sulfameter

Sulfameter (sulfamethoxydiazine) exists in at least six different forms (Moustafa *et al.*, 1971). Form I (see Figure 10.32 and Table 10.10) is obtained by crystallization from boiling water or by heating any other form to 150 °C. Form II is prepared by rapid cooling of a saturated ethanol solution. Form III (see Figure 10.33 and Table 10.10) is obtained from a number of solvents including methanol, isopropanol, and ethanol. Forms IV and V are probably solvates and are obtained from dioxane and chloroform, respectively. An amorphous form is also known.

These forms were characterized by their infrared spectra, which are all slightly different, particularly in the 800-875, 900-970, 1550-1600, and 3000-3500 cm^{-1} regions of the spectrum. The powder diffraction patterns of these forms are also significantly different.

The forms can be interconverted by heating or grinding. Heating converts all forms to Form I, while grinding or suspension in water converts all forms to Form III. This behavior is discussed in more detail in the interconversion section (see Section 13.2B).

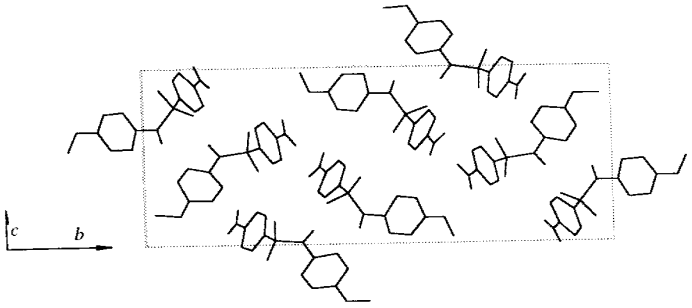

Figure 10.32 Crystal packing of sulfameter Form I (Giuseppetti *et al.*, 1977).

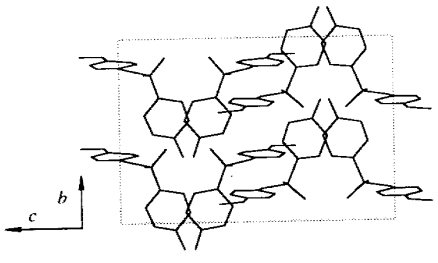

Figure 10.33 Crystal packing of sulfameter Form III (Giuseppetti *et al.*, 1977).

Table 10.10 Crystallographi

Parameter	
Space Group	
a (Å)	
b (Å)	
c (Å)	
β	1
Z	
ρ_{calc} (gm cm^{-3})	
V (Å^3)	

Giuseppetti *et al.*, 1977.

The dissolution rates
their relative bioavailabilit
ments are shown in Figu
dissolve most rapidly. F
Form II. It is also interest
amorphous form, sugges
surface area of Form II ma

Commercial preparati
mixtures of Forms I and I
ing. The significance of a
to be determined in separa

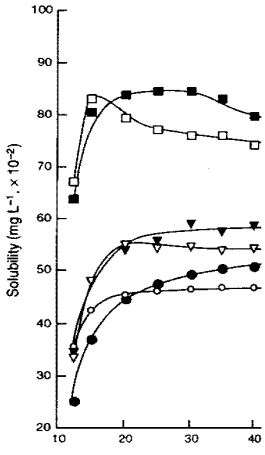

Figure 10.34 Dissolution rate

Table 10.10 Crystallographic Parameters for Sulfameter Forms I and III

Parameter	Form I	Form III
Space Group	$P2_1/c$	$C2/c$
a (Å)	8.358	13.370
b (Å)	26.833	11.735
c (Å)	11.964	15.928
β	111.36°	97.90°
Z	8	8
ρ_{calc} (gm cm^{-3})	1.490	1.504
V (Å^3)	2499	2475

Giuseppetti *et al.*, 1977.

The dissolution rates of these forms have been measured as a means of estimating their relative bioavailabilities (Moustafa *et al.*, 1971). The results of these measurements are shown in Figure 10.34. Obviously, Form II and the amorphous form dissolve most rapidly. Form III has the slowest dissolution rate, about half that of Form II. It is also interesting to note that Form II has a faster dissolution rate than the amorphous form, suggesting that the amorphous form may crystallize or that the surface area of Form II maybe much larger than that of the amorphous form.

Commercial preparations were also studied and, in general, contained Form I or mixtures of Forms I and III. These forms are the most stable and the slowest dissolving. The significance of any such differences with respect to bioavailability would have to be determined in separate experiments.

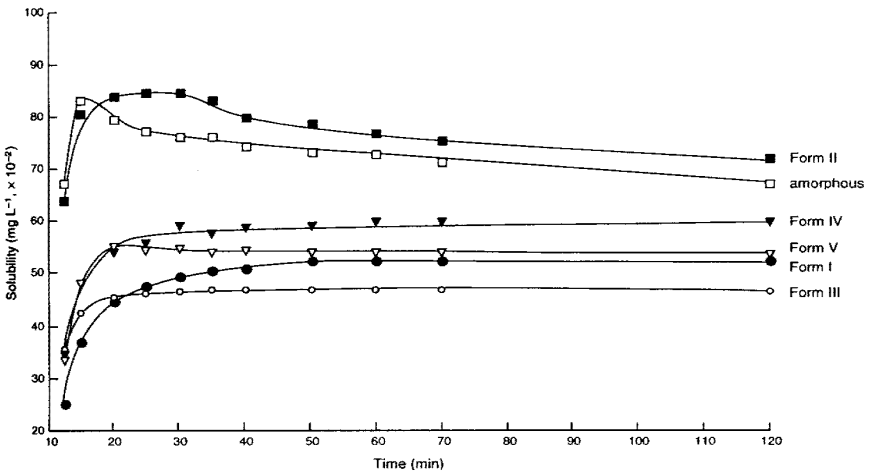

Figure 10.34 Dissolution rates of the different forms of sulfameter (Moustafa *et al.*, 1971).

E. Other Sulfonamides

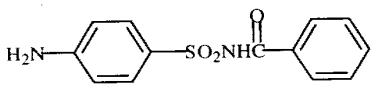

sulfabenzamide

Sulfabenzamide. Sulfabenzamide exists in four polymorphs and three solvates (Yang and Guillory, 1972). Form III can be transformed to Form I by **trituration**, and Form IV can be transformed to Form III and then Form I by heating. Desolvation of two of the solvates yielded Form II (see Figure 10.35).

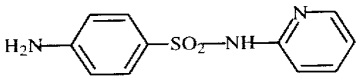

sulfapyridine

Sulfapyridine. Sulfapyridine (see Figures 10.35–10.39) exists in at least four polymorphs and one amorphous form (Yang and Guillory, 1972). The infrared spectra of two of these forms are identical, but their X-ray diffraction patterns are completely different. In addition, hot-stage experiments indicated that sulfapyridine crystallized in at least seven forms (Kuhnert-Brandstätter, 1971).

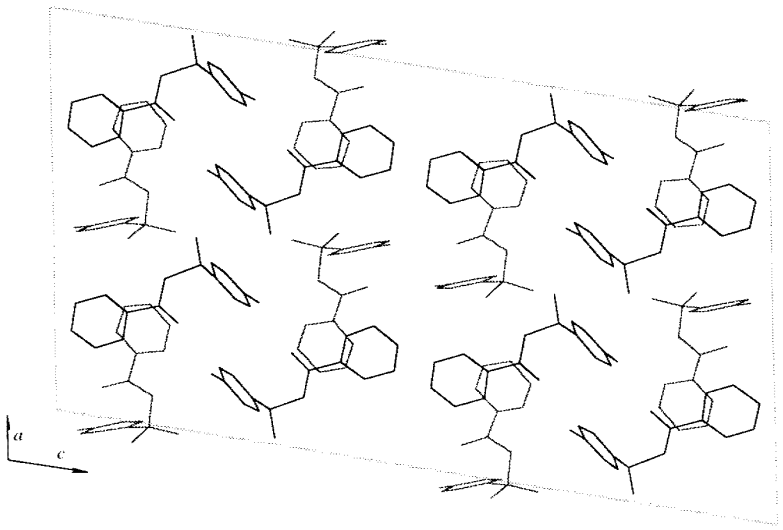

Figure 10.35 Crystal packing of sulfabenzamide Form II (Rambaud *et al.*, 1980).

Figure 10.36 Cryst

Figure 10.37 Cryst

Figure 10.38 Cryst

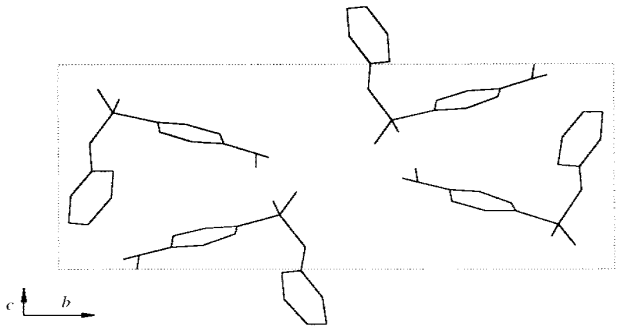

Figure 10.36 Crystal packing of sulfapyridine Form II (Bar and Bernstein, 1985).

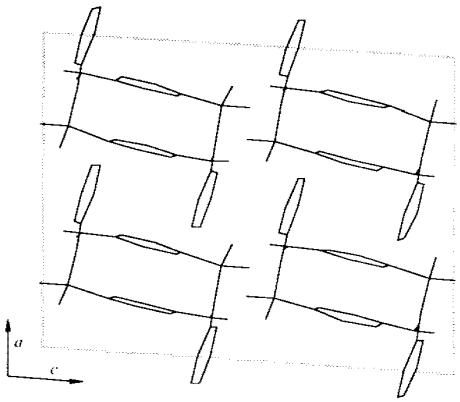

Figure 10.37 Crystal packing of sulfapyridine Form III (Basak *et al.*, 1984).

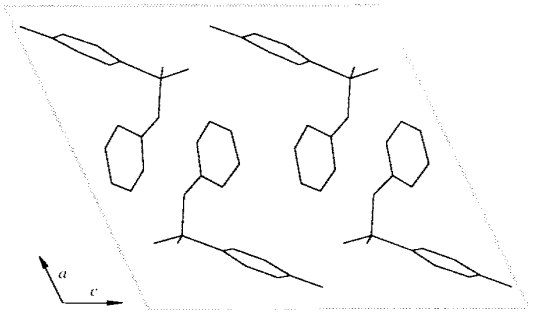

Figure 10.38 Crystal packing of sulfapyridine Form IV (Bernstein, 1988).

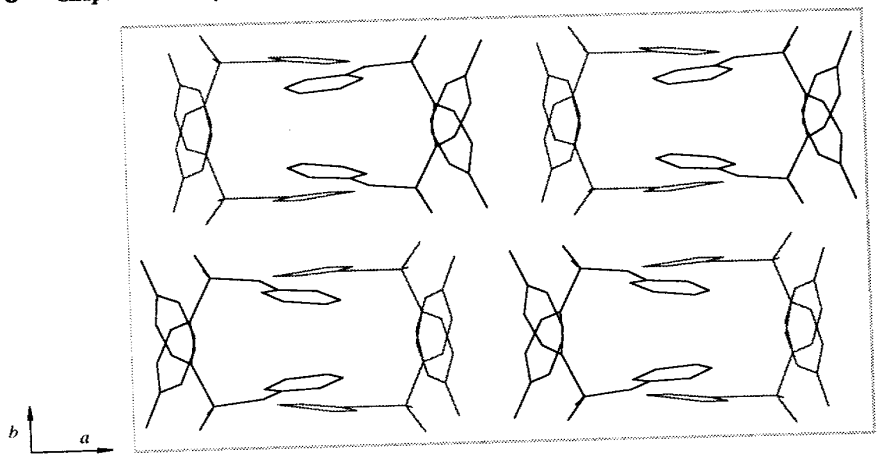

Figure 10.39 Crystal packing of sulfapyridine Form V (Bar and Bernstein, 1985).

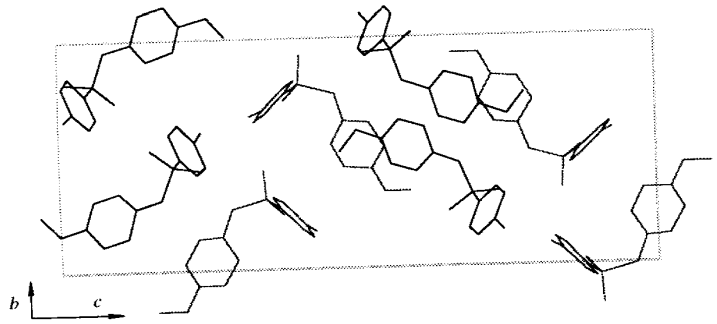

Figure 10.40 Crystal packing of sulfamethoxypyridiazine Form I (Basak *et al.*, 1987).

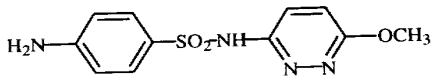

sulfamethoxypyridazine

Sulfamethoxypyridiazine. Sulfamethoxypyridiazine (see Figure 10.40) exists in at least three crystalline forms (Yang and Guillory, 1972). Form II can be transformed to Form I at 154 °C.

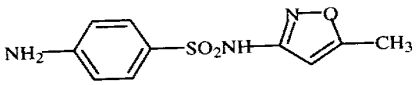

sulfamethoxazole

Sulfamethoxazole. Sulfamethoxazole (see Figures 10.41–10.42) exists in three polymorphs, and Form II can be converted to Form I at 164 °C (Yang and Guillory, 1972). These studies are in agreement with Kuhnert-Brandstätter (1971) who also

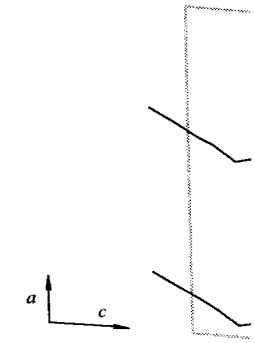

Figure 10.41 Crystal packing

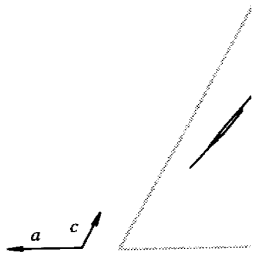

Figure 10.42 Crystal packing

showed there were three p
two forms of sulfamethox
10.41 and 10.42 show the
the conformations of the n

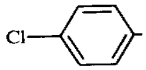

Chlorpropamide. Ch
morphs that have differe
obtained from aqueous et
or II at 110 °C. The infi

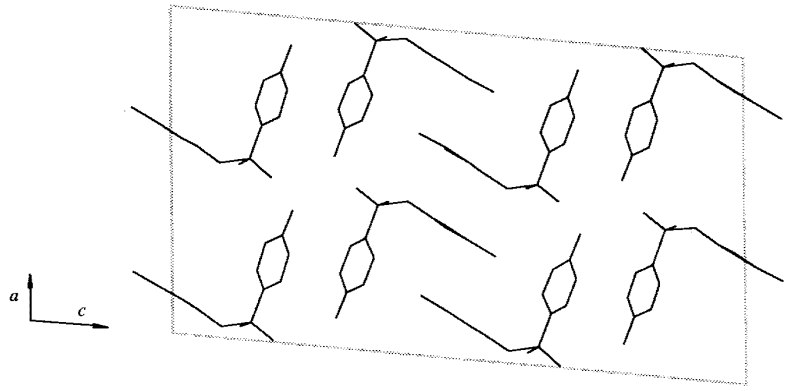

Figure 10.41 Crystal packing of sulfamethoxazole Form I (Bettinetti *et al.*, 1982).

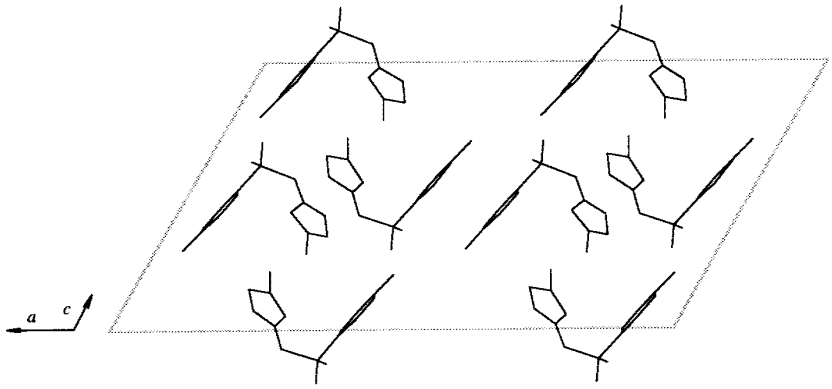

Figure 10.42 Crystal packing of sulfamethoxazole Form II (Bettinetti *et al.*, 1982).

showed there were three polymorphs of sulfamethoxazole. The crystal structures of the two forms of sulfamethoxazole were determined by Bettinetti *et al.* (1982). Figures 10.41 and 10.42 show the crystal packing in these two different forms. It appears that the conformations of the molecule in the two crystal forms are similar.

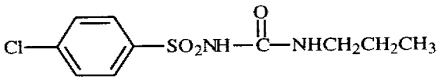

chlorpropamide

Chlorpropamide. Chlorpropamide (see Figure 10.43) exists in at least three polymorphs that have different diffraction patterns (Simmons *et al.*, 1973). Form I is obtained from aqueous ethanol, Form II from benzene, and Form III by heating Form I or II at 110 °C. The infrared spectra of all three forms are slightly different and the

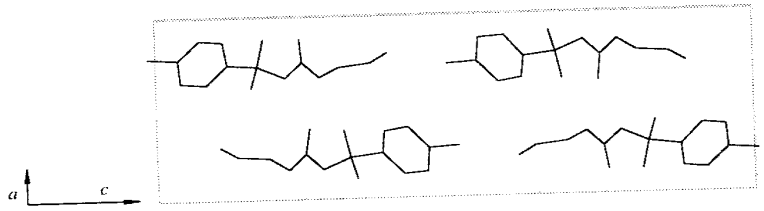

Figure 10.43 Crystal packing of chlorpropamide Form I (Koo *et al.*, 1980).

X-ray powder patterns of all three forms are significantly different, whereas the DSC thermograms obtained for the three forms are very similar.

The three forms of chlorpropamide have different dissolution rates. The dissolution rates of Forms I and III in water are identical, while Form II dissolves about half as fast. However, in beagle dogs, the serum levels following oral administration are identical for all three forms (Simmons *et al.*, 1973). Further single-crystal studies are necessary to completely characterize these forms and explain these results.

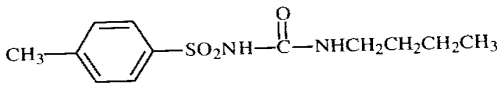

tolbutamide

Tolbutamide. Early studies (Simmons *et al.*, 1972) showed that tolbutamide crystallizes in two forms. Form I (see Figure 10.44) is obtained from benzene-hexane, and the crystals are prismatic with mp 127–128 °C. Form II is obtained from aqueous ethanol and the crystals are plates with mp 126–128 °C. Both the infrared spectra and the DTA thermograms of Forms I and II are slightly different. The DTA of Form II shows an endotherm at 113 °C that is not present in Form I. This endotherm apparently corresponds to the conversion of Form II to Form I. The dissolution rates of Forms I and II are the same in water at pH 5.5 and 7.3. The serum levels of these two forms are also identical. One explanation of this data is that, upon exposure to liquid, Form II is converted to Form I by a solution-mediated phase transformation.

More recent studies showed that tolbutamide exists in four crystal forms (Burger, 1975). In addition, aqueous suspensions of tolbutamide were found to thicken to an unpourable state upon occasional agitation. Analysis of the IR spectra and X-ray diffraction patterns confirmed that Form III had crystallized (Rowe and Anderson,

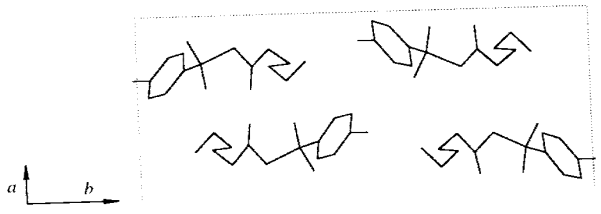

Figure 10.44 Crystal packing of tolbutamide Form I (Donaldson *et al.*, 1981; Nirmala and Gowda, 1981).

ln [Solubility] (mol/kg of Solvent)

Figure 10.45 Van
trans

1984). This is su
thought to be the
shown in Figure
close. Because
suspensions; how
lower energy fo
other solvents.

These data s
and that Form I i
was verified by
were placed in m
for several hours
the temperature v
grow throughout
room temperatur
dissolved. These
shown in Figure
thermal microsco

F. Conclusion

This section sho
polymorphism of
availability of a
number of ring-

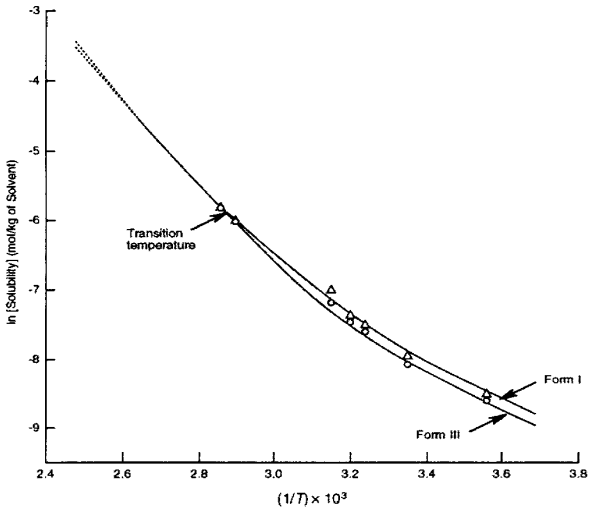

Figure 10.45 Van't Hoff plot of the solubilities of Forms I and III of tolbutamide showing the transition temperature (Rowe and Anderson, 1984).

1984). This is surprising since the suspensions were prepared with Form I which was thought to be the most stable polymorph. Solubility studies gave the van't Hoff plot shown in Figure 10.45. The aqueous solubilities of Form I and Form III are very close. Because of this, Form I may appear to be quite stable at low temperatures in suspensions; however, given sufficient time, Form I will transform to the Form III, the lower energy form. This interconversion was observed at room temperature in ten other solvents.

These data suggests that Form III is more stable than Form I at room temperature and that Form I is more stable than Form III at higher temperatures. This observation was verified by microscopy (Rowe and Anderson, 1984) in which Form III crystals were placed in mineral oil on a microscope hot stage. The sample was heated at 100 °C for several hours with periodic agitation by pressing and rotating the cover slip. When the temperature was reduced to 95 °C, prismatic crystals, typical of Form I, began to grow throughout the oil mixture and the Form III crystals dissolved. Upon cooling to room temperature, fine needles, typical of Form III, grew and the Form I crystals dissolved. These observations experimentally verify the result of the van't Hoff plot shown in Figure 10.45. These studies show the power of van't Hoff plots and also thermal microscopy in studying the interconversion of polymorphs.

F. Conclusion

This section shows the extent of polymorphism in the sulfonamides. The fact that polymorphism of these drugs is widespread yet unpredictable is probably due to (a) the availability of a variety of hydrogen-bonding schemes and (b) the occurrence of a number of ring-ring stacking modes. Further study of the polymorphism of these

compounds using single-crystal X-ray techniques should, no doubt, lead to a better general understanding of polymorphism.

10.5 STEROIDS

Steroids exhibit widespread polymorphism that may affect their bioavailability. A few examples of the polymorphism of steroids have been discussed in preceding sections.

Kuhnert-Brandstätter (1971) has studied the polymorphism of steroids using a Kofler hot stage, and the results of her studies are summarized in Table 10.11. This table clearly shows the extent of polymorphism in this important class of compounds. It should be noted that these studies are based mainly on hot-stage results. Other methods would be useful to verify the existence of these polymorphs and clarify the possible involvement of solvates.

Table 10.11 Melting Points of Polymorphic Steroids[a]

Compound	Forms I	II	III	IV	V
Allopregnane-3β,20α-diol	215–219	162–168			
Allopregnane-3,20-dione	202–206	198–203			
Androstane-3β,17β-diol	168–169	163–164	158–161	146–147	
Androstane-3,17-dione	132–134	128–130			
Androstanolone	182	168			
Δ^5-Androstene-3β,17α-diol	202–205	180–195			
Δ^5-Androstene-3β,17β-diol	181–185	177–180	155–158		
Δ^4-Androstene-3,17-dione	170–174	142–145			
Corticosterone	180–186	175–179	162–168	155–160	
Cortisone enanthate	138–140	135–137	129–132		
Dehydroepiandrosterone	149–153	139–141	137–140	130–136	
Dehydroepiandrosterone acetate	170–172	132–135	94–96	65–69	
Epiandrosterone	174–176	167–169			
α–Estradiol	225	223			
β–Estradiol	178	169			
Estradiol benzoate	188–195	177.5	176		
Estradiol dipropionate	107	97	82		
Estradiol 17-propionate	198–200	154–156			
Estrone	260–263	256	254		
Estrone methyl ether	172–174	123–126	88–92		
Etiocholane-3α-ol-17-one	150–152	141–143	133		
Etiocholane-17β-ol-3-one	141–143	103			
Fluorocortisone trimethylacetate	192–198	184–190			
9α-Fluorohydrocortisone acetate	225–233	208–212	205–208		
Hydrocortisone hemisuccinate	198–205	182–188	168–172		
Methandriol	205–208	202–205	196–198		
Methandriol dipropionate	83–86	74–75			
17α-Methandrostane-3β,17β-diol	213	205			

a Data from Kuhnert-Brandstätter (1971)

Table 10.11 (continued) Me

Compound
1-Methylandrostenolone acet
17α-Methylestradiol
6α-Methylprednisolone aceta
17-Norethisterone
Prednisolone
Prednisolone acetate
Progesterone
Testosterone
Testosterone isobutyrate
Testosterone nicotinate
Testosterone propionate

a Data from Kuhnert-Brandstät

A. ESTRONE

As indicated in Table 10.1
of all three polymorphs ha
of the estrone molecule is
three forms is shown in
molecules, but not obviou
and stacks of estrone mol
molecules. The crystal pa
of 2.26 and 2.47 Å; the c

Table 10.12 Crystallographic

	Form I
Space group	$P2_12_12_1$
a (Å)	12.188
b (Å)	16.301
c (Å)	7.463
β	90.00°
Z	4
V (Å^3)	1481
Source	Sublimati

Busetta *et al.*, 1973

Table 10.11 (continued) Melting Points of Polymorphic Steroids[a]

Compound	Forms I	II	III	IV	V
1-Methylandrostenolone acetate	143	106			
17α-Methylestradiol	190–194	188			
6α-Methylprednisolone acetate	225–229	208–212	205–210		
17-Norethisterone	200–207	199			
Prednisolone	218–234	215			
Prednisolone acetate	232–241	225–228	217–220		
Progesterone	131	123	111	106	100
Testosterone	155	148	144	143	
Testosterone isobutyrate	131–133	88–90			
Testosterone nicotinate	194–196	185–188			
Testosterone propionate	122	74			

a Data from Kuhnert-Brandstätter (1971)

A. Estrone

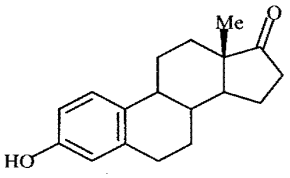

estrone

As indicated in Table 10.12 estrone exists in three polymorphs. The crystal structures of all three polymorphs have been determined (Busetta *et al.*, 1973). The conformation of the estrone molecule is similar in all three polymorphs. The crystal packing of these three forms is shown in Figures 10.46–10.48. Form I contains layers of estrone molecules, but not obvious stacks of estrone molecules. Form III contains both layers and stacks of estrone molecules. Form II has a herringbone arrangement of estrone molecules. The crystal packing of Form I appears to be controlled by H···H contacts of 2.26 and 2.47 Å; the crystal packing of Form II appears to be controlled by C···C

Table 10.12 Crystallographic Parameters of Three Estrone Polymorphs

	Form I	Form II	Form III
Space group	$P2_12_12_1$	$P2_12_12_1$	$P2_1$
a (Å)	12.188	10.043	9.271
b (Å)	16.301	18.424	22.285
c (Å)	7.463	7.787	7.610
β	90.00°	90.00°	111.45°
Z	4	4	4
V (Å^3)	1481	1440	1461
Source	Sublimation	Acetone	Sublimation

Busetta *et al.*, 1973

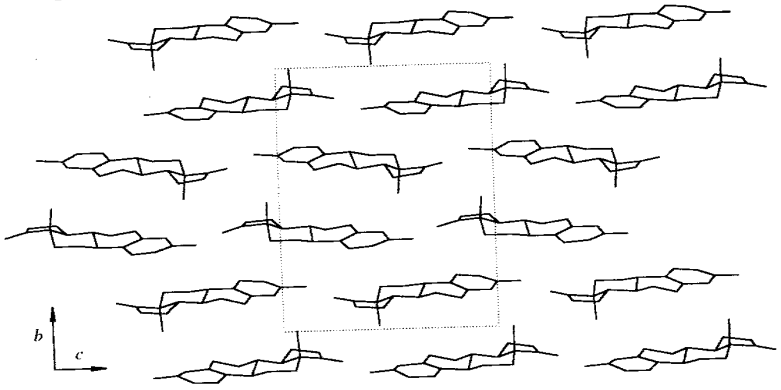

Figure 10.46 Crystal packing of estrone Form I (Busetta *et al.*, 1973).

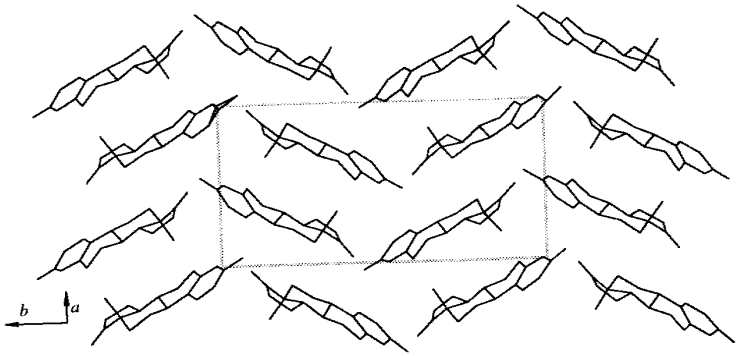

Figure 10.47 Crystal packing of estrone Form II (Busetta *et al.*, 1973).

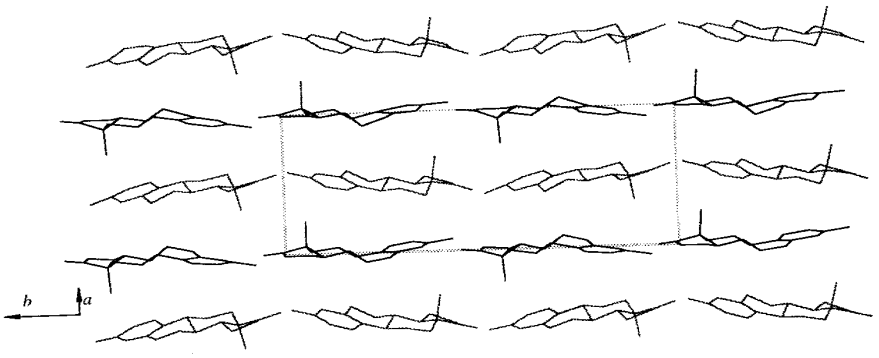

Figure 10.48 Crystal packing of estrone Form III (Busetta *et al.*, 1973).

contacts of 3.35
reported; howeve

B. PREDNISOLO

In our laboratory
Three crystal for
parameters and c
10.13. The cryst
ture of Form III
prednisolone in t

Table 10.13 Cryst

Space Group
a (Å)
b(Å)
c (Å)
β
Z
ρ_{calc} (g cm^{-3})
V (Å^3)
R

Sutton, 1984

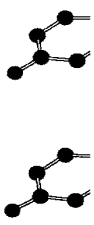

Figure 10.49 Stereo
(Sutto

contacts of 3.35 Å. No transformations or interconversions of these forms have been reported; however, it is likely that the densest form, Form II, is the most stable.

B. Prednisolone

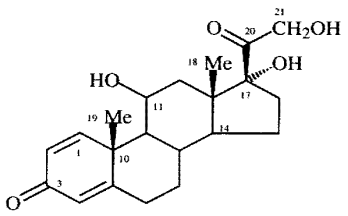

prednisolone

In our laboratory we have investigated the polymorphs of prednisolone (Sutton, 1984). Three crystal forms were obtained by crystallization from various solvents. The cell parameters and other crystallographic data for these three forms are shown in Table 10.13. The crystal structures of Forms I and II were determined but the crystal structure of Form III could not be refined to an acceptable R value. The conformation of prednisolone in the two crystal forms (Forms I and II) is shown in Figure 10.49 and

Table 10.13 Crystallographic Data for the Polymorphs of Prednisolone

	Form I	Form II	Form III
Space Group	$P2_1$	$P2_12_12_1$	$P2_12_12_1$
a (Å)	6.350 (3)	11.808 (7)	24.56 (2)
b (Å)	12.985 (8)	6.009 (2)	24.77 (4)
c (Å)	10.971 (9)	25.643 (12)	6.415 (3)
β	91.24°	90.00°	90.00°
Z	2	4	8
ρ_{calc} (g cm^{-3})	1.32	1.32	1.29
V (Å^3)	904.4	1819.5	3903.5
R	0.672	0.672	> 0.10

Sutton, 1984

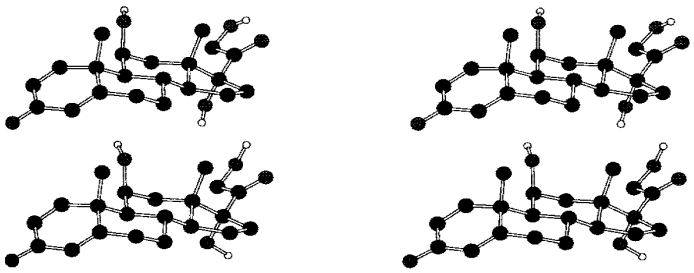

Figure 10.49 Stereoview of prednisolone Forms I (upper) and II (lower) conformations in the crystal (Sutton, 1984).

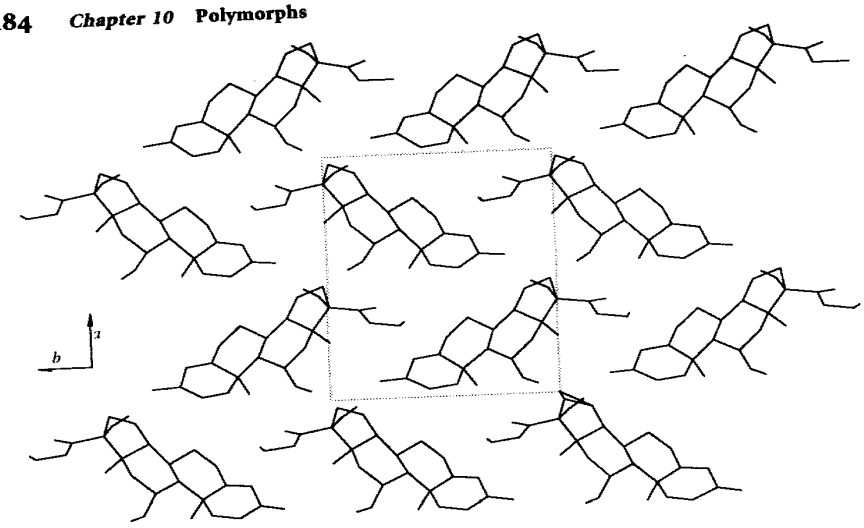

Figure 10.50 Crystal packing stereoview of prednisolone Form I (Sutton, 1984).

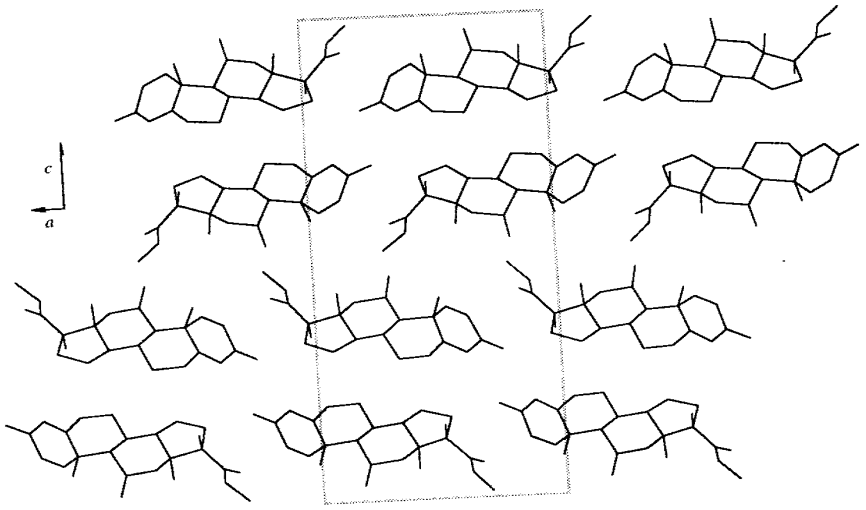

Figure 10.51 Crystal packing stereoview of prednisolone Form II (Sutton, 1984).

the crystal packing is shown in Figures 10.50–10.51.

The crystal packing shows that the arrangements of the prednisolone molecules in the unit cells of Forms I and II are similar but not identical. However, the solid-state NMR spectra of Forms I and II of prednisolone are different as illustrated by the spectra and the chemical shifts in Figure 10.52 and Table 10.14 (Saindon *et al.*, 1993).

Especially important for pu
the resonances assigned to
respectively.

The solid-state CP/MA
(labeled amount of 5 mg)
10.53 and required long a
comprises only about 5%
spectra shows that product
Further analysis showed th

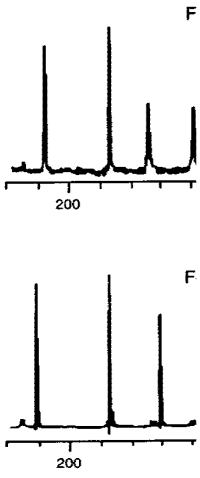

Figure 10.52 Solid-state CP/
(Saindon *et al.*,

Table 10.14 ^{13}C NMR Chem

Atom	Form I	Form II
C20	209.5	211.8
C3	188.1	187.g
C5	175.1	171.0
C13	159.8	157.3
C2	125.9	130.2
C4	121.8	123.8
C17	91.4	90.2
C11	69.9	70.4
C21	67.1	67.7
C9	55.4	54.8
C14	52.2	52.8

The assignment of this peak

Especially important for purposes of identification is the difference in chemical shifts of the resonances assigned to carbons C2 and C4 which occur between 120 and 140 ppm, respectively.

The solid-state CP/MAS ^{13}C NMR spectra of three generic prednisolone products (labeled amount of 5 mg) were also determined. These spectra are shown in Figure 10.53 and required long acquisition times since the active ingredient (prednisolone) comprises only about 5% of the approximately 100 mg tablets. Inspection of these spectra shows that products A and B contain Form I while product C contains Form II. Further analysis showed that all three products passed the USP dissolution test. Thus,

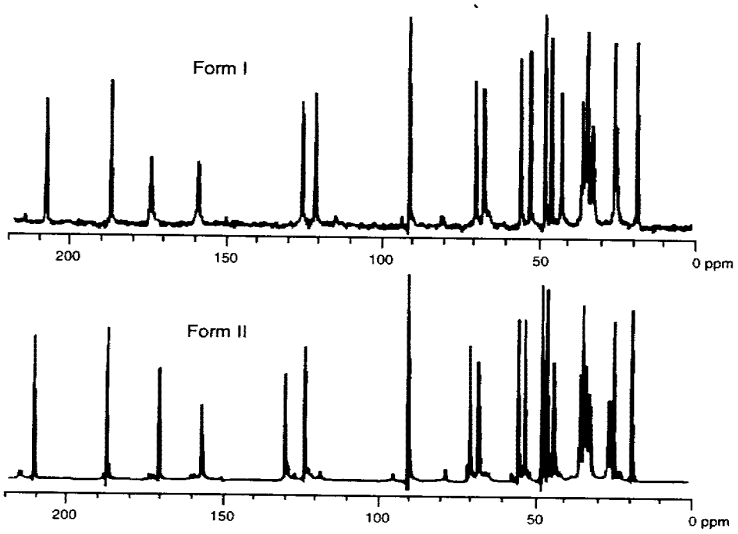

Figure 10.52 Solid-state CP/MAS ^{13}C NMR spectra of prednisolone Forms I (top) and II (bottom) (Saindon *et al.*, 1993).

Table 10.14 ^{13}C NMR Chemical Shifts of Prednisolone in the Solid-State and Solution

Atom	Form I	Form II	Solution	Atom	Form I	Form II	Solution
C20	209.5	211.8	211.5	C13	47.5	47.1	46.7
C3	188.1	187.g	185.1	C10	45.3	45.1	43.9
C5	175.1	171.0	170.5	C12	42.1	43.1	39.0
C13	159.8	157.3	156.8	C8[a]	35.3	34.7	34.1
C2	125.9	130.2	127.2	C16[a]	34.3	33.5	33.0
C4	121.8	123.8	121.7	C15[a]	33.5	32.7	32.7
C17	91.4	90.2	88.5	C6[a]	31.8	31.5	31.6
C11	69.9	70.4	68.6	C7[a]	24.6	25.4	31.2
C21	67.1	67.7	66.1	C18[a]	23.9	23.7	21.0
C9	55.4	54.8	55.5	C19[a]	17.3	18.1	17.0
C14	52.2	52.8	51.2				

a The assignment of this peak should be considered tentative (Saindon *et al.*, 1993)

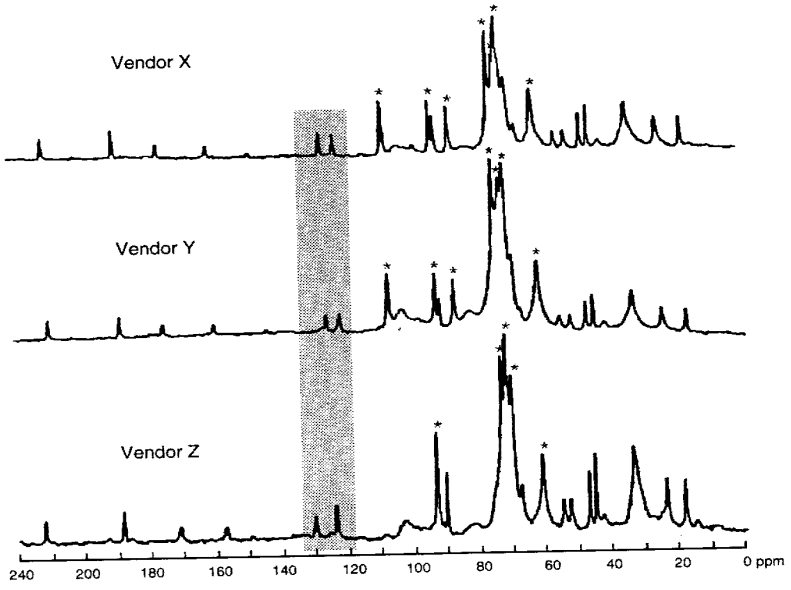

Figure 10.53 Solid-state CP/MAS ^{13}C NMR spectra of prednisolone tablets from three different vendors. The most evident differences are noted within the shaded region and the excipient signals are labeled with a star. (Byrn *et al.*, 1988).

these tablets represent a control problem because they contain different crystal forms but hopefully do not represent a serious clinical problem since they all meet the USP dissolution test.

C. Spironolactone

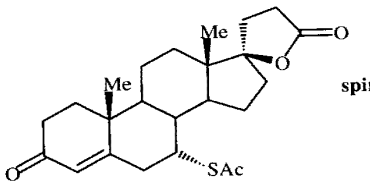

spironolactone

The polymorphism of spironolactone has been carefully studied using X-ray crystallography (Agafonov *et al.*, 1991). The data for the different forms are described in Table 10.15.

Spironolactone is of interest because it shows variable solubility and dissolution rate as well as pharmaceutical performance as an oral drug. Recently, a number of crystal forms of this compound have been discovered (see Table 10.15). As is the case for many steroids, both solvated and unsolvated crystal forms have been obtained. Figure 10.54 shows the TGA curves of the different crystal forms, clearly Forms III

Table 10.15 Spironolacto

Solvent	Method[a]
Acetone	1
Acetone	2
Dioxane	1
Dioxane	2
Chloroform	1
Chloroform	2
Acetonitrile	—[b]
Ethanol	—[b]
Ethyl acetate	—[b]
Methanol	—[b]

a Method 1—the sample is
0° C within a few hours; m
ture and the solvent allowe
the two methods of prepar
fraction pattern. (Agafono

through VI are solvate
crystal forms confirmin

Table 10.16 lists t
spironolactone, clearly
10.17 tabulates the pow
that Forms I through I
(Agafonov *et al.*, 1991
crystal forms of spiron
(Form I) is shown in Fi
Figure 10.57. The conf
it is clear that the crystal

Mass (mg)

Figure 10.54 TGA curves

Table 10.15 Spironolactone Single-Crystal Preparation Methods and Thermodynamic Data

Solvent	Method[a]	Form Obtained	T_{dec} (°C)	ΔH_{dec} (J/g)	T_f (°C)	ΔH_f (J/g)
Acetone	1	I	...	...	205 ± 1	48 ± 3
Acetone	2	II	...	...	210 ± 1	53 ± 4
Dioxane	1	Glass[c]	...	...	...	...
Dioxane	2	II	...	...	210 ± 1	53 ± 4
Chloroform	1	Glass[c]	...	...	...	...
Chloroform	2	II	...	...	210 ± 1	53 ± 4
Acetonitrile	—[b]	Solvate (2:1) (III)	137 ± 2	38 ± 2	210 ± 1	52 ± 4
Ethanol	—[b]	Solvate (2:1) (IV)	100 ± 2	28 ± 2	210 ± 1	54 ± 4
Ethyl acetate	—[b]	Solvate (4:1) (V)	102 ± 6	28 ± 1	210 ± 1	54 ± 4
Methanol	—[b]	Solvate (1:2) (VI)	25-126	50 ± 2	210 ± 1	52 ± 3

a Method 1—the sample is dissolved in the solvent at close to its boiling point and cooled to 0° C within a few hours; method 2—the sample is dissolved in the solvent at room temperature and the solvent allowed to evaporate slowly during several weeks. *b* For these solvents, the two methods of preparation give the same results. *c* Glass-like solid without X-ray diffraction pattern. (Agafonov *et al.*, 1991)

through VI are solvates. Figure 10.55 shows the DSC thermograms of the different crystal forms confirming that Forms III through VI contain solvent of crystallization.

Table 10.16 lists the crystallographic parameters of the different crystal forms of spironolactone, clearly showing that the different forms have distinct structures. Table 10.17 tabulates the powder patterns for Forms I through III. It is clear from this table that Forms I through III have different powder diffraction patterns. These workers (Agafonov *et al.*, 1991) were able to determine the crystal structures of three of the crystal forms of spironolactone and the contents of the unit cell for the needle form (Form I) is shown in Figure 10.56, the contents of the unit cell for Form II is shown in Figure 10.57. The conformation of the steroid is the same in all three crystal forms but it is clear that the crystal packing is different.

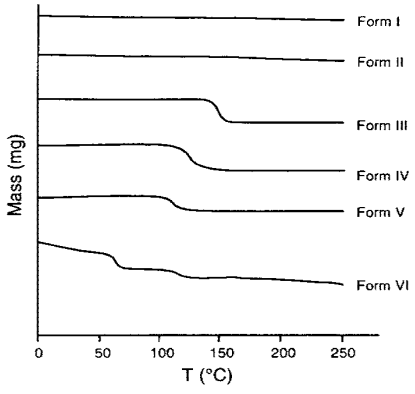

Figure 10.54 TGA curves of spironolactone crystal forms (Agafonov *et al.*, 1991).

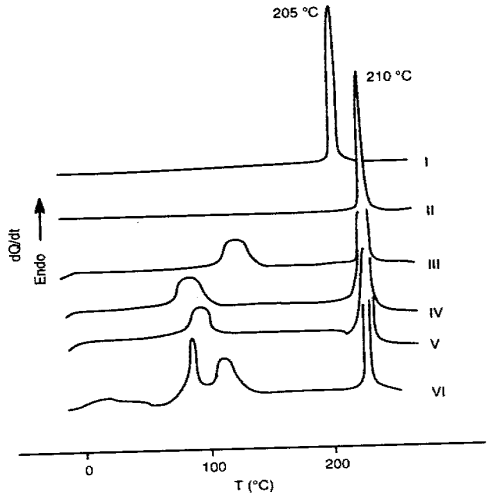

Figure 10.55 DSC thermograms of spironolactone crystal forms (Agafonov *et al.*, 1991).

Table 10.16 Crystallographic Data for the Crystal Forms of Spironolactone

Parameter	Form I	Form II	Form III	Form IV	Form V
Space group	$P2_12_12_1$	$P2_12_12_1$	$P2_1$	$P2_12_12_1$	$P2_12_12_1$
a (Å)	9.979	10.584	11.857	10.14	10.15
b (Å)	35.573	18.996	19.655	36.21	36.22
c (Å)	6.225	11.005	11.346	6.28	6.29
β	90.00	90.00	118.13	90.00	90.00
Z	4	4	2	4	4
V (Å^3)	2209.8	2212.6	2318.7	2306	2315
Crystal System	Orthorhombic	Orthorhombic	Monoclinic	Orthorhombic	Orthorhombic
Morphology	Needle-like	Prisms	Trigonal prisms	Needle-like	Needle-like
Solvate	...	...	½ acetonitrile	½ ethanol	¼ ethyl acetate

Agafonov *et al.*, 1991.

Table 10.17 X-ray Powder Diffraction Data for the Different Crystal Forms of Spironolactone

Form I			Form II			Form III		
d_{hkl} (Å)	I^a	$h\ k\ l$	d_{hkl} (Å)	I^a	$h\ k\ l$	d_{hkl} (Å)	I^a	$h\ k\ l$
17.8	w	0 2 0	9.5	s	0 2 0	9.8	s	0 2 0
8.9	m	0 4 0	7.63	w	1 0 1	8.9	w	0 1 1
8.7	vs	1 2 0	7.00	m	1 2 0	8.8	w	1 1 1
7.63	s	1 3 0	5.43	s	1 3 0	6.99	w	1 2 1
6.64	m	1 4 0	5.29	s	0 1 2	5.55	s	1 3 0

a vs–very strong intensity, s–strong intensity, m–medium intensity, w–weak intensity, vw–very weak intensity (Agafonov *et al.*, 1991).

Table 10.17 (continued)

Form I		
d_{hkl} (Å)	I^a	$h\ k\ l$
6.13	w	0 1 1
5.93	vw	0 6 0
5.10	w	1 6 0
4.94	m	2 1 0
4.68	vs	0 5 1
4.599	s	2 3 0
4.528	s	1 7 0
4.351	m	2 4 0
3.870	m	2 0 1
3.699	m	1 9 0

a vs–very strong intensit
intensity (Agafonov *et a*

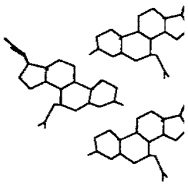

Figure 10.56 Contents o

Figure 10.57 Contents of

Table 10.17 (continued) X-ray Powder Diffraction Data for the Different Crystal Forms of Spironolactone

Form I			Form II			Form III		
d_{hkl} (Å)	I^a	*h k l*	d_{hkl} (Å)	I^a	*h k l*	d_{hkl} (Å)	I^a	*h k l*
6.13	w	0 1 1	5.10	m	2 1 0	5.48	s	0 3 1
5.93	vw	0 6 0	4.87	w	1 0 2	5.46	s	1 3 1
5.10	w	1 6 0	4.73	w	1 1 2	5.09	s	1 2 1
4.94	m	2 1 0	4.333	m	1 4 0	5.05	w	2 1 0
4.68	vs	0 5 1	4.263	w	2 1 2	4.97	m	2 0 –2
4.599	s	2 3 0	4.032	m	1 4 1	4.91	s	0 4 0, 1 2 2
4.528	s	1 7 0	3.815	w	2 0 2	4.456	m	0 2 2, 1 4 0
4.351	m	2 4 0	3.741	w	2 1 2	4.287	m	1 3 2
3.870	m	2 0 1	3.576	w	1 5 0	3.931	w	2 0 1
3.699	m	1 9 0	3.540	w	2 2 2	3.837	w	3 1 1, 3 0 2

a vs–very strong intensity, s–strong intensity, m–medium intensity, w–weak intensity, vw–very weak intensity (Agafonov *et al.*, 1991).

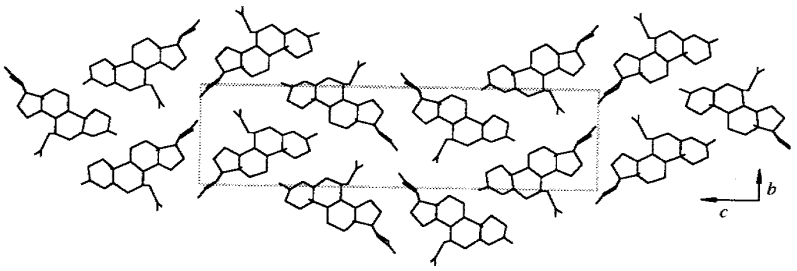

Figure 10.56 Contents of the unit cell of Form I of spironolactone (Dideberg *et al.*, 1972).

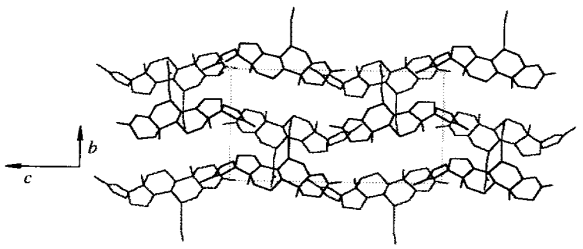

Figure 10.57 Contents of the unit cell of Form II of spironolactone (Agafonov *et al.*, 1989).

D. Methylprednisolone

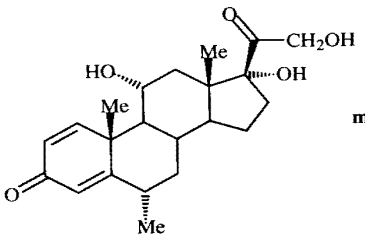

methylprednisolone

Methylprednisolone exists in two polymorphs. Form I can be prepared by recrystallization from acetone, and Form II by sublimation at 190 °C (Hamlin *et al.*, 1962). Dissolution rates of pellets of these two forms were studied under varying conditions of agitation. Under all conditions, except the most rapid agitation, Form II has a faster dissolution rate than Form I. *In vivo* tests of the rate of dissolution of Forms I and II using pellet implants in rats showed that Form II has a faster dissolution rate than Form I.

Studies of the intrinsic dissolution rates (see Chapter 6) of Forms I and II also showed that Form II has a faster dissolution rate than Form I. At increased stirring rates, Forms I and II had more similar dissolution rates. These studies also indicated that low agitation rates give data that correlate with the pellet-implant *in vivo* data, while higher agitation rates are required to give results that correlate with data from trials involving tablets dissolving in the stomach (Levy and Procknal, 1964).

Infrared spectroscopy showed that the surfaces of pellets of Form II revert to Form I in water, even after only a 2-minute exposure. This appears to be a water-mediated phase transformation of the type discussed by Haleblian and McCrone (1969). This observation explains some of the conflicting data obtained in measuring the dissolution rates of Form II in water (Higuchi *et al.*, 1969).

E. Hydrocortisone 21-*tert*-Butylacetate

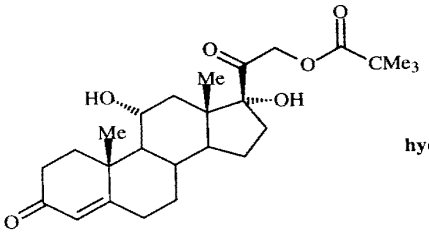

hydrocortisone 21-*tert*-butylacetate

Biles (1963) reported that hydrocortisone 21-*tert*-butylacetate crystallizes in three forms. X-ray diffraction studies in our laboratory indicate that there are actually at least four different forms, and elemental analysis shows that two of these forms contain different amounts of ethanol. The results of these studies are shown in Table 10.18. Several other forms (from other solvents or from desolvation of a solvate by heating) are also known and have a melting point of 234–238 °C (Lin *et al.*, 1982).

Table 10.18 Crysta

Crystal Form
I
II
III
IV

a The exact melting
at this temperature
melt resolidified as

During recrys
III, often formed
new form, design
120 °C. Forms I
while Form III ch

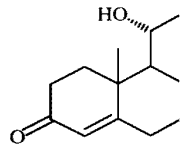

hydrocortiso

All crystal fo
light. Form I
ultraviolet light i
°C. The formatio
NMR chemical sh
by gas chromato
21-*tert*-butylaceta

Table 10.19 Desol
Butyl

Days
1
2
3
6
10
14
21

Lin *et al.*, 1982.

Table 10.18 Crystal Forms of Hydrocortisone 21-*tert*-Butylacetate

Crystal Form	Ethanol Content (mole ratio)	Oxidation in UV Light	Mp[a] (°C)
I	0.9 (variable)	Reaction	170-180
II	1.0	No Reaction	110-120[b]
III	0	No Reaction	123-126[c]
IV	0	No Reaction	234-238

a The exact melting temperature may vary from one crystal to another. *b* Opaque at this temperature range with final melting at 234–238 °C. *c* After melting, the melt resolidified as the temperature was increasing. (Lin *et al.*, 1982)

During recrystallization from ethanol, a mixture of crystal forms, Forms I, II, and III, often formed but a pure single form could be obtained under certain conditions. A new form, designated Form IV, was produced when Forms I, II, and III were heated at 120 °C. Forms I and II underwent desolvation and phase transformation to Form IV, while Form III changed from one phase to another.

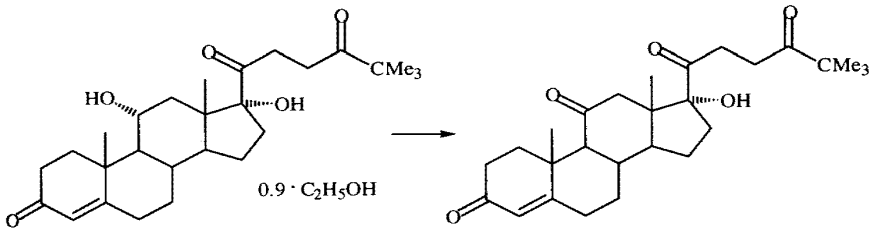

hydrocortisone 21-*tert*-butylacetate **cortisone 21-*tert*-butylacetate**

All crystal forms, except for Form I, were stable upon irradiation with ultraviolet light. Form I was oxidized to cortisone 21-*tert*-butylacetate upon irradiation with ultraviolet light in air. A known weight of crystals was put in vials and irradiated at 30 °C. The formation of cortisone 21-*tert*-butylacetate was determined by the change in the NMR chemical shift of the C18 methyl signal, and the content of ethanol was measured by gas chromatography. The percent of desolvation and oxidation of hydrocortisone 21-*tert*-butylacetate to cortisone 21-*tert*-butylacetate is shown in Table 10.19. The loss

Table 10.19 Desolvation and Oxidation of Crystalline Hydrocortisone 21-*tert*-Butylacetate Form I (0.9 Ethanolate) upon Exposure to UV Light

Days	% Oxidation	Ethanol Lost
1	20.0	43.3%
2	38.9	75.6%
3	50.0	83.3%
6	52.9	88.9%
10	56.3	93.3%
14	66.7	95.6%
21	71.4	96.7%

Lin *et al.*, 1982.

of ethanol is faster than oxidation but does not completely precede oxidation. In addition, ethanol loss does not occur from crystals stored in the dark, indicating that oxidation is required for ethanol loss to begin. Further studies of this interesting reaction are in order. This behavior is different from that of dihydrophenylalanine hydrate, in which water loss almost completely preceded oxidation (Byrn and Lin, 1976).

F. Conclusion

The steroids exhibit a wide range of polymorphic and solvate behavior which appears to affect both the bioavailability and stability of these compounds. Of particular interest are the cases where one form is chemically reactive in the solid state while the others are stable.

10.6 Barbiturates

Barbiturates are another class of drugs which generally exhibit polymorphism. As in the discussions of the polymorphism of sulfonamides and steroids just presented, this section begins with Table 10.20 describing the results of hot-stage experiments on barbiturates (Kuhnert-Brandstätter, 1971).

Table 10.20 Melting Points of Polymorphs of Barbiturates[a]

Compound	I	II	III	IV	V	VI	VII	VIII	IX	X	XI
Allobarbital	173	~122									
5-Allyl-5-(2-Cyclopentenyl-1-yl)barbituric acid	148	126	124	115	—						
5-Allyl-5-phenyl-barbituric acid	159	133	130	129	128	126					
Amobarbital	157	151									
Aprobarbital	141	139	133	130	~116	~95					
Barbital	190	184	183	181	176	159					
Butallylonal	131	128	104								
Buthalitone	149	117	~95								
5-Crotyl-5-ethyl-barbituric acid	117	90									
Cyclobarbital	173	161									
Dipropylbarbital	148	146	126	120	~110	105	85				
Dormovit	171	146									
Ethallobarbital	160	149	137	129	117	108					
5-Ethyl-5-(1-piperidyl)-barbituric acid	217	210	204								
Heptabarbital	174	150	145	143	141	137	127	100			
Hexobarbital	146										

a Kuhnert-Brandstätter (1971).

Table 10.20 (continued) Melting Points

Compound	I
5-Methyl-5-phenyl-barbituric acid	226
Pentobarbital	129
Phenobarbital	176
Propallylonal	184
Secobutabarbital	166
Thialbarbital	146
Thiothyr	176
Vinbarbital	166

a Kuhnert-Brandstätter (1971).

A. Amobarbital

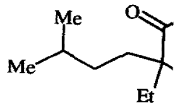

ven and Vizzini (1969) have det
phs of amobarbital (5-ethyl-5-iso
parameters shown in Table 10.21
The conformation of amobarbita
rystal packing is different (see F
double-ribbon arrangement; ho
ets, while in Form II an interl
density.

.21 Crystallographic Parameters fo

eter	Form I
oup	*C2/c*
	21.480
	11.590
	10.370
	97.07°
	8
	2562.0
³)	1.171
t	Plates developed on
	154–156

zini, 1969.

Table 10.20 (continued) Melting Points of Polymorphs of Barbiturates[a]

Compound	I	II	III	IV	V	VI	VII	VIII	IX	X	XI
5-Methyl-5-phenyl-barbituric acid	226	226	200								
Pentobarbital	129	114	108								
Phenobarbital	176	174	167	163	160	157	153	141	133	126	112
Propallylonal	184	180	~179	~127	~123						
Secobutabarbital	166	—									
Thialbarbital	146	125									
Thiothyr	176	172									
Vinbarbital	166	129	106								

a Kuhnert-Brandstätter (1971).

A. Amobarbital

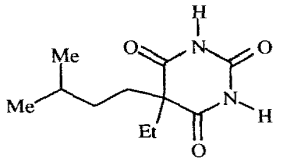

amobarbital

Craven and Vizzini (1969) have determined the crystal structures of the two polymorphs of amobarbital (5-ethyl-5-isopentylbarbituric acid). The two forms have the cell parameters shown in Table 10.21.

The conformation of amobarbital is virtually identical in the two polymorphs but the crystal packing is different (see Figures 10.58–10.59). Both forms show the so-called double-ribbon arrangement; however, in Form I there is no interaction between the sheets, while in Form II an interlocking structure is present resulting in a slightly higher density.

Table 10.21 Crystallographic Parameters for the Two Forms of Amobarbital

Parameter	Form I	Form II
Space group	$C2/c$	$P2_1/c$
a (Å)	21.480	10.281
b (Å)	11.590	22.061
c (Å)	10.370	11.679
β	97.07°	109.10°
Z	8	8
V (Å^3)	2562.0	2503.1
ρ_{calc} (g cm^{-3})	1.171	1.178
Crystal habit	Plates developed on 1 0 0	Needles elongated along b-axis
Mp (°C)	154–156	160–162

Craven and Vizzini, 1969.

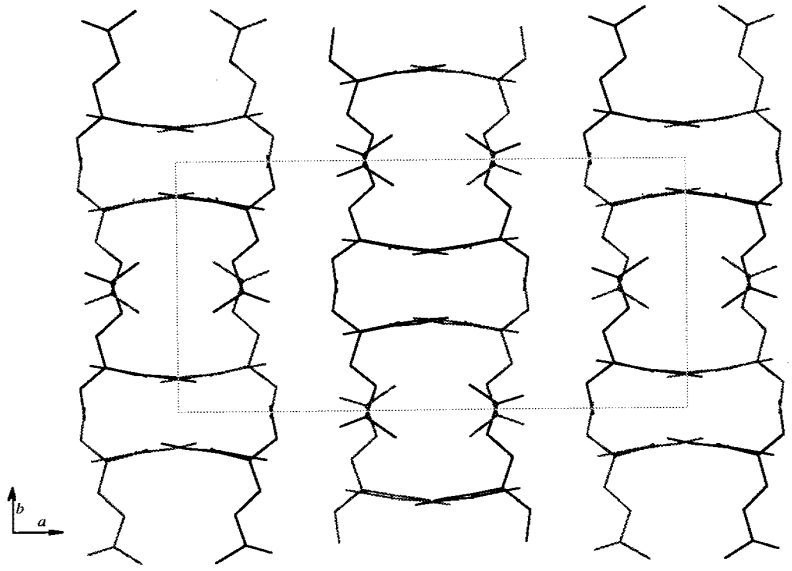

Figure 10.58 The crystal structure of Form I of amobarbital viewed down the *c* axis (Craven and Vizzini, 1969).

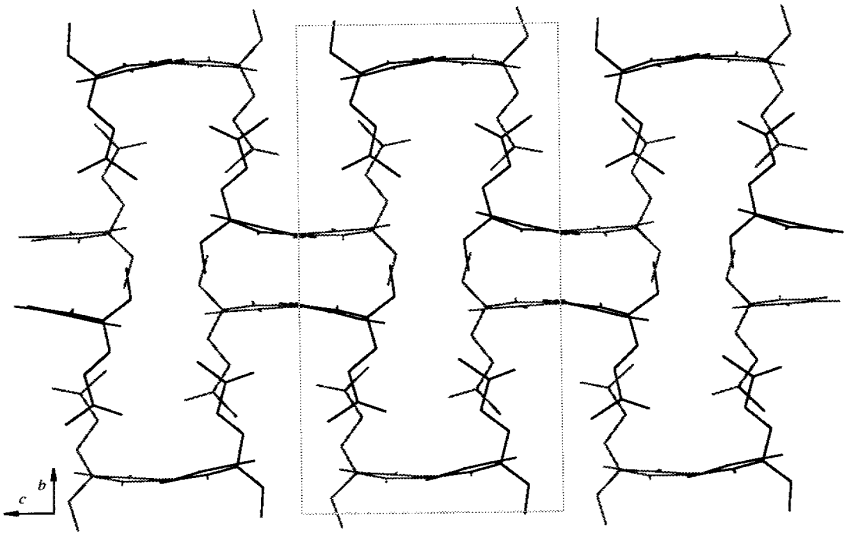

Figure 10.59 The crystal structure of Form II of amobarbital viewed down the *a* axis (Craven and Vizzini, 1969).

B PHENOBARBITAL

Phenobarbital (5-ethyl-5-ph
many as thirteen modificati
least four distinct anhydrou

The crystal structures
have been determined (W
phenobarbital, including the
two forms. The crystal pac
somewhat different; howev
hydrogen-bonded pyrimidi

Kopp *et al.* (1988) repo
of polymorphic phenobarbi
can easily lead to misunder
to identify the different cry
obtained if different heating
also influenced the DSC re
DSC methodology outlined

A study by Szabó-Révé
ers Avicel® PH 101 or Hew
(obtained by heating a comr
two commercial sources lab
phenobarbital. The dissolut
were different as shown in
and other similar observat
dissolution rates.

Table 10.22 Crystallographic

Parameter	Form I[a]
Space group	$P2_1/n$
a (Å)	6.800
b (Å)	47.174
c (Å)	10.695
α	90.00°
β	94.18°
γ	90.00°
Z	12
V (Å^3)	3421.7
ρ_{calc} (gm cm^{-3})	1.352

a Williams, 1973. *b* Williams,

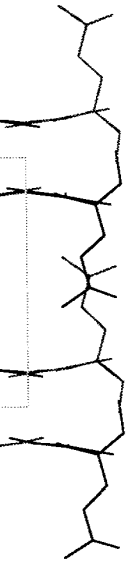

c axis (Craven and

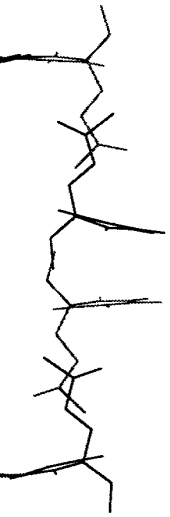

e *a* axis (Craven and

B PHENOBARBITAL

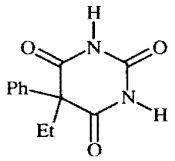

phenobarbital

Phenobarbital (5-ethyl-5-phenylbarbituric acid) has been reported to crystallize in as many as thirteen modifications. Single-crystal studies of these polymorphs revealed at least four distinct anhydrous forms and one hydrate (see Table 10.22).

The crystal structures of the hydrate (Form XIII) and of Forms I, II, III, and V have been determined (Williams, 1973; Williams, 1974). The conformations of phenobarbital, including the angle between the two rings, are slightly different in these two forms. The crystal packing of these two forms, shown in Figures 10.60–10.61, is somewhat different; however, both forms contain layers of phenyl rings and layers of hydrogen-bonded pyrimidine rings.

Kopp *et al.* (1988) reported a study of DSC and X-ray powder diffraction patterns of polymorphic phenobarbital. Their work demonstrates that using one technique alone can easily lead to misunderstandings. It was not possible to use the DSC thermograms to identify the different crystal forms of phenobarbital because different results were obtained if different heating rates were used. In addition, they found that particle size also influenced the DSC results. These results are consistent with the discussion of DSC methodology outlined in Chapter 5.

A study by Szabó-Réveśz *et al.* (1987) used direct compression with the dry binders Avicel® PH 101 or Heweten® 40 to evaluate manufactured tablets containing Form I (obtained by heating a commercial product near 160 °C for 3 h), Form II (obtained from two commercial sources labeled II_1 and II_2), or Form III (obtained by spray drying) of phenobarbital. The dissolution rates of the tablets containing the various crystal forms were different as shown in Figure 10.62 but by only a few percent. This observation and other similar observations suggest that different polymorphs may give similar dissolution rates.

Table 10.22 Crystallographic Parameters for the Crystal Forms of Phenobarbital.

Parameter	Form I[a]	Form II[a]	Form III[b]	Form V[a]	Form XIII (hydrate)[a]
Space group	$P2_1/n$	$P\bar{1}$	$P2_1/c$	$P2_1/c$	$Pbca$
a (Å)	6.800	6.784	9.534	12.66	7.157
b (Å)	47.174	23.537	11.855	6.75	30.879
c (Å)	10.695	10.741	10.794	27.69	10.87
α	90.00°	91.89°	90.00°	90.00°	90.00°
β	94.18°	94.43°	111.56°	106.9°	90.00°
γ	90.00°	89.03°	90.00°	90.00°	90.00°
Z	12	6	4	8	8
V (Å^3)	3421.7	1708.8	1134.6	2264.1	2402.3
ρ_{calc} (gm cm^{-3})	1.352	1.354	1.360	1.362	1.384

a Williams, 1973. *b* Williams, 1974.

The effect of additives on the crystallization of phenobarbital has also been investigated (Kato *et al.*, 1984). Kato and co-workers prepared two forms of phenobarbital by adding barbital or cyclobarbital to the crystallization. In these studies rather large quantities of additive (7.5% for barbital and 7% cyclobarbital) were required to achieve the effect.

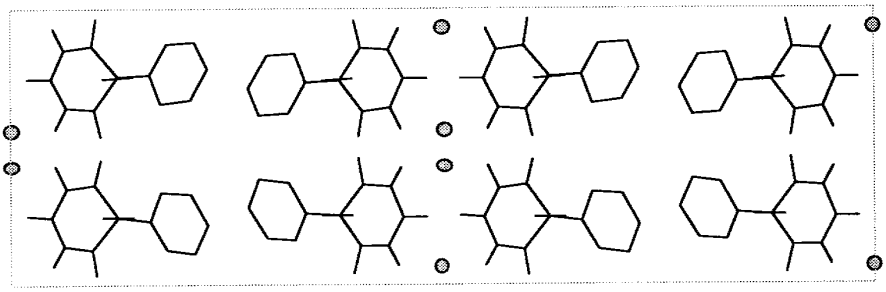

Figure 10.60 Crystal packing of phenobarbital Form XIII hydrate (◎ water molecule) viewed down the *z* axis. (Williams, 1973).

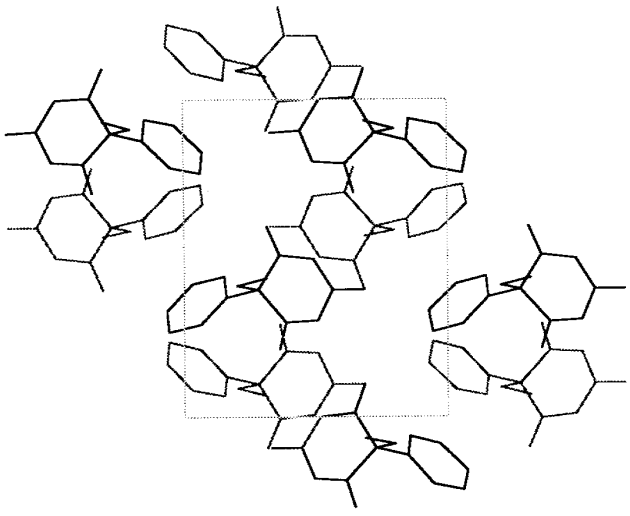

Figure 10.61 Crystal packing of phenobarbital Form III viewed down the *b* axis (Williams, 1974).

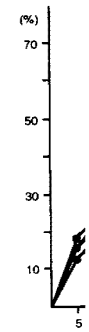

Figure 10.62 Dissolution rate of
pressure of 20 kN,
cial sources), and II

10.7 OTHER DRUGS

In this section the polymorph
this review is not exhaustive,
pharmaceuticals.

A. PROMEDOL ALCOHOL

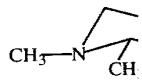

DeCamp and Ahmed (1972
monoclinic and rhombohedr
methyl-4*e*-phenylpiperidin-4*a*
alcohol is the same in bot

Table 10.23 Crystallographic Pa

Parameter	Mono
Space Group	
a (Å)	
b (Å)	
c (Å)	
β	
Z	
V (Å^3)	1
ρ_{calc} (gm·cm^{-3})	

a DeCamp and Ahmed, 1972a. *b*

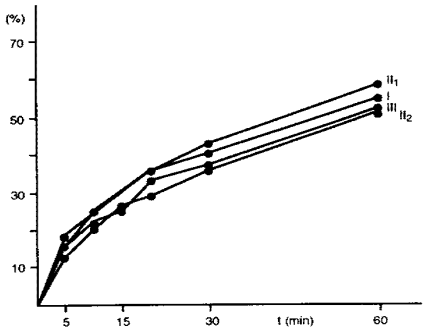

Figure 10.62 Dissolution rate of phenobarbital tablets prepared using the binder Heweten® 40, a pressure of 20 kN, and the four different crystal forms, Forms I, II (from two commercial sources), and III (Szabó-Réveśz *et al.*, 1987).

10.7 Other Drugs

In this section the polymorphic properties of several other drugs are reviewed. While this review is not exhaustive, it illustrates several important studies of polymorphism in pharmaceuticals.

A. Promedol Alcohol

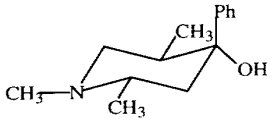

(±)-β-promedol alcohol

DeCamp and Ahmed (1972a–b) have determined the crystal structure of both the monoclinic and rhombohedral forms of (±)-β-promedol alcohol, (±)-α-1,2*a*,5*e*-trimethyl-4*e*-phenylpiperidin-4*a*-ol, (see Table 10.23). The conformation of β-promedol alcohol is the same in both forms, but the crystal packing differs (see Figures

Table 10.23 Crystallographic Parameters for the Two Forms of (±)-β-Promedol Alcohol

Parameter	Monoclinic Form[a]	Rhombohederal Form[b]
Space Group	$P2_1/n$	$R\bar{3}$
a (Å)	13.298	29.754
b (Å)	7.721	29.754
c (Å)	12.776	7.713
β	90.09°	60.0°
Z	4	18
V (Å^3)	1311.8	5913.5
ρ_{calc} (gm·cm^{-3})	1.109	1.110

a DeCamp and Ahmed, 1972a. *b* DeCamp and Ahmed, 1972b

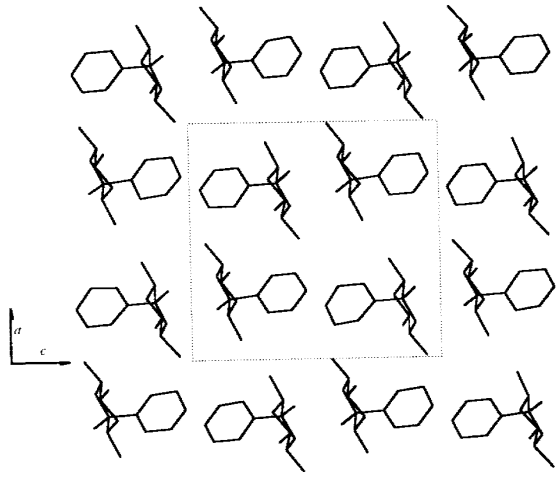

Figure 10.63 Crystal packing of (±)-β-promedol alcohol monoclinic form (DeCamp and Ahmed, 1972a).

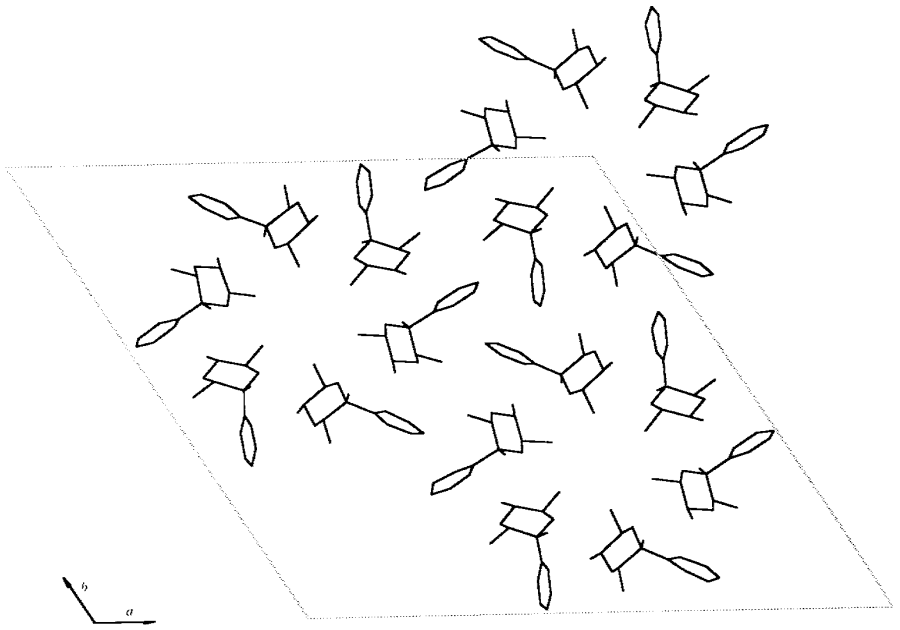

Figure 10.64 Crystal packing of (±)-β-promedol alcohol rhombohedral form (DeCamp and Ahmed, 1972b).

10.63–10.64). In the
same chirality to form
gen bonds; however,
Despite the differenc
have almost the sam
104.5–105 °C, where
difference in melting
since the OH···N dis
the densities indicate
DeCamp and Ahmed
rings of molecules of
molecules of the sam
ordering results in a
monoclinic form. S
(1971).

B. Enalapril Ma

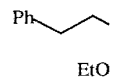

This example illustra
morphs. Enalapril
different solid-state
ethyl ester methyl a
respectively. The
forms as shown in F
of the two crystal fo
the DSC analysis, th
solution data, as sho
dissolution for the

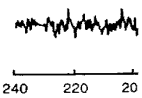

Figure 10.65 Solid-st

10.63–10.64). In the monoclinic form, OH···N hydrogen bonds link molecules of the same chirality to form chains. In the rhombohedral form, there are also OH···N hydrogen bonds; however, these link molecules of alternating chirality into hexameric rings. Despite the differences in crystal packing, the monoclinic and rhombohedral crystals have almost the same density. The melting point of the rhombohedral form is 104.5–105 °C, whereas the melting point of the monoclinic form is 90.5–91 °C. This difference in melting point is probably not related to differences in hydrogen bonding since the OH···N distances are approximately the same in the two forms. In addition, the densities indicate that the two forms have nearly equal packing energies. Thus, DeCamp and Ahmed (1972a) suggested that, since the rhombohedral form contains rings of molecules of alternating chirality while the monoclinic form contains stacks of molecules of the same chirality, the monoclinic form is more ordered. This increased ordering results in an entropy difference that results in a lower melting point for the monoclinic form. Similar arguments were also advanced by Krigbaum and Wildman (1971).

B. Enalapril Maleate

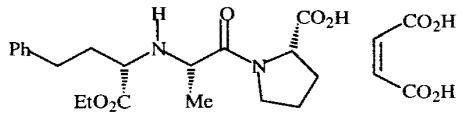

enalapril maleate

This example illustrates the need for using more than one method in looking for polymorphs. Enalapril maleate (Ip *et al.*, 1986) exists in two crystal forms which give different solid-state ^{13}C NMR spectra. (Figures 10.65 and 10.66). The signals of the ethyl ester methyl and maleate carbon signals are at 11–13 ppm and 137–138 ppm, respectively. The XRPD patterns also display a difference between the two crystal forms as shown in Figures 10.67 and 10.68. However, the FT-IR and Raman spectra of the two crystal forms are very similar. Under the experimental conditions used in the DSC analysis, the thermograms of both forms cannot be distinguished. Heat of solution data, as shown in Table 10.24, indicate that there are differences in the heats of dissolution for the two forms, although both crystal forms have virtually identical

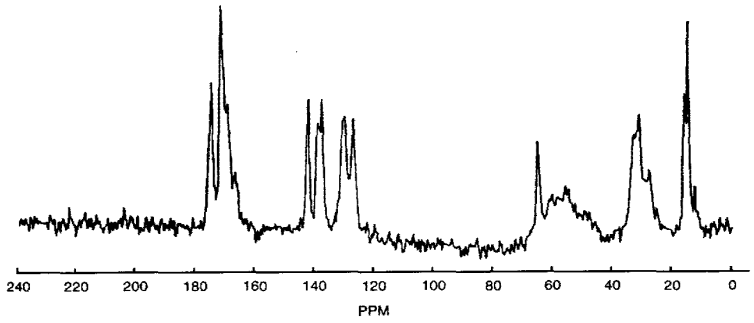

Figure 10.65 Solid-state ^{13}C NMR of enalapril maleate Form I (Ip *et al.*, 1986).

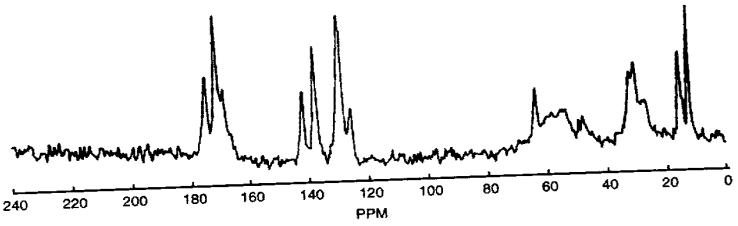

Figure 10.66 Solid-state ^{13}C NMR of enalapril maleate Form II (Ip *et al.*, 1986).

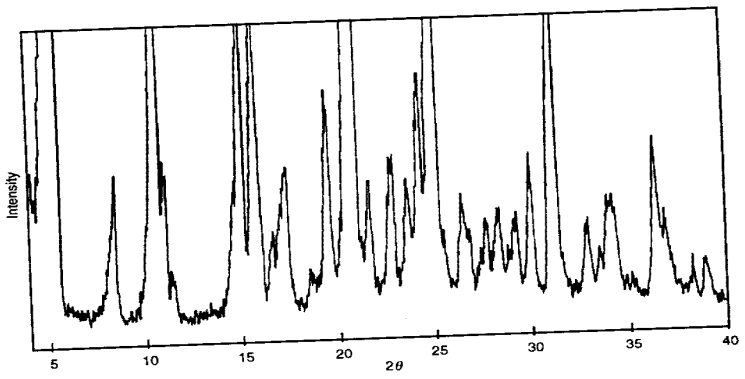

Figure 10.67 Powder X-ray diffraction pattern of enalapril maleate Form I (Ip *et al.*, 1986).

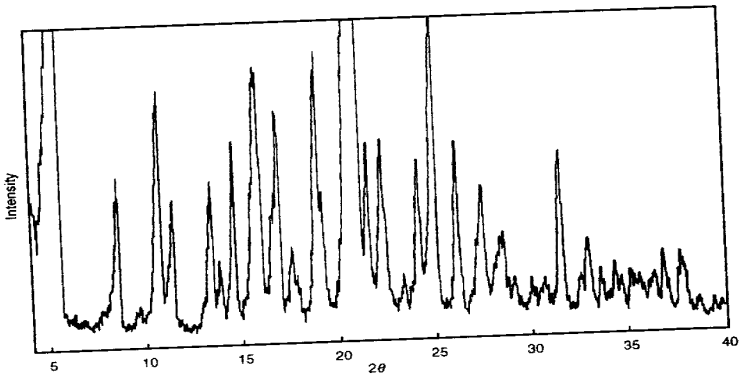

Figure 10.68 Powder X-ray diffraction pattern of enalapril maleate Form II (Ip *et al.*, 1986).

in vitro dissolution rates (s
number of methods on two
two crystal forms are very
properties.

Table 10.24 Heats of Solution

Solvent	**Form I Δ** (kJ/mo
Methanol	36.5(
	35.6
	35.9
	36.2(
	36.4
Mean ± S.D.	36.33 ±
Acetone	59.4
	59.7
	59.1
	59.7
Mean ± S.D.	59.52 ±

Ip *et al.*, 1986.

Table 10.25 Dissolution Dat

Enalapril Maleate Formulation	**Crys**
Capsules	
	I
	I
Tablets	

Ip *et al.*, 1986.

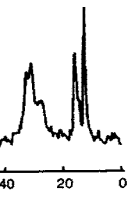

86).

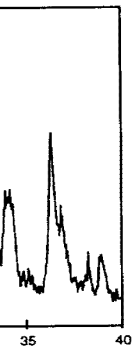

p *et al.*, 1986).

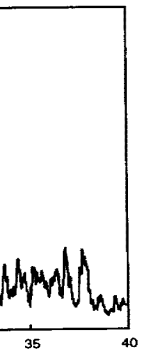

(Ip *et al.*, 1986).

in vitro dissolution rates (see Table 10.25). In summary, this represents a study by a number of methods on two crystal forms of an important compound. It is clear that the two crystal forms are very similar in structure and have very similar pharmaceutical properties.

Table 10.24 Heats of Solution and Transition of Enalapril Maleate Polymorphs

Solvent	Form I ΔH_{soln} (kJ/mol)	Form II ΔH_{soln} (kJ/mol)	ΔH_{Trans} (kJ/mol)
Methanol	36.50	38.47	
	35.64	38.21	
	35.95	38.54	
	36.20	38.62	
	36.46		
Mean ± S.D.	36.33 ± 0.25	38.46 ± 0.11	2.05
Acetone	59.44	62.71	
	59.73	61.99	
	59.19	62.66	
	59.73	62.54	
Mean ± S.D.	59.52 ± 0.25	62.41 ± 0.29	2.89

Ip *et al.*, 1986.

Table 10.25 Dissolution Data for Enalapril Maleate Capsules and Tablets

Enalapril Maleate Formulation	Crystal Form	Potency (mg)	Average Percent Dissolved at 30 min
Capsules	II	2.5	89
	I	2.5	100
	I and II	2.5	101
	I	2.5	96
	I and II	20	82
	I	20	99
	II	20	95
	I	20	92
Tablets	I	10	100
	II	10	99
	I	10	99
	I and II	10	98
	I	40	103
	I and II	40	102
	II	40	96

Ip *et al.*, 1986.

C. Metoclopramide and Metoclopramide Monohydrochloride

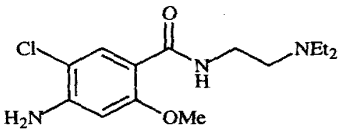

metoclopramide

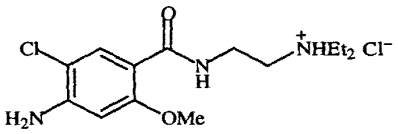

metoclopramide monohydrochloride

Mitchell (1985) has studied the polymorphism of both metoclopramide and metoclopramide monohydrochloride. Each exists in two crystal forms and metoclopramide monohydrochloride also forms a monohydrate. Metoclopramide exists in two enantiotropic polymorphs with a transition temperature of 125 °C from Form I (stable at low temperature) to Form II (stable at high temperature) having a melting point of 147 °C. This process can also be reversed. Dehydration of metoclopramide monohydrochloride monohydrate, depending on the conditions, give rise to one of two anhydrous polymorphs; Form I (mp 187 °C) is formed from the melt under slow crystallization conditions, whereas, Form II (mp 155 °C) is formed from the melt under fast crystallization conditions. All of these crystal forms were detected by DSC, thermal microscopy, X-ray diffraction, and infrared spectroscopy.

D. Furosemide

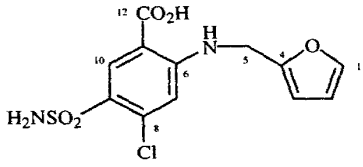

furosemide

Doherty and York (1988) described the two crystal forms of furosemide readily detected by X-ray powder diffraction. In a more recent study, Matsuda and Tatsumi (1990) discovered three additional polymorphs as well as two solvates and an amorphous form. Interestingly, it was found that the forms produced could be related to the boiling point of the solvent. Thus, Form I was obtained from the lower boiling solvents used [acetone (bp 57 °C), methanol (bp 65 °C), ethanol (bp 79 °C), and methyl ethyl ketone (bp 80 °C)], Form II was obtained from the higher boiling solvents used [isobutyl alcohol (bp 108 °C), butanol (bp 118 °C), and pentanol (bp 138 °C)], and mixtures of both forms were obtained from solvents with intermediate boiling points used [isopropyl alcohol (bp 83 °C) and propanol (bp 97 °C)] by slow crystallization from a hot solution. To our knowledge this is the first such relationship which has been reported. In addition, they reported that the rate of solvent evaporation affected the crystal form obtained. Figure 10.69 shows the XRPDs of furosemide and Figure 10.70 shows the IR spectra of the different crystal forms.

Doherty and York (1988) also showed that Forms I and II had different solid-state NMR spectra as shown in Figure 10.71. Figure 10.72 shows the DSC and TG

thermograms of the six dif
all forms are unique and w

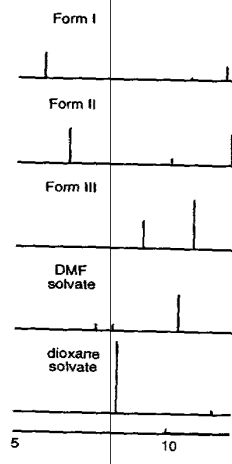

Figure 10.69 X-ray powder di
and Tatsumi, 19

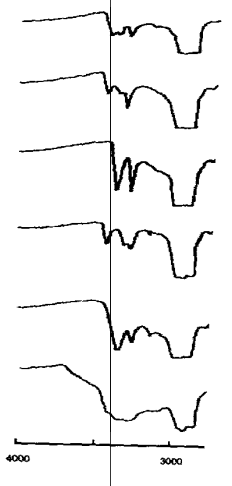

Figure 10.70 Infrared spectra
1990).

thermograms of the six different forms of furosemide. It is clear from these studies that all forms are unique and well characterized.

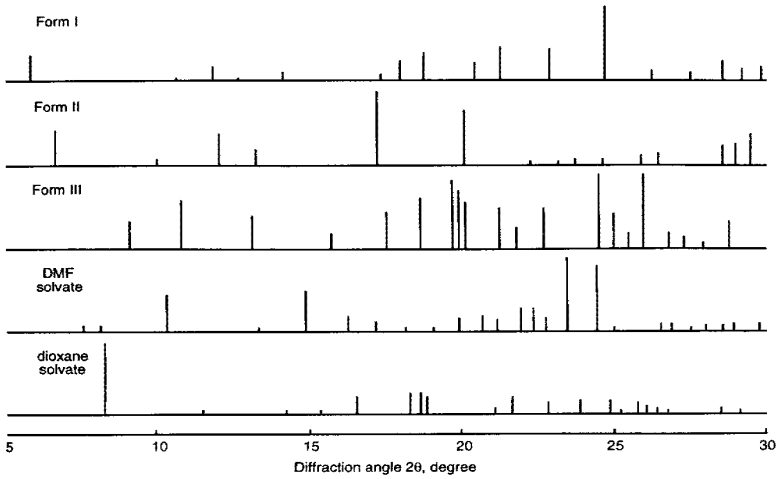

Figure 10.69 X-ray powder diffraction patterns of the different crystal forms of furosemide (Matsuda and Tatsumi, 1990).

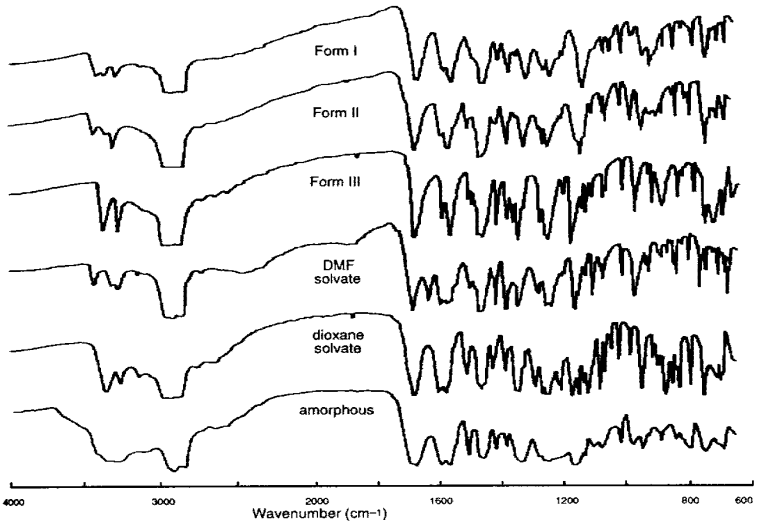

Figure 10.70 Infrared spectra of the different crystal forms of furosemide (Matsuda and Tatsumi, 1990).

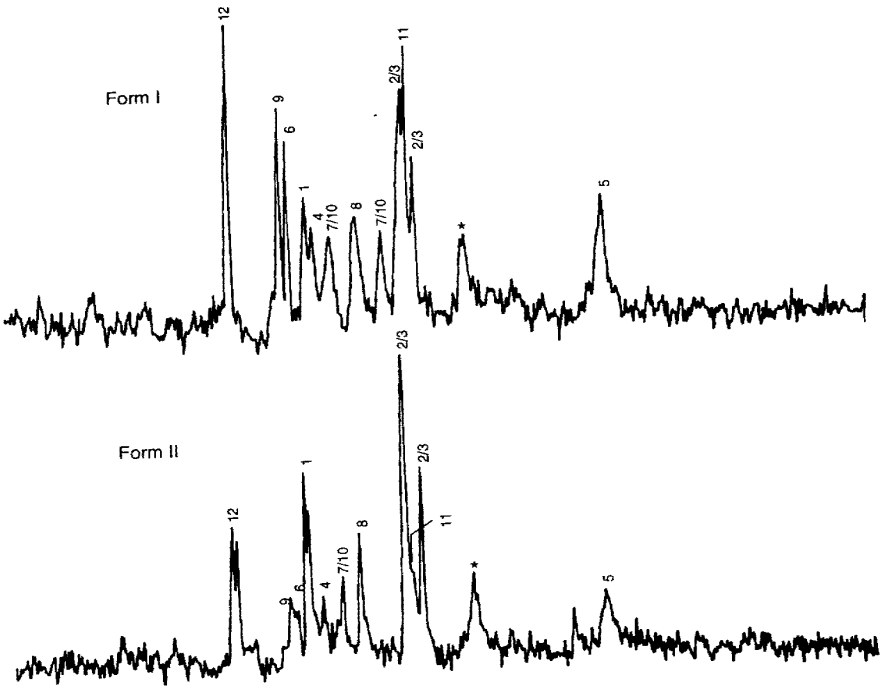

Figure 10.71 Solid-state ^{13}C CP/MAS NMR spectra for two furosemide forms at ambient temperature with peak assignments. The peaks marked with a star are due to the Delrin® rotor (Doherty and York, 1988).

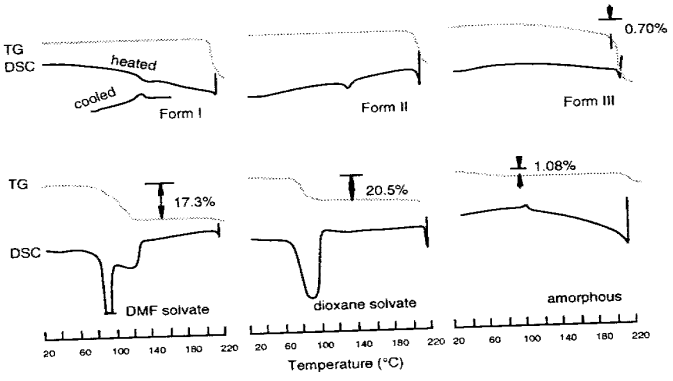

Figure 10.72 DSC and TG thermograms of the different crystal forms of furosemide (Matsuda and Tatsumi, 1990).

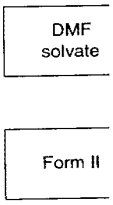

Figure 10.73 Interconvers
and Tatsum

Matsuda and Tats
which could be obtaine
studied the interconvers
rized in Figure 10.73.
most stable form, Form
Form I upon heating (s
Matsuda and Tats

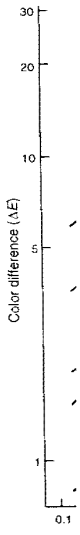

Figure 10.74 Double-log
forms unde

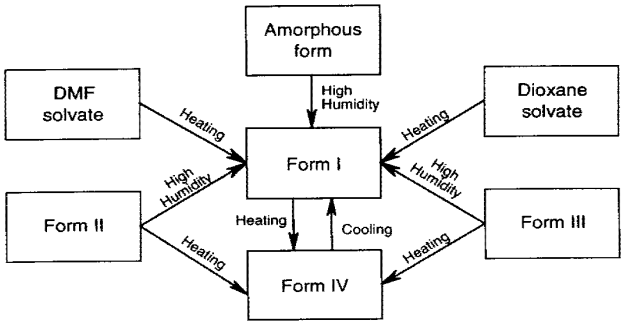

Figure 10.73 Interconversion scheme of furosemide crystal forms under various conditions. (Matsuda and Tatsumi, 1990).

Matsuda and Tatsumi (1990) found a high temperature crystal form (Form IV) which could be obtained by heating Forms I, II, or III to 180 °C. In addition, they studied the interconversion of the crystal forms and these interconversions are summarized in Figure 10.73. It is clear that all of the crystal forms can be converted into the most stable form, Form I, at room temperature. The solvated forms also converted to Form I upon heating (see Figure 10.73).

Matsuda and Tatsumi also studied the physical and chemical properties of the

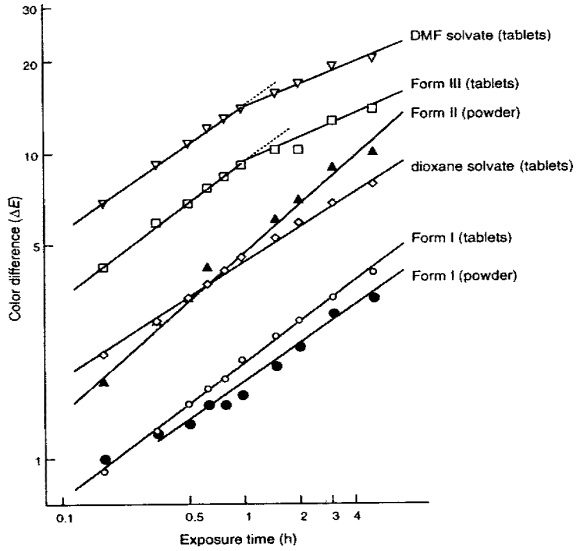

Figure 10.74 Double-logarithmic plots for the coloration process of different furosemide crystal forms under irradiation by a mercury vapor lamp (Matsuda and Tatsumi, 1990).

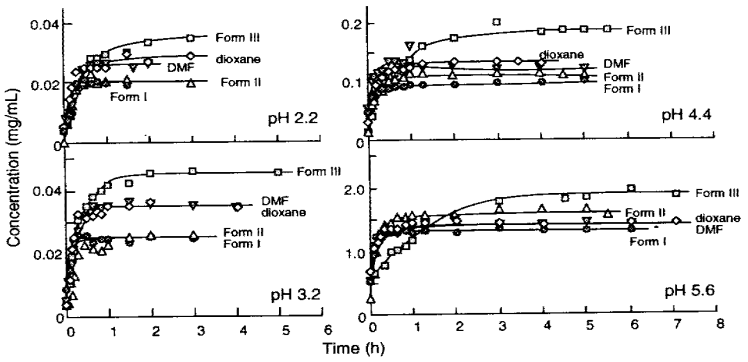

Figure 10.75 Dissolution profiles of the different crystal forms of furosemide in buffer solution at various pH values at 37° C (Matsuda and Tatsumi, 1990).

different crystal forms of furosemide. Figure 10.74 shows the studies on the photostability of the different crystal forms. It is apparent that the different crystal forms have a different amount of coloration initially but that the rate of change in coloration is about the same for all crystal forms. However, the relationship between coloration and degradation remains unknown.

Figure 10.75 shows the dissolution profiles of furosemide at different pH (2.2, 3.2, 4.4, and 5.6). It is apparent that Form II reaches the highest solubility at all pH's and that Form II and the DMF solvate are the least soluble. Judging by these profiles, some of the forms appear to interconvert in these experiments.

E. 14-Hydroxymorphinone—Color Dimorphism

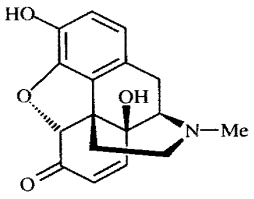

14-hydroxymorphinone

The phenolic α,β-unsaturated ketone 14-hydroxymorphinone exists in two crystalline modifications (see Table 10.26), which are interconvertible by dissolution and recrystallization (Chiang *et al.*, 1978). Recrystallization from polar solvents (ethanol) yields yellow crystals, while crystallization from benzene gives colorless (white) crystals. Both forms are stable indefinitely in the solid state.

Infrared spectra show that the yellow form has a carbonyl absorption at 1685 cm^{-1}, while the colorless form has a carbonyl absorption at 1660 cm^{-1}. Since both forms have a carbonyl absorption, neither form contains an enol tautomer.

Crystallographic studies show that the conformation of 14-hydroxymorphinone in the two forms is similar; however, the yellow form contains an intermolecular OH···O

Table 10.26 Crystallogr

Parameter
Space group
a (Å)
b (Å)
c (Å)
Z
ρcalc (g cm^{-3})
V (Å^3)

Chiang *et al.*, 1978.

hydrogen bond, while bond.

The color of the y hydrogen bond, since dihydroxyterephthalate is that there is a weak adjacent phenyl ring in tion between these two

Numerous other re that are not drugs. The *et al.*, 1978; Byrn *et a* important compound I thebaine gave metathe sodium bicarbonate and NaOH or NH_3 and recry melting point, and both solution in benzene. U color and no investigati been reported.

M

F

F. Miscellaneous St

Kuhnert-Brandstätter an polymorphs of pharmac spectroscopy, and in so shown in Table 10.27. I of the different polymo

Table 10.26 Crystallographic Parameters for the Two Forms of 14-Hydroxymorphinone

Parameter	Colorless Form	Yellow Form
Space group	$P2_12_12_1$	$P2_12_12_1$
a (Å)	12.918	13.150
b (Å)	14.074	13.508
c (Å)	8.035	7.837
Z	4	4
ρ_{calc} (g cm^{-3})	1.36	1.428
V (Å^3)	1460.8	1392.1

Chiang *et al.*, 1978.

hydrogen bond, while the white form contains an intramolecular OH···O hydrogen bond.

The color of the yellow form may, in part, result from the intermolecular OH···O hydrogen bond, since a similar effect was found for dimethyl 3,6-dichloro-2,5-dihydroxyterephthalate (Byrn *et al.*, 1972; see Section 8.1). An alternative explanation is that there is a weak charge-transfer interaction between the C=O group and an adjacent phenyl ring in the yellow form, but not in the colorless form. A clear distinction between these two explanations is not possible.

Numerous other reports of color dimorphism have been published for compounds that are not drugs. These reports are briefly reviewed by (Desiraju *et al.*, 1977; Chiang *et al.*, 1978; Byrn *et al.*, 1972). Color dimorphism of at least one other biologically important compound has been reported (Small and Meitzner, 1933); reduction of thebaine gave metathebainone. Neutralization of a metathebainone solution with sodium bicarbonate and recrystallization gave yellow crystals, while neutralization with NaOH or NH_3 and recrystallization gave colorless crystals. Both crystals had the same melting point, and both gave a yellow solution in ethanol or water and a colorless solution in benzene. Unfortunately, no structural explanations of these differences in color and no investigation of differences in polymorphism of these compounds have been reported.

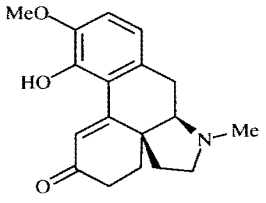

metathebainone

F. Miscellaneous Studies by Kuhnert-Brandstätter and Co-workers

Kuhnert-Brandstätter and co-workers have carried out an extensive study on the polymorphs of pharmaceuticals. Their studies generally use thermal microscopy, IR spectroscopy, and in some cases powder diffraction. The results of these studies are shown in Table 10.27. In many cases they were able to determine the relative stability of the different polymorphs and whether they were monotropic (one forms is most

Table 10.27 Studies of Polymorphic Pharmaceuticals by Kuhnert-Brandstätter's Group

Pharmaceutical	No. of Forms	Thermodynamics*	Reference
Amiperone	2	II → I	Kuhnert-Brandstätter and Porsche, 1989b
Anilamate	3	III → II, II → I	Kuhnert-Brandstätter *et al.*, 1982c
Benactyzine HCl	2	II → I	Kuhnert-Brandstätter. and Wurian, 1982a
Bentiromide	3 + hydrates	II → I, ···	Kuhnert-Brandstätter and Porsche, 1989b
Bromopride	2	II → I	Kuhnert-Brandstätter *et al.*, 1982b
Brotizolam	4	IV → III, III → I, ···	Kuhnert-Brandstätter and Porsche, 1989b
Bumetanide	2	II → I	Kuhnert-Brandstätter *et al.*, 1982b
Bupicomide	3	Monotropic	Kuhnert-Brandstätter and Porsche, 1989a
Buspirone HCl	2	Monotropic	Kuhnert-Brandstätter and Porsche, 1989a
Clenbuterol HCl	2	II → I	Kuhnert-Brandstätter. and Wurian, 1982a
Dimethoxanate HCl	2	II → I	Kuhnert-Brandstätter *et al.*, 1982c
Diphenadione	2	II → I	Kuhnert-Brandstätter *et al.*, 1982c
Diphenidol HCl	3	III → II, III → I	Kuhnert-Brandstätter. and Wurian, 1982a
Dipyridamole	2	II → I	Kuhnert-Brandstätter. and Wurian, 1982a
Dobutamine HCl	4	···	Kuhnert-Brandstätter and Porsche, 1989b
Famotidine	2	II → I	Kuhnert-Brandstätter and Porsche, 1990
Fenbufen	3	III → II, III → I	Kuhnert-Brandstätter and Porsche, 1989b
Flucabril	2	II → I	Kuhnert-Brandstätter *et al.*, 1982b
Flupirtine Maleate	2	II → I	Kuhnert-Brandstätter and Porsche, 1990
Gallic Acid Ethyl Ester	3	III → II, III → I	Kuhnert-Brandstätter. and Wurian, 1982a
Halofenate	3	Monotropic	Kuhnert-Brandstätter and Völlenklee, 1986
Heptolamide	3	···	Kuhnert-Brandstätter and Porsche, 1989a
Iprindol HCl	3	III → II, ···	Kuhnert-Brandstätter *et al.*, 1982b
Levobunolol HCl	5		Kuhnert-Brandstätter and Porsche, 1989a
Lorcainide HCl	2	II → I	Kuhnert-Brandstätter and Völlenklee, 1986
Maprotiline HCl	3	III → II, II → I	Kuhnert-Brandstätter *et al.*, 1982c
Mexiletine HCl	3	III → I, II → I	Kuhnert-Brandstätter and Völlenklee, 1987
Minoxidil	3	III → II, II → I	Kuhnert-Brandstätter and Völlenklee, 1986
Mopidamol	4	IV → I, II → I, ···	Kuhnert-Brandstätter and Völlenklee, 1986
Nafoxidine HCl	3	III → I, II → I	Kuhnert-Brandstätter *et al.*, 1982c
Naftifine HCl	3	Monotropic	Kuhnert-Brandstätter and Porsche, 1989a
Oxypendyl 2HCl	4	III → I, II → I, ···	Kuhnert-Brandstätter and Völlenklee, 1987
Paxamate	2	II → I	Kuhnert-Brandstätter and Porsche, 1990
Penbutolol Sulfate	4	IV → III, III → II, ···	Kuhnert-Brandstätter and Völlenklee, 1987
Piretanide	4	II → I, ···	Kuhnert-Brandstätter and Porsche, 1989a
Pirprofene	2	Monotropic	Kuhnert-Brandstätter and Völlenklee, 1987
Propentofylline	4	Monotropic	Kuhnert-Brandstätter and Porsche, 1990
Renytoline HCl	3	III → II, II → I	Kuhnert-Brandstätter *et al.*, 1982b
Terconazole	2	Monotropic	Kuhnert-Brandstätter and Porsche, 1989b
Triclabendazole	2	Monotropic	Kuhnert-Brandstätter and Porsche, 1990

* Some forms undergo inhomogeneous melting rather than transformation.

stable at all temperatures) o
peratures). Specifically, Ku
this table as cases where the
the highest melting point.

G. (2*R*,4*S*)-6-FLUORO-2-M

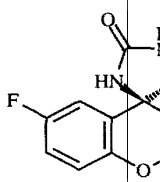

This aldose reductase inhil
studied by DSC, X-ray pow
1988). Figure 10.76 show
indicates that the β–form is
tent with the X-ray powder
sion of the β–form to the α
the α– and β–forms as wel
heating the β–form, indicati
α–form to the β–form appe

Figure 10.76 The DSC curv
dione (Ashizawa

stable at all temperatures) or enantiotropic (different forms are stable at different temperatures). Specifically, Kuhnert-Brandstätter defined enantiotropy for the purposes of this table as cases where the most stable form at room temperature is not the form with the highest melting point.

G. (2*R*,4*S*)-6-Fluoro-2-methylspiro[chroman-4,4′-imidazoline]-2′,5-dione

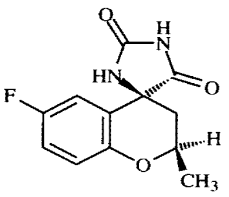

(2*R*,4*S*)-6-fluoro-2-methylspiro-[chroman-4,4′-imidazoline]-2′,5-dione

This aldose reductase inhibitor exists in two crystal forms, α and β, which were studied by DSC, X-ray powder diffraction, and infrared spectroscopy (Ashizawa *et al.*, 1988). Figure 10.76 shows the DSC behavior of the β–form. This thermogram indicates that the β–form is converted to the α–form at high temperature and is consistent with the X-ray powder diffraction and infrared spectra which showed interconversion of the β–form to the α-form. Figure 10.77 shows the X-ray powder patterns of the α– and β–forms as well as that of a 1:1 mixture and the product obtained upon heating the β–form, indicating it is being transformed into the α–form. Addition of the α–form to the β–form appears to provide nuclei which allow the conversion to occur

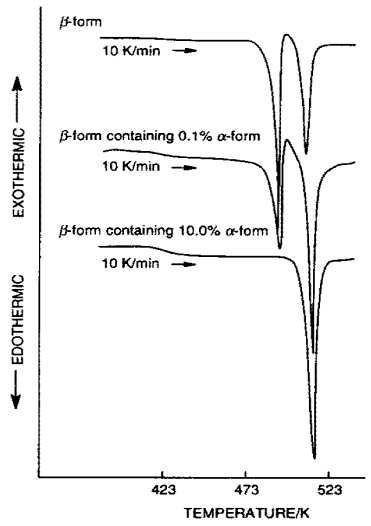

Figure 10.76 The DSC curve for (2*R*,4*S*)-6-fluoro-2-methylspiro[chroman-4,4′-imidazoline]-2′,5-dione (Ashizawa *et al.*, 1988).

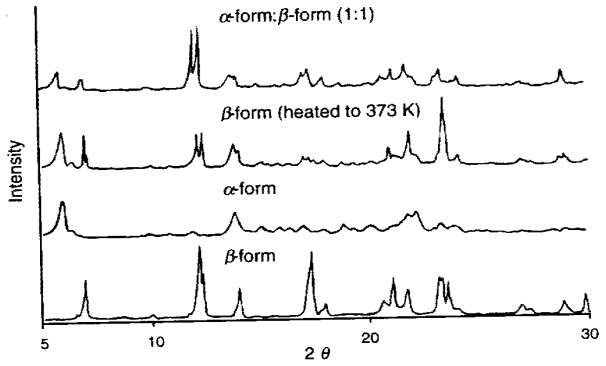

Figure 10.77 X-ray diffraction patterns of (2*R*,4*S*)-6-fluoro-2-methylspiro[chroman-4,4′-imidazoline]-2′,5-dione (Ashizawa *et al.*, 1988).

before melting of the β–form. This indicates the importance of nucleation in polymorphic interconversions.

The crystal structure of the β–form has been determined by single crystal X-ray methods (Ashizawa, 1989). They suggested that the crystal structure of the α–form is disordered and thus the structure could not be determined.

H. Cyclopenthiazide

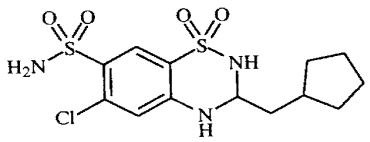

cyclopenthiazide

The diuretic cyclopenthiazide exists in three polymorphic forms which are obtained by crystallization from ethanol:heptane:methanol (Form I), ethanol (Form II), and ethanol:water (Form III) (Gerber *et al.*, 1991).

These forms were characterized by DSC, thermomicroscopy, X-ray powder diffraction, scanning electron micrographs, IR, solid-state NMR, solution calorimetry, dissolution rates, and solubility determinations.

Figure 10.78 shows the DSC thermograms, Figure 10.79 shows the X-ray powder diffraction patterns, and Figure 10.80 shows the solid-state CP/MAS spectra. The DSC thermograms gave the following heats of fusion for the different polymorphs: Form I, 105.5 kJ/mol; Form II, 98.4 kJ/mol and Form III, 62.5 kJ/mol. The value for Form III is too low to be the ΔH_f and most likely represents a transformation process This was confirmed by thermomicroscopy in which Form III melted at 181 °C and recrystallized to Form I.

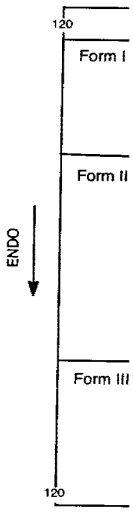

Figure 10.78 DSC the
238 °C;

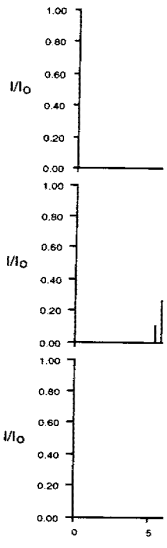

Figure 10.79 X-ray pov
1991).

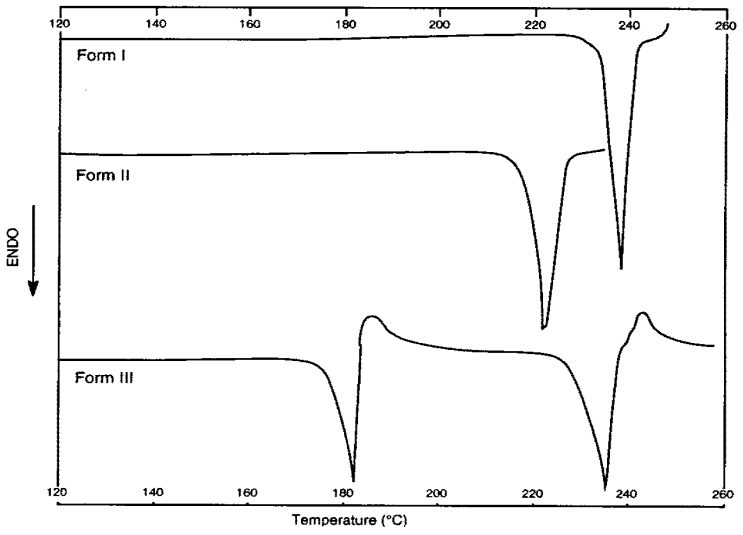

Figure 10.78 DSC thermograms of cyclopentathiazide polymorphs with melting points: Form I, 238 °C; Form II, 225 °C; and Form III, 181° and 235 °C (Gerber *et al.*, 1991).

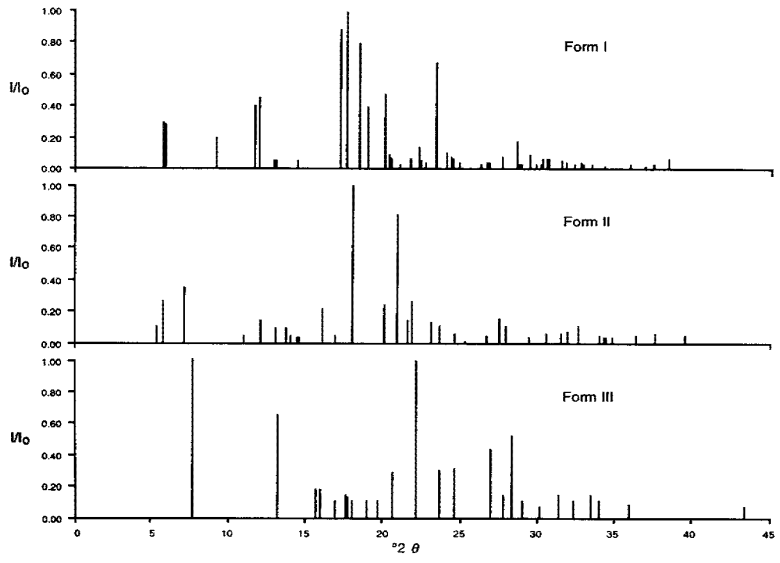

Figure 10.79 X-ray powder diffraction patterns of cyclopentathiazide polymorphs (Gerber *et al.*, 1991).

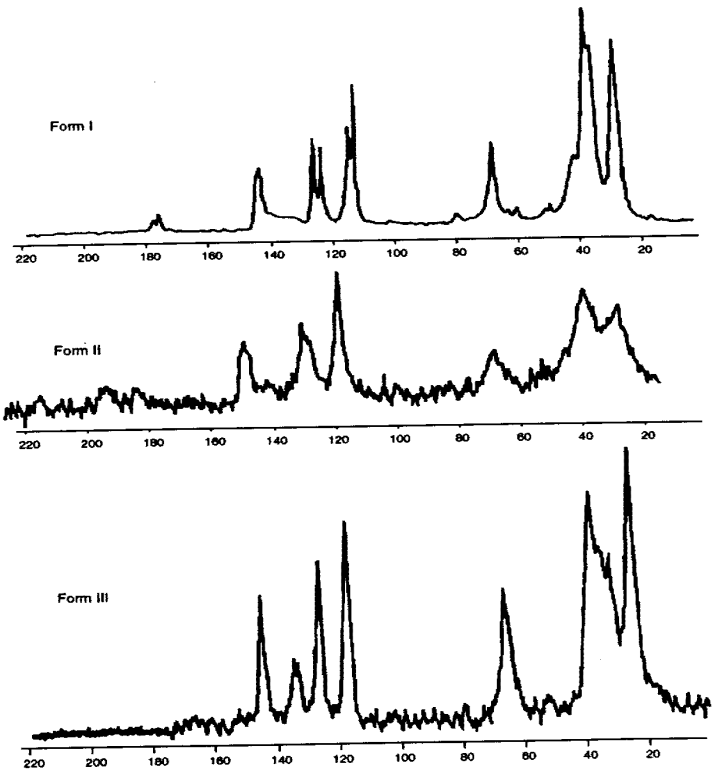

Figure 10.80 Solid-state ^{13}C NMR spectra of cyclopentathiazide polymorphs (Gerber *et al.*, 1991).

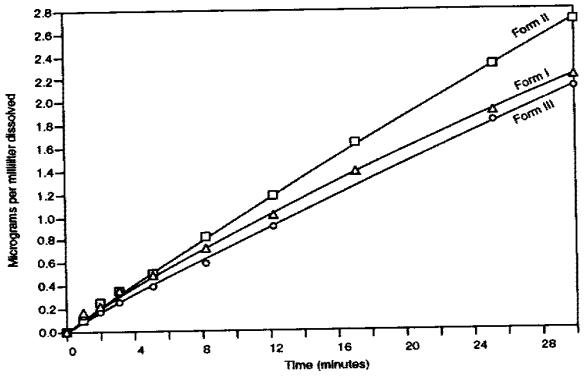

Figure 10.81 Intrinsic dissolution rates of cyclopentathiazide polymorphs (Gerber *et al.*, 1991).

It is evident from
of solution of the diff
Form I, 0.34 kJ/mol;
these measurements ra
solution within experi
were measured and are
tion rates but Form II h
three forms were also
solubility was Form II
most stable polymorph

I. Tamoxifen Citra

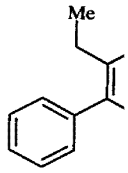

Tamoxifen citrate is w
(1987) have reported th
Form B. Figure 10.82
morph of tamoxifen citr
of Form A; however, t
organized and less sta

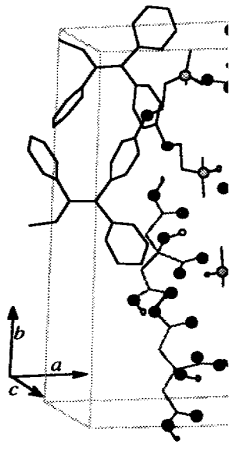

Figure 10.82 Stereoview o
Becker, 1987)

It is evident from all these data that these are truly different polymorphs. The heats of solution of the different polymorphs in 95% ethanol were also determined and are: Form I, 0.34 kJ/mol; Form II, 0.35 kJ/mol; and Form III, 0.86 kJ/mol. The errors in these measurements range 0.03–0.06 kJ/mol; thus Forms I and II have the same heat of solution within experimental error. The intrinsic dissolution rates of the three forms were measured and are shown in Figure 10.81. Forms I and III have similar dissolution rates but Form II has a significantly higher dissolution rate. The solubilities of the three forms were also determined in several solvents and in all cases the order of solubility was Form II > Form I > Form III. These data suggest that Form III is the most stable polymorph.

I. Tamoxifen Citrate

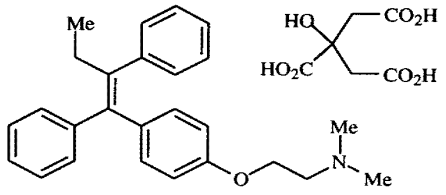

tamoxifen citrate

Tamoxifen citrate is well known as an antiestrogenic agent. Goldberg and Becker (1987) have reported the crystal structure of the more stable of two polymorphic forms, Form B. Figure 10.82 shows a stereoview of the crystal packing of the stable polymorph of tamoxifen citrate. Unfortunately they were not able to determine the structure of Form A; however, they point out that there are several indications that it is a less organized and less stable structure. For instance, they observed that at room

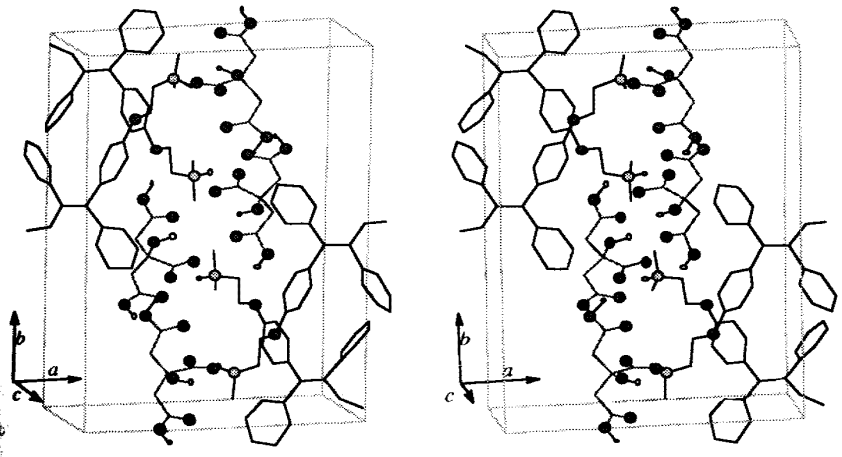

re 10.82 Stereoview of the crystal structure of Form B of tamoxifen citrate (Goldberg and Becker, 1987).

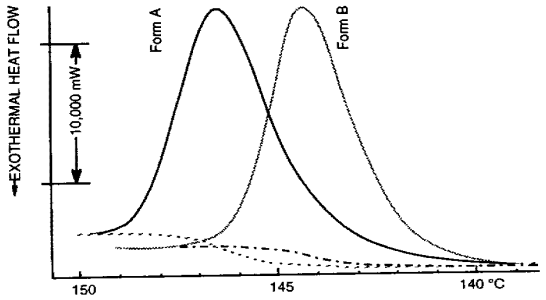

Figure 10.83 DSC thermograms of the two crystal forms of tamoxifen citrate (Goldberg and Becker, 1987).

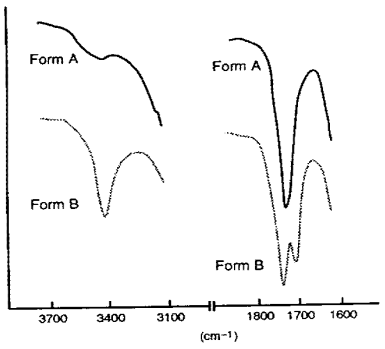

Figure 10.84 Infrared spectra of the two crystal forms of tamoxifen citrate: Form A, solid lines; Form B, dashed lines (Goldberg and Becker, 1987).

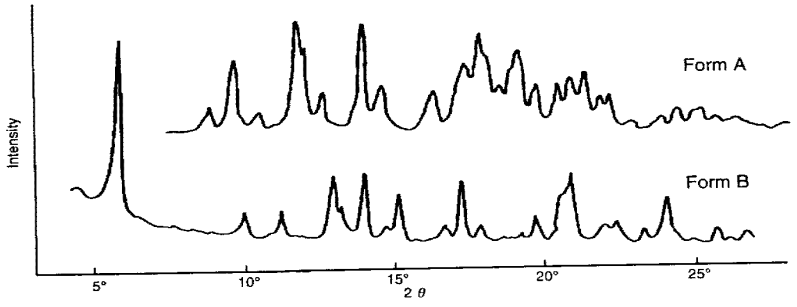

Figure 10.85 X-ray powder diffraction patterns of the two crystal forms of tamoxifen citrate (Goldberg and Becker, 1987).

temperature in an ethanol suspension, Form A rearranges spontaneously to Form B. They also reported the DSC thermograms (Figure 10.83), the IR spectra (Figure 10.84), and the XRPDs (Figure 10.85) of the two polymorphs.

J. Antiulcer Agent FR101853

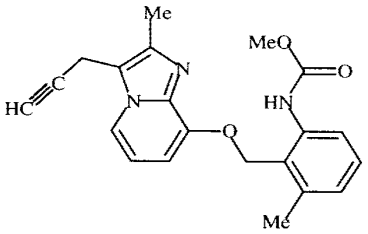

8-(2-methoxycarbonyl-amino-6-methylbenzyloxy)-2-methyl-3-(2-propynyl)-imidazo[1,2-*a*]pyridine (FR101853)

Miyamae and co-workers (1990) have carried out an extensive study of the polymorphism of an orally-active antiulcer compound 8-(2-methoxycarbonylamino-6-methylbenzyloxy)-2-methyl-3-(2-propynyl)imidazo[1,2-*a*]pyridine (FR101853) which exists in two crystal Forms A and B. Table 10.28 shows the crystallographic data for the two crystal forms which exhibit significantly different crystal packing (see Figures 10.86–10.87). In addition, the different crystal forms have different X-ray powder diffraction patterns and different DSC thermograms (Figure 10.88). Interestingly, the IR spectra of the two crystal forms are very similar (Figure 10.89) perhaps because the complicated absorptions of the molecule obscure any differences in infrared spectra that might be caused by different crystal packing.

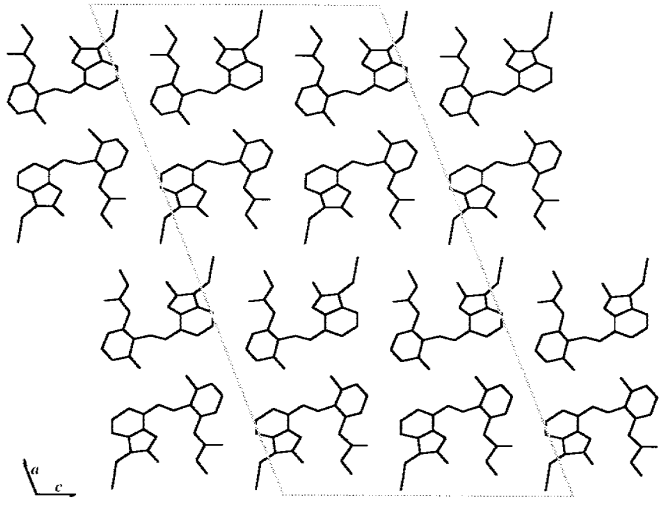

re 10.86 Stereoview of the crystal packing of FR101853, Form A (Miyamae *et al.*, 1990).

Table 10.28 Crystal Data for the Two Crystal Forms of FR101853

Parameter	Form A	Form B
Space Group	$C2/c$	$P2_1/c$
a (Å)	42.936(14)	4.367(1)
b (Å)	4.356(1)	38.214(3)
c (Å)	21.536(6)	11.253(1)
β	109.92(4)°	95.47(2)°
Z	8	4
ρcalc (g cm^{-3})	1.275	1.292
V (Å^3)	3786.7(20)	1869.4(3)

Miyamae *et al.*, 1990.

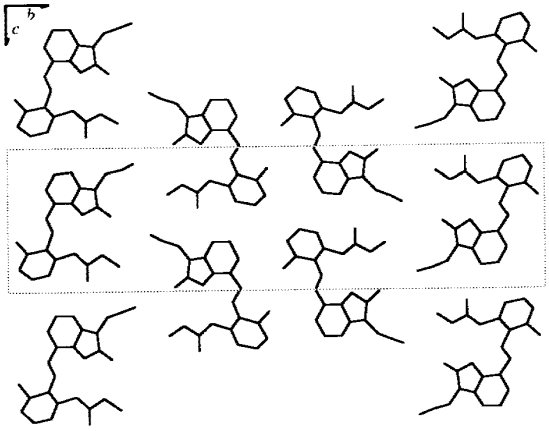

Figure 10.87 Stereoview of the crystal packing of FR101853, Form B (Miyamae *et al.*, 1990).

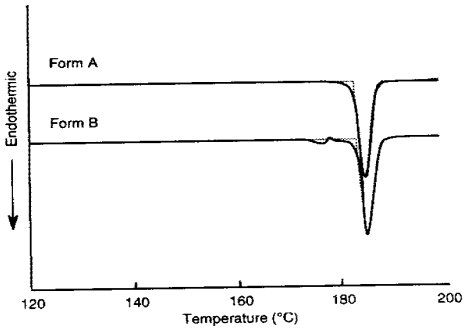

Figure 10.88 DSC thermograms of the different crystal forms of FR101853 (Miyamae *et al.*, 1990).

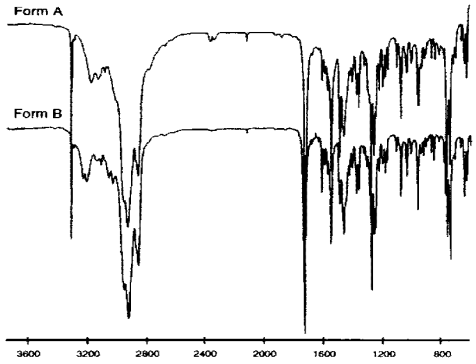

Figure 10.89 Infrared spectra of the different crystal forms of FR101853 (Miyamae *et al.*, 1990).

10.8 CARBOHYDRATES

In this section, polymorphism of carbohydrates is briefly discussed. This area is of substantial interest since carbohydrates are often used as excipients. Although numerous carbohydrates exhibit polymorphism, relatively few studies of these compounds have been reported.

Mannitol exists in four forms (Debord *et al.*, 1987). The α- and β-form have been isolated in the pure state, the δ-form has been isolated containing the α-form as an impurity. In addition, a fourth form was found but could not be characterized further. The different compressibilities and particle shapes of these forms could have important implications for their use as excipients. Figure 10.90 shows the X-ray powder diffraction patterns of the α- and β-forms as well as the "unknown" form. Figure 10.91 shows the X-ray powder patterns of different commercial products of mannitol. It is apparent that material from supplier 4 (S_4) contains a crystal form different from the other preparations. The water contents of the crystal forms and the different commercial products were determined after two months storage. Compression studies were also carried out and it was found that compression of the different samples produced tablets of different hardness. The different products and crystal forms took up small but different amounts of water, but the amount of water uptake did not seem to be related to the crystal form. The amounts of water uptake are so small that these measurements may be subject to variations from the amount of amorphous material present in the different crystal forms. Such studies have important implications for tablet preparation and demonstrate that it may be important to control the polymorphic form of excipients used in tablets.

Several other carbohydrates also exist in polymorphs. For example, the carbohydrate 4-methoxyphenyl-β-D-glucopyranoside exists in two forms (Forms I and II). Each form has a distinct powder pattern, and Form II can be converted to Form I at 161 °C (Shafizadeh and Susott, 1973). Phenyl-2-acetamidotri-*O*-acetyl-β-D-glucopyranoside also exists in two polymorphs that have different powder patterns. Form II can be converted to Form I at 185 °C (Shafizadeh and Susott, 1973). 4-Methoxy-2-acetamidotri-*O*-acetyl-β-D-glucopyranoside exists in four forms which have different

powder patterns (Shafizadeh and Susott, 1973). Form IV is converted to Form III at 158 °C, Form III can be converted to Form II at 177 °C, and Form II can be converted to the least stable form, Form I, at 183 °C. Form I melts at 192 °C.

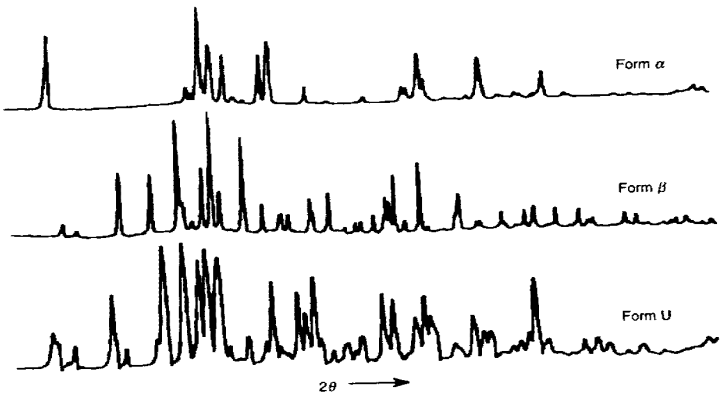

Figure 10.90 X-ray powder diffraction patterns of the α-, β-, and unknown forms of mannitol (Debord *et al.*, 1987).

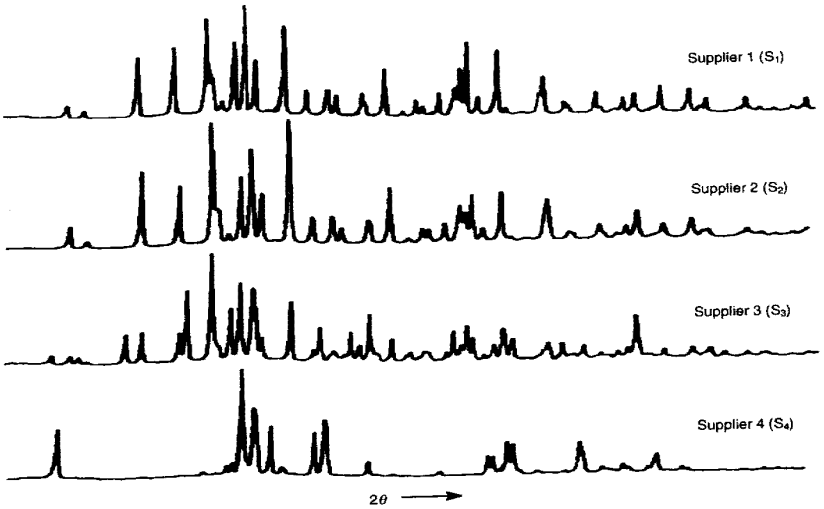

Figure 10.91 X-ray powder diffraction patterns of the commercial mannitol products S_1 through S_4 (Debord *et al.*, 1987).

10.9 POLYMORPHS OF ANTIBIOTICS

Antibiotics exhibit polymorphism which could affect their stability and bioavailability. In addition, cephalosporin antibiotics crystallize in an extensive series of hydrates and solvates as discussed in Chapter 11.

For the polyene antibiotics, mepartricin and nystatin, different conditions of crystallization have resulted in products with different activity and acute toxicity. These differences are not due to particle size effects (Ghielmetti *et al.*, 1976). Evaporation of mepartricin in methylene chloride–methanol (9:1) at room temperature gave an oil which crystallized upon standing to form a solid which had one-fourth the oral activity and between one-sixth and one-tenth the LD_{50} (for mice) compared to the solid obtained by cooling an acetone–water–ether solution.

Studies of nystatin showed that crystals obtained by crystallization of a water–methyl ethyl ketone solution had approximately the same activity against microorganisms, but half the solubility and half to one-tenth the LD_{50} of crystals obtained from chloroform–methanol–ammonia. While the existence of nystatin polymorphs has not been proven by X-ray powder diffraction or other experimental techniques, it is likely that the differences in activity of the crystals are due to differences in solubility and solution rate. These solubility differences may, in turn, be due to polymorphic differences.

A. CONFORMATIONAL POLYMORPHISM OF SPIPERONE

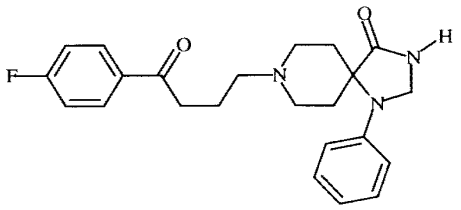

spiperone

Azibi *et al.* (1983) described the conformational polymorphism of spiperone. This compound exists in two crystal forms (the structures and data are shown in Figures 10.92–10.93 and Table 10.29). Form I melted at 208.9 °C and Form II melted at 207 °C. The infrared spectra of the two crystal forms are different, and the crystal structure

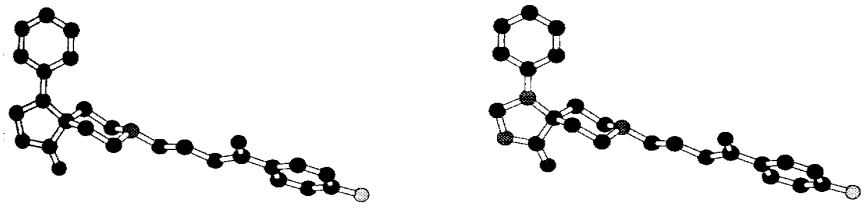

Figure 10.92 Stereoview of the molecular conformation of spiperone in Form I where: ● C, ○ F, ● N, ● O (Azibi *et al.*, 1983).

Figure 10.93 Stereoview of the molecular conformation of spiperone in Form II where: ● C, ◎ F, ● N, ● O (Koch and Germain, 1972).

Table 10.29 Crystal Data of Spiperone Forms I and II

Parameter	Form I[a]	Form II[b]
Space Group	$P2_1/a$	$P2_1/c$
a (Å)	12.722	18.571
b (Å)	7.510	6.072
c (Å)	21.910	20.681
β	95.08°	118.69°
Z	4	4
V (Å^3)	2085.1	2045.7

a Azibi *et al.*, 1983. *b* Koch and Germain, 1972.

showed that the conformation of the two forms are significantly different (see Figures 10.92–10.93). The authors analyzed the crystal packing and determined that hydrogen bonding was responsible for the polymorphism.

B. Sulfapyridine

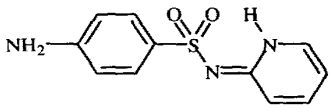

"imide"

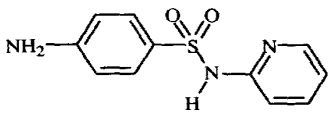

"amide"

Bar and Bernstein (1985) described the conformational polymorphism of 4-amino-*N*-2-pyridinylbenzenesulfonamide, sulfapyridine. The crystal structures of four forms of sulfapyridine were determined and are summarized in Table 10.30. The bond lengths and bond angles among the four structures are virtually identical, and are consistent with the imide structure. However, the conformations of the molecules are different in the different crystal structures, producing the phenomenon termed "conformational polymorphism." The conformations of the four different crystal forms are shown in Figure 10.94. It is clear that there is a different conformation about the —SO_2— bond in different molecules with some of the sulfapyridine rings pointing to the left in some forms and to the right in other forms.

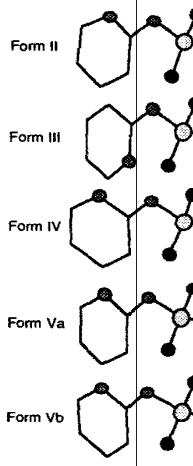

Figure 10.94 Stereoview of the
Bernstein, 1985; I

Table 10.30 Crystal Data for Su

Parameter	Form II[a]
Space group	$P2_1/c$
a (Å)	6.722
b (Å)	20.593
c (Å)	8.505
β	101.14°
Z	4
ρ_{calc} (g cm^{-3})	1.43
V (Å^3)	1155.1

a Bar and Bernstein, 1985. *b* Ba

Bar and Bernstein (19
dine in the different crystal
tions showed that all four fo

Finally, the authors co
single crystal structures obt
the different crystal forms.
well with the published diff
of Form II and III did not a
that there are additional crys
that a given powder patter
calculated pattern from a sin
either from observed single
nates using a program such

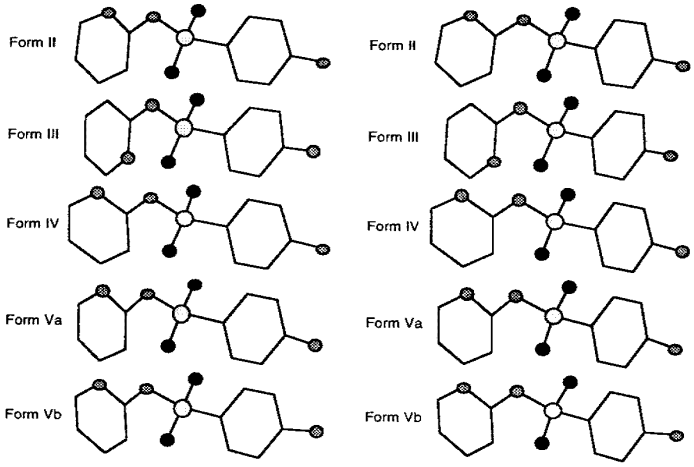

Figure 10.94 Stereoview of the molecular conformations in the four forms of sulfapyridine (Bar and Bernstein, 1985; Basak *et al.*, 1984; Bernstein, 1988).

Table 10.30 Crystal Data for Sulfapyridine

Parameter	Form II[a]	Form III[b]	Form IV[c]	Form V[a]
Space group	$P2_1/c$	$C2/c$	$P2_1/c$	$Pbca$
a (Å)	6.722	12.830	13.560	24.722
b (Å)	20.593	11.714	6.480	15.710
c (Å)	8.505	15.400	14.120	12.147
β	101.14°	94.12°	113.70	...
Z	4	8	4	16
ρ_{calc} (g cm^{-3})	1.43	1.44	1.46	1.41
V (Å^3)	1155.1	2308.5	1136.1	4717.7

a Bar and Bernstein, 1985. *b* Basak *et al.*, 1984. *c* Bernstein, 1988.

Bar and Bernstein (1985) also investigated the molecular energetics of sulfapyridine in the different crystal forms using extended Hückel calculations. These calculations showed that all four forms are within about 2.1 kJ/mol in energy.

Finally, the authors compared their data to research from other laboratories. The single crystal structures obtained allowed calculation of the X-ray powder patterns of the different crystal forms. The calculated X-ray powder pattern of Form I compared well with the published diffractogram. However, the calculated X-ray powder patterns of Form II and III did not agree with any previously reported patterns. This suggests that there are additional crystal forms. This study illustrates that the best way to prove that a given powder pattern is that of a pure polymorph is by comparing it with a calculated pattern from a single crystal structure. The powder pattern may be calculated either from observed single crystal diffraction intensity data or from the atomic coordinates using a program such as *Cerius*[2] (see Section 3.5).

10.10 POLYMORPHISM AND CHEMICAL STABILITY

Because polymorphs have different properties, including different melting points, densities, and crystal structures, it is not surprising that polymorphs have different chemical stabilities.

Perhaps the most striking effect of polymorphism on chemical reactivity is seen in the polymorphs of *trans*-2-ethoxycinnamic acid (see Figure 10.95). Irradiation of this compound in solution produces *trans*- to *cis*-isomerization, but no dimerization (Cohen and Green, 1973). Crystallization of this cinnamic acid yields three polymorphs, α, β, and γ. The α-form is obtained from ethyl acetate, ether, or acetone; the β-form is obtained from benzene or petroleum ether; and the γ-form is obtained from aqueous ethanol. Irradiation of the α-form gives the centrosymmetric dimer, irradiation of the β-form gives the mirror symmetric dimer, and irradiation of the γ-form produces no reaction. These reactions are summarized in Figure 10.95. Numerous examples of similar behavior have been found in other cinnamic acid derivatives and in anthracene dimerizations.

A number of pharmaceutical examples of different stabilities of polymorphs are also known. For example, methylprednisolone crystallizes in two forms. One form is stable while the other is reactive when exposed to heat, ultraviolet light, or high humidity (Munshi, 1973).

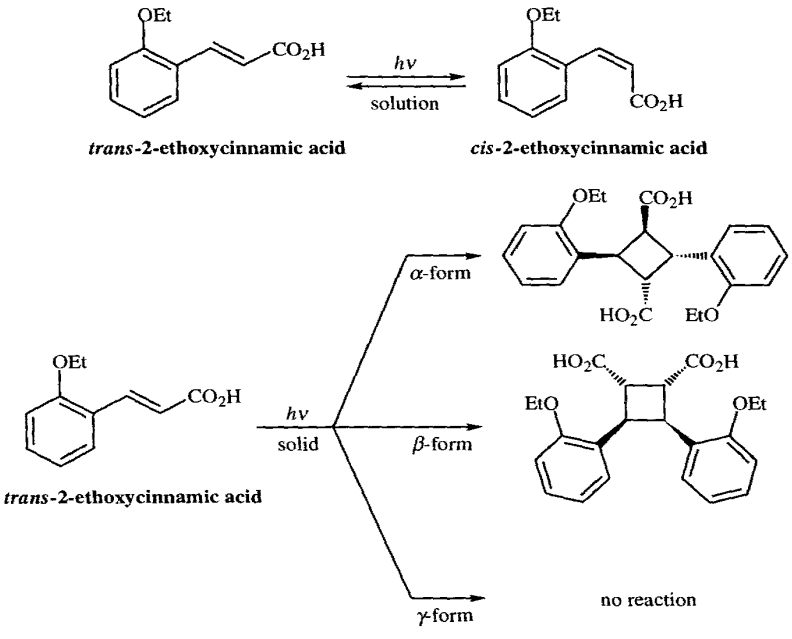

Figure 10.95 Summary of the reactivities of the α-, β-, and γ-crystalline forms of *trans*-2-ethoxycinnamic acid upon exposure to ultraviolet light (Cohen and Green, 1973).

In closely related stu
been reported. In our lab
polymorphs of hydrocort
ethanol in three crystalline
light, one of the solvates is
there are numerous cases
crystalline form. Macek (1
potassium penicillin G are
of the potassium salt can w
of the amorphous form re
have found similar differ
applied to sensitivity discs
detail in Chapter 12 (see S
This discussion clearly
there is a need for careful c

10.11 POLYMORPHISM AN

The rate of absorption of a
dissolution rate is affected
the lowest solubility and, i
polymorphs will usually
ignored, significant dose-t
In a particular striking
taining various ratios of F
(*i.e.*, blood levels) (Aguia

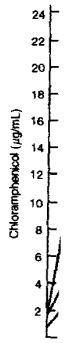

Figure 10.96 Comparison
suspensions c
oral dose equi
creases, the pe
the next 25%
McCrone, 19

In closely related studies, different stabilities of polymorphs and solvates have been reported. In our laboratory, we have reinvestigated the behavior of the various polymorphs of hydrocortisone 21-*tert*-butylacetate. This steroid crystallizes from ethanol in three crystalline forms, one anhydrous and two solvates. When exposed to light, one of the solvates is reactive while the other two forms are stable. In addition, there are numerous cases where amorphous forms are much more reactive than the crystalline form. Macek (1965) has reported that the amorphous forms of sodium and potassium penicillin G are significantly less stable than the crystalline forms. Crystals of the potassium salt can withstand heating for several hours, while identical treatment of the amorphous form results in a significant loss of activity. Pfeiffer *et al.* (1976) have found similar differences between amorphous and crystalline cephalosporins applied to sensitivity discs. The reactivity of amorphous drugs is discussed in more detail in Chapter 12 (see Sections 12.1C–D).

This discussion clearly shows that in cases where chemical stability is a problem, there is a need for careful control of the polymorph or solvate.

10.11 Polymorphism and Bioavailability

The rate of absorption of a drug is sometimes dependent upon the dissolution rate. The dissolution rate is affected by the polymorph present, with the most stable form having the lowest solubility and, in most cases, the slowest dissolution rate. Other less stable polymorphs will usually have higher dissolution rates. Thus, if polymorphism is ignored, significant dose-to-dose variations can occur (Haleblian and McCrone, 1969).

In a particular striking example, a suspension of chloramphenicol palmitate containing various ratios of Form A and B showed significant variations in bioavailability (*i.e.*, blood levels) (Aguiar *et al.*, 1967). Figure 10.96 shows a comparison of mean

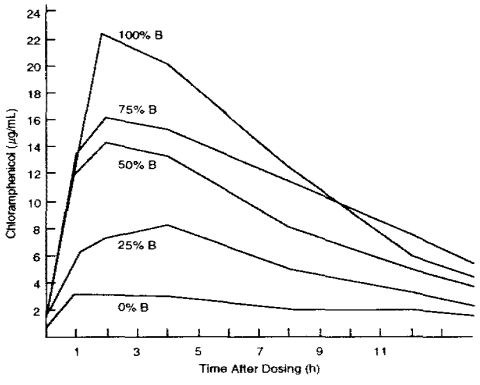

Figure 10.96 Comparison of the mean serum levels obtained with chloramphenicol palmitate suspensions containing varying ratios of the A and B polymorphs following a single oral dose equivalent to 1.5 gm of chloramphenicol palmitate. As the blood level increases, the percent of polymorph B increases. The lowest curve corresponds to 0% B, the next 25% B, the next 50% B, then 75% B, and the highest 100% B (Haleblian and McCrone, 1969).

blood serum levels of suspensions containing varying ratios of Form A and B. Clearly, the maximum blood levels are quite different, ranging from 3 to 22 μg/mL or by approximately a factor of seven. (Interestingly, a plot of peak blood levels versus percent Form B gave a straight line, as shown in Figure 10.97.) These data show that bioavailability is influenced by the type and concentration of the polymorph present. Obviously, if products are manufactured containing Form A, they will be largely inactive, while products containing Form B will show activity.

In another study, serum levels of the amorphous form and Form A of chloramphenicol palmitate have been compared in both children and Rhesus monkeys. Table 10.31 lists the results of these studies (Banerjee *et al.*, 1971) which show that the amorphous form has greater bioavailability than Form A.

Fluprednisolone crystallizes in three polymorphs and two solvates. These forms were pressed into pellets and implanted into rats, and their *in vivo* dissolution rates

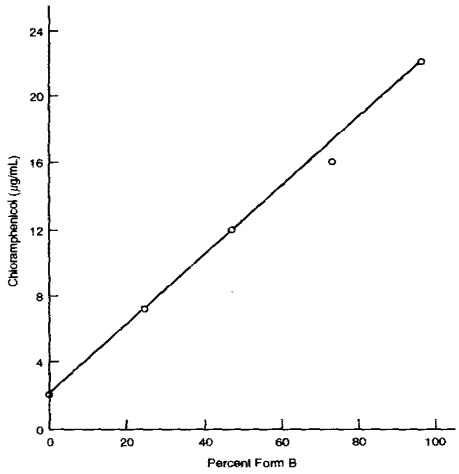

Figure 10.97 Plot of the peak chloramphenicol palmitate blood levels versus the percent of polymorph B (Haleblian and McCrone, 1969).

Table 10.31 Blood Levels (μg/100 mL) for Various Suspensions of Chloramphenicol Palmitate[a]

Suspension used	Hours after Feeding 2	4	6	8
		In Children		
Amorphous	102	60	42	26
Polymorph A	34	35	57	23
		In Rhesus Monkeys		
Amorphous	58	39	18	
Polymorph A	22	17	17	

a Banerjee *et al.*, 1971.

were measured (Haleblian and McCrone, 1969). The dissolution rates showed the following order and value: Form I (0.237 mg cm^{-2} M^{-1}) > Form III (0.209 mg cm^{-2} M^{-1}) > Form II (0.186 mg cm^{-2} M^{-1}) > β-monohydrate (0.162 mg cm^{-2} M^{-1}) > α-monohydrate (0.147 mg cm^{-2} M^{-1}). Thus, the variation in dissolution rate is approximately a factor of 1.6 when comparing Form I to the α-monohydrate.

The examples discussed in this section show that the polymorph present can dramatically affect the bioavailability of a drug.

10.12 Polymorphism and Its Pharmaceutical Application

Because polymorphs have different physical properties, it is often advantageous to choose the proper polymorph for the desired pharmaceutical application (see Section 22.10). In general, the pharmaceutical applications of polymorphism depends on the answers to the following questions:

1. What are the solubilities of each form?
2. Can pure, stable crystals of each form be prepared?
3. Will the form survive processing, micronizing, and tableting?

Furthermore, several more basic questions about polymorphs also need to be answered:

1. How many polymorphs exist?
2. What is the chemical and physical stability of each of these polymorphs?
3. Can the metastable states be stabilized?

These basic questions can be answered as follows: The number of polymorphs can be determined by microscopic examination and by subsequent analytical studies using DSC, IR, solid-state NMR, X-ray powder diffraction, and single-crystal X-ray studies (see Section 22.3). The physical stability of each form can be determined using the solution phase transformation method. This method involves placing two polymorphs in a drop of saturated solution under the microscope. Under these conditions, the crystals of less stable form will dissolve and crystals of the more stable form will grow until only the most stable form remains. Comparison of the relative stabilities of pairs of forms in succession gives the order of stability of the various forms. This method can also be used to prepare metastable forms. In this case, the temperature is increased or decreased to the temperature where the metastable form is most stable and then the experiment repeated.

There are numerous activities in the pharmaceutical industry that require consideration of polymorphism; these have been reviewed by Haleblian and McCrone (1969). Tableting behavior depends upon the polymorph present. For example, Simmons *et al.* (1972) showed that tolbutamide exists in Forms A and B. Form B is plate-like and causes **powder bridging** in the hopper and **capping** problems during tableting. Form A, which is not plate-like, showed no problems during tableting.

The behavior of suspensions also depends upon the polymorph present. If the wrong polymorph of a drug is used, a phase transformation to a more stable form may occur producing a change in crystal size and possibly caking. A change in particle size is often undesirable as it may cause serious caking problems, as well as changes in the syringeability of the suspension. In addition, the new polymorph may have altered

dissolution properties and, thus, bioavailability. Caking is a particularly serious problem since a caked suspension cannot be resuspended upon shaking. For example, oxyclozanide, upon standing in quiescent (undisturbed) suspensions, undergoes an increase in particle size (Pearson and Varney, 1969). This is due to a solvent-mediated phase transformation between two polymorphs. As discussed earlier, under these conditions, crystals of the more stable form grow and those of the less stable form dissolve. This produces cakes that cannot be resuspended by shaking.

REFERENCES

Agafonov, V., B. Legendre, and N. Rodier (1989) "A new crystalline modification of spironolactone" *Acta Crystallogr., Sect. C. Cryst. Struct. Commun.* **45** 1661–1663.

Agafonov, V., B. Legendre, N. Rodier, D. Wouessidjewe, and J.-M. Cense (1991) "Polymorphism of spironolactone" *J. Pharm. Sci.* **80** 181–185.

Aguiar, Arondo J., John Krc, Jr., Arlyn W. Kinkel, and Joseph C. Samyn (1967) "Effect of polymorphism on the absorption of chloramphenicol from chloramphenicol palmitate" *J. Pharm. Sci.* **56** 847–853.

Alleaume, Marc, and Joseph Decap (1965) "Tridimensional refinement of β-sulfanilamide" *Acta Crystallogr.* **18** 731–736.

Alleaume, Marc, and Joseph Decap (1966) "Tridimensional refinement of γ-sulfanilamide" *Acta Crystallogr.* **19** 934–938.

Armour Research Foundation (1949) "Sulfasuxidine (*p*-2-thiazolylsulfamylsuccinanilic acid)" *Anal. Chem.* **21** 1293–1294.

Ashizawa, Kazuhide, Kiyohiko Uchikawa, Teiichi Hattori, Tadashi Sato and Yasuo Miyake (1988) "Polymorphic differences in α- and β-form crystals of 2*R*,4*S*,6-fluoro-2-methyl-spiro[chroman-4,4'-imidazoline]-2',5-dione (M79175) as determined by X-ray diffraction, infrared spectroscopy, and differential scanning calorimetry" *J. Pharm. Sci.* **77** 635–637.

Ashizawa, Kazuhide (1989) "Polymorphism and crystal structure of 2*R*,4*S*,6-fluoro-2-methyl-spiro[chroman-4,4'-imidazoline]-2',5-dione (M79175)" *J. Pharm. Sci.* **78** 256–260.

Azibi, M., M. Draguet-Brughmans, R. Bouche, B. Tinant, G. Germain, J. P. DeClercq, and M. Van Meerssche (1983) "Conformational study of two polymorphs of spiperone: possible consequences on the interpretation of pharmacological activity" *J. Pharm. Sci.* **72** 232–235.

Banerjee, Sachchidananda, Asok Bandyopadhyay, Ramesh Chandra Bhattacharjee, Arun Kumar Mukherjee, and Arup Kumar Halder (1971) "Serum levels of chloramphenicol in children, rhesus monkeys, and cats after administration of chloramphenicol palmitate suspension" *J. Pharm. Sci.* **60** 153–155.

Bar, I. and J. Bernstein (1985) "Conformational polymorphism. VI. The crystal and molecular structures of Form II, Form III, and Form V of 4-amino-*N*-2-pyridinylbenzenesulfonamide (sulfapyridine)" *J. Pharm. Sci.* **74** 255–263.

Basak, A. K., S. Chaudhuri, and S. K. Mazumdar (1984) "Structure of 4-amino-*N*-2-pyridylbenzenesulfonamide (sulfapyridine), $C_{11}H_{11}N_3O_2S$" *Acta Crystallogr., Sect. C, Cryst. Struct. Commun.* **C40** 1848–1851.

Basak, A. K., S. K. Mazumdar, and S. Chaudhuri (1987) "Structure of N'-(6-methoxy-3-pyridazinyl)sulfanilamide (sulfamethoxypyridazine)" *Acta Crystallogr., Sect. C, Cryst. Struct. Commun.* **C43** 735–738.

Bernstein, J. and A. T. Hagler (1978) "Conformational polymorphism. The influence of crystal structure on molecular conformation" *J. Am. Chem. Soc.* **100** 673–681.

Bernstein, Joel (1987) "Conformational polymorphism" in *Organic Solid State Chemistry*; G. R. Desiraju, Ed.; Studies in Organic Chemistry 32; Elsevier: Amsterdam; Chapter 13.

Bernstein, J. (1988) "Polymorph IV of 4-amino-*N*-2-pyridinylbenzenesulfonamide (sulfapyridine)" *Acta Crystallogr., Sect. C, Cryst. Struct. Commun.* **C44** 900–902.

Bettinetti, G. P., F. Giordano, and A. La Manna (1982) "Solid state molecular arrangements of sulfamethoxazole $C_{10}H_{11}N_3O_3S$: the crystal structure of two polymorphs" *Cryst. Strucut. Comm.* **11** 821–828.

Biles, John A. (1963) "Some crystalline modifications of the *tert*-butylacetates of prednisolone and hydrocortisone" *J. Pharm. Sci.* **52**, 1066–1070.

Borchardt, Thomas B. (1997) "The derivatization, solid-state characterization, and crystallization of a pharmaceutical precursor that expresses color polymorphism in the solid state" Ph.D. Thesis, Purdue University: West Lafayette, IN 47907-1333.

Brown, Herbert C. and Sei Sujishi (1948) "Tri-1-naphthylboron as a highly hindered reference acid: a case of polymorphism ascribed to hindered rotation" *J. Am. Chem. Soc.* **70** 2793–2802.

Burger, A. (1973) "The polymorphs of sulfanilamide" *Sci. Pharm.* **41** 290–303.

Burger, A. (1973) "Solubility studies in the determination of thermodynamic data of a polymorphic pharmaceutical (sulfanilamide)" *Sci. Pharm.* **41** 303–314.

Burger, Artur (1975) "Polymorphism of oral antidiabetics. II. Tolbutamide" *Sci. Pharm.* **43** 161–168.

Burger, Artur and Regine D. Dialer (1983) "New research results on the polymorphism of sulfathiazole" *Pharm. Acta Helv.* **58** 72–78.

Burger, A. and U. J. Griesser (1989) "The polymorphic drug substances of the European Pharmacopoeia. IV. Identification and characterization of 11 crystal forms of succinylsulfathiazole" *Sci. Pharm.* **57** 293–305.

Burger, Artur and Ulrich J. Griesser (1991) "Physical stability, hygroscopicity and solubility of succinylsulfathiazole crystal forms. The polymorphic drug substances of the European Pharmacopoeia. VII" *Eur. J. Pharm. Biopharm.* **37** 118–124.

Busetta, Bernard, Christian Courseille, and Michel Hospital (1973) "Crystal and molecular structure of three polymorphous forms of estrone" *Acta Crystallogr., Sect. B., Struct. Sci.* **B29** 298–313.

Byrn, Stephen R., David Y. Curtin, and Iain C. Paul (1972) "X-ray crystal structures of the yellow and white forms of dimethyl 3,6-dichloro-2,5-dihydroxyterephthalate and a study of the conversion of the yellow form to the white form in the solid state" *J. Am. Chem. Soc.* **94** 890–898.

Byrn, Stephen R. and Chung-Tang Lin (1976) "The effect of crystal packing and defects on desolvation of hydrate crystals of caffeine and L-(−)-1,4-cyclohexadiene-1-alanine" *J. Am. Chem. Soc.* **98** 4004–4005.

Byrn, Stephen R., Brian Tobias, Donald Kessler, James Frye, Paul Sutton, Patricia Saindon, and John Kozlowski (1988) "Relationship between solid state NMR spectra and crystal structures of polymorphs and solvates of drugs" *Trans. Am. Crystallogr. Assoc.* **24** 41–54.

Chiang, Chian C., Wilson H. DeCamp, David Y. Curtin, Iain C. Paul, Sidney Shifrin, and Ulrich Weiss (1978) "Color dimorphism of 14-hydroxymorphinone. X-ray analysis of two different crystalline modifications" *J. Am. Chem. Soc.* **100** 6195–6201.

Cohen, M. D. and Bernard S. Green (1973) "Organic chemistry in the solid state" *Chem. Brit.* **9** 490–497.

Craven, B. M. and E. A. Vizzini (1969) "Crystal structures of two polymorphs of 5-ethyl-5-isoamylbarbituric acid (amobarbital)" *Acta Crystallogr., Sect. B., Struct. Sci.* **B25** 1993–2009.

Curtin, D. Y. and S. R. Byrn (1969) "Stereoisomerism at the oxygen-carbon single bond due to hydrogen bonding. Structures of the yellow and white crystalline forms of dimethyl 3,6-dichloro-2,5-dihydroxyterephthalate" *J. Am. Chem. Soc.* **91** 1865–1866.

Curtin, David Y. and John H. Englemann (1972) "Intramolecular oxygen-nitrogen benzoyl migration of 6-aroyloxyphenanthridines" *J. Org. Chem.* **37** 3439–3443.

Dabrowski, Janusz (1963) "Infrared spectra and structure of substituted unsaturated carbonyl compounds. I. Enamino ketones with primary amino group" *Spectrochim. Acta* **19** 475–496.

Debord, B., C. Lefebvre, A. M. Guyot-Hermann, J. Hubert, R. Bouché, and J. C. Guyot (1987) "Study of different crystalline forms of mannitol: comparative behavior under compression" *Drug Dev. Ind. Pharm.* **13** 1533–1546.

DeCamp, Wilson H. and F. R. Ahmed (1972a) "Structural studies of synthetic analgesics. II. Crystal and molecular structure of the monoclinic form of (±)-β-promedol alcohol" *Acta Crystallogr., Sect. B., Struct. Sci.* **B28** 1796–1800.

DeCamp, Wilson H. and F. R. Ahmed (1972b) "Structural studies of synthetic analgetics. III. Crystal and molecular structure of the rhombohedral form of (±)-β-promedol alcohol" *Acta Crystallogr., Sect. B., Struct. Sci.* **B28** 3484–3489.

Desiraju, Gautam R., Iain C. Paul, and David Y. Curtin (1977) "Conversion in the solid state of the yellow to the red form of 2-(4'-methoxyphenyl)-1,4-benzoquinone. X-ray crystal structures and anisotropy of the rearrangement" *J. Am. Chem. Soc.* **99** 1594–1601.

Dideberg, O., and L. Dupont (1972) "Crystal and molecular structure of spironolactone, 7α-acetylthio-3-oxo-17α-4-pregnene-21,17β-carbolactone" *Acta Crystallogr., Sect. B., Struct. Sci.* **28** 3014–3022.

Doherty, Chris and Peter York (1988) "Frusemide crystal forms; solid state and physiochemical analyses" *Int. J. Pharm.* **47** 141–155.

Donaldson, J. D., J. R. Leary, S. D. Ross, M. J. K. Thomas, and C. H. Smith (1981) "The structure of the orthorhombic form of tolbutamide (1-*n*-butyl-3-*p*-toluenesulphonylurea)" *Acta Crystallogr., Sect. B., Struct. Sci.* **B37** 2245–2248.

Dudek, Gerald O. and Gert P. Volpp (1963) "Nuclear magnetic resonance studies of keto-enol equilibria. V. Isomerization in aliphatic Schiff bases" *J. Am. Chem. Soc.* **85** 2697–1702.

Dunitz, Jack D. and Joel Bernstein (1995) "Disappearing polymorphs" *Acc. Chem. Res.* **28** 193–200.

Eistert, Bernd, Friedrich Weygand, and Ernst Csendes (1952) "Polymorphism of the chalcones" *Chem. Ber.* **85** 164–168.

Fletton, Richard A., Robert W. Lancaster, Robin K. Harris, Alan M. Kenwright, Kenneth J. Packer, David N. Waters, and Alan Yeadon (1986) "A comparative spectroscopic investigation of two polymorphs of 4'-methyl-2'-nitroacetanilide using solid-state infrared and high-resolution solid-state nuclear magnetic resonance spectroscopy" *J. Chem. Soc., Perkin Trans. 2* **1986** 1705–1709.

Gerber, J. J., J. G. vander Watt, and A. P. Lötter (1991) "Physical characterization of solid forms of cyclopenthiazide" *Int. J. Pharm.* **73** 137–145.

Ghielmetti, G., T. Bruzzese, C. Bianchi, and F. Recusani (1976) "Relationship between acute toxicity in mice and polymorphic forms of polyene antibiotics" *J. Pharm. Sci.* **65** 905–907.

Giuseppetti, G., C. Tadini, G. P. Bettinetti, and F. Giordano (1977) "2-Sulfanilamido-5-methoxypyrimidine, $C_{11}H_{12}N_4O_3S$" *Cryst. Struct. Commun.* **6** 263–274.

Goldberg, Israel and Yigal Becker (1987) "Polymorphs of tamoxifen citrate: detailed structural characterization of the stable form" *J. Pharm. Sci.* **76** 259–264.

Gougoutas, J. Zanos and L. Lessinger (1974) "Solid state chemistry of organic polyvalent iodine compounds. III. The crystal structures of 3-oxo-3*H*-2,1-benzoxiodol-1-yl *m*-chlorobenzoate (two polymorphs) and its isostructural derivative, 3-oxo-3*H*-2,1-benzoxiodol-1-yl benzoate" *J. Solid State Chem.* **9** 155–164.

Griesser, Ulrich J. and Xiaorong He (1998) Personal communication; Purdue University: West Lafayette, IN 47907-1336.

Guillory, J. Keith (1967) "Heats of transition of methylprednisolone and sulfathiazole by a differential thermal analysis method" *J. Pharm. Sci.* **56** 72–76.

Haleblian, John and Walter McCrone (1969) "Pharmaceutical applications of polymorphism" *J. Pharm. Sci.* **58** 911-929.

Hamlin, W. E., E. Nelson, B. E. Ballard, and J. G. Wagner (1962) "Loss of sensitivity in distinguishing real differences in dissolution rates due to increasing intensity of agitation" *J. Pharm. Sci.* **51** 432–435.

Herbstein, F. H. and G. M. J. Schmidt (1955) "The crystal and molecular structures of heterocyclic compounds. I. The analysis of the crystal structure of α-phenazine" *Acta Crystallogr.* **8** 399–405.

Higuchi, W. I., P. D. Bernardo, and S. C. Mehta (1967) "Polymorphism and drug availability. II. Dissolution rate behavior of the polymorphic forms of sulfathiazole and methylprednisolone" *J. Pharm. Sci.* **56** 200–207.

Higuchi, W. I., W. E. Hamlin, S. C. Mehta (1969) "Infrared attenuated total reflectance (ATR) method for observing the water-mediated surface phase reversion of methylprednisolone II to I during dissolution" *J. Pharm. Sci.* **58** 1145–1146.

Ip, Dominic P., Gerald S. Brenner, James M. Stevenson, Siegfried Lindenbaum, Alan W. Douglas, S. David Klein, and James A. McCauley (1986) "High resolution spectroscopic evidence and solution calorimetry studies on the polymorphs of enalapril maleate" *Int. J. Pharm.* **28** 183–191.

Kato, Yuriko, Yumi Okamoto, Sayoko Nagasawa, and Ichiko Ishihara (1984) "New polymorphic forms of phenobarbital" *Chem. Pharm. Bull.* **32** 4170–4174.

Koch, Michael H. J. and Gabriel Germain (1972) "Crystal and molecular structure of 4-[1-(4-hydroxy-4-*p*-fluorophenyl)piperidinyl]-4'-fluorobutyrophenone and its hydrochloride" *Acta Crystallogr., Sect. B., Struct. Sci.* **B28** 121–125.

Koo, Chung Hoe, Sung Il Cho, and Young Hee Yeon (1980) "The crystal and molecular structure of chlorpropamide" *Arch. Pharmacal. Res.* **3** 37–49.

Kopp, Sabine, Christian H
misinterpretations of D
Pharm. Technol. **34** 21

Krigbaum, W. R. and G.
Crystallogr., Sect. B,

Kruger, G. J. and G. Gafner
Crystallogr., Sect. B.,

Kruger, G. J. and G. Gafner
Struct. Sci. **B27** 326–3

Kuhnert-Brandstätter, M. (1
New York, NY.

Kuhnert-Brandstätter, M. an
tions on enantiotropic p

Kuhnert-Brandstätter, M., I.
investigations on enanti

Kuhnert-Brandstätter, M., I.
investigations on enanti

Kuhnert-Brandstätter, M. an
Halofenate, lorcainide h
71–82.

Kuhnert-Brandstätter, M. an
Mexiletine hydrochloric
Pharm. **55** 13–25.

Kuhnert-Brandstätter, M. an
Bupicomide, buspirone
chloride and piretanide"

Kuhnert-Brandstätter, M. an
Amiperone, bentiromide
Pharm. **57** 81–96.

Kuhnert-Brandstätter, M. an
Famotidine, flupirtine m
Pharm. **58** 55–67.

Levy, Gerhard and Josephin
polymorphs" *J. Pharm.*

Lin, Chung-Tang, Phillipe H
"Solid-state photooxidati
Chem. **47** 2978–2981.

Macek, Thomas J. (1965) "Th
forms for new pharmace

Matsuda, Yoshihisa and Ets
modifications" *Int. J. Pha*

Mesley, R. J. (1971) "The pol

Milosovich, George (1964) "
53 484–487.

Mitchell, A. G. (1985) "Pol
Pharm. Pharmacol. **37** 6(

Miyamae, Akira, Shigetaka K
(1990) "X-ray crystallogr
6-methylbenzyloxy)-2-me

Molecular Simulations, Inc. (

Moustafa, M. A., A. R. Ebi
crystal forms" *J. Pharm.*

Munshi, Mayank V. (1973)
Thesis, University of Mic

Nirmala, K. A., and D. S. Sak
logr., Sect. B., Struct. Sci

Kopp, Sabine, Christian Beyer, [illegible] (1988) "Potential misinterpretations of DTA/DSC [illegible] phenobarbital" *Acta Pharm. Technol.* **34** [illegible]

Krigbaum, W. R. and [illegible] Wildman [illegible] bromotoluene" *Acta Crystallogr., Sect. B: Struct. Sci.* **B27** [illegible]

Kruger, G. J. and G. Gafner (1971) [illegible] sulfathiazole" *Acta Crystallogr., Sect. B: Struct. Sci.* **B27** [illegible]

Kruger, G. J. and G. Gafner (1971) [illegible] *Crystallogr., Sect. B: Struct. Sci.* **B27** 326–[illegible]

Kuhnert-Brandstätter, M. [illegible] Pergamon, New York, NY.

Kuhnert-Brandstätter, M. and [illegible] optical investigations on enantiotropic polymorphs [illegible]

Kuhnert-Brandstätter, M., [illegible] IR spectroscopical investigations on enantiotropic [illegible] **50** [illegible]

Kuhnert-Brandstätter, M., [illegible] and IR spectroscopical investigations on enantiotropic [illegible] **50** [illegible] 216.

Kuhnert-Brandstätter, M. and [illegible] of Drugs. II: Halofenate, lorcainide [illegible] *Pharm.* **54** 71–82.

Kuhnert-Brandstätter, M. [illegible] of Drugs. III: Mexiletine hydrochloride [illegible] pirprofene" *Sci. Pharm.* **55** 13–25.

Kuhnert-Brandstätter, M. and [illegible] of Drugs. VI: Bupicomide, buspirone hydrochloride [illegible] naftifine hydrochloride and piretanide" [illegible] **58** [illegible]

Kuhnert-Brandstätter, M. [illegible] of Drugs [illegible]: Amiperone, bentiromide [illegible] fenticonazole" *Sci. Pharm.* **57** 81–96.

Kuhnert-Brandstätter, M. [illegible] of Drugs. VII: Famotidine, flupirtine [illegible] albendazole" *Sci. Pharm.* **58** 55–67.

Levy, Gerhard and Joseph [illegible] methylprednisolone polymorphs" *J. Pharm.* [illegible] **53** [illegible]

Lin, Chung-Tang, Phillipe Perrier [illegible] R. Byrn (1982) "Solid-state photooxidation [illegible] acetate" *J. Org. Chem.* **47** 2978–298[illegible]

Macek, Thomas J. (1965) [illegible] formulation of dosage forms for new pharmaceuticals [illegible]

Matsuda, Yoshihisa and [illegible] of furosemide modifications" *Int.* [illegible] **60** [illegible]

Mesley, R. J. (1971) "The [illegible] 604.

Milosovich, George (1964) [illegible] *Pharm.* [illegible] **53** 484–487.

Mitchell, A. G. (1985) [illegible] clopamide" *J. Pharm. Pharmacol.* **37** [illegible]

Miyamae, Akira, Shigetaka Koda [illegible] Yoshi Morimoto (1990) "X-ray crystallographic [illegible] carbonylamino-6-methylbenzyloxy-2-methyl [illegible] **79** 189–[illegible]

Molecular Simulations, Inc. [illegible]

Moustafa, M. A., A. R. Ebian [illegible] methoxydiazine crystal forms" *J. Pharm. Pharmacol.* [illegible] **23** [illegible]

Munshi, Mayank V. (19[illegible]) [illegible] Thesis, University of Michigan [illegible]

Nirmala, K. A., and D. S. Sake Gowda [illegible] *Crystallogr., Sect. B: Struct.* [illegible]

O'Conner, B. H. and E. N. Maslen (1965) "The crystal structure of α-sulfanilamide" *Acta Crystallogr.* **18** 363–366.

Pearson, J. T. and G. Varney (1969) "Crystal growth studies involving phase transitions in aqueous drug suspensions" *J. Pharm. Pharmacol., Suppl.* **21** 60S–96S.

Perrin, M. and P. Michel (1973a) "Polymorphism of *p*-chlorophenol. I. Crystal structure and morphology of the stable form" *Acta Crystallogr., Sect. B., Struct. Sci.* **B29** 253–258.

Perrin, M. and P. Michel (1973b) "Polymorphism of *p*-chlorophenol. I. Crystal structure of the metastable form (β-form) at low temperature" *Acta Crystallogr., Sect. B., Struct. Sci.* **B29** 258–263.

Pfeiffer, Ralph R., Gary L. Engel, and Dennis Coleman (1976) "Stable antibiotic sensitivity disks" *Antimicrob. Agents Chemother.* **9** 848–851.

Phillips, D. C. (1956) "The crystallography of acridine. II. The structure of acridine III" *Acta Crystallogr.* **9** 237–250.

Phillips, D. C., F. R. Ahmed, and W. H. Barnes (1960) "The crystallography of acridine. III. The structure of acridine II" *Acta Crystallogr.* **13** 365–377.

Rambaud, J., R. Roques, S. Alberola, and F. Sabon (1980) "Crystallographic structure of 3-(4-aminobenzenesulfonamido)-5-methylisoxazole" *Bull. Soc. Chim. Fr.* **1980** 56–60.

Richardson, Mary Frances, Quing-Chuan Yang, Elisabeth Novotny-Bregger, and Jack D. Dunitz (1990) "Conformational polymorphism of dimethyl 3,6-dichloro-2,5-dihydroxyterephthalate. II. Structural, thermodynamic, kinetic and mechanistic aspects of phase transformations among the three crystal forms" *Acta Crystallogr., Sect. B* **B46**, 653–660.

Robertson, J. Monteath and J. G. White (1947) "The crystal structure of the orthorhombic modification of 1,2,5,6-dibenzathracene. A quantitative X-ray investigation" *J. Chem. Soc.* **1947** 1001–1010.

Robertson, J. Monteath and J. G. White (1956) "The crystal structure of the monoclinic modification of 1,2,5,6-dibenzanthracene. A quantitative X-ray investigation" *J. Chem. Soc.* **1956** 925–931.

Rowe, Englebert L. and Bradley D. Anderson (1984) "Thermodynamic studies of tolbutamide polymorphs" *J. Pharm. Sci.* **73** 1673–1675.

Saindon, Patricia J., Nina S. Cauchon, Paul A. Sutton, C.-j. Chang, Garnet E. Peck, and Stephen R. Byrn (1993) "Solid-state nuclear magnetic resonance (NMR) spectra of pharmaceutical dosage forms" *Pharm. Res.* **10** 197–203.

Schulenberg, John W. (1968) "Isolation of crystalline keto-enol tautomers. Conversion into indoles and oxindoles" *J. Am. Chem. Soc.* **90** 7008–7014.

Shafizadeh, Fred and Ronald A. Susott (1973) "Crystalline transitions of carbohydrates" *J. Org. Chem.* **38** 3710–3715.

Shefter, Eli and Takeru Higuchi (1963) "Dissolution behavior of crystalline solvated and nonsolvated forms of some pharmaceuticals" *J. Pharm. Sci.* **52** 781–791.

Shenouda, Latif S. (1970) "Various species of sulfathiazole Form I" *J. Pharm. Sci.* **59** 785–787.

Shieh, Tiee-Leou, Chung-Tang Lin, Ann T. McKenzie, and Stephen R. Byrn (1983) "Relationship between the solid-state and solution conformations of β-(benzylamino)crotonate" *J. Org. Chem.* **48** 3103–3105.

Simmons, D. L., R. J. Ranz, N. D. Gyanchandani, and P. Picotte (1972) "Polymorphism in pharmaceuticals. II. Tolbutamide" *Can. J. Pharm. Sci.* **7** 121–123.

Simmons, D. L., R. J. Ranz, and N. D. Gyanchandani (1973) "Polymorphism in pharmaceuticals. III. Chlorpropamide" *Can. J. Pharm. Sci.* **8** 125–127.

Small, Lyndon F. and Erich Meitzner (1933) "Metathebainone" *J. Am. Chem. Soc.* **55** 4602–4610.

Smith, Jay, Ernesto MacNamara, Daniel Raftery, Thomas Borchardt, and Stephen Byrn (1998) "Application of two-dimensional ^{13}C solid-state NMR to the study of conformational polymorphism" *J. Am. Chem. Soc.* **120** 11710–11713.

Stephenson, G. A., T. B. Borchardt, S. R. Byrn, J. Bowyer, C. A. Bunnell, S. V. Snorek, and L. Yu (1995) "Conformational and color polymorphism of 5-methyl-2-[(2-nitrophenyl)amino]-3-thiophenecarbonitrile" *J. Pharm. Sci.* **84** 1385–1386.

Sunwoo, Chimin and Henry Eisen (1971) "Solubility parameter of selected sulfonamides" *J. Pharm. Sci.* **60** 238–244.

Sutton, Paul Allen (1984) "Crystal packing effects on the photochemical oxidation and solid state carbon-13 NMR chemical shifts of several anti-inflammatory steroids" Ph.D. Thesis, Purdue University, West Lafayette, IN 47907-1330.

Szabó-Révész, Piroská, Klárá Pintye-Hódi, Máriá Miseta, B. Selmeczi, G. Kedvessy, J. Traue, H. Kala, and U. Wenzel (1987) "Investigations about polymorphism of drugs in powders and tablets. IV. The influence of the polymorphism of drugs on the physical properties and drug release of phenobarbitone tablets" *Pharmazie* **42** 179–181.

Weintraub, H. J. R. and A. J. Hopfinger (1975) "*CAMSEQ* [conformational analysis of molecules in solution by empirical and quantum mechanical techniques] software system in drug design calculations" *Int. J. Quantum Chem., Quantum Biol. Symp.* **1975** 203–208.

Williams, P. P. (1973) "Polymorphism of phenobarbitone: the crystal structure of 5-ethyl-5-phenylbarbituric acid monohydrate" *Acta Crystallogr., Sect. B., Struct. Sci.* **B29** 1572–1579.

Williams, P. P. (1974) "Polymorphism of phenobarbitone. II. Crystal structure of modification III" *Acta Crystallogr., Sect. B., Struct. Sci.* **B30** 12–17.

Yang, Shiu Shiang and J. Keith Guillory (1972) "Polymorphism in sulfonamides" *J. Pharm. Sci.* **61** 26–40.

Yang, Qing-Chuan, Mary Frances Richardson, and Jack D. Dunitz (1989) "Conformational polymorphism of dimethyl 3,6-dichloro-2,5-dihydroxyterephthalate. I. Structures and atomic displacement parameters between 100 and 350 K for three crystal forms" *Acta Crystallogr., Sect. B* **B45** 312–323.

Yu, Lian (1998) Personal communication; Eli Lilly and Company: Indianapolis, IN 46285–0001.

Hydrates and Solvates

The occurrence of hydrated or solvated crystal forms (see Table 11.1), crystals in which solvent molecules occupy regular positions in the crystal structure, is widespread but by no means universal among drug substances. Some classes of drugs (*e.g.*, steroids, antibiotics, and sulfonamides) are particularly prone to form solvates, but this impression may be partly related to the considerable attention these drugs have received. In her classic book on thermomicroscopy, Kuhnert-Brandstätter

Table 11.1 Partial List of Drugs Discovered Prior to 1971 that Form Solvates

Drug	Reference
Ampicillin	Austin *et al.*, 1965
Cephaloridine	Chapman *et al.*, 1968; Pfeiffer *et al.*, 1970
Chloramphenicol	Himuro *et al.*, 1971
Cholesterol	Shefter and Higuchi, 1967
Cortisone acetate	Carless *et al.*, 1966
Eluprednisolone	Haleblian *et al.*, 1971
Erythromycin	Rose, 1955
Estradiol	Kuhnert-Brandstatter and Gasser, 1971
Fluorohydrocortisone acetate	Shefter and Higuchi, 1967
Gramicidin	Olsen and Szabo, 1959
Griseofulvin	Sekiguchi *et al.*, 1968
Hydrocortisone 21-acetate	Shell, 1955
Hydrocortisone 21-*tert*-butylacetate	Biles, 1963
Nitrofurmethone	Borka *et al.*, 1972
Prednisolone 21-*tert*-butylacetate	Biles, 1963
Succinylsulfathiazole	Shefter and Higuchi, 1967
Sulfabenzamide	Yang and Guillory, 1972
Sulfaguanidine	Yang and Guillory, 1972
Sulfameter	Moustafa *et al.*, 1971
Sulfanilamide	Lin, 1972

(Kuhnert-Brandstätter, 1971)

(1971) summarized in tabular form some of these examples (see Table 11.2). Nevertheless, many drugs, including some members of the aforementioned classes, even after intensive investigation, are found to always crystallize without solvent inclusion (*e.g.*, aspirin and ibuprofen).

In a classic study, Kuhnert-Brandstatter (1971) characterized the behavior of hydrates of pharmaceuticals known at that time using thermomicroscopy (see Table 10.2). Many of the hydrates listed in this table show unusual behavior that may be caused by dehydration prior to melting. Many of these crystals are reported to become opaque, and appear dark when viewed by transmitted light (see Chapter 14). Some of these hydrates crack and "jump" during dehydration. This behavior is characteristic of rapid solid-state reactions that produce gaseous products.

Another aspect of solvate formation is that virtually any laboratory solvent can be involved; Table 11.3 lists solvents in solvates reported in the crystal structure literature on organic compounds which, naturally, includes many crystalline drugs. In some solvates, two or even three different solvents occupy their own positions in the structure. Furthermore, a compound may form solvates with a given solvent in different ratios, 2:1, 1:1, etc., and in rare cases, a fixed ratio in polymorphic forms.

Because prediction of crystal structures is not yet generally possible, we must be content with examining the crystal structures of compounds after the fact in looking for explanations of why solvates do or do not form. On doing so, however, we are left with only vague impressions, to wit:

- Certain molecular shapes and features favor the formation of crystals without solvent. These structures tend to be stabilized by an efficient packing that also utilizes intermolecular hydrogen bonding and other bonding capacity to a maximum extent. The slightest molecular differences may conceivably interfere with this cooperative effect. As a result, solvate formation within a series of related compounds tends to lack a discernible pattern—each compound has a unique response to solvate formation.
- Including specific solvent molecules can stabilize a crystal structure by improving either the packing or the intermolecular bonding, especially hydrogen bonding. Some of the solvents listed in Table 11.3 are nonhydrogen-bonding solvents and thus must serve only in a space-occupying capacity. The hydrogen-bonding capacity of included solvent molecules is usually fully exploited, although some structures are known where such bonding capacity is not exercised at all.
- Lower temperatures favor formation of solvates and also higher stoichiometric amounts of a given solvent. This is probably due to the increased strength of hydrogen bonding at lower temperatures.
- The ease with which solvent is lost varies widely among solvates. At one extreme some retain solvent at temperatures well above the boiling point of the solvent, at the other extreme, others lose solvent readily at room temperature. In the latter case, the formation of a solvate may be overlooked unless special precautions are taken to preserve the composition of the crystals.

Table 11.2 Thermomicroscopic Behavior of Drug Hydrates

Drug	Mp (°C)	Remarks
Apomorphine hydrochloride	220–260	From 220 °C, turbidity and carbonization
Atropine sulfate	190–193	Substance partially dehydrates
Brucine	170	Crystals are rarely clear
Brucine sulfate	130–165	Gradual loss of water
Chloroquine sulfate	209–213	
Citric acid	152–155	Loss of H_2O and turbidity at 60–70 °C
Cocaine nitrate	55–59	Needles of decomposition product appear
Codeine	156	Loss of water with turbidity
Codeine hydrochloride	260–275	
Codeine phosphate	225–240	
Cyclophosphamide	40–47	Melts as hydrate
Dihydrocodeinone bitartrate	115–130	
Dipropylbarbituric acid	148	Commercial product partly dehydrated
Emetine hydrochloride	205–215	
L-Ephedrine	38–40	
Heroine hydrochloride	218–232	Turbidity of crystals from 115–120 °C
Histidine monohydrochloride	155–176	
Hydrocortisone hemisuccinate	198–205	From 85 °C, loss of water with turbidity
Hyoscyamine hydrochloride	152–155	Turbidity with loss of water during heating
Lidocaine hydrochloride	65–78	
Mercaptopurine	300–325	From 160 °C, turbidity of crystals
Mescaline sulfate	230–250	From 125 °C, water escapes with turbidity
Methicillin sodium	182–186	Loss of birefringence
Morphine	245–255	At 115–140 °C, loss of water with turbidity
Morphine hydrochloride	285–310	From 80 °C, loss of water with turbidity
Morphine sulfate	230–240	
Ouabain	178–184	Loses H_2O from 90 °C
Oxycodone hydrochloride	245–260	From 70 °C, loss of water with turbidity
Phloroglucinol	218–220	At 55–90 °C, turbidity with loss of water
Pyrogallol	133	Turbidity
Quercetin	300–320	
Quinidine hydrochloride	262–265	From 90 °C, loss of water
Quinidine sulfate	205–210	
Quinine bisulfate	155–160	Turbidity at 60 °C
Quinine hydrobromide	145–152	Water evolved at 90 °C
Raffinose pentahydrate	132–135	Transforms to anhydrous
Reserpine hydrochloride	125–225	From 180 °C, turbidity of crystals
α-Rhamnose	70–95	
Succinylsulfathiazole	190–193	
Sulphaguanidine	187–191	From 90 °C loss of water
Terpin hydrate	105.5	Transforms to anhydrous
Theophylline	274	At 70–80 °C, loss of water
L-Thyroxine sodium	195–202	From 70 °C, effervescence with jumping

(Kuhnert-Brandstätter, 1971)

Table 11.3 Solvents that Form Solvates with Drugs and Organic Compounds

water
methanol, ethanol, 1-propanol, isopropanol, 1-butanol, *sec*-butanol, isobutanol, *tert*-butanol
acetone, methyl ethyl ketone
acetonitrile
diethyl ether, tetrahydrofuran, dioxane
acetic acid, butyric acid, phosphoric acids
hexane, cyclohexane
benzene, toluene, xylene
ethyl acetate
ethylene glycol
dichloromethane, chloroform, carbon tetrachloride, 1,2-dichloroethane
N-methylformamide and *N*,*N*-dimethylformamide, *N*-methylacetamide
pyridine
dimethylsulfoxide

Most drug crystals that fall into the category of solvates are, for obvious reasons, hydrates—exceptions being ethanol or freon solvates. The organically solvated structures, nevertheless, also deserve our attention for several reasons:

- They are often the penultimate solid form of the drug (which should therefore be monitored carefully in the interests of good control).
- They are often specifically chosen for recovery or purification.
- They may have a morphology conducive to good filtration or other bulk processes.
- They may be the only crystalline form available for X-ray structure determination of a new molecular species.
- They may be useful in their desolvated form as a drug product due to superior dissolution properties.
- They may be patentable for any of the above reasons, thus prolonging the manufacturing exclusivity of the drug.

11.1 HYDRATES

The water molecule, because of its small size, is particularly suited to fill structural voids. The multidirectional hydrogen bonding capability of water is also ideal for linking a majority of drug molecules into stable crystal structures. Figure 11.1 shows how a water molecule in an ice crystal forms hydrogen bonds in four directions by acting twice as an hydrogen acceptor and twice as an hydrogen donor to neighboring molecules with identical bonding.

In hydrated crystal structures, we find that water molecules bind not only to other water molecules but also to any available functional groups like carbonyls, amines, alcohols and many others that can accept or donate an active hydrogen atom to form hydrogen bonds. As a result, the total hydrogen bonding of water in crystal hydrates is almost always one of the most important forces holding the structure together.

Owing to their high solubility and biocompatibility, sodium salts are commonly the derivative chosen for acidic drug products. Because the formation of crystal hydrates

is common for sodium salts of all drug classes, a look at why this is so prevalent may be helpful to our discussion of water in crystals.

The sodium ion in most crystal structures is coordinated to six ligands in an octahedral array. In sodium chloride, for example, six chloride ions surround each sodium ion. In monensin, a crown ether with extraordinary affinity for sodium, the coordinated ligands are bidentate, forming five-member rings with the sodium (see Figure 11.2). In sodium salts of drugs and other organic compounds, this strong coordination tendency of the sodium ion is satisfied by linkages to any suitable ligand to be found in the structure, such as carboxylate, alcohol, carbonyl, amide, sulfonate, and many others, particularly water. While hydrogen bonding between the various ligands tends to distort the regularity of the coordination octahedra around the sodium ion, the trend to octahedral coordination is almost universal.

The high affinity of the sodium ion for water is perhaps most striking when we find that some sodium ions in acid structures actually coordinate to water molecules and the charged oxygen atoms of the acid are relegated to a position more distant from the sodium ion, yet always hydrogen bonded to an intervening water molecule. Analysis of the charge distribution in some of these structures shows the charges to be quite diffuse rather than being concentrated at single atomic positions.

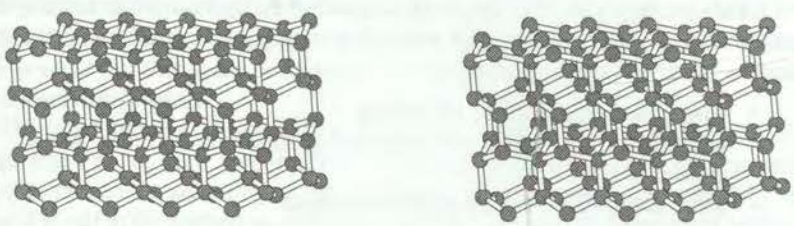

Figure 11.1 Stereoview of the hydrogen bonding in ice Form *Ih*. Only the the oxygen atoms are shown (Peterson and Levy, 1957).

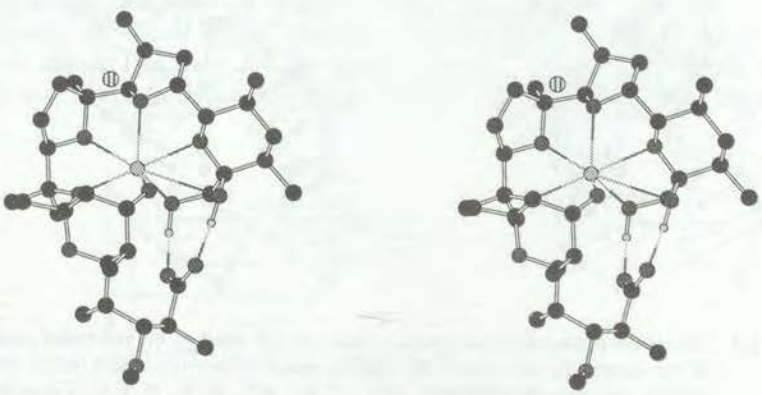

Figure 11.2 Stereoview of monensin sodium monohydrate showing the coordination of the sodium ion (only the non-hydrogen atoms, expept for the two hydrogens involved in intramolecular hydrogen-bonds to the carboxylate group, are shown; key: ● C, ● O, ◍ Na, ⏀ H_2O, ◍ H) (Barrans *et al.*, 1982).

The coordination octahedra around sodium ions, in addition to accommodating different ligands, also show a remarkable flexibility in how they propagate throughout a crystal. Thus, neighboring octahedra can be independent or share points, edges, or sides in any combination, usually leading to highly polar chains or sheets that traverse the entire crystal. Many properties of the crystal are dependent on structural features of this kind. Figure 11.3 is a view of a typical structure of a sodium salt hydrate.

The counterpart to sodium salts are amine hydrochlorides, again commonly encountered among drug products because they are soluble and biocompatible. Of the roughly 130 hydrochloride salts listed in the *Physicians' Desk Reference* (Greenberg, 1994), about ten are reported to exist as hydrates. Hydrated forms of amine hydrochlorides do not, however, fall into the orderly patterns shown by the sodium salts. Nevertheless, a few generalizations can be made with regard to the role of water in hydrated hydrochloride crystals:

- The charged ions—the ammonium ion and the chloride ion—are most often in proximity and hydrogen bonded to one or more water molecules.
- These water molecules tend to be extensively involved with any other hydrogen bond donors or acceptors in the structure.

Figure 11.4 shows the location of the water in fenethazine hydrochloride monohydrate.

In summary, we have shown that water plays many roles critical to drug crystal structures:

- water occupies vacancies in packing
- water hydrogen bonds to functional groups and to other water molecules
- water coordinates sodium and other cations

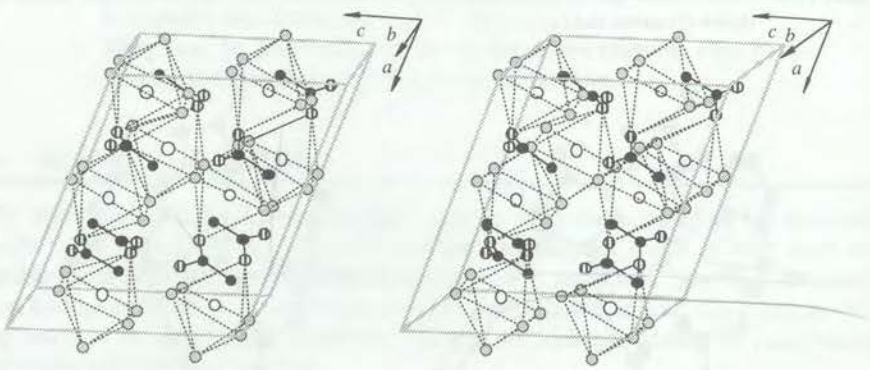

Figure 11.3 Stereoview of the sodium acetate trihydrate unit cell showing the octahedral arrangement of the oxygen ligands around the sodium atoms (symmetry related waters have been added to complete the octahedra; Key: ○ Na, ● C, ◑ O, ◎ H_2O (Cameron *et al.*, 1976).

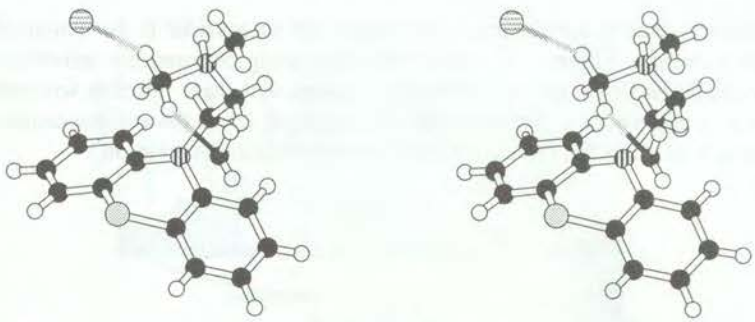

Figure 11.4 Stereoview of the coordination of water in fenethazine hydrochloride monohydrate. Key: ○ H, ● C, ◑ N, ● O, ◯ S, ⊖ Cl (Obata *et al.*, 1985).

11.2 Conditions Under which Hydrates May Form

When we see the manifold ways in which water can be bound in various crystal-structures we should expect and indeed find that each hydrate structure has its own characteristic binding energy for the water molecules in it. Thus, the mere presence of water in a system is not sufficient reason to expect hydrate formation, rather, it is the *activity* of water that determines whether a given hydrate structure forms. We have already pointed out that some compounds do not seem to form hydrates, even though they are soluble in water.

The most obvious situation that favors the formation of crystal hydrates is of course when an aqueous solution of a substance is evaporated, cooled, or otherwise altered to reduce the solubility of the substance. Supersaturation followed by nucleation will result in the formation of hydrate crystals provided that that form exists. Figure 11.5 shows an example of how different crystal forms may be obtained when evaporation of an aqueous solution is conducted at different temperatures. The solubility profile in Figure 11.5 shows relationships that typify drug systems capable of forming several structures with different degrees of hydration.

Figure 11.6 shows typical solubility relationships that govern formation of hydrates in mixtures of water and an organic solvent. This diagram would naturally change with temperature, with the higher hydrates becoming unstable as the tempera-

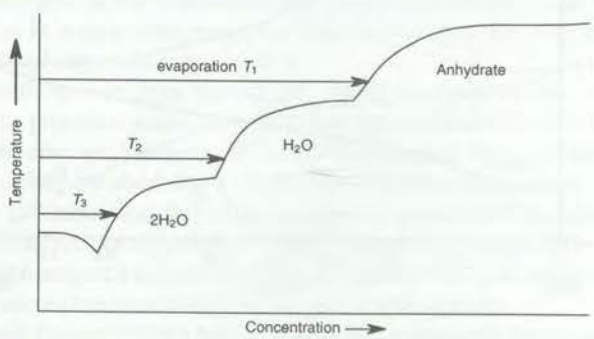

Figure 11.5 Crystal forms produced when evaporations are performed at different temperatures.

ture increases. One factor that many researchers fail to consider is the *activity* of water in mixed solvents. Figure 11.7 shows the relationship between the activities and the activity coefficients of water and ethanol in solutions of these miscible solvents. (Recall that $\alpha_i = \gamma_i x_i$, where α_i is the activity of component i, γ_i is the activity coefficient for component i, and x_i is the mole fraction of component i in the solution.)

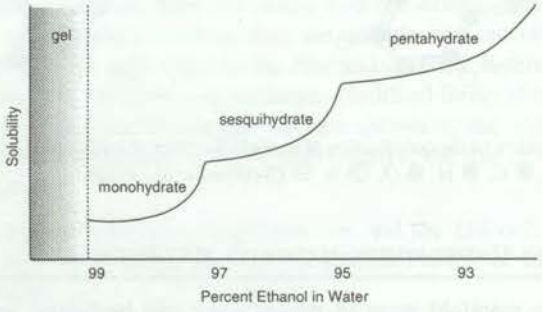

Figure 11.6 Hydrates of cefazolin sodium formed in water-ethanol mixtures.

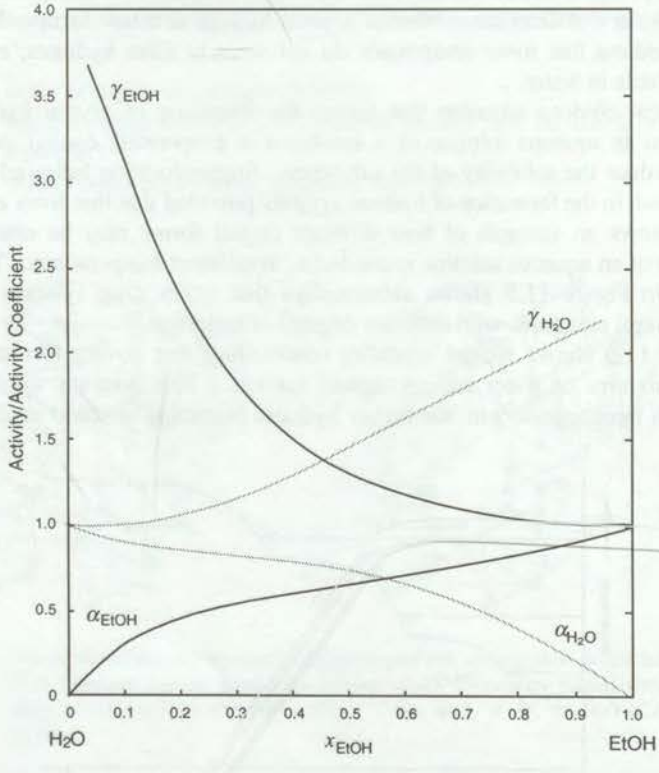

Figure 11.7 Activity (α) and activity coefficient (γ) plot for the ethanol–water system at 20 °C (Data from the *International Critical Tables*; Washburn *et al.*, 1928).

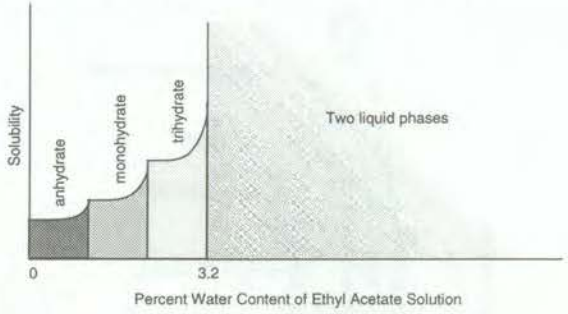

Figure 11.8 Crystallization of hydrated crystal forms from so-called water-immiscible solvents. (Note that the water activity increases from zero to one over the range of water content from 0% to 3.2% water.)

So-called water-immiscible solvent mixtures sometimes present problems in controlling crystal form because the finite, but very low, water solubility means that the water activity in that solvent can vary from zero to one with only slight changes in water concentration. Therefore, when substances that are capable of forming multiple hydrates are dissolved in water-immiscible solvents, different hydrates can be encountered if the water content of the system is not rigorously controlled (see Figure 11.8). This can prove difficult in large scale operations.

At this point it should be obvious that good solubility data are vital to understanding the crystallization behavior of a compound, particularly if multiple forms are encountered.

11.3 Formation of Hydrates in Air: Stability of Hydrates at Different Relative Humidities

One of the most important characteristics to be determined for any drug is how it responds to changes in relative humidity. This knowledge is essential to providing proper conditions for the handling and storage of any solid drug product in order to avoid possible recrystallization into a new and perhaps undesired form. For example, plaster or cement is purchased as a free-flowing powder, but after the addition of water, the material undergoes a recrystallization to the hydrated forms. The quantitative aspects of changes in a drug with respect to relative humidity are also important to the proper execution of any mass-based analysis.

The best method to describe the moisture-uptake or moisture-loss characteristics of a compound is to prepare a water content versus relative humidity (RH) diagram based on data obtained after equilibration of the solid at various RH. This can be accomplished rather simply by obtaining a single Karl Fischer measurement or other water analysis of the substance and following changes by gravimetric monitoring until constant weight is obtained for a multiple of samples stored in various RH chambers. Another method is to subject a single sample to gravimetric analysis using a recording microbalance connected to a system with controllable atmosphere.

Griesser and Burger (1995) have developed a **semimicro hygrostat** (see Figure 11.9) which is a modification of a hygrostat reported by Schepky (1982). The semimi-

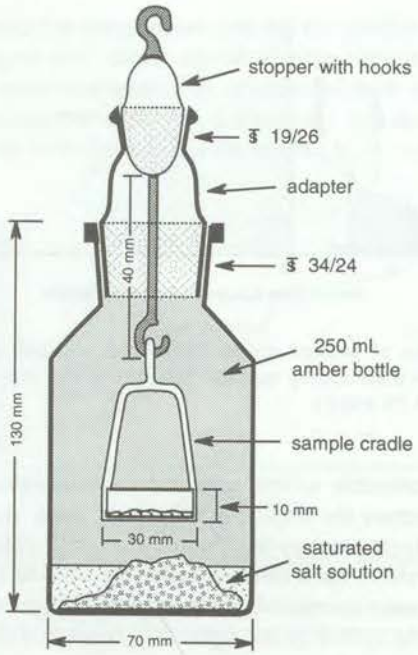

Figure 11.9 Semimicro hygrostat for gravimetric sorpton-desorption moisture studies (Griesser and Burger, 1995).

cro hygrostat consists of an amber wide-mouth reagent bottle with a 34/24 standard-tappered ground-glass joint, a 34/23 male to 19/26 female standard-tappered ground-glass adapter, and a modified 19/26 standard-tapper ground-glass hollow stopper. The amber bottle contains a saturated salt solution to control the relative humidity (Nyqvist, 1983). The stopper has a long hook on the bottom (inserted through the adapter to hold the glass sample basket directly above the saturated salt solution) and a short hook on the top (attached to a bottom-weighing balance when weighing). The sample to be studied (approximately 300 mg) is distributed evenly in the sample basket and then the semimicro hygrostat is assembled and sealed. At various time periods, the hygrostat is positioned below the bottom-weighing balance and the stopper–sample assembly is slighly separated from the adapter and suspended from a wire loop attached to the balance arm of the balance to determine any change in the sample weight. After recording the data, the stopper–sample assembly is detached from the loop and the hygrostat re-sealed. In this manner, weighings can be made without disturbing the equilibrium of the system. Several automated systems have been developed to measure moisture uptake (*e.g.*, Surface Measurement Systems. 1998; VTI Corp. , 1998).

Figure 11.10 shows the kind of behavior that might be found for a compound that can exist as an anhydrate, monohydrate, or dihydrate at room temperature. The stepwise changes in moisture content, of course, are verifiable by other methods covered in Chapter 2.

Note that Gibbs' phase rule considerations dictate the depicted behavior: when there are two condensed phases present, vapor pressure cannot vary; when there is

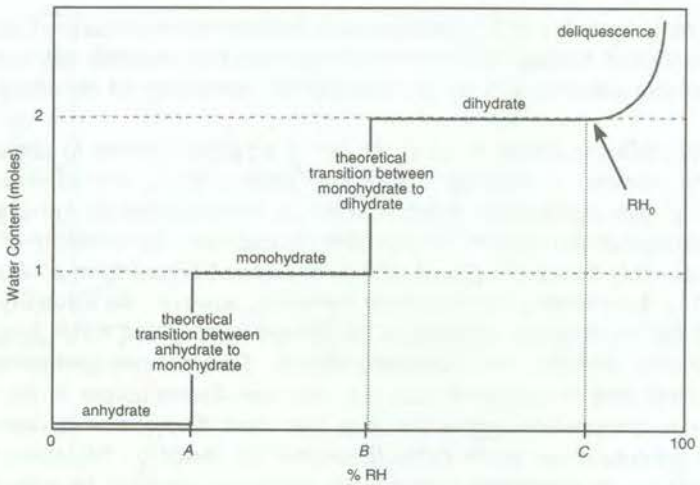

Figure 11.10 Idealized moisture-uptake profile. Starting with a sample of the anhydrous form at 0% RH and increasing the percent relative humidity, the sample will transform to the monohydrate form at point *A*. Increasing the percent relative humidity further, the sample will transform to the dihydrate at point *B*. Increasing the percent relative humidity still further, the sample will begin to deliquesce (RH_0) at point *C*.

only one condensed phase, vapor pressure will vary over a range. (This principle provides the *constant humidity* in environment chambers containing *the condensed phase*, that is, crystals and saturated solution.)

11.4 Deliquescence and Efflorescence

At this time, in the interests of good communication, we should clarify the terms **deliquescence** (to become liquid from the adsoption of atmospheric water) and **efflorescence** (to change to a powder from the loss of water of crystallization), because they are often used without recognizing the fact they are relative terms, not absolute terms. In other words, the conditions under which the respective behavior is observed to spontaneously gain or lose moisture must be stated. It is incorrect to make the blanket statement that a substance is, or is not, "deliquescent" or "efflorescent." Thus, a substance may have been observed to deliquesce or effloresce, but this observation is valid only above or, respectively, below a certain RH value and at a fixed temperature. These limiting values, of course, vary considerably from one substance to another.

11.5 Factors Governing the Formation of Solvates in Mixed Solvents

When a solution of a compound in an organic solvent is evaporated, the results are analogous to the formation of hydrates depicted in Figure 11.5. Depending on the forms available to the given system, the resulting crystals may be unsolvated or solvated with the relevant solvent, again dependent on temperature.

It is common practice in the pharmaceutical industry to use mixtures of solvents for the crystallization of a drug. Because many drugs can form multiple solvates, the use of mixed solvent solutions can greatly multiply the probability of obtaining a crystal solvate.

Often crystallizing a drug involves the use of a "good" solvent to obtain a fairly concentrated solution. A miscible "antisolvent," chosen for its low solubility for the given drug, is then added to the solution to induce crystallization by forming a supersaturated solution of the mixture. In the most desired case, the solubility of the drug decreases smoothly during this process and an unsolvated crystal form is obtained (see Figure 11.11). In systems prone to solvate formation, however, the solubility behavior of the drug can be strikingly different as the solvent composition varies from one extreme to the other (Pfeiffer *et al.*, 1970; and others). Rather than a gradual decrease in solubility, these authors found not only that there are discontinuities in the solubility versus solvent composition curves but also that these discontinuities demarcate the boundaries between zones where different solvates are obtained. Moreover, the solubility maxima can be remarkably higher in the mixed solvents than in either pure solvent, a finding that can be extremely useful in process design. Figure 11.12, adapted from Pfeiffer *et al.* (1970), gives examples of solubility diagrams that correlate solubility behavior with formation of different solvates. Hydrate formation is included in these considerations, as are examples of solvates containing two solvents.

The interpretation of solubility curves like those in Figure 11.12 is that they reveal some kind of strong solute-solvent interactions. We can postulate that:

1. The nature and concentration of differently solvated solute species that exist at different solvent ratios will change considerably as we move from one side of the diagram to the other.
2. Each alternative crystal form in the diagram will grow best when the solvated solution species it favors is at maximum concentration.

Thus, a methanolate crystal might grow well when all of the solute molecules in the solution are surrounded by dipole-oriented methanol molecules, and the growth of a methanol-hydrate crystal would be favored by a high concentration of solute molecules surrounded by a certain ratio of water *and* methanol molecules, and so forth.

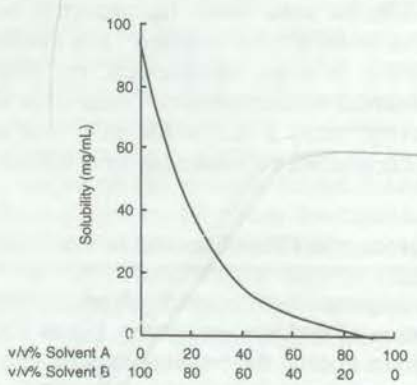

Figure 11.11 Solubility of a substance versus concentration of two solvents A and B.

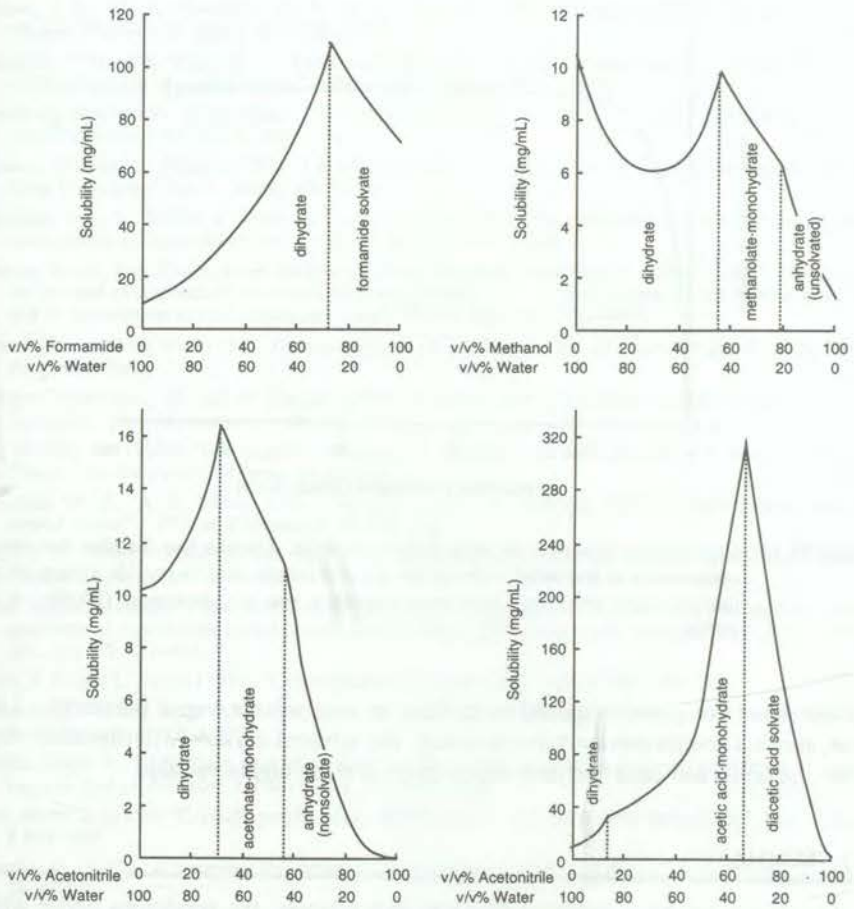

Figure 11.12 Solubility diagrams for a drug in mixtures of organic solvents and water (Pfeiffer, *et al.*, 1970).

We again find ourselves dependent on adequate solubility data if we expect to control crystallizations in mixed solvents.

11.6 Stability of Organic Solvates in Air

Like hydrates, organic solvates also respond to changes in the vapor pressure of the relevant solvent by losing or gaining weight. From a diagram of solvent vapor pressure versus solvent content, as in Figure 11.13, we see behavior analogous to the hydrates in the percent relative humidity versus water-content diagram as in Figure 11.10. In this case, however, the non-solvated form transforms directly to the disolvate form at approximately 15% v/v acetonitrile in triethylene glycol. Even without absolute values, the vapor pressure is the most convincing evidence of the true stoichiometry of a solvate. Just as all hydrates lose water at zero RH, organic solvates will eventually lose

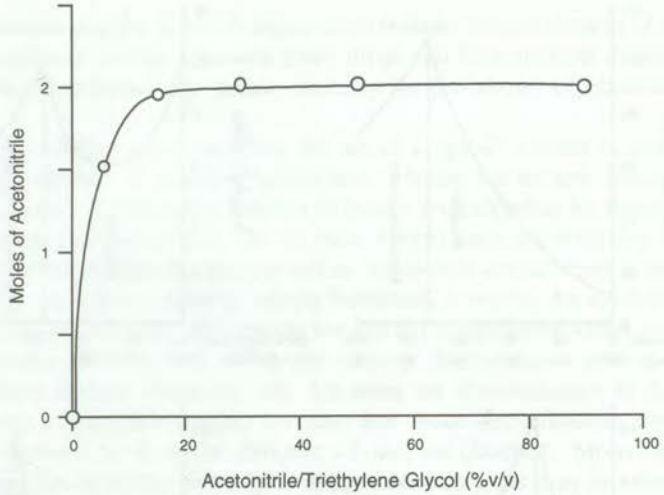

Figure 11.13 Crystal-vapor equilibria for cephalexin–acetonitrile. The abscissa describes the volume composition of acetonitrile–triethylene glycol mixtures used to provide a range of acetonitrile vapor pressures whose exact magnitude was not determined (Pfeiffer, *et al.*, 1970).

solvent when completely exposed to air (*i.e.*, at zero solvent vapor pressure). Likewise, above a certain solvent vapor pressure, the solvated crystals will dissolve. Once more, the limits and rates that pertain to a given case are highly variable.

11.7 SUMMARY

In this chapter we have reviewed hydrates and solvates, the conditions under which they form, and their stability. In addition, deliquescence and efflorescence are defined and the use of solubility versus composition diagrams to understand crystallizations is reviewed. This review provides insight into approaches which can be used to understand solvates and hydrates.

REFERENCES

Austin, K. W. B., A. C. Marshall, and H. Smith (1965) "Crystalline modifications of ampicillin" *Nature* **208** 999–1000.

Barrans, Yvette, Marc Alleaume, and Georges Jeminet (1982) "Sodium complex of the ionophore

Carless, J. E., M. A. Moustafa, and H. D. C. Rapson (1966) "Cortisone acetate crystal forms" *J. Pharm. Pharmacol. Suppl.* **18** 190*S*–197*S*.

Chapman, J. H., J. E. Page, A. C. Parker, D. Rodgers, C. J. Sharp, and Susan E. Staniforth (1968) "Polymorphism of cephaloridine" *J. Pharm. Pharmacol.* **20** 418–429.

Greenberg, Stephen B., Prod. Mgr. (1994) *Physicians' Desk Reference*, 48th ed.; Medical Economics Data Production: Montvale, NJ.

Griesser, U. J. and A. Burger (1995) "The effect of water vapor pressure on desolvation kinetics of caffeine ⅔–hydrate" *Int. J. Pharm.* **120** 83–93.

Haleblian, John K., Robert T. Koda, and John A. Biles (1971) "Isolation and characterization of some solid phases of fluprednisolone" *J. Pharm. Sci.* **60** 1485–1488.

Himuro, Ikuzo, Yoji Tsuda, Keiji Sekiguchi, Isamu Horikoshi, and Motoko Kanke (1971) "Studies on the method of size reduction of medicinal compounds. IV. Solvate formation on chloramphenicol and its application to size reduction" *Chem. Pharm. Bull.* **19** 1034–1040.

Kuhnert-Brandstätter, M. (1971), *Thermomicroscopy in the Analysis of Pharmaceuticals*. New York, Pergamon Press.

Kuhnert-Brandstätter, M. and P. Gasser (1971) "Solvates and polymorphic modifications of steroid hormones. III." *Microchem. J.* **16** 590–601.

Lin, Hwaing Ou (1971) "Investigation of physical properties of sulfanilamide polymorphs" Ph. D. Thesis, The University of Iowa, Iowa City, IA.

Moustafa, M. A., A. R. Ebian, Said A. Khalil, and M. M. Motawi (1971) "Sulphamethoxydiazine crystal forms" *J. Pharm. Pharmacol.* **23** 868–874.

Nyqvist, H. (1983) "Saturated salt solutions for maintaining specified relative humidities" *Int. J. Pharm. Tech. & Mfr.* **4** 47–48.

Obata, Atsuo, Masahiro Yoshimori, Kohichi Yamada, Hiroshi Kawazura (1985) "Crystal and molecular structures of fenethazine hydrochloride and its cation radical-copper(II) complex salt" *Bull. Chem. Soc. Jpn.* **58** 437–441.

Olsen, P. E. and L. Szabo (1959) "Crystallization of gramicidin" *Nature* **183** 749–750.

Peterson, S. W. and Henri A. Levy (1957) "A single-crystal neutron diffraction study of heavy ice" *Acta Crystallogr.* **10** 70–76.

Pfeiffer, Ralph R., K. S. Yang, and Mary Ann Tucker (1970) "Crystal pseudopolymorphism of cephaloglycin and cephalexin" *J. Pharm. Sci.* **59** 1809–1814.

Rose, Harry A. (1954) "Crystallographic data. Erythromycin and some of its derivatives" *Anal. Chem.* **5** 938–939.

Schepky, G. (1982) "A hydrostat for simple and trouble-free sample weighings" *Acta Pharm. Technol.* **28** 87–88.

Sekiguchi, Keiji, Isamu Horikoshi, and Ikuzo Himuro (1968) "Studies on the method of size reduction of medicinal componds. III. Size reduction of griseofulvin by solvation and desolvation method using chloroform" *Chem. Pharm. Bull.* **16** 2495–2502.

Shefter, Eli and Takeru Higuchi (1967) "Dissolution behavior of cyrstalline solvated and nonsolvated forms of some pharmaceuticals" *J. Pharm. Sci.* **52** 781–791.

Shell, John W. (1955) "Hydrocortisone acetate" *Anal. Chem.* **27** 1665–1666.

Surface Measurement Systems (1998) 3 Warple Mews, Warple Way, London, W3 ORF, UK.

VTI Corp. (1998) 7650 W. 26th Avenue, Hialeah, Florida 33016–5611.

Washburn, Edward W., Ed. (1928) *International Critical Tables of Numerical Data, Physics, Chemistry and Technology*; Clarence J. West, N. Ernest Dorsey, F. R. Bichowsky, and Alfons Klemenc, Eds.; McGraw-Hill: New York, NY; Vol 3; p 290.

Yang, Shiu Shiang and J. Keith Guillory (1972) "Polymorphism in sulfonamides" *J. Pharm. Sci.* **61**

13

Polymorphic Interconversions

This chapter is divided into a review of polymorphs of organic chemicals which interconvert and a review of pharmaceutical polymorphs which interconvert. Transformations induced by heat, stress, grinding, and tableting are discussed. Pharmaceutical aspects of polymorphic transformations, such as those that occur during dissolution testing, are reviewed since these can have profound effects on interpretation of these tests.

13.1 Interconversion of Polymorphs in the Solid State

This section reviews several organic polymorphs known to interconvert. Of particular interest is the carefully studied equilibration of the two forms of 4-dichlorobenzene.

A. 4-Dichlorobenzene

4-dichlorobenzene

The polymorphic transformation of α- $\rightleftharpoons$ β-4-dichlorobenzene has been carefully studied (Kitaigorodskii *et al.*, 1965). The results are suggested to have more general significance and serve to indicate why solid-state reactions are apt to be very difficult to characterize quantitatively. Microscopic and crystallographic studies of the phase transformation showed that the reaction occurred by the growth of one crystal within another. In general, there appears to be a great deal of similarity between the growth of one phase in the other and the growth of a crystal from solution. During the solid-state interconversion, a crystal of the α-form grows in a crystal of the β-form or vice versa, showing front advancement in much the same way that 4-dichlorobenzene crystals

grow from solution. In addition, the growth direction of the product crystal could be reversed by merely raising (or lowering) the temperature.

Crystallographic studies showed that there is no relationship between the orientation of the product crystal and the starting crystal. These crystallographic studies also showed that, if the transformations are nucleated at a single site, they are single-crystal-to-single-crystal transformations while, if they are nucleated at n sites, then n crystals of different orientation are formed. In addition, it was impossible to predict which crystals would nucleate spontaneously at single sites and which at multiple sites. It was also found that in some cases, even if the phase transformation nucleated at one site, the product crystal contained microcrystallites of arbitrary relative orientation. In these cases, stresses and defects that occur during reaction are thought to induce the nucleation and crystallization of many orientations of the product phases.

Studies of the nucleation process showed that, in "perfect crystals" (*i.e.*, relatively "defect-free" crystals) of either phase, it was often impossible to induce a phase transformation, and these crystals simply melted at the melting point of the respective initial phase. However, with less perfect crystals, it was often possible to induce the phase transformation by artificial creation of a defect using a pin.

Studies of repeated transformations, $\alpha \rightarrow \beta \rightarrow \alpha \rightarrow \beta$, showed that when the transformation of a crystal began at one site, subsequent transformations always began at that same site, whether it was a $\beta \rightarrow \alpha$ or an $\alpha \rightarrow \beta$ transformation. Thus, the crystal seemed to "remember" its nucleation site. This memory effect is explained by the conservation of the nucleation site at crystal defects. In other words, repeated transformations do not destroy the nucleation site for this transformation.

The rates of the $\alpha \rightarrow \beta$ and $\beta \rightarrow \alpha$ polymorphic transformations were best studied by measuring the rate of advancement of the phase boundary or front under a microscope during heating. Each rate was determined by measuring the volume of the crystal transformed per unit time and was shown to be dependent on the location of the nucleus in the crystal, as well as the crystal shape. For example, if the nucleus is in the center of the crystal and the reaction expands symmetrically, after a fixed time, twice as much crystal will be reacted than if the reaction started on the end. Thus, the rate of volume transformation depends on non-crystallographic factors and is, therefore, not a true measure of the absolute rate. This observation probably explains (at least in part) why there is great variation in the measured rates of solid-state reactions when measurements depend on the volume transformed (amount transformed) and not the rate of front advancement. Because of these observations, the rates were measured by determining the rate of advancement of the front in crystals that nucleated at a single site. Even with these measurements, the rates of transformation of apparently similar crystals differed by a factor of 6. The rates were determined at different temperatures allowing calculation of the activation energy of the process. The activation energy for the $\alpha \rightarrow \beta$ reaction was 72.8± 10 kJ/mol, while that for the $\beta \rightarrow \alpha$ process was 71.6 ± 10 kJ/mol. Thus, these measurements indicate the α- and β-phasesare within experimental error of each other in energy.

Table 13.1 Crystal Parameters of the Two Polymorphs of 4-Nitrophenol

Parameter	α-Form[a]	β-Form[b]
Space group	$P2_1/a$	$P2_1/a$
a (Å)	14.8	15.40
b (Å)	8.9	11.12
c (A)	6.17	3.79
β	130°25'	107°6'
Z	4	4
ρ_{calc} (g·cm^{-3})	1.51	1.49
V (Å^3)	618.8	620.3

a Coppens and Schmidt, 1965a. *b* Coppens and Schmidt, 1965b.

B. 4-Nitrophenol

4-nitrophenol

The phase transformation of β- to α-4-nitrophenol has been extensively studied (Cohen *et al.*, 1964) and resembles, in many respects, the behavior of 4-dichlorobenzene. The crystallographic properties of these polymorphs are shown in Table 13.1. The crystal structures of both polymorphs are similar and, in both polymorphs, the molecules are linked by head-to-tail hydrogen bonding into infinite chains parallel to (100).

The $\beta \longrightarrow \alpha$ phase transformation occurs upon heating a crystal of the β-form. During this transformation, the crystals retain their original shape, and the product consists of one or a small number of single crystals. This is quite similar to the behavior of 4-dichlorobenzene. In addition, experiments with thin films showed that the orientation of the product crystal was not dependent upon the orientation of the starting one, again in marked similarity to the behavior of 4-dichlorobenzene. Similar experiments with single crystals show that the orientation of the product crystal was not related to the starting crystal.

C. 5-Methyl-1-thia-5-azacyclooctane-1-oxide Perchlorate

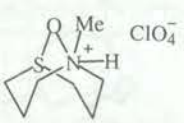

5-methyl-1-thia-5-azacyclooctane-1-oxide perchlorate

5-Methyl-1-thia-5-azacyclooctane-1-oxide perchlorate crystallizes in an α- and a β-form with the crystal parameters shown in Table 13.2 (Paul and Go, 1969). The crystal structures of both forms have been determined and are shown in Figures 13.1 and 13.2. The transformation can be explained in terms of either a ring-flipping mechanism or slipping of layers within the crystal. Regardless of the mechanism, the transformation is reversible and occurs upon cooling the α-form (which is stable at 25 °C) to 3 °C,

at which point the β-form is generated; raising the temperature reverses this process. This is another of the few examples of a single-crystal-to-single-crystal transformation.

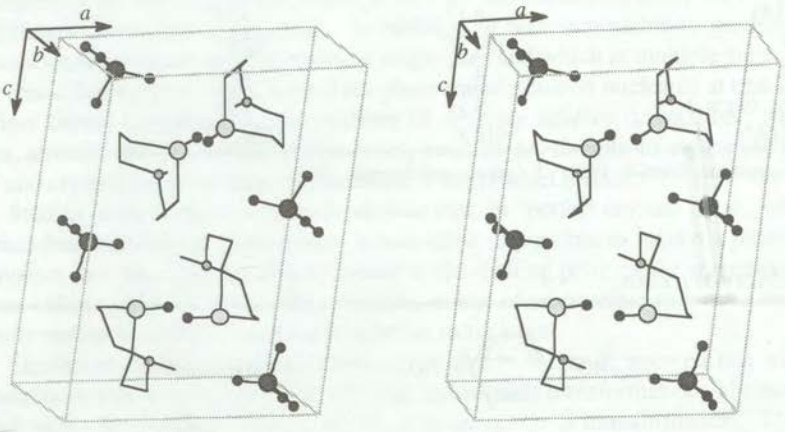

Figure 13.1 Crystal lattice of the α-form of 5-methyl-1-thia-5-azacyclooctane-1-oxide perchlorate. Key: ○ sulfur; ● chlorine; • oxygen; ∘ nitrogen (Paul and Go, 1969).

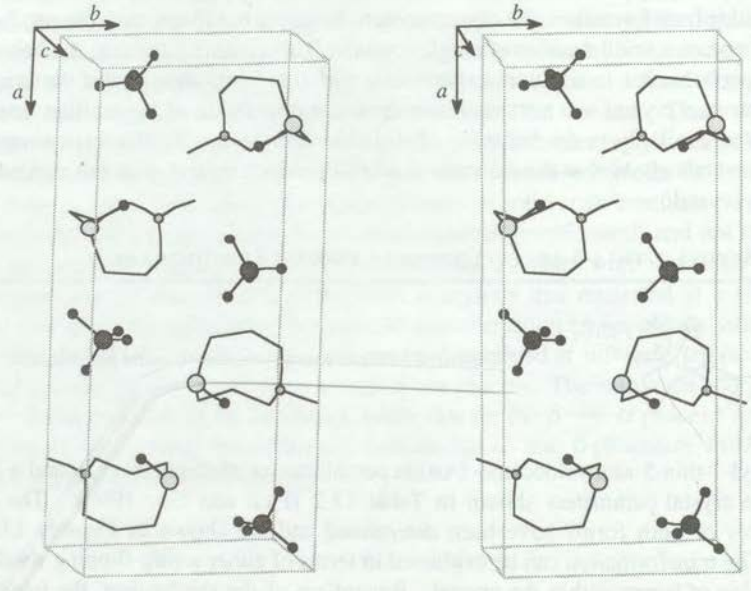

Figure 13.2 Stereoview of the β-form of 5-methyl-1-thia-5-azacyclooctane-1-oxide perchlorate. Key: ○ sulfur; ● chlorine; • oxygen; ∘ nitrogen (Paul and Go, 1969).

Table 13.2 Crystal Parameters of Two Polymorphs of 5-Methyl-1-thia-5-azacyclooctane-1-oxide Perchlorate

Parameter	α-Form	β-Form
Space Group	$P2_1/c$	$P2_1/a$
a (Å)	9.87	20.10
b (Å)	8.78	8.89
c (Å)	13.26	6.67
β	97.90°	97.80°
Z	4	4
V (Å^3)	1138.2	1108.8

(Paul and Go, 1969)

D. Resorcinol

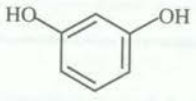

resorcinol

Resorcinol exists in two polymorphs, α and (Robertson and Ubbelohde, 1938). The α-form is more stable than the β-form at room temperature; however, it is less dense than the β-form. Resorcinol is one of the few substances known for which the denser polymorph is the metastable polymorph at room temperature. Studies showed that, upon transformation to the high-temperature β-form, there is a contraction in volume with no change in crystal symmetry. In addition, the atomic displacement parameters obtained from crystallographic studies show that the thermal motion in α- and β-resorcinol is nearly the same.

A comparison of the crystal structure of the α- and β-forms provides an explanation for the fact that the less dense α-form is more stable at room temperature. The α-form has significantly shorter hydrogen bonds than the β-form. Thus, in this case, the hydrogen-bonding energy overcomes the loss in packing energy and renders the α-form more stable than the β-form. This explanation is also consistent with the experimental observations mentioned above.

13.2 The Induction of Phase Transformations by Stress

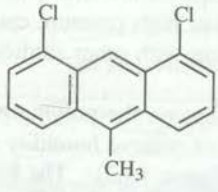

1,8-dichloro-10-methylanthracene

Stress-induced phase transformations were studied by Thomas (1974) using mechanical deformations with a pin or cleaving with a razor blade to induce stress. For example, 1,8-dichloro-10-methylanthracene undergoes a stress-induced phase transformation. In addition, the orientation of the product crystal is related to the starting crystal.

Thus, for this compound, the generalizations of Kitaigorodskii and co-workers (1965) based on 4-dichlorobenzene do not seem to apply. It is interesting to note that 1,8-dichloro-9-methylanthracene, unlike the 10-methyl isomer, does not undergo a phase transformation (*e.g.*, a change in the crystal structure), but merely deformation twinning (the crystal structure does not change, merely the crystal shape).

13.3 Polymorphic Transformations of Pharmaceuticals

In this section, studies of drugs that undergo polymorphic transformation are reviewed and discussed. This is an important area of research because of its implications in the physical stability of drug dosage forms. As mentioned earlier, different polymorphs possess different physical properties—solubility and bioavailability being the most important. In addition, keep in mind that changing the temperature or pressure during a manufacturing operation, such as tableting, could induce a polymorphic transformation.

A. Phenylbutazone

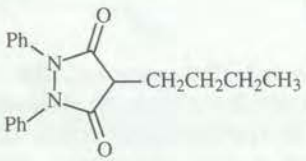

phenylbutazone

Studies of phenylbutazone illustrate several of the practical consequences of polymorphic interconversions. Ibrahim and co-workers (1977) prepared four batches of phenylbutazone by crystallization: Form I, from *tert*-butyl alcohol; Form II, from cyclohexane; Form III, from heptane; and Form IV, from 2-propanol–water. The X-ray powder patterns and infrared spectra of these four forms were different. However, because it is possible that some batches of crystals contained mixtures of forms, single-crystal X-ray diffraction studies of these forms are in order. At any rate, studies of the dissolution rates of these four forms show that the crystals from cyclohexane have the slowest dissolution rate and that the other three batches have nearly equal dissolution rates. The differences in dissolution rate were attributed to differences in surface area. However, the possibility that a solution-mediated phase transformation converted all three forms to the same form during the dissolution tests was not ruled out.

All four batches of crystals were pressed into disks. This treatment caused Form III to transform to Form IV, and Forms I and II to transform to a fifth phase. Grinding produced the same changes. These studies indicate that high pressure can cause polymorphic transformations. This suggestion is consistent with other studies reported by Ibrahim and co-workers (1977).

Matsuda *et al.* (1984b) have extended these studies on the polymorphic interconversions of phenylbutazone by determining the effect of relative humidity and temperature on the rate of polymorphic transformation (see Figure 13.3). The kinetic data for the transformations were fitted to the Avrami–Erof'ev model and first-order kinetic models (see Chapter 22). One of the transformations was affected by humidity, and the temperature dependence of this transformation rate was remarkable. Matsuda *et al.*

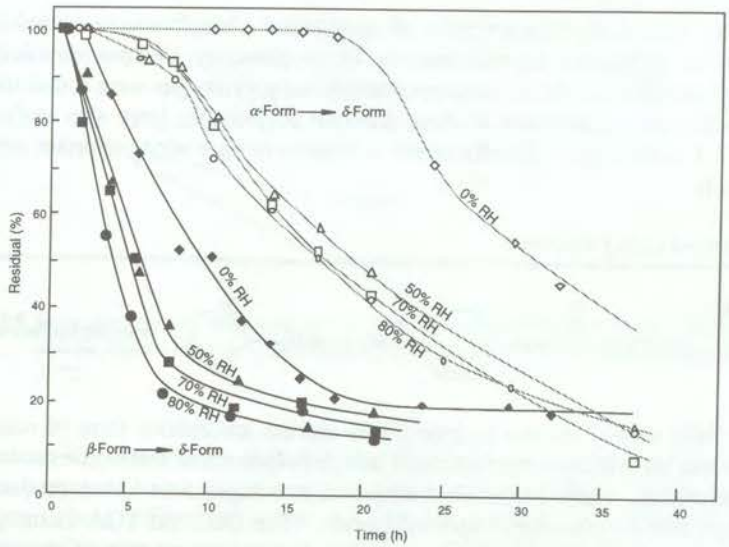

Figure 13.3 Time course for phenylbutazone $\alpha \rightarrow \delta$ and $\beta \rightarrow \delta$ transformations at 60 °C and various relative humidities (Matsuda *et al.*, 1984b).

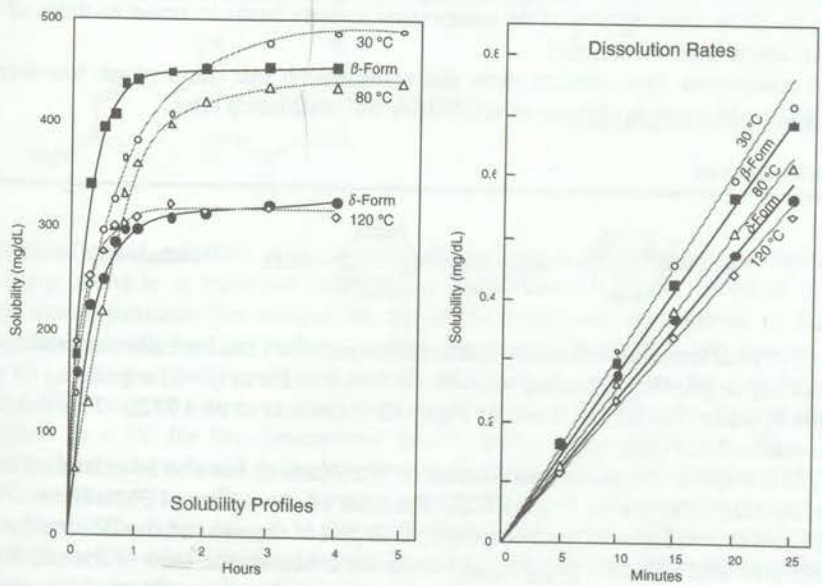

Figure 13.4 Solubility profiles and dissolution rates in simulated intestinal fluid at 37 °C of phenylbutazone pure modifications (black symbols and black lines) and spray-dried samples prepared at different drying temperatures (white symbols and gray lines) (Matsuda *et al.*, 1984a).

(1984a) also studied the characteristics of spray-dried phenylbutazone samples by X-ray diffraction, differential thermal analysis, IR spectroscopy, electron microscopy, and hot-stage photomicroscopy. A number of additional polymorphs were found using this approach. The dissolution rates of these different polymorphs were also analyzed (see Figures 13.3 and 13.4). Phenylbutazone continues to be a very important subject for further study.

B. Succinylsulfathiazole

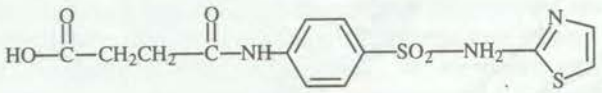

succinylsulfathiazole

Rankell (1969) studied the two hydrate forms and the amorphous form of succinylsulfathiazole and showed that pressure could induce polymorphic interconversions of succinylsulfathiazole. These forms were subjected to compression forces produced by a tablet punch and die placed in a hydraulic press. The DSC and TGA thermograms of the two hydrates were altered after compression, but the thermogram of the anhydrous form was unaffected. In addition, the extent of the change was related to the compression force.

Grinding also alters both the water content and the crystal structure of the two hydrates, but has little effect on the anhydrous form. This may indicate that grinding accelerates solid-state transformations by increasing the number of defects. Grinding also causes the DTA thermograms of the compressed hydrate forms to revert to those of the ground, uncompressed material.

In conclusion, these studies show that compression can cause phase transformations that could result in changes in solubilities and dissolution rates.

C. Sulfameter

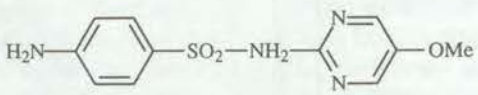

sulfameter

Various crystal forms of sulfameter (sulfamethoxydiazine) can be interconverted by either heating or grinding. Heating converts all forms to Form I, while grinding or suspension in water converts all forms to Form III (Moustafa *et al.* 1972). This behavior is summarized in Figure 13.5.

The kinetics of the phase transformations of sulfameter has also been studied using IR spectroscopy (Moustafa *et al.*, 1972). The rates of conversion of Form II → Form I and Form II → Form III were determined. A plot of the ratio of the IR absorbances at 1595 cm^{-1} and 950 cm^{-1} (A_{950}/A_{1595}) versus the concentration ratio of the two forms (C_I/C_{II}) gave curved but well-behaved lines that allowed the measurement of the amount of Form I in Form II. The rate of conversion of Form II → Form I was studied at 100, 105, and 110 °C. The rate of conversion of Form II → Form III was studied in water suspension at 20, 25, 30, and 37 °C. Plots of log (C_{II}) versus time were linear for both the heat-induced reaction and the suspension reaction. In addition, both reactions follow first-order kinetics. Analysis of these kinetic data gave an activation en-

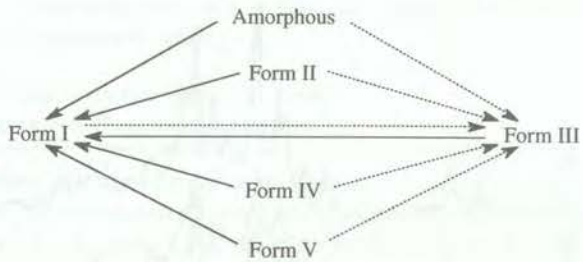

Figure 13.5 Interconversion of sulfameter crystal forms. The solid lines show the effect of heating and the dashed lines show the effect of suspension in water or grinding (Moustafa, *et al.*, 1972).

ergy of about 100 kcal/mol for the solid-state conversion of Form II ⟶ Form I and an activation energy of about 20 kcal/mol for the conversion of Form II ⟶ Form III in suspension. These differences in rate and activation energy may be because the phase transformation in suspension is water-mediated. Thus, the conversion in water suspension may actually be a dissolution-recrystallization process as described by McCrone (1965) for other compounds.

D. Effect of Seed Crystals on Transformations of Chloramphenicol Palmitate

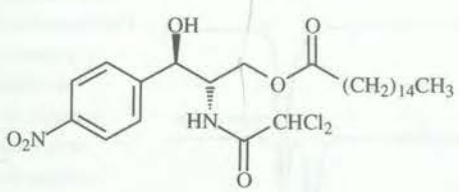

chloramphenicol palmitate

Chloramphenicol palmitate was observed to undergo a polymorphic transformation during grinding in an agate ball mill (Otsuka and Kaneniwa, 1986). Form B of chloramphenicol palmitate (the desired yet metastable form) was transformed to Form A (the therapeutically least active form) during grinding for more than 150 minutes (Figure 13.6). In the presence of seed crystals of Form A, however, the transformation occurred in only 40 minutes. The transformations were fitted to the Avrami–Erof'ev equation ($n = ½$) for two-dimensional growth processes (see Chapter 22). These studies clearly show that if, in the preparation of drugs such as chloramphenicol palmitate there are mixtures of crystal forms, the stable form can seed or accelerate the transformation of the entire sample to the stable form. This is one of the scientific studies that indicate that unstable crystal forms should be marketed only after adequate investigation of the transformation kinetics.

Chloramphenicol palmitate can also undergo transformation to a more stable polymorph (less bioavailable) upon heating. (De Villiers *et al.*, 1991) These researchers used X-ray powder diffraction and DSC to study the thermal transformation of Forms A, B, and C. Form B can be converted to Form A upon heating at 82 °C for 1600 min. Form C is also converted to Form A through Form B by grinding or heating as shown

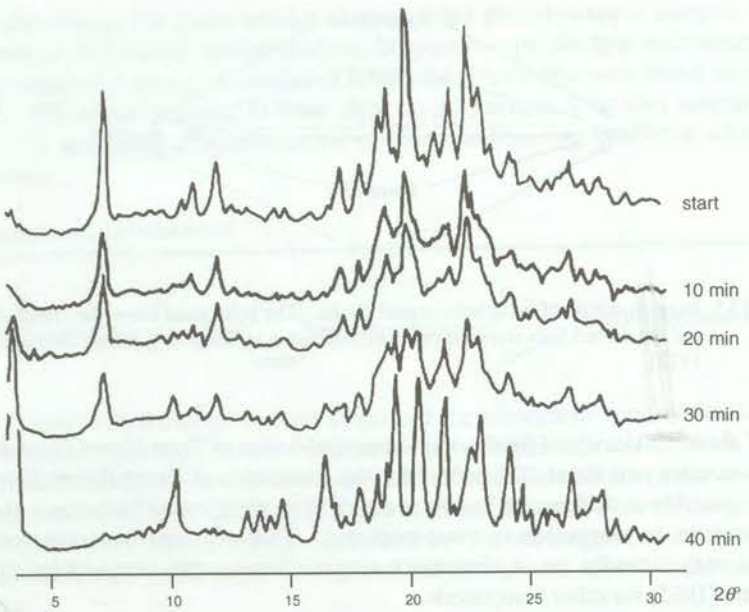

Figure 13.6 Effect of grinding on the X-ray diffraction profiles of chloramphenicol palmitate Form B containing 1% Form A (Otsuka and Kaneniwa, 1986).

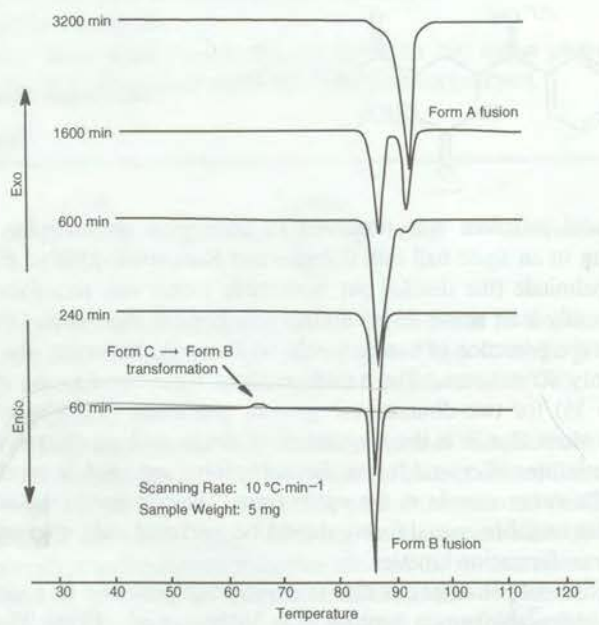

Figure 13.7 Change in the DSC curve of Form C of chloramphenicol palmitate when kept at 75 °C for various periods of time (De Villiers *et al.*, 1991).

in Figure 13.7. These studies show how DSC can be effectively used to study the polymorphic transformations of drugs.

E. Effect of Compression and Grinding on Polymorphic Transformations

Chan and Doelker (1985) have reported an extensive study of the effect of grinding on the polymorphic transformation of several drugs. The results of their study are summarized in Table 13.3. It appears that, in general, the number of polymorphs decrease upon grinding, possibly indicating that transformation to the most stable crystal form is occurring.

Chan and Doelker (1985) also found that maprotiline hydrochloride underwent a

Table 13.3 Drugs Tested for Polymorphic Transformation During Grinding

Drug	Polymorphic Transformation[a]	Number[b] Before Grinding	Number[b] After Grinding
Acetohexamide	–		
Azaperone	–		
Barbitone	+	2	1
Bumetanide	–		
Butobarbitone	–		
Caffeine	+	2	1
Chlorpropamide	+	3	2
Clenbuterol HCl	+	2	3
Diazepam	–		
Digitoxin	–		
Dipyridamole	+	2	3
Fluanisone	–		
Indomethacin	–		
Maprotiline HCl	+	3	1
Mebendazole	+	4	5
Mefenamic acid	–		
Meprobamate	–		
Methylprednisolone	–		
Nafoxidine HCl	+	4	3
Pentobarbitone	+	3	2
Sulfabenzamide	+	2	1
Sulfaethidol	–		
Sulfadimidine	–		
Sulfamethoxazole	–		
Sulfapyridine	–		
Sulfaisoxazole	–		
Theophylline	–		
Tolbutamide	–		
Trimethoprim	–		

a (+) Undergoes a polymorphic transformation upon grinding; (–) does not undergo a polymorphic transformation upon grinding. *b* Number of polymorphs (Chan and Doelker, 1985).

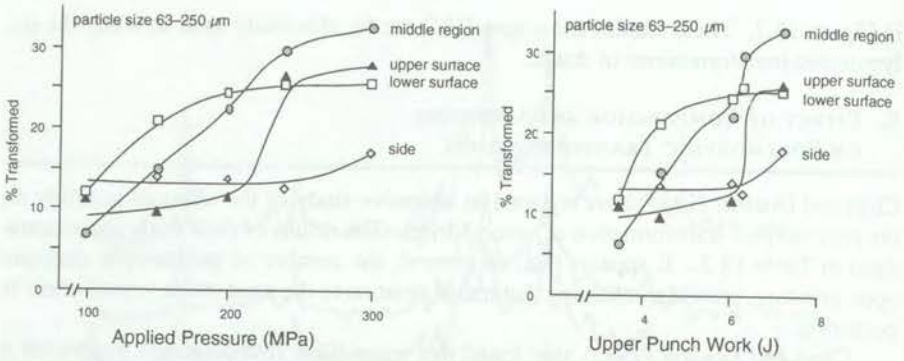

Figure 13.8 Percentage of maprotiline hydrochloride Form III transformed to Form II versus applied pressure and the work delivered by the upper punch in the tablet press (Chan and Doelker, 1985).

polymorphic transformation when pressed in a tablet press. The extent of transformation is shown in Figure 13.8. This is an example of the influence of pressure (tableting) on the transformation of a crystal form.

F. Isothermal Solid-Solid Polymorphic Transformation of Tolbutamide and Mefenamic Acid

Umeda *et al.* (1985) studied the kinetics of solid-solid polymorphic transformations at high temperatures. The percent conversion of tolbutamide and mefenamic acid was analyzed using DSC. Figures 13.9 and 13.10 show the DSC curves for tolbutamide and mefenamic acid, respectively. Quantitative analysis of the DSC curves of mixtures (see Section 5.2) gave straight lines with correlation coefficients of 0.999 and 0.997 for tolbutamide and mefenamic acid, respectively. Figure 13.11 shows the residual fraction of Form A of tolbutamide upon heating and Figure 13.11 shows the residual fraction of Form I of mefenamic acid upon heating. It is clear from these figures that as the

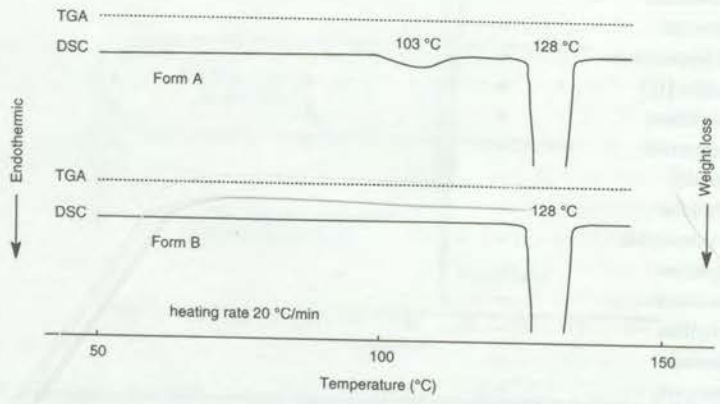

Figure 13.9 DSC–TG Curves of tolbutamide polymorphs (Umeda et al., 1985).

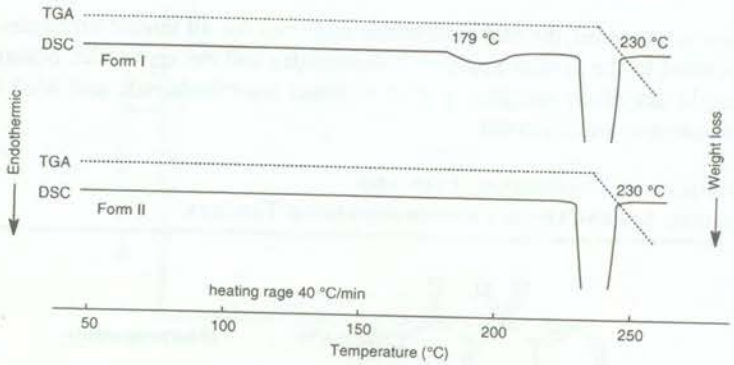

Figure 13.10 DSC–TG Curves of mefenamic acid polymorphs (Umeda *et al.*, 1985).

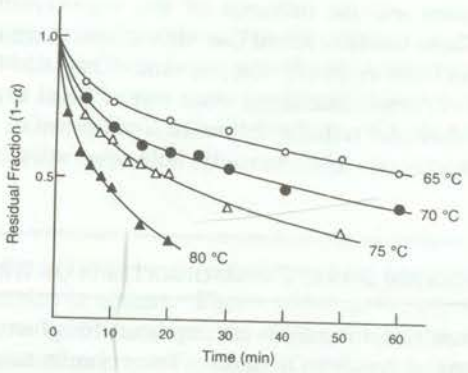

Figure 13.11 Residual fraction of tolbutamide Form B during the isothermal transition to Form A (Umeda *et al.*, 1985).

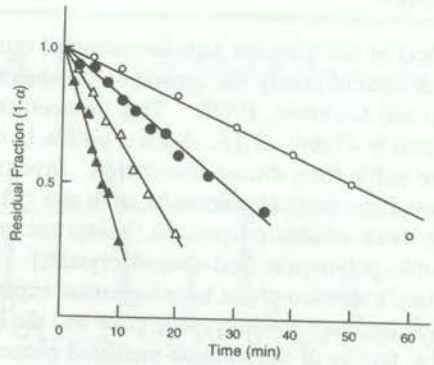

Figure 13.12 Residual fraction of mefenamic acid Form I**Error! Bookmark not defined.** during the isothermal transition to Form II (Umeda *et al.*, 1985).

temperature is increased, the rate increases as expected for all kinetic processes. These data were fitted to the Jander equation (tolbutamide) and the zero-order equation (mefenamic acid); activation energies of 37.3 kcal/mol for tolbutamide and 86.4 kcal/mol for mefenamic acid were derived.

G. Polymorphic Transformation and Crushing Strength of Chlorpropamide Tablets

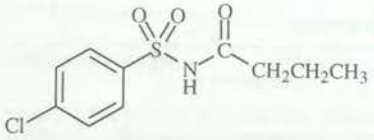

chlorpropamide

Matsumoto *et al.* (1991) have reported the polymorphic transformation of chlorpropamide during compression and the influence of this transformation on the crushing strength of tablets. These workers found that high temperatures accelerated the transformation of Form C to Form A during compression. They also found that the crushing strength of tablets of Form A was about twice that of Form C even at the same porosity. These studies show that transformations of significance to product performance can occur during compression. Unfortunately, little other work has been done in this important area.

13.4 Solution-Mediated Phase Transformations of Drugs

Solution-mediated phase transformations are important for pharmaceuticals since they explain the conversions of one form to another that occur in suspensions or slurries. Such phase transformations can also occur upon granulation and thus need to be monitored during dosage form preparation. Finally, solution-mediated phase transformations can occur during dissolution testing and may provide anomalous results.

A. A Hypertension Drug

The solution-phase method of studying the transformation of one crystalline form of a drug to another has been used to clarify the apparently anomalous dissolution rates of an antihypertensive (Lin and Lachman, 1969). This unspecified compound gave the dissolution profile depicted in Figure 13.13. Such a profile is characteristic of phase transformation to a more stable form during dissolution. Investigation of this process under a microscope showed that there appears to be an *in situ* crystalline transformation in which crystals of the more soluble polymorph (hexagonal crystals) transform into crystals of the less soluble polymorph (rod-shaped crystals). This transformation is closely related to McCrone's solution-phase transformation experiments (Haleblian and McCrone, 1969) in which the more stable crystals grow and the less stable crystals disappear. The most notable feature of the solution-mediated phase transformation of this antihypertensive is that it is rapid, nearing completion in 30 minutes.

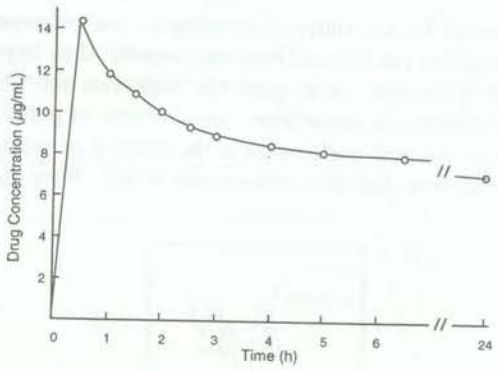

Figure 13.13 Dissolution rate of an undisclosed, hypertension drug in 0.1 *N* HCl (Lin and Lachman 1969)

These studies suggest the hypothesis that in cases where polymorphs appear to have the same dissolution rate, there might actually be a solution-mediated phase transformation taking place. In such cases, one would expect to see anomalous dissolution profiles, such as that shown in Figure 13.13, if the rate of nucleation is slow relative to the time frame of the study.

B. Indomethacin

Kaneniwa and coworkers (1985) have studied the phase transformation of indomethacin polymorphs suspended in ethanol. Figure 13.14 shows the X-ray diffraction profile. Figure 13.15 shows the infrared spectra. Figure 13.16 shows the DTA curves of the polymorphs of indomethacin and Figure 13.17 shows the change in the DTA curve of indomethacin upon storage in ethanol suspension at 45 °C. It is apparent from Figure 13.17 that the α-form is transformed to the γ-form after 18 hr. Additional studies showed that the rate of transformation increased as the temperature was raised. This

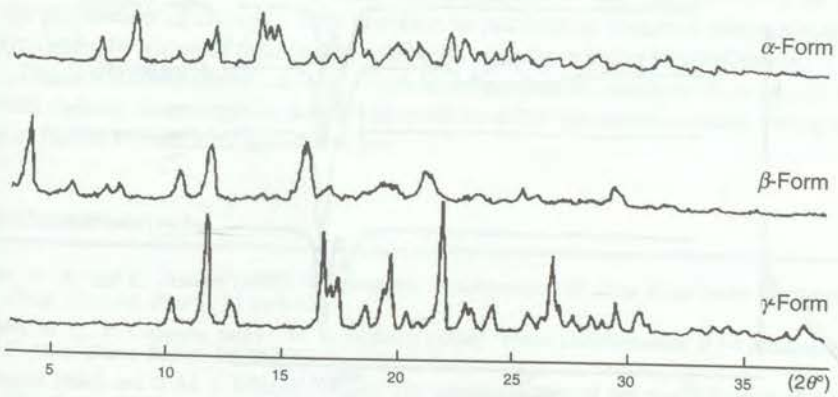

Figure 13.14 X-ray powder diffraction profiles for pure polymorphs of indomethacin (Kaneniwa *et al.*, 1985).

transformation is a model for the slurry conversion of one polymorph to another and indicates that these reactions can proceed relatively rapidly, thus having potential use in production processes. It is important to recall that Haleblian and McCrone (1969) first described this type of transformation in their classic review of polymorphs.

One variable that is not well understood is the kinetics of solution-mediated phase transformation. That is, how fast does conversion occur? Why do some conversions

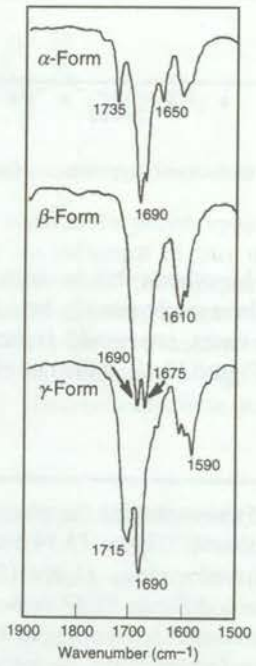

Figure 13.15 IR spectra for the pure polymorphs of indomethacin (Kaneniwa *et al.*, 1985).

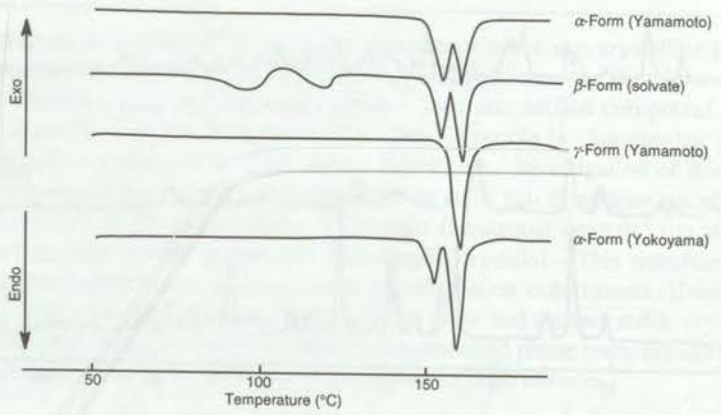

Figure 13.16 DTA curves of the polymorphs of indomethacin (Yokoyama *et al.*, 1979).

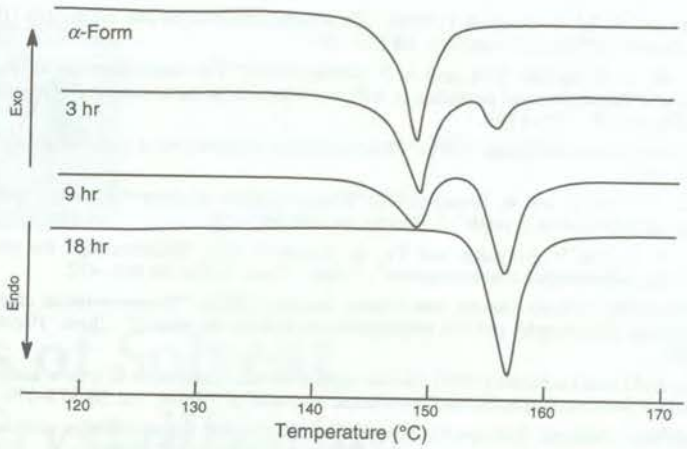

Figure 13.17 Change of DSC curves of the α-form of indomethacin upon storage in ethanol at 45 °C (Kaneniwa *et al.*, 1985).

occur very rapidly and others take hours or days? Further research needs to be done in order to understand the kinetics of solvent-mediated transformations and the factors which affect these, such as temperature, solubility, solvent composition, nucleation, rates of dissolution, and rates of crystal growth.

C. Suspensions

Polymorphic transformations can affect the properties of creams and suspensions. If the wrong polymorph is used in the preparation, a phase transformation can often occur, resulting in crystal growth of the new phase. The cream can then become gritty and cosmetically unacceptable. Similarly, transformations in suspensions can result in caking and a change in the physical properties. Thus, it is best to select the polymorph that is least susceptible to phase transformations and crystal growth. This is the most stable polymorph and, therefore, least soluble in the cream base. On the other hand, some metastable polymorphs may transform at such a slow rate that they could be used in the preparation of creams. This situation is particularly attractive since metastable polymorphs, by virtue of their higher solubility, often have better bioavailability.

Phase transformations can also occur in suppositories, resulting in products with altered melting characteristics that could result in either premature melting during storage or failure to melt after administration.

References

Chan, H. K. and E. Doelker (1985) "Polymorphic transformation of some drugs under compression" *Drug. Dev. Ind. Pharm.* **11** 315–332.

Cohen, M. D., P. Coppens, and G. M. J. Schmidt (1964) "Phase transformation $\beta \rightarrow \alpha$ *p*-nitrophenol" *J. Phys. Chem. Solids.* **25** 258-260.

Coppens, Philip and G. M. J. Schmidt (1965a) "The crystal structure of the α-modification of *p*-nitrophenol near 90 K" *Acta Crystallogr.* **18** 62–67.

Coppens, Philip and G. M. J. Schmidt (1965b) "The crystal structure of the metastable (β) modification of *p*-nitrophenol" *Acta Crystallogr.* **18** 654–663.

De Villiers, M. M., J. G. van der Watt, and A. P. Lötter (1991) "The interconversion of the polymorphic forms of chloramphenicol palmitate (CAP) as a function of environmental temperature" *Drug Dev. Ind. Pharm.* **17** 1295–1303.

Haleblian, John and Walter McCrone (1969) "Pharmaceutical applications of polymorphism" *J. Pharm. Sci.* **58** 911-929.

Ibrahim, H. G., F. Pisano, and A. Bruno (1977) "Polymorphism of phenylbutazone: properties and compressional behavior of crystals" *J. Pharm. Sci.* **66** 669–673.

Kitaigorodskii, A. I., Yu. V. Mnyukh, and Yu. G. Asadov (1965) "Relationships for single crystal growth during polymorphic transformation" *J. Phys. Chem. Solids* **26** 463–472.

Kaneniwa, Nobuyoshi, Mokato Otsuka, and Tetsuo Hayashi (1985) "Physiochemical characterization of indomethacin polymorphs and the transformation kinetics in ethanol" *Chem. Pharm. Bull.* **33** 3447–3455.

Lin, Song-Ling and Leon Lachman (1969) "*In situ* crystalline transformation of a new antihypertensive determined by photomicrographic and dissolution methods" *J. Pharm. Sci.* **58** 377–379.

Matsuda, Yoshihisa, Sachiyo Kawaguchi, Hitomi Kobayashi, and Jujiro Nishijo (1984a) "Physiochemical characterization of spray-dried phenylbutazone polymorphs" *J. Pharm. Sci.* **73** 173–179.

Matsuda, Yoshihisa, Etsuko Tatsumi, Etsuko Chiba, and Yukie Miwa (1984b) "Kinetic study of the polymorphic transformations of phenylbutazone" *J. Pharm. Sci.* **73** 1453–1460.

Matsumoto, Takahiro, Nobuyoshi Kaneniwa, Shigesada Higuchi, and Makoto Otsuka (1991) "Effects of temperature and pressure during compression on polymorphic transformation and crushing strength of chlorpropamide tablets" *J. Pharm. Pharmacol.* **43** 74–78.

McCrone, Walter C. (1965) "Polymorphism" in *Physics and Chemistry of the Organic Solid State*; David Fox, Mortimer M. Labes, and Arnold Weissberger, Eds.; Interscience: New York, NY; Vol. 2, Chapter 8, pp 725–767.

Moustafa, M. A., Said A. Khalil, A. R. Ebian, and M. M. Motawi (1972) "Kinetics of interconversion of sulphamethoxydiazine crystal forms" *J. Pharm. Pharmacol.* **24** 921–926.

Otsuka, Makoto and Nobuyoshi Kaneniwa (1986) "Effect of seed crystals on solid-state transformation of polymorphs of chloramphenicol palmitate during grinding" *J. Pharm. Sci.* **75** 506–511.

Paul, Iain C. and Kuan Tee Go (1969) "Crystal and molecular structure of 5-methyl-1-thia-5-azacyclooctane 1-oxide perchlorate" *J. Chem. Soc. B* **1969** 33–42.

Rankell, A. S. (1969) "Influence of compressional force on solid-state crystal conversion of succinylsulfathiazole" Ph.D. Thesis, University of Wisconsin, Madison, WI .

Robertson, J. Monteath and A. R. Ubbelohde (1938) "A new form of resorcinol. II. Thermodynamic properties in relation to structure" *Proc. Roy. Soc London Ser. A.* **167** 136–147.

Thomas, J. M. (1974) "Topography and topology in solid state chemistry" *Philos. Trans. R. Soc. London, Ser. A.* **277** 251–287.

Umeda, Tsuneo, Noriaki Ohnishi, Teruyoshi Yokoyama, Tsutomu Kuroda, Yoshiaki Kita, Koji Kuroda, Etsuko Tatsumi, and Yoshihisa Matsuda (1985) "A kinetic study on the isothermal transition of polymorphic forms of tolbutamide and mefenamic acid in the solid state at high temperatures" *Chem. Pharm. Bull.* **33** 2073–2078.

Yokoyama, Teruyoshi, Tsuneo Umeda, Koji Kuroda, Takako Nagafuku, Tomoko Yamamoto, and Shozo Asada (1979) "Studies on drug nonequivalence. IX. Relationship between polymorphism and rectal absorption of indomethacin" *Yakugaku Zasshi* **99** 837–842.

Miscellaneous Topics

In this chapter we review a number of topics that can be expected to receive more interest in the future.

22.1 CRYSTALLIZATION

Once polymorphs or solvates are characterized, there is a need to be able to control the production of a desired form. Whenever possible, a single crystal form (polymorph or solvate) should be selected. The final crystallization should be designed to control the crystal form and particle size.

In cases involving pharmaceuticals where the new crystal form does not influence bioavailability or chemical stability, it may be simpler to switch the process to accommodate the new crystal form and request an exception from the FDA than to invest the time needed to discover a process which reliably produces the old form. It is important to note that the above phenomenon is one of the main reasons the FDA is interested in more careful studies of polymorphs.

Extensive studies early in the development process should lead to the discovery of most of the polymorphs and to a method whereby the desired pure polymorph can be reproducibly prepared. However, even a systematic search may not always reveal all of the polymorphs of a substance because so many factors, as we have seen, can affect polymorph nucleation and growth.

Crystallizations are affected by numerous factors including:

a. concentration (degree of supersaturation)
b. temperature and cooling profile
c. seeding and agitation
d. interconversion of solid forms
e. composition, polarity, and pH (important for crystallization of salts; the exact pH may have important influences on the crystallization)
f. additives and impurities

The effect of each of these factors on crystallization will be reviewed and discussed in the remainder of this section.

A. Concentration (Degree of Supersaturation)

An important factor which influences crystallizations is degree of supersaturation (*i.e.*, the ratio of the concentration of the solution to that of a saturated solution). In a study of polymorphism of cimetidine, Sudo and co-workers (1991a–b) showed that the crystal forms obtained through crystallization in isopropyl alcohol were dependent on supersaturation ratios. At supersaturation ratios greater than 3.6, Form A crystallized regardless of the presence or absence of Form A or Form B seeds. In supersaturation ratios less than 2, the form that crystallized was dependent upon seeding (*i.e.*, Form A crystallized if there were Form A seeds and Form B crystallized if there were Form B seeds). In this study, Sudo and co-workers also suggested the size of the nucleus for crystallization was very small (about 8 Å), containing seven molecules. Sato and Boistelle (1984) studied the polymorphic modifications of stearic acid and found that high supersaturation in non-polar solvents favored Forms A and C whereas lower supersaturation favored Form B.

B. Temperature and Cooling Profile

Crystallization at higher temperatures may produce one polymorph whereas crystallization at lower temperatures may produce a second polymorph. Kitamura (1989) in studies on the crystallization of L-glutamic acid showed that at 45 °C the α-form nucleates slowly and the β-form grows, whereas at 25 °C, only the α-form nucleates and grows. In their study of the crystallization of tripalmetin, Kellens and co-workers (1992) found that crystallization at 42 °C favored the α-form whereas crystallization at 56 °C favored the β-form. In between these temperatures, other β-type polymorphs were formed. Nass (1991) has reviewed the effect of temperature on the crystallization of polymorphs. Other examples may be found in *Particle Design via Crystallization* (Ramanarayanan *et al.*, 1991).

C. Seeding and Agitation

The effect of seeding on crystallization has been the subject of many studies. Typically, seeding can be used to control crystallization and the extent of primary nucleation. For example, Suzuki and Hara (1974) showed that the α-form of inosine could be obtained directly by crystallization from water whereas to obtain the β-form, seeds of the β-form must be used.

A study of the effect on seeding was reported by Kondepudi and co-workers (1990). Sodium chlorate crystallizes in a chiral and a racemic crystal form. Since sodium chlorate is not chiral in solution, quiescent crystallization of an aqueous solution produces equal numbers of *d*- and *l*-crystals. Surprisingly, crystallization of an aqueous solution with stirring gives mostly crystals of only one chirality, either *d* or *l*. Investigation showed that this effect was due to the fact that once a particular crystal (either *d* or *l*) has formed, then that crystal collides with the stirrer and is broken into many small seeds which then nucleate crystallization of that chirality. This supports the idea that one seed can produce one crystal form. This also suggests that in this particular crystallization, if a seed of either *d*- or *l*-crystals was initially added then only crystals of that chirality would be obtained. In a related study, Belyustin and Ro-

gacheva (1966) showed that seeding with a right-handed crystal produced a right-handed crystal form of magnesium sulfate.

In a study of cimetidine by Sudo and co-workers (1991a–b), an effect of seeding was also observed. Seeding at high supersaturation levels with either Form A or Form B crystal always led to Form A, that is, seeds of Form B had no effect on controlling the crystallization. However, at lower supersaturation levels the crystal form obtained was dependent on the crystal form of the added seeds.

In a study of the crystallization of glutamic acid, Sugita (1988) found that seeding with α-crystals controlled the crystal form of the product. However, many of the α-seeds that were used were contaminated with the β-form, therefore causing mixtures to crystallize. This study illustrates the importance of having pure seeds.

Questions of the size of seeds are often raised and several studies have indicated that seeds can be as small as 10 Å in diameter (Powers, 1971; Belyustin and Rogacheva, 1966), 100 Å (Van Hook, 1961), or as large as 1000 Å (Mullin and Leci, 1972; Mullin, 1993). A study by Rousseau and co-workers (1976) found that seeds must be at least several hundred nanometers (several hundred-thousand Ångstroms) to control nucleation rate.

Cases are known where a crystal form that has been produced for a long period of time can no longer be obtained. Suddenly a more stable form that had not been observed before is now the only form that can be isolated. All attempts to produce the original, less-stable crystal form fail. Dunitz and Bernstein (1995) have reported on cases involving these "disappearing polymorphs." Woodard and McCrone (1975), suggested that seeding was the best explanation for this phenomenon. Jaciewicz and Nayler (1979) suggested that it should be possible to produce the earlier form but that discovering the correct conditions may require considerable effort.

In other studies, Mullin and Leci (1972) have investigated the crystallization of seeded citric acid solutions. They found that by decreasing the seed size, the latency period in crystallization decreased while the de-supersaturation rate increased. Based on these studies they proposed a mechanism of secondary nucleation by cluster formation. The importance of secondary nucleation (see Section 1.5B), that is, seeds produced by factors such as agitation and equipment, must also be recognized. Treatment of this special subject may be found in the literature on crystal engineering and unit operations.

D. Interconversion of Solid Forms

Interconversion of crystal forms is another phenomenon which affects the production of crystalline materials and, like an ordinary crystallization, involves nucleation and growth of a new phase. Davoll and co-workers (1952) found two crystal forms of tetraacetyl-D-ribofuranose. The presence of any of the higher-melting form caused spontaneous conversion of the lower-melting form to the higher-melting form. The practical effect of this process is the inability to obtain the lower-melting form. A similar observation was made by Anchel and Blatt (1948) in the synthesis of 9,9-dimethylfluorene. They found that the crystal form which was first obtained as needles from ligroin had a melting point of 71 °C. However, upon standing this form converted to a second crystal form with a melting point of 95–96 °C. Again, this appears to be a solid-state interconversion initiated by seeds of the higher-melting crystal form.

The interconversion of crystal forms by a solution-mediated process is well known. For example, the α- and γ-forms of oleic acid transform to the β-form in a saturated solution (Suzuki *et al.*, 1985; Sato and Suzuki, 1986). This is clearly a case where the less soluble (more stable) crystal form grows and the more soluble crystal form dissolves. In another study, the lower melting form (melting point 111–117 °C) of α-D-lyxopyranose tetrabenzoate (Fletcher *et al.*, 1951) has been shown to convert to the higher melting form by slurrying in alcohol. Davey (1982) reported a more extensive study of this phenomenon in his review and suggested that the rate of a solution-mediated phase transformation depends on the relative solubilities of the two substances in that solution. However, this is a theoretical statement and there may be cases where other factors such as nucleation become more important. In our laboratory, we have occasionally had great difficulty in achieving interconversion even in solutions where the crystal forms are somewhat soluble.

When crystalline solvates undergo desolvation, three possibilities can occur that may not be mutually exclusive:

1. a new, anhydrous crystalline form is produced
2. amorphous material is produced
3. the original crystal lattice is maintained

When crystalline solvates undergo desolvation, the most likely outcome is that a new, anhydrous crystalline form is produced. The XRPD pattern of the resulting crystalline product is different from the starting material and corresponds to that of an anhydrous form obtained by crystallization from another solvent. Caffeine hydrate is a good example (Griesser and Burger, 1995).

However, there are two other possible outcomes from the desolvation of a crystalline solvate. An amorphous material may be produced; for example, Xu (1997) found that the acetonitrile solvate of quinapril hydrochloride desolvates *in vacuo* to produce amorphous material. Alternatively, the original crystal lattice may be maintained after the desolvation of a crystalline solvate. An example of this third behavior is hydrocortisol 21-*tert*-butylacetate monoethanol solvate, in which the solvent is lost yet the original crystal structure is unchanged, resulting in a crystal with voids and cavities (Kessler, 1986).

E. Composition, Polarity, and pH

Crystallization from a pure solvent may favor one polymorph whereas crystallization from a mixed solvent may favor a different polymorph. For example, in the mannitol system, the α'-form is obtained by evaporation of 100% ethanol while the β-form is obtained by crystallization from aqueous ethanol (Berman *et al.*, 1968). In a study of inosine (Suzuki and Hara, 1974) showed that crystallization from water gave the α-form whereas crystallization from 70% DMSO gave the β-form.

Nass (1991) demonstrated how the polarity of the solvent can be important for controlling the polymorph. Sato's study (Sato and Boistelle, 1984; Sato *et al.*, 1985) of the crystallization of stearic acid showed that non-polar solvents at high supersaturations favor Forms A and C while the Form B crystallizes at lower supersaturation in polar solvents. These studies indicate that polarity is an important factor to consider in choosing a crystallization solvent.

It should be obvious that the pH and ionic strength of the crystallization solvent play a major role in the crytallization of proteins because of the many acidic and basic functionalities present in these macromolecules. However, one variable that is often overlooked during the crystallization of small organic compounds is the pH of the solvent. The crystal habit of cytosine monohydrate is influenced by the pH of the crystallization solvent (Pazourek, 1979). Figure 22.1 illustrates the crystal lattice of cytosine monohydrate and Figure 22.2 shows the morphologies of the crystal habits obtained at pH values of 7.20, 6.44, and 5.70. The crystal form of glycine is influenced by the pH of the crystallization solvent (Iitaka, 1961). There are three polymorphic forms of glycine: α, β, and γ. The α-form is the most common form. The β-

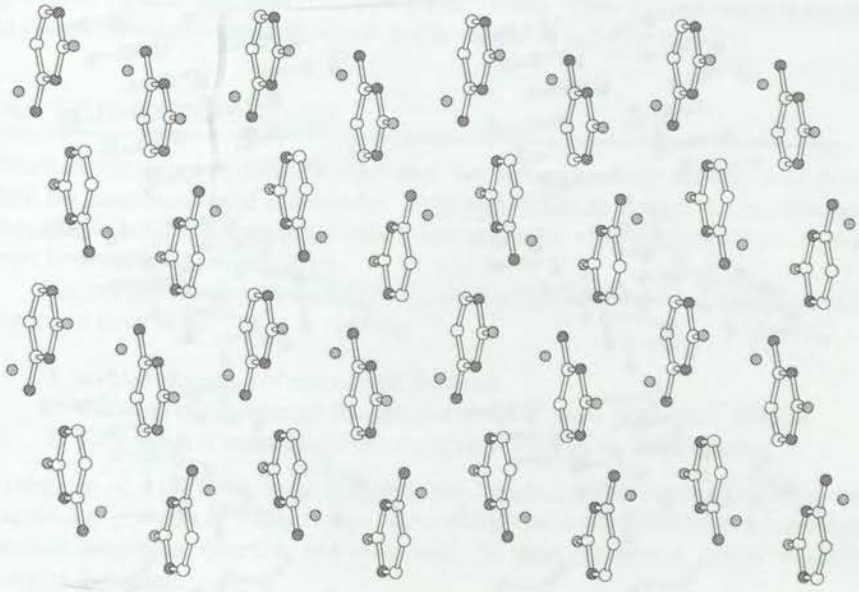

Figure 22.1 Cytosine monohydrate crystal lattice (carbon ○; nitrogen ●; oxygen ⊙) viewed in the same orientation as the habits illustrated in Figure 22.2 (McClure and Craven, 1973).

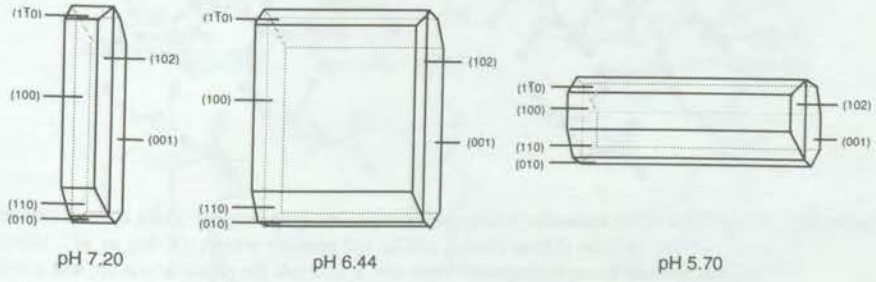

Figure 22.2 Habits of cytosine monohydrate crystals grown from solutions of different pH values (Pazourek, 1979).

form is metastable and converts to the α-form upon heating. The γ-form is obtained from non-neutral aqueous solutions. Figure 22.3 shows stereoviews of the crystal lattices of these three forms of glycine.

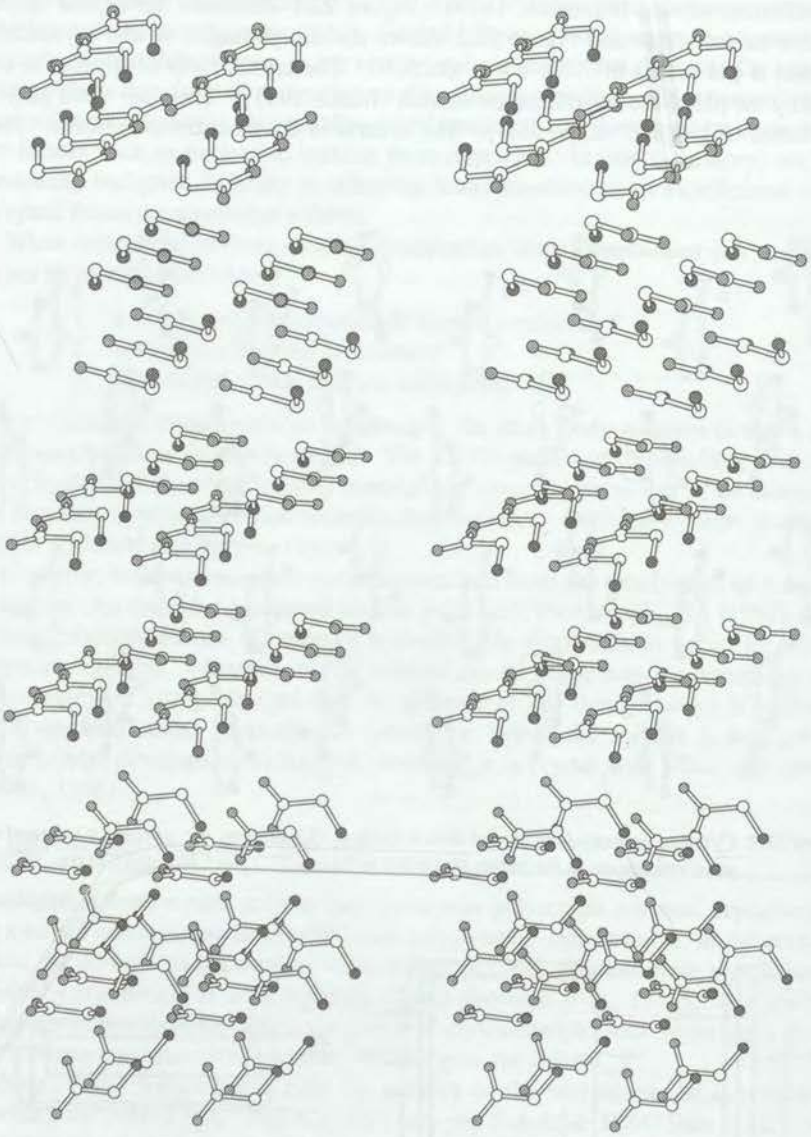

Figure 22.3 Stereoviews of the molecular arrangements in glycine polymorphs: (top) α-form (Power *et al.*, 1976); (middle) β-form (Iitaka, 1960); and bottom) γ-form (Kvick *et al.*, 1980). The directions of the crystallographic axes are: *a*-axis into the paper; *b*-axis up; and *c*-axis to the left.

F. Additives and Impurities

Because additives or impurities can dictate the morphology and crystal form produced in a crystallization process, the effect of additives on crystallization has been of interest for many years. Early work by Simonelli indicated that polymeric additives could inhibit the crystallization of certain forms. He presented a diagram which shows how a polymer can poison the crystallization of a given phase (Simonelli *et al.*, 1970). Grant and co-workers have shown the effect of additivies on the crystallization of adipic acid (Grant and York, 1986; Chow *et al.*, 1986). Studies of the crystallization of sucrose showed that additives were capable of slowing its crystallization (Powers, 1971). Lahav and co-workers have shown that the presence of as little as 0.03% of an additive can inhibit nucleation and crystal growth of a stable polymorph, thereby favoring the growth of a metastable form (Weissbuch *et al.*, 1991). They suggest that it is possible to design crystal nucleation inhibitors for the control of polymorphism.

22.2 Solid-Solid Reactions

Reactions between two different solids have not been extensively studied, even though they are sometimes used industrially. Although drugs in dosage forms sometimes degrade via solid-solid reactions, only a few studies of solid-solid reactions of drugs have been reported (Byrn, 1976).

According to Rastogi *et al.* (1977a–b), solid-solid reaction can be thought of as occurring in three steps:

1. surface migration of one or both reactants
2. diffusion of one reactant into the grains and crevices of the other reactant
3. penetration of one reactant into the crystal lattice of the other reactant

Rastogi *et al.* (1977a–b) used this three-step mechanism to explain the solid-solid reactions of powders of 8-hydroxyquinoline with phthalic anhydride, maleic anhydride, succinic anhydride, catechol, and resorcinol. In these reactions a yellow molecular complex is formed.

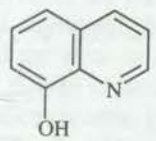

8-hydroxyquinoline

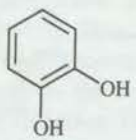

catechol

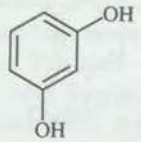

resorcinol

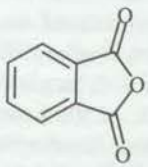

phthalic anhydride

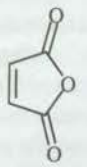

maleic anhydride

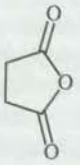

succinic anhydride

The kinetics of diffusion of 8-hydroxyquinoline into the solid anhydrides and the phenols were measured using a capillary technique. The powders of 8-hydroxyquinoline and the reactant were placed in capillary tubes, in contact or with an air gap separating them. The reaction was monitored by measuring the increase in thickness of the yellow product layer. When the powders were in contact, the data fit Equation 22.1, where k is the rate constant, t is the time, and n is an integer.

$$\text{Thickness of the product layer} = kt^n \tag{22.1}$$

The activation energy for this reaction, determined by measuring the rate at various temperatures, was 45–156 kJ/mol. The lower activation energies were interpreted in terms of a surface migration of 8-hydroxyquinoline into the anhydrides or phenols (Rastogi *et al.*, 1977a–b). No migration of the phenols or anhydrides into the 8-hydroxyquinoline layer was observed.

When there was an air gap separating 8-hydroxyquinoline from the reactants, the reaction was much slower and followed a different kinetic equation (Equation 22.2). As the lengths of the air gap increased, the rate of reaction decreased. These results indicate that when the powders are in contact the reaction is dominated by a mechanism other than vapor diffusion.

$$\text{Thickness of the product layer} = kt \tag{22.2}$$

The diffusion of 8-hydroxyquinoline inside the grains of the reactant anhydrides and phenols was also studied by reacting 8-hydroxyquinoline vapor with solid anhydride or phenol. This process has an activation energy of 96.3 kJ/mol and is similar to the ΔH_{vap} of 8-hydroxyquinoline. Thus this process may occur by vapor-phase diffusion.

These studies points out several important aspects of solid-solid reactions. Of particular interest to pharmaceutical scientists is the observation that intimate contact of the reactant powders allows surface migration of the reactant. The reaction dependant on surface migration has a very low activation energy relative to the reaction dependant on vapor-phase diffusion.

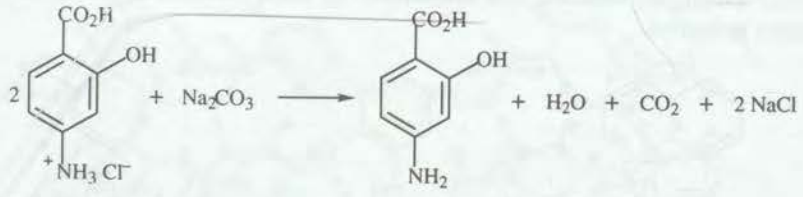

4-aminosalicylic acid hydrochloride **4-aminosalicylic acid**

In our laboratory, we have studied the reaction of single crystals of 4-aminosalicylic acid hydrochloride with powdered sodium carbonate (Lin *et al.*, 1978). This reaction was carried out by placing powdered Na_2CO_3 in contact with single crystals of 4-aminosalicylic acid hydrochloride in order to study the details of the penetration of reactants. 4-Aminosalicylic acid hyrochloride commonly exists in three crystal habits, and all three undergo solid-solid reaction with sodium carbonate (see Figure 22.4 for illustrations of the three habits, Figure 22.5 for photographs of a typical reaction, and Figure 22.6 for the crystal lattice). These reactions always began at the point where the

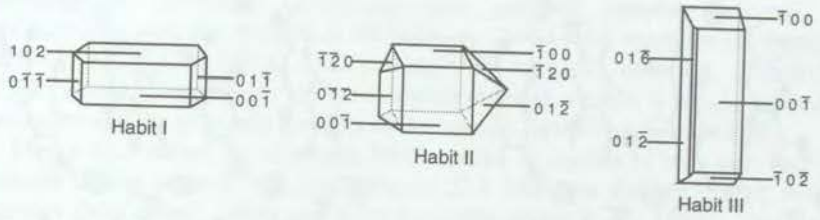

Figure 22.4 Representations of three habits of 4-aminosalicylic acid hydrochloride (Lin *et al.*, 1978).

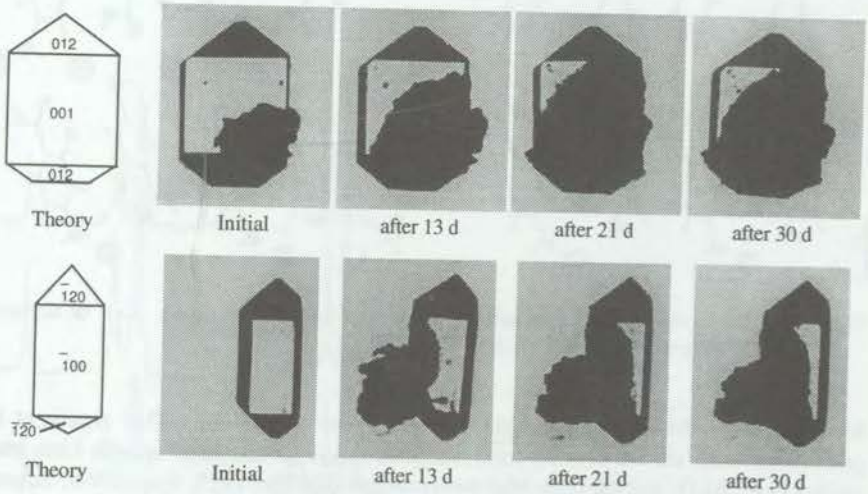

Figure 22.5 Reaction of a 4-aminosalicylic acid hydrochloride crystal (Habit II) with Na_2CO_3 (dark mass) on the (001) face (upper) and on the ($\bar{1}00$) face (lower) (Lin *et al.*, 1978).

acid crystal and base touched. They were quite slow and took more than 40 days to reach completion at 60° C.

Analysis of the end-products of the reaction indicated that both 4-aminosalicylic acid and 4-aminosalicylate ions were present. Thus, solid-solid acid-base reactions do occur and are slow in comparison to their solution counterparts. The slow rate is probably due to slow diffusion of ions in the 4-aminosalicylic acid hydrochloride crystal lattice (Hauffe, 1955; Jost, 1960; Girifalco, 1964; Schmalzried, 1968; Schmalzried, 1981). In addition, the fact that these reactions always began at the point of contact of the acid crystals and base and spread through the crystal from that point indicates that these reactions can be artificially nucleated and that the reaction proceeds from the nucleation site (which may involve a defect) throughout the crystal. This behavior is similar to that of the degradation of 4-aminosalicylic acid hydrochloride single crystals at 95 °C, since once these crystals begin to react the reaction spreads from that nucleation site throughout the crystal (Lin *et al.*, 1978). It should be noted that while the thermal reaction of 4-aminosalicylic acid hydrochloride probably involves loss of HCl by diffusion, these solid-solid acid-base reactions could involve either diffusion of HCl to the sodium carbonate or counterdiffusion of the H^+ and Na^+ ions to

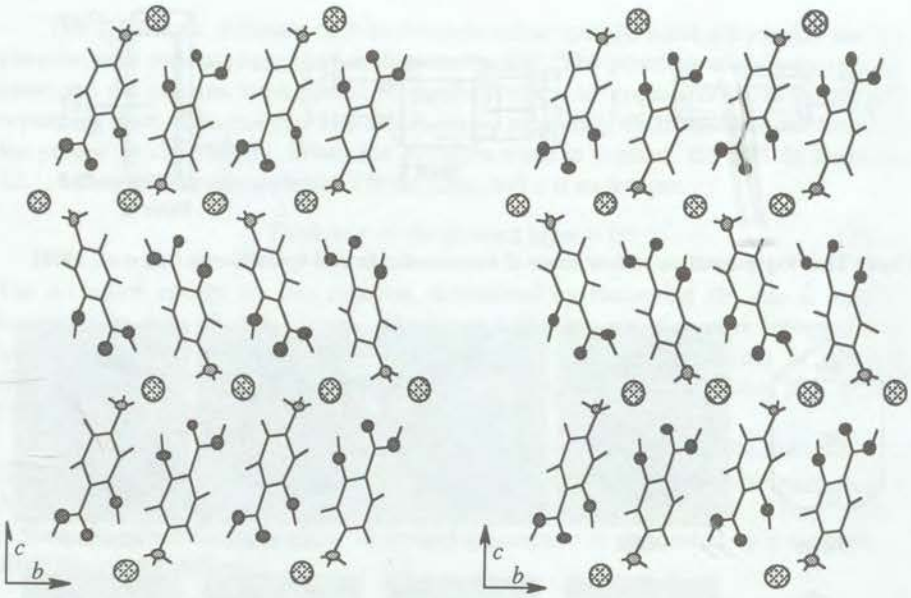

Figure 22.6 Stereoview of the 4-aminosalyclic acid hydrochloride crystal lattice. Key: ◍ nitrogens; ● oxygens; ⊗ chlorines (Lin *et al.*, 1978).

form H_2CO_3 in the base and sodium chloride in the acid lattice. This argument has precedents in the studies of solid-solid inorganic reactions that form spinels from metal oxides (*e.g.*, Al_2O_3 and MgO) at high temperatures (Hauffe, 1955; Jost, 1960; Schmalzried, 1968; Schmalzried, 1981); the most probable mechanism of these reactions involves counterdiffusion of cations.

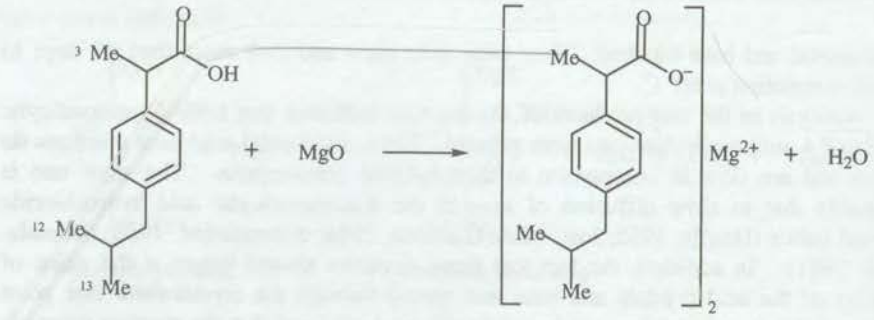

ibuprofen **magnesium oxide** **magnesium diibuprofenate**

Other solid-solid acid-base reactions have been reported including the reaction of ibuprofen with magnesium oxide (Kararli, *et al.*, 1989) and the reaction of sodium bicarbonate with tartaric acid (Usui and Carstensen, 1985; Wright and Carstensen, 1986). The solid-solid reaction of MgO with ibuprofen was observed for both 1:1 and 2:1 mixtures of ibuprofen with MgO stored at 55 °C. Evidence for the reaction included disappearance of the ibuprofen melting endotherm on DSC and changes in the infrared

spectrum after reaction. Comparison with authentic samples indicated that $Mg(ibuprofen)_2$ was the product of the reaction. Solid-solid reactions of ibuprofen with Na_2HCO_3, $K_2CO_3 \cdot 1\frac{1}{2}H_2O$, CaO, and $Mg(OH)_2$ were also observed. Research in our laboratories (Stephenson, 1994) has shown that this reaction is greatly influenced by moisture and the molecular mobility of the reactant crystal (see Section 22.8).

Figure 22.7 shows the solid-state NMR spectra of crystals of both (+)- and (±)-ibuprofen during reaction with MgO; Figure 22.8 illustrates the unit cell of racemic ibuprofen (McConnell, 1974) and *S*-(+)-ibuprofen (Freer *et al.*, 1993). Solid-state NMR proved to be the best method for studying these reactions, since the powder

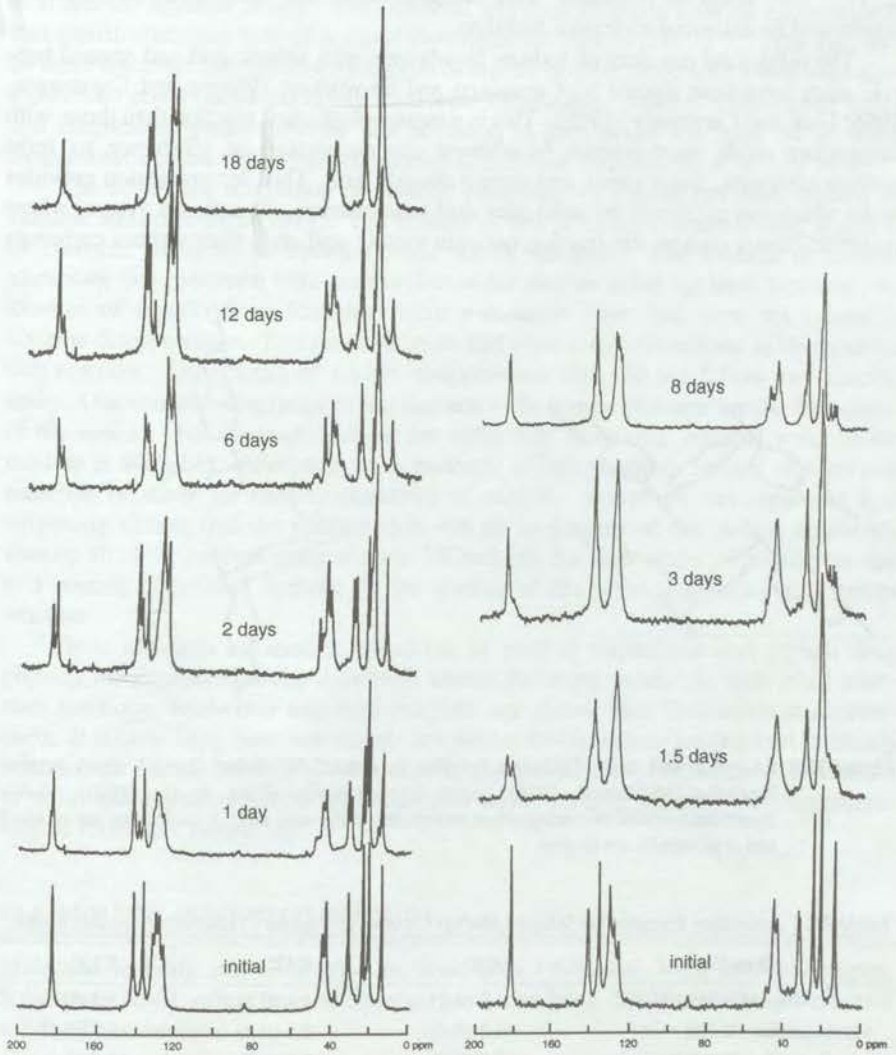

Figure 22.7 CP/MAS solid-state NMR spectra of (±)-ibuprofen (left) and (+)-ibuprofen (right) during reaction with MgO at 20 °C and 81% RH (Stephenson, 1994).

diffraction pattern of ibuprofen disappeared during the reaction and solution methods obscure the reaction products. It is clear from the growth of the new carbonyl resonance at 190 ppm that the chiral (+)-crystals react significantly faster than the racemic crystals.

Stephenson (1994) also studied the molecular mobility of (+)-ibuprofen and (±)-ibuprofen crystals by measuring the T_1 relaxation times of the methyl carbon atoms in ibuprofen at different temperatures using solid-state NMR (Table 22.1). The relaxation times were then plotted versus the reciprocal of temperature to yield an activation energy for the motion being studied. These studies showed that all three methyl carbon atoms had lower activation energies in the more reactive (+)-ibuprofen crystals (Table 22.1). This result is consistent with the hypothesis that solid-solid reactions are accelerated by enhanced molecular mobility.

The solid-solid reactions of sodium bicarbonate with tartaric acid and several benzoic acids have been studied by Carstensen and co-workers (Wright and Carstensen, 1986; Usui and Carstensen, 1985). This is a more complicated reaction than those with magnesium oxide since sodium bicarbonate can decompose or effervesce to form sodium carbonate, water vapor, and carbon dioxide gas. This decomposition provides water which can accelerate the solid-state acid-base reaction. In a closed system where moisture cannot escape, the reaction between tartaric acid and either sodium carbonate

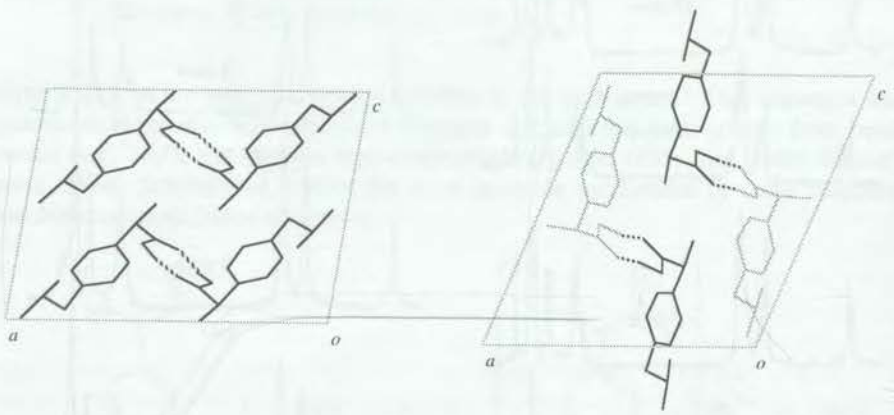

Figure 22.8 Ibuprofen unit cells (hydrogen bonding is denoted by dashed lines): (left) racemic ibuprofen (McConnell, 1974); (right) *S*-(+)-ibuprofen (Freer *et al.*, 1993). *S*-(+)-Ibuprofen contains two independent molecules in the unit cell; *A* molecules are in black and *B* molecules are in grey.

Table 22.1 Activation Energies for Selected Methyl Carbons in Various Crystalline Ibuprofen Forms

Sample	C3[a]	C12[a]	C13[a]
(*S*)-(+)-ibuprofen 1% RH	4.3 (0.2)	4.4 (0.2)	5.3 (0.5)
(±)-ibuprofen 1% RH	9.9 (0.4)	8.8 (0.4)	9.1 (0.5)
(±)- ibuprofen 98% RH	10.0 (0.7)	10.3 (1.2)	10.3 (1.3)
(±)-ibuprofen during reaction	9.0 (0.8)	9.8 (0.9)	9.6 (0.5)

a The energies of activiation are in kJ/mol with standard deviations in paretheses (Stephenson, 1994).

or sodium bicarbonate was found to be relatively rapid, taking only a few hours. Similarly, the reaction of sodium bicarbonate with benzoic acids was also relatively rapid in the presence of varying amounts of moisture (Wright and Carstensen, 1986). In an open system, they found that tartaric acid did not react; instead, the sodium bicarbonate decomposed to sodium carbonate and no solid-state acid-base reaction was observed in the timeframe of their studies (up to 400 hr). These results are consistent with studies of the acid-base reaction of 4-aminosalicylic acid hydrochloride and sodium carbonate, where in an open system at 40 °C a solid-state acid-base reaction was observed only after many days.

Tablets containing both aspirin and an easily acylated drug degrade to give salicylic acid and the acylated drugs. For example, mixtures of phenylephrine hydrochloride and aspirin contained 80% of acylated phenylephrine after 34 d at 70 °C. The first step of these reactions may involve hydrolysis of aspirin to form acetic acid which may have a profound effect on the putatively solid-state mechanism. Indeed, a mixture of starch and magnesium stearate slowed this acylation to only about 1% after 34 d, while magnesium stearate without starch resulted in complete decomposition in only 16 d.

The solid-state acetylation of codeine phosphate by aspirin has been studied by Galante and coworkers (1979). The kinetics of this acetylation reaction were found to be complex and a single equation could not be obtained. The kinetics of codeine phosphate disappearance were pseudo-first-order after an initial lag time; however, the kinetics of acetylcodeine formation were a complex order and were not related to codeine disappearance. This result suggests that there is an intermediate in this acetylation reaction. The kinetics of aspirin disappearance also did not follow any specific order. One complicating factor in this reaction is the source of water for the hydrolysis of the aspirin. For the hydrolysis of the initial few molecules, residual water in the mixture is available. After this, each molecule of acetylcodeine formed releases one molecule of water for further hydrolysis of aspirin. Based on this argument it is surprising to note that the reaction does not go to completion but instead apparently uses up all of the residual water at about 7% reaction and then stops. This may be due to a coating of product forming on the reactant at this point, preventing any further reaction.

These reactions are models which can be used to understand and explain drug physical incompatibilities that have been known for many years. As with other solid-state reactions, solid-solid acid-base reactions are slower than their solution counterparts. It is clear from these few studies that further investigations are required to clearly establish the factors controlling the course of these solid-solid reactions. A discussion of solid–gas reactions which also addresses issues in drug physical incompatibilites will be found in Chapter 16.

22.3 Molecular Mobility in Solids

Molecular mobility can be studied by solid-state NMR and X-ray crystallography. Solid-state NMR offers several approaches to studying the molecular mobility of solids. These include:

1. Study of processes which result in peak coalescence of solid-state NMR resonances using variable-temperature solid-state NMR to detect conformational changes.

2. Determination of the T_1 relaxation of individual carbon atoms using variable temperature solid-state NMR.
3. Use of interrupted-decoupling (or other pulse sequences) to detect methylene and possible methine groups with unusual mobility.
4. Comparison of solid-state MAS spectra measured with and without cross polarization to detect mobile groups or atoms.

The rate of the carbon-spin relaxation towards equilibrium is characterized by the spin-lattice relaxation time, T_1 (Fukushima and Roeder, 1981). In this process the excess energy from the spin system is given to the surroundings or lattice. Interactions of randomly fluctuating magnetic fields at the **Larmor frequency** of the nucleus stimulate these transitions. Such fields arise from motions of other nuclear magnetic moments such as those from protons. Spin-lattice relaxation is thus most efficient when these motions are near the Larmor frequency. Studies of T_1 can give valuable information about fast motions in the MHz range such as methyl-group rotations (Bloembergen *et al.*, 1948; Andrew *et al.*, 1974).

In the rotating frame, the relaxation of the ^{13}C nuclei is affected by motions having frequencies comparable to the spin-lock field B_1. The determination of $T_{1\rho}$ in this rotating frame can provide information about slow molecular motions. Numerous studies of molecular motion using relaxation times have been published (Fyfe, 1983). In the field of polymer science, for example, solid-state NMR has been used to study both main chain and side group motion (Lyerla, 1979; Garroway *et al.*, 1979; Tonelli *et al.*, 1990; Axelson and Mandelkern, 1979). In addition, studies have been made of the relationship between polymer crystallinity and relaxation parameters including T_1, $T_{1\rho}$, and T_2 (Menger *et al.*, 1982; Kitamaru *et al.*, 1986; Earl and VanderHart, 1979; Schilling *et al.*, 1984; Cholli *et al.*, 1988).

Variable temperature solid-state NMR spectroscopy has been shown to be a powerful technique for the study of molecular motion in polymers and amino acids (Andrew *et al.*, 1976a–b; Andrew *et al.*, 1978; Schaefer *et al.*, 1977; Garroway *et al.*, 1982; Fyfe, 1983; Imashiro *et al.*, 1983; Naito *et al.*, 1983; Schaefer *et al.*, 1984a–b; Poliks and Schaefer, 1990). In addition, solid-state NMR has been used to study the activation energies of spinning methyl groups (Andrew *et al.*, 1976a–b; Andrew *et al.*, 1978; Fyfe, 1983). The activation energy for the spinning of methyl groups in triethylphosphine oxide was reported to be 7.9 kJ/mol by T_1 studies and 8.69 kJ/mol by $T_{1\rho}$ studies (Schaefer *et al.*, 1984a–b). Relaxation studies of *peri*-substituted naphthalenes were used to determine the barrier to methyl rotation when substituents at the *peri*-position were —H (9.7 kJ/mol), —CH_3 (13.5 kJ/mol), —Cl (15.2 kJ/mol), and —Br (18.4 kJ/mol). The barriers follow the sequence of the van der Waals radii and indicate that if a large group abuts the methyl group it can restrict methyl rotation. Rotation barriers for methyl groups in several amino acids have also been reported (Andrew *et al.*, 1976a–b; Andrew *et al.*, 1978).

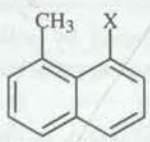

***peri*-substituted naphthalenes**

X = H, Me, Cl, Br

Trueblood, Dunitz, and Shomaker have shown that the molecular motion in a crystalline material can be studied by variable-temperature X-ray crystallography (Trueblood, 1985; Dunitz *et al.*, 1988a–b). They showed that simple harmonic theory can be used to relate the mean-squared displacement amplitudes of the atoms to the temperature. That is, motion of atoms in crystals can be described by the simple harmonic oscillator model. The notion that mean-squared displacement amplitude is related to the molecular mobility of an atom is, of course, consistent with the general concept of crystallographic atomic displacement parameters. It is important, however, to be aware of the fact that static disorder can complicate such studies. Nevertheless, it is apparent that X-ray crystallography also provides important information on the molecular mobility of atoms in solids.

hydrocortisone 21-cyclopentylmethylacetate

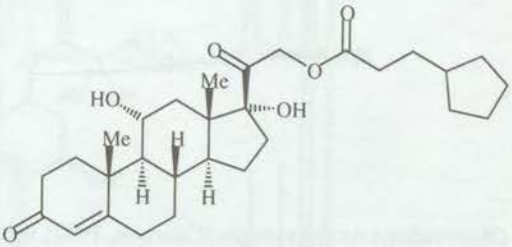

Early solid-state NMR studies of the molecular mobility in pharmaceuticals were conducted by our group jointly with Frye on hydrocortisone 21-cyclopentylmethyl-

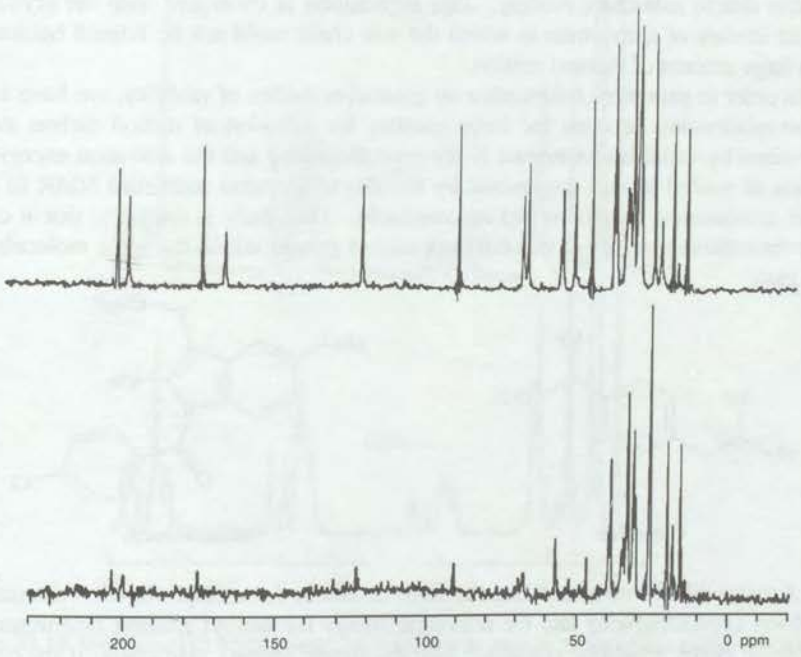

Figure 22.9 Solid-state FT-NMR spectra of hydrocortisone 21-cyclopentylmethylacetate: (upper) with cross polarization; and (lower) without cross polarization (Byrn *et al.*, 1988.)

acetate (Byrn *et al.*, 1988). Crystallographic studies showed that the cyclopentyl group in the side chain had extremely large thermal motion. A comparison of Fourier-transform (FT) NMR spectra with and without cross polarization (Figure 22.9) clearly showed that the cyclopentyl group peak was the most intense in the spectrum without cross polarization whereas in the spectrum acquired with cross polarization there were several signals with greater or equal intensity. The enhancement of this signal in the spectrum acquired without cross polarization indicates that this group has a large amount of thermal motion.

simvastatin

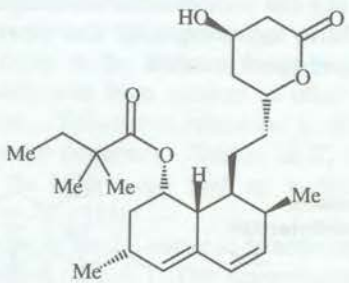

Observations on simvastatin (Cauchon, 1992) led to related conclusions. A signal from one of the side chain methylene carbon atoms was present in the interrupted-decoupling spectrum which normally shows the presence of only quarternary carbon atoms and methyl groups having a great deal of thermal motion. This was interpreted to mean that the methylene carbon atom has mobility similar to a methyl group, presumably due to side-chain motion. This explanation is consistent with the crystallographic studies of simvastatin in which the side chain could not be refined because it had a large amount of thermal motion.

In order to gain more information on quantative studies of mobility, we have studied the relationship between the force constant for vibration of methyl carbon atoms determined by variable temperature X-ray crystallography and the activation energy for rotation of methyl groups determined by variable temperature solid-state NMR in two model compounds, ibuprofen and indomethacin. This study is unique in that it compares the relative mobility of two different methyl groups within the same molecule for each case.

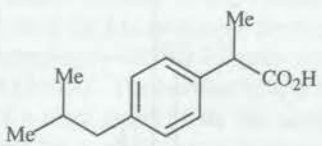

ibuprofen

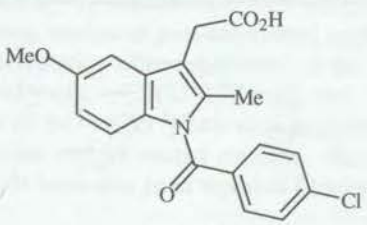

indomethacin

A priori there is no reason that the force constants for methyl vibration determined by X-ray crystallography and the activation energy for methyl rotation determined by solid-state NMR would be correlated (see discussion above). However, if the crystal packing in the vicinity of two different methyl groups in the same molecule is different one might expect that the methyl group which is not as tightly packed might exhibit a

lower force constant for vibration and also a lower activation energy for rotation. In order to test this idea, variable temperature solid-state NMR spectra of ibuprofen and indomethacin along with the variable temperature single crystal structures of these two model compounds were obtained.

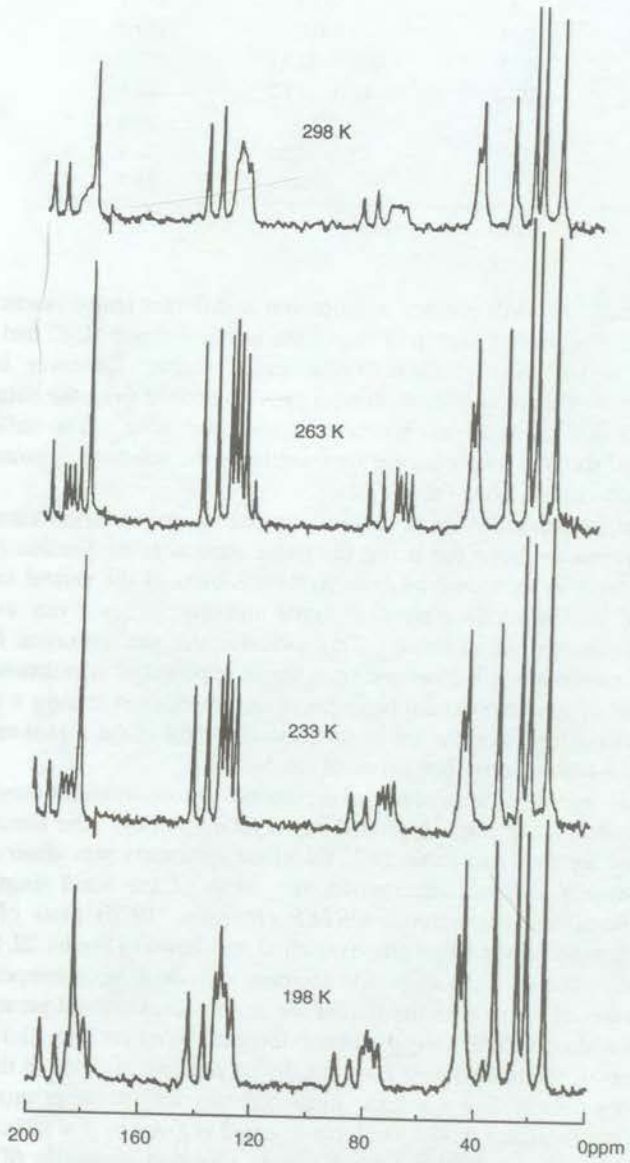

Figure 22.10 Solid-state ^{13}C NMR spectra of ibuprofen at various temperatures. The doublet and broad peak at 80 and 180 ppm are spinning side bands from the signals in the range of 125–145 ppm. The sharp peak at 183.3 ppm is due to the carbonyl absorption (Stephenson, 1994).

Table 22.2 ^{13}CMR Chemical Shift Assignments of Ibuprofen

Structure	Carbon Assignment	Chemical Shift Solid-State[a]	Chemical Shift Solution[b]
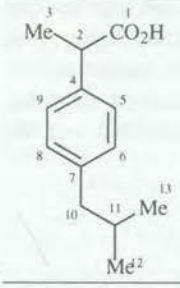	1	183.3	181.5
	7	142.1	140.7
	4	137.3	137.1
	6, 8	130.9	129.4
	5, 9	129.3, 127.1	127.4
	10, 2	46.0, 44.2	45.1
	11	32.7	30.2
	12, 13	25.1, 22.1	22.4
	3	15.4	18.7

a Cauchon, 1992. *b* $CDCl_3$; Smeyers *et al.*, 1985.

The solid-state ^{13}C NMR spectra of ibuprofen at different temperatures are shown in Figure 22.10. The methyl carbon atoms of the isobutyl group (C12 and C13) have identical chemical shifts in solution due to rotational averaging. However, in the solid-state spectrum, one of them is shifted about 3 ppm downfield from the solution value, indicating a different chemical environment in the solid state. The solid-state and solution chemical shifts of ibuprofen are very similar so the solid-state resonances were assigned by direct comparison (Table 22.2).

The spin-lattice relaxation times were measured at various temperatures for the three methyl groups in ibuprofen using the pulse sequences of Torchia (1978), and their activation energies were derived from Arrhenius plots of the natural log of the T_1 values versus T^{-1}. The semilog plots of signal intensity versus τ that were used to calculate the T_1 values were all linear. This indicates that the relaxation function for each individual carbon atom is governed by a single exponential correlation time; there was no evidence of non-exponential behavior in this case, even at long τ times. The low observed standard deviations are a consequence of the good signal-to-noise ratio which reflects the highly crystalline nature of the sample.

The crystal structure of ibuprofen was determined at four different temperatures on two separate crystals using single crystal X-ray crystallography. The structural data at each temperature are shown in Table 22.3. Excellent agreement was observed between the two independent structure determinations. Most of the bond lengths decrease slightly with increasing temperature. *ORTEP* (Johnson, 1976) plots of the crystal structures of ibuprofen at the temperatures studied are shown in Figure 22.11.

Clearly, the volumes of the ellipsoids decrease with decreasing temperature as expected. The slopes of the plots of the size of the atomic-displacement-parameter (ADP) ellipsoids versus temperature were calculated for each atom and are shown in Table 22.4. The atoms of the phenyl ring have smaller slopes, while those in the side-chain have larger slopes, indicating a weaker force constant for the latter atoms. In the classical harmonic oscillator model, the force constant is given by $f = kT/\langle\phi^2\rangle$ where k is the Boltzmann constant, $\langle\phi^2\rangle$ the mean square vibration amplitude of the motion, and T the absolute temperature. Thus, a plot of $\langle\phi^2\rangle$ versus temperature would yield a slope that was inversely proportional to the force constant. Since $\langle\phi^2\rangle$ for a particular atom is directly related to the ADP value for that atom, the slopes of ADP values versus

T give information about the relative magnitudes of the force constant k, assuming that atom can be treated as a harmonic oscillator.

Table 22.5 is a summary of the solid-state NMR and X-ray crystallographic data for the three methyl groups in ibuprofen. In this case, the methyl carbon atom, C3,

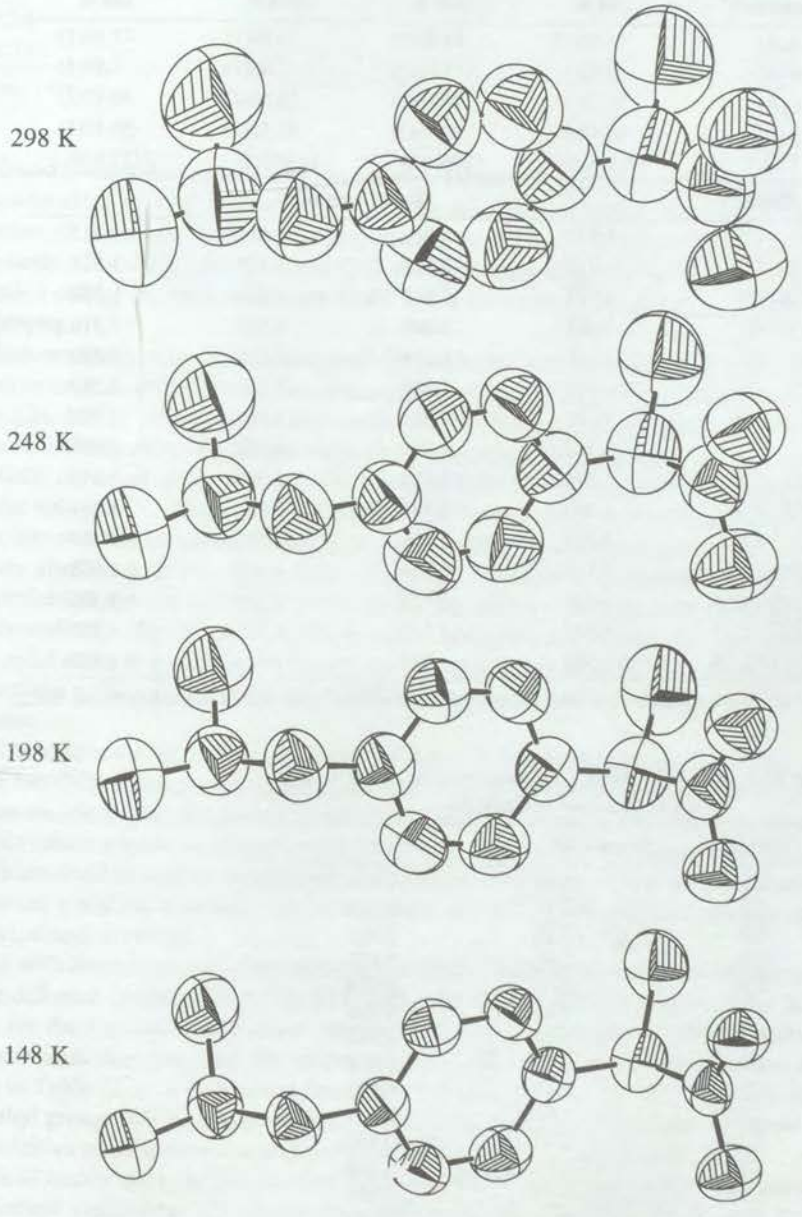

Figure 22.11 Atomic displacement-parameter ellipsoids (50% probability) of ibuprofen at different temperatures (Toma, 1993).

Table 22.3 Single-Crystal X-ray Data at Different Temperatures for Ibuprofen

Space group = $P2_1/c$ (monoclinic)
Average $R = 0.04$ Average $R_w = 0.07$
Crystal Dimensions = 0.54 × 0.47 × 0.43 mm

Cell Constants[a]	Temperature 298 K	248 K	198 K	148 K
a (Å)	14.65(1)	14.60(2)	14.54(1)	14.50(1)
b (Å)	7.88(1)	7.86(1)	7.85(1)	7.83(1)
c (Å)	10.71(1)	10.66(2)	10.58(2)	10.52(2)
β (°)	99.42(1)	99.46(1)	99.55(1)	99.55(1)
V (Å^3)	1219.6(3)	1206.3(6)	1190.9(5)	1177.9(5)
Bonds	**Bond Length (Å)**			
C1—C2	1.515	1.516	1.515	1.512
C2—C3	1.514	1.517	1.523	1.524
C2—C4	1.522	1.528	1.524	1.526
C1—O1	1.302	1.309	1.314	1.316
C1—O2	1.219	1.214	1.215	1.219
C4—C5	1.377	1.380	1.384	1.389
C5—C6	1.381	1.381	1.381	1.380
C6—C7	1.384	1.387	1.388	1.396
C7—C8	1.374	1.382	1.386	1.390
C8—C9	1.383	1.388	1.382	1.381
C4—C9	1.384	1.389	1.391	1.391
C7—C10	1.511	1.514	1.511	1.508
C10—C11	1.529	1.528	1.534	1.536
C11—C12	1.513	1.517	1.516	1.522
C11—C13	1.508	1.517	1.524	1.520

a The values in parentheses are the estimated standard deviation in the last place quoted (Toma, 1993).

Table 22.4 Slopes of Atomic Displacement Parameter Values versus Temperature for Ibuprofen

Atom	Slope × 10^4 Å^3·K^{-1}	r
C1	2.13	0.983
C2	2.34	0.985
C3	3.20	0.995
C4	2.04	0.987
C5	2.49	0.984
C6	2.64	0.986
C7	2.24	0.982
C8	2.45	0.988
C9	2.41	0.987
C10	2.67	0.988
C11	2.70	0.990
C12	3.71	0.994
C13	3.70	0.993
O1	2.62	0.993
O2	2.70	0.988

Toma, 1993.

Table 22.5 Comparison of Activation Energies from Solid-State NMR and Slopes of Atomic Displacement Parameters from X-ray for the Methyl-Carbon Atoms in Ibuprofen

Carbon	Chemical Shift (ppm)	E_a (kJ/mol)	Slope $\times 10^4$ ($Å^3$ K^{-1})
C3	15.4	10.0	3.20
C12/C13	22.1	8.8	3.70
C12/C13	25.1	9.1	3.71

Toma, 1993.

was found to have the highest activation energy (from the solid-state NMR study), and the lowest slope of ADP values versus T (from the single-crystal X-ray study). Since the value of the slope is inversely proportional to the force constant, the trend is in agreement. Similarly, the C12 and C13 methyls were found to have both a lower activation energy by both solid-state NMR and a lower force constant by X-ray crystallography.

Indomethacin was also investigated for a similar comparison. Indomethacin is known to exist in several crystalline polymorphic states (*et al.*, 1984; Kaneniwa *et al.*, 1985; Lin, 1992). However, in this study, the NMR relaxation properties and crystal structure for only Form I (also known as the γ-form) were determined. The solid-state ^{13}C NMR chemical shifts for crystalline indomethacin were assigned by comparison with the solution ^{13}C NMR shifts in DMSO-d_6 (O'Brien *et al.*, 1984) and with the help of the interrupted-decoupling experiment. The solution and solid-state chemical shifts are very similar, with two exceptions. The peak assigned as C4 is shifted almost 4 ppm upfield in the solid-state spectrum, while the carboxyl carbon is shifted about 7 ppm downfield. This latter observation can be attributed to hydrogen-bonding effects in the solid state; as hydrogen bonding to the carboxyl oxygen increases, the difference between the solid-state and solution ^{13}C NMR chemical shifts for the carboxyl carbon increases.

The solid-state ^{13}C NMR spectrum of Form I of indomethacin did not show any significant differences as the temperature was lowered (apart from variations in the position and intensity of spinning side-bands due to changes in the spinning speed). The spin-lattice relaxation times for each of the two methyls in crystalline indomethacin were determined at various temperatures. A plot of the natural log of the signal intensity versus τ yielded a straight line with a slope of $-1/T_1$. The activation energy was then calculated as before.

As with ibuprofen, the crystal structure of Form I of indomethacin was determined at four different temperatures (172, 214, 225, and 298 K) and the slopes of the ADP values for the various carbon atoms were plotted versus temperature. The T_1 values, their activation energies, and the slopes of the ADP values versus temperature are shown in Table 22.6. It is apparent from this table that, as was the case for ibuprofen, the methyl group with the lowest activation energy as determined from the T_1 values is most sensitive to temperature and therefore has the smallest force constant.

These results strongly indicate that solid-state NMR activation energies and atomic displacement parameters are related, thus indicating that solid-state NMR is a good method for studying the mobility of methyl groups in indomethacin and ibuprofen. Because solid-state NMR can be used to study pharmaceutical dosage forms and other

Table 22.6 Comparison of Activation Energies from Solid-State NMR and Slopes of Atomic Displacement Parameters from X-Ray for the Methyl-Carbon Atoms in Indomethacin

Carbon	Chemical Shift (ppm)	E_a (kJ/mol)[a]	Slope $\times 10^4$ ($Å^3 \cdot K^{-1}$)[b]
C17	13.8	8.0	2.12
C20	55.5	9.3	1.91

a Cauchon, 1992. *b* Toma, 1993.

mixtures (Saindon *et al.*, 1993), this powerful method will find increased application in the determination of the molecular mobility of drugs in mixtures and dosage forms.

22.4 Mobility and Reactivity of Solids

Molecular loosening was hypothesized by Paul and Curtin (1973) to be the first step in a solid-state reaction. In this first step, the molecules achieve enough molecular mobility to undergo the molecular change (bond making or breaking) required for the chemical reaction. This first step, molecular loosening or molecular mobility, could be the most important step in solid-state degradations. Thus, study of molecular mobility in crystals can provide important insights into their reactivity.

A significant body of research over the years has indicated that molecular mobility is required for the degradation of many pharmaceuticals. Pikal and co-workers (1977) and Oberholzer and Brenner (1979) showed that amorphous forms of pharmaceuticals were more reactive than their crystalline counterparts. In addition, Ahlneck and Zografi (1990) have suggested that water absorption enhances the molecular mobility of amorphous pharmaceutical solids, perhaps explaining the enhanced chemical reactivity of these materials in the presence of water.

Earlier, we hypothesized that desolvation preceded oxidation of steroids and dihydrophenylalanine derivatives, rendering them more reactive (Byrn and Lin, 1976; Byrn and Kessler, 1987; Byrn *et al.*, 1988). It is suggested that, in the case of steroids and dihydrophenylalanine, disordered or "amorphous" regions in the desolvated crystal can explain their enhanced reactivity. This concept explains why disordered regions or mobile functional groups (such as side chains) could be important factors in crystal stability. Additional studies of disordered regions in crystals are appropriate. However, further study of the relationship between molecular mobility and solid-state reactivity requires the development of new approaches. Determining the molecular mobility could help predict physical and chemical stability, especially in mixtures (*e.g.*, pharmaceutical dosage forms) where single-crystal X-ray methods cannot be used. During the next few years, additional studies of the relationship between molecular mobility and reactivity by solid-state NMR are expected.

22.5 Role of Defects in Solid-State Reactions

There are three major classifications of crystal defects in organic crystals: point defects (vacancies, interstitials, orientations, and substitutional); line defects (edge, slip, and screw dislocations); and surface defects (grain, tilt, and twist boundaries). Surface

defects may be a result of irregular crystal growth, mechanical stress (*e.g.*, grinding or milling), or thermal stress. See Tiller (1991), Mullin (1993), or Wright (1995) for additional reading.

Thomas and his group (Thomas and Williams, 1969; Thomas, 1970; Thomas *et al.*) have carried out extensive studies of the influence of crystal defects on solid-state reactions of inorganic compounds. They have also studied the influence of defects on the solid-state photochemical reactions of organic compounds, mainly involving the identification of three types of defects: the screw dislocation, the slip dislocation, and the orientation defect. These dislocations can bring molecules into different spatial orientations and create molecular cavities that differ from those in the bulk crystal. The objective of their studies was to explain the breakdown of the topochemical postulate (see Sections 15.4 and 19.1) in certain solid-state photochemical dimerizations. For example, the topochemical postulate predicts that the dimerization of 1,8-dichloro-9-methylanthracene should not take place because the molecules are too far apart, yet the *trans*-photodimer is produced exclusively.

Through their studies, Desvergne and co-workers (1974) demonstrated that the formation of the photodimer occurs at defects in the crystal. Thus, the molecules at these defects reoriente such that they are close enough to dimerize. For example, they hoped to show that the dimerization of 9-cyanoanthracene, which leads to the centrosymmetric photodimer rather than the mirror-symmetric photodimer predicted on the basis of the topochemical postulate, occurs at defects that bring the monomer into a centrosymmetric relationship with another monomer molecule. Both transmission electron microscopy and optical microscopy were used to study these reactions. In the electron microscopic procedure, single crystals are cleaved and one of the matched faces is irradiated while the other is **wet-etched**. The faces are then compared. In general, these studies show that photochemical reactions begin at defects (Thomas and Williams, 1969; Thomas, 1970; Thomas *et al.*, 1972; Desvergne, 1973; Sloan *et al.*, 1975; Jones and Williams, 1975). The topochemical postulate will still apply, but the products will be determined by the geometry at the screw or slip dislocation and not by the geometry in the bulk crystal (Thomas, 1972).

Reaction at dislocations could explain why 9-cyanoanthracene forms centrosymmetric photodimers rather than the mirror-symmetric dimers predicted from the bulk crystal structure. Unfortunately, it is difficult to prepare stable thin samples of this solid, so this explanation cannot be considered confirmed. In addition, it is important to realize that reaction at defects cannot occur unless photochemical energy is transferred to the defect site. If energy transfer is slow relative to the rate of reaction, then reaction will occur in the bulk crystal. If energy transfer is fast relative to the rate of reaction then the reaction will occur at defects, because defects often trap the energy. The 9-cyanoanthracene dimerization is apparently a defect-sensitive reaction, since the quantum yield of this reaction increases as the reaction proceeds. This idea is further confirmed by the fact that a small concentration of fluorescent dopants decreases the yield of dimers (Cohen *et al.*, 1971).

At orientation defects, the tenant molecule takes up an abnormal orientation. This defect is believed to occur in 1,5-dichloroanthracene, which when irradiated produced 20% of the head-to-tail dimer and 80% of the head-to-head dimer (Thomas, 1979).

In our laboratory, we have observed the effect of defects on dehydration reactions of crystal solvates. Three observations on different crystal hydrates illustrate the effect of defects on these solid $\longrightarrow$ solid + gas reactions. First, the temperature and time at

which a desolvation occurs is dependent upon defects. For example, individual crystals of cycloserine began to desolvate at very different times when heated at 50 °C. Apparently, the faster reacting crystals had defects that initiated the reaction. Second, mechanical defects produced by cutting the ends off the crystal greatly accelerated the reaction. For example, crystals of dihydrophenylalanine·¾H_2O lost water much more rapidly when the ends of the crystal were removed with a razor blade. Similar observations were made for 4-dichlorobenzene where mechanical defects initiated the phase transformation. Third, Perrier (1980) found that seeding unreacted crystals with desolvated powder in some cases accelerated the desolvation. For example, brushing the desolvated powder of cytosine hydrate onto the ends of single crystals of cytosine hydrate induced the reaction to begin on the ends of the crystal and move to the center. However, in other compounds this treatment had no effect.

In conclusion, it should be noted that defects can have important influences on the solid-state reactions of drugs. In particular, defects can determine when the reaction begins and in special cases possibly even determine the products of solid-state reactions.

22.6 Solid-State Stability of Protein Pharmaceuticals

There are a large number of protein products in early clinical trials as the result of the ability to produce proteins via recombinant DNA technology. These solids will be produced by either lyophillization or precipitation and in many cases will be amorphous or partially amorphous. As with other drug substances, there is a need to produce solid forms of proteins with consistant properties and to develop methods to characterize the solid-state properties of proteins.

The stability of protein pharmaceuticals presents special problems. A variety of chemical degradation reactions of proteins are known to occur in solution (Manning *et al.*, 1989). These include oxidation of sulfur-containing peptides to form sulfoxides or sulfones as shown in Figure 22.12 and deamidation of aspartyl and asparaginyl residues to form cyclic imides and isoaspartyl peptides as shown in Figure 22.13.

Other solution reactions include proteolysis, incorrect disulfide bond formation, racemization, and β-elimination. Furthermore, some proteins not only chemically degrade but also undergo denaturation during handling or storage, resulting in the formation of products which have different properties. Of these reactions, deamidation

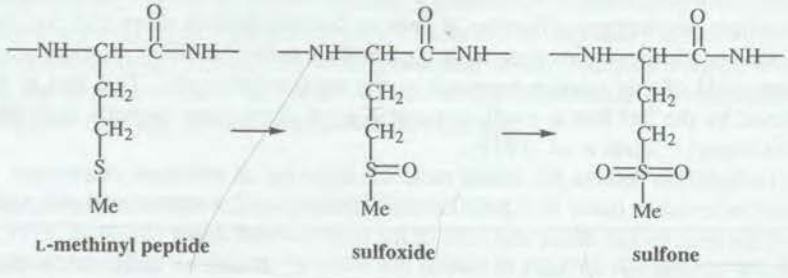

Figure 22.12 Reaction scheme for the oxidation of sulfur-containing peptides to sulfoxides or sulfones.

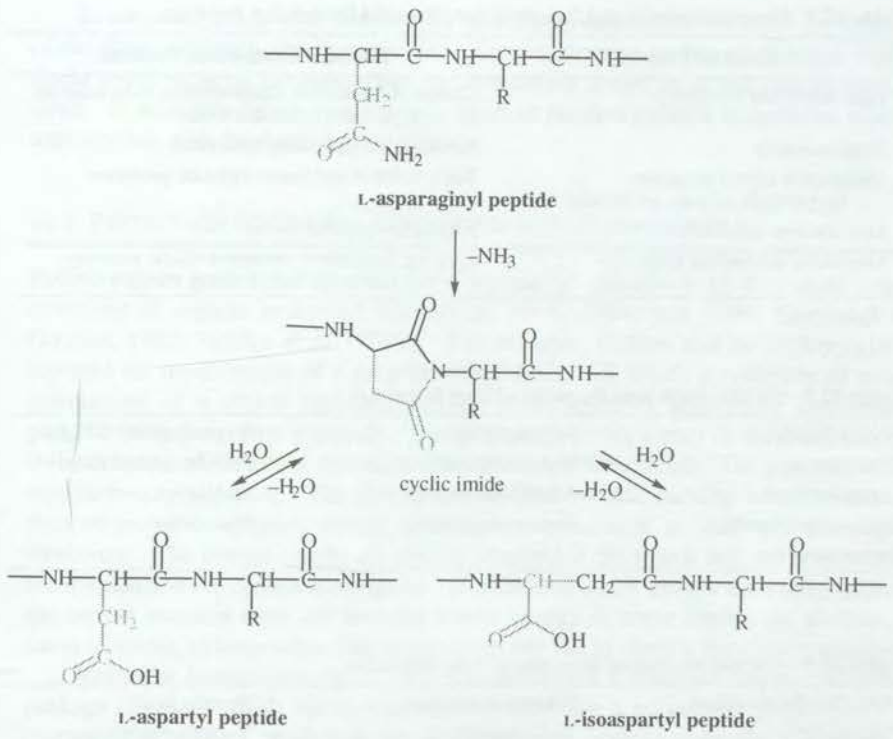

Figure 22.13 Deamidation reaction scheme of asparaginyl residues to form cyclic imides which hydrolize to aspartyl and and isoaspartyl peptides.

and oxidation are probably the most common reactions in the dry solid state. In solids which contain substantial moisture, all of the degradations described above can occur. Very little has been published on the solid-state degradation of proteins, making this an important area for additional research.

22.7 Particle Design and the Physics of Tablet Compaction

In recent years there has been growing interest in using solid-state chemistry to understand the reasons for tableting problems and to design and engineer particles and crystals with optimum tableting properties (Wray, 1992; York, 1992). Table 22.7 lists the undesirable material properties which often lead to compaction problems. To avoid these problems, materials without these properties need to be designed and synthesized.

Table 22.8 provides a list of the solid-state properties that vary from one drug to another and Table 22.9 lists the mechanical properties which are dependent on these solid-state properties. At present it is not possible to directly correlate a single solid-state property to a mechanical property; however, it is clear that variation in the solid-state properties of a substance will result in changes in mechanical properties of that substance. This is one of the reasons for the desire to consistently manufacture a drug substance with the same solid-state properties.

Table 22.7 Material Properties and their Associated Potential Compaction Problems

Material Property	Potential Compaction Problem
High strain rate sensitivity	Change of mechanical characteristics upon scale-up to high-speed tablet machines
Hygroscopicity	Handling and processing difficulties
Variation in crystal properties (polymorph, solvate, amorphous form)	Batch-to-batch and source variation problems
Low aqueous solubility	Inadequate drug dissolution
Unsuitable mechanical properties	Capping; lamination; excessive elastic recovery too high or too low crushing strength

York, 1992

Table 22.8 Variable Solid-State Properties of Drug Substances

Crystal density	Polymorphism	Hygroscopicity (RH_o)
Crystal habit	Hydrates/solvates	Particle size and shape
Crystal hardness	Amorphous material	Stability
Crystal order/disorder	Surface properties	Wettability
Crystal structure		

York, 1992

Table 22.9 Variable Mechanical Properties of Drug Substances

Brittle/ductile transitions	Indentation hardness	Poisson ratio
Fracture stress	Yield pressure	Young's modulus
Stress/strain relaxation	Deformation characteristics	

York, 1992

Table 22.10 Processing Stresses and Treatments Affecting Drug Substance Properties

Processing Stresses	Pretreatment of Drug Substance	Manufacturing Unit Operations
Temperature	Milling	Flow
Pressure	Crystallization	Milling
Mechanical	Precipitation	Drying
Exposure to liquids, gases, and vapors vapors	Freeze drying	Compression
		Coating

York, 1992

In addition, as discussed in several previous sections, there are several processing stresses that can be produced by unit operations (see Table 22.10). These stresses can affect the drug and in some cases even result in change of the crystal form of the drug or the production of an amorphous form. Obviously such changes will result in additional changes in the properties of the substance. Thus every effort should be made to find a method of processing the drug substance which does not result in changes of its properties.

In conclusion, it is clear that there is an intimate relationship between the structure of the drug substance and its properties. Careful attention to this relationship will no doubt avoid some of the compaction and processing problems which can be encountered. In addition, future research may result in the development of methods to engineer crystals with the desired properties.

22.8 Prediction of Crystal Structures and Polymorphs

Recently there have been reports of the successful calculation of theoretical crystal structures of organic molecules (Gavezzotti, 1991, 1994, and 1996; Karfunkel and Gdanitz, 1992; Holden *et al.*, 1993). For example, Holden and co-workers (1993) reported the development of a program called *MOLPAK* which investigates all unique orientations of a central molecule and the construction of appropriate coordination patterns about the central molecule. This program provides a map of the minimum unit cell volume as a function of the orientation of the central molecule. The program uses a repulsion-only potential. The five to ten smallest volume packing arrangements are then subjected to a lattice energy minimization refinement to yield possible crystal structures. The correct results are usually obtained if the search and refinement steps are restricted to the correct space group. If additional space groups are examined, then the correct structure does not have the lowest energy in some cases. In addition, in cases of strong hydrogen-bonding the program can fail to identify the correct structure.

Molecular Simulations Inc. (1997) has developed a materials science computing package (*Cerius*^{2}) which has several modules including a polymorph predictor. This module is capable of prediciting the polymorphs of organic molecules; however, its application to pharmaceutical problems is in its infancy. Nevertheless, the introduction of this program in an easy-to-use software package marks a milestone in the development of computational methods for the prediction and analysis of polymorphs and will probably lead to the eventual development of approaches to the *ab initio* prediction of polymorphs for other than small, rigid molecules.

The forerunner to the polymorph prediction software is described by Karfunkel and Gdanitz (1992), who reported a program which searches for the global crystal energy minimum. This program allows the investigation of crystal packing forces. They suggested that one published crystal structure was incorrect based on their calculations.

Approaches to the prediction of crystal structure and polymorphs are based on early work by Kitaigorodski and Gavezzotti (Kitaigorodskii and Mirskaya, 1972; Gavezzotti, 1991). Their work has laid the groundwork for these calculations by developing potential functions for use with crystals.

Gavezzotti used his *PROMET*3 program (1994), which allows for geometrical crystallography and symmetry relationships as input to generate polymorphic crystal structures, to investigate the conformational differences between two polymorphs of 7-dimethylaminocyclopenta[*c*]coumarin (Gavezzotti, 1996). Gavezzotti (1994) argues that it may never be possible to predict polymorphs and crystal structures *ab initio* because the errors in calculations of the heat of sublimation are of the same order of magnitude as the differences in energies of polymorphs. Furthermore, Gavezzotti has enumerated seven questions which must be answered in order to allow calculation of the crystal structure of an organic solid (Gavezzotti, 1994):

1. *Will the compound crystallize at all?* Just because a low energy solid is predicted, there is no assurance that experiments will lead to the formation of a crystal. As described above, many factors can influence the crystallization of the substance.
2. *Is the crystal high-melting?* The melting point of a solid is extremely difficult to predict due to entropic factors and the possiblility that the melt will be highly associated. Thus even the prediction of a crystal with a large heat of sublimation does not ensure a high melting point.
3. *What is the lattice energy (heat of sublimation)?* This is the parameter predicted by the polymorph prediction software and can be subject to relative large errors due to errors in parameter sets.
4. *Will the crystal structure be non-centrosymmetric?* Crystal structure predictions rely upon a knowledge of the symmetry of the crystal and can be greatly assisted by the initial choice of a unit cell. It is difficult to predict *ab initio* whether a solid will spontaneously resolve and produce non-centrosymmetric crystals.
5. *What will be the conformation of a flexible molecule in the crystal?* In some cases the crystal packing can alter the conformation of a solid. The prediction of crystal structures is dependent upon a knowledge of the molecular conformation and thus can be thwarted in such instances.
6. *What is the space group and the number of molecules per asymmetric unit?* It is extremely difficult to predict the space group of a crystal. Monte Carlo approaches are probably best in this case.
7. *What are the cell parameters?* In addition, to the space group, the cell parameters and resultant density are an important factor in crystal structure prediction and analysis.

Even with all of these questions and uncertainties, the order of calculated energies of polymorphs may be conserved thus making it possible to predict the order of stability of different polymorphs in at least some cases.

It should be noted that the program *Cerius*[2] (Molecular Simulations Inc., 1997) provides a **Rietveld** module to refine any proposed crystal structure of a substance from its powder-diffraction pattern. This program, in combination with high-resolution powder-diffraction data, has potential to solve structures of low-molecular weight drugs for which good single crystals cannot be obtained (Gavezzotti, 1994; Karfunkel and Gdanitz, 1992).

22.9 Atomic Force Microscopy (AFM)

Atomic force microscopy is a powerful new technique for studying solid-state reactions (Frommer, 1992; Kaupp, 1992a–c). This technique provides Ångstrom-scale images of reacting crystals, providing new insight into solid-state reactions. Using this method, Kaupp has studied the photodimerizations of cinnamic acids (Kaupp, 1992a) and anthracenes (Kaupp, 1992b) and suggested that the phase transitions in the surface regions of the crystal are of foremost importance in the reaction. In fact, he suggested that the photodimerization of cinnamic acids involved a surface reaction with considerable mass transport to the active site. In this regard, it is interesting to note that Enkel-

mann and co-workers (1993) have recently reported that a single-crystal to single-crystal photodimerization of cinnamic acid can be accomplished by irradiating the crystal at a wavelength corresponding to the chromophore's absorption tail. It is interesting to speculate whether the mechanism of the dimerization of cinnamic acid is different depending upon the wavelength of irradiation.

Kaupp (1992c) has also studied solid-gas reactions using AFM and has suggested that these studies provide new insight into the mechanisms of these reactions and, in particular, how the product phases build up.

AFM has also been used to probe the surface structure of crystals and determine whether the structure on the surface is different from the bulk structure as determined by single crystal X-ray methods (Overney *et al.*, 1992). For example, the surface of pyrene crystals consists of monomers while the bulk consists of dimer pairs. In contrast, the AFM of tetracene showed that the intermolecular spacings on the crystal surface correspond to those in the bulk crystal.

22.10 Regulatory Aspects of the Solid-State Chemistry of Drugs

Interest in this subject stems in part from the Food and Drug Administration's (FDA) drug substance guideline that states "appropriate" analytical procedures should be used to detect polymorphic, solvated (including hydrated), or amorphous forms of the drug substance. The guideline also states that it is the applicant's responsibility to control the crystal form of the drug substance and, if bioavailabilty is affected, to demonstrate the suitability of the control methods. This highlights the importance of controlling the crystal form of the drug substance.

While it is clear that the New Drug Application (NDA) should contain information on solid-state properties, particularly when bioavailability is an issue, an applicant may be unsure how to scientifically approach the gathering of information and even what kind of information is needed. This section is intended to provide a strategic approach to remove much of this uncertainty by presenting concepts and ideas in the form of decision trees rather than a list of guidelines or regulations (Byrn *et al.*, 1995). This is especially important because each individual compound has its own peculiarities which require flexibility in approach. The studies proposed herein are part of the Investigational New Drug (IND) process.

As pointed out in this book, solid drug substances display a wide and largely unpredictable variety of solid-state properties. Nevertheless, application of basic physicochemical principles combined with appropriate analytical methodology can provide a strategy for scientific and regulatory decisions related to solid-state behavior in the majority of cases. By addressing *fundamental* questions about solid-state behavior at an early stage of drug development, both the applicant and the FDA are in a better position to assess the possible effects of any variations in the solid-state properties of the drug substance. The resulting early interaction of the parties with regard to these fundamental questions would not only tend to ensure uniformity of the materials used throughout the clinical trials but also would virtually resolve solid-state issues before the critical stages of drug development. A further benefit of these scientific studies is the development of a meaningful set of solid-state specifications which critically describe the solid form of the drug substance. These specifications also facilitate the approval of a change in supplier or chemical process.

We suggest a series of decision trees for collecting data on a drug substance that will efficiently answer specific questions about solid-state behavior in a logical order. In "difficult" cases, perhaps where mixtures of forms must be dealt with or other unusual properties are encountered, the decision trees should still be followed as a first stage in the investigation.

Decision trees provide a conceptual framework for understanding how the justification for different crystal forms might be presented in the drug application. Industry may wish to use these decision trees as a strategic tool to organize the gathering of information early in the drug development process. Put another way, these decision trees provide a thought process that will lead to development of the most appropriate analytical controls. Since it is the responsibility of the industry to select the appropriate test or tests to identify the phase of the solid and determine its relevant pharmaceutical properties, this approach is superior to simply performing a broad range of tests without regard to their relevance.

We have chosen to present this approach in the form of a series of decision trees, one for each of the most common solid-state forms. The charts are accompanied by examples from the literature representing the kind of data that would be useful in supporting the various decisions.

We should point out that, from a regulatory standpoint, if a company can establish a specification or test to ensure production of a well defined solid form of the drug substance, then it is not necessary to do all of the physical and chemical testing outlined in the decision trees. From a scientific standpoint, however, such an approach is risky since new forms may appear unpredictably during various stages of the development process. The appearance of these new forms usually slows the drug approval process and makes planning difficult.

Four decision trees are described in the sub-sections that follow:

a. polymorphs
b. solvates (including hydrates)
c. desolvated solvates
d. amorphous forms

All of the decision trees end (*e.g.*, Figure 22.14) with an indication of the types of controls which will be required based on whether a single morphic form or a mixture will be produced as the drug substance. Although this ending provides a simplified view of a very complicated process of selecting appropriate controls, it is included to illustrate the consequence of the decisions made with regard to the drug substance. The reader should realize that the actual selection of the appropriate control could be the subject of another review which might contain another set of decision trees.

In addition, when using the decision trees, one should bear in mind that for some solids a combination of trees or even all four trees will have to be used to completely characterize all of the materials.

A. Polymorphs

The decision tree for polymorphs is shown in Figure 22.14. It outlines investigations of the formation of polymorphs, the analytical tests available for identifying polymorphs, studies of the physical properties of polymorphs, and the controls needed to

ensure the integrity of a drug substance containing either a single morphic form or a mixture.

The first step in the polymorphs decision tree is to crystallize the substance from a number of different solvents in order to attempt to answer the question: Are polymorphs possible? Solvents should include those used in the final crystallization steps and those used during formulation and processing and may also include water, methanol, ethanol, propanol, isopropanol, acetone, acetonitrile, ethyl acetate, hexane and mixtures if appropriate. The solids produced are analyzed using X-ray diffraction and at least one of the other methods. In these analyses, care must be taken to show that the method of sample preparation (*i.e.*, drying, grinding) has not affected the solid form. If the analyses show that the solids obtained are identical (*e.g.*, have the same X-ray diffraction patterns and IR spectra) then the answer to the question "Are polymorphs possible?" is probably "No," and further research may not be needed.

If polymorphs exist then it is necessary to examine those physical properties of the different polymorphs that can affect dosage form performance (bioavailability and stability) or manufacturing reproducibility. The properties of interest are solubility profile (intrinsic dissolution rate, equilibrium solubility), stability (chemical and physical), crystal morphology (including both shape and particle size), calorimetric behavior, and percent relative humidity profile. If there are no discernible differences between these physico-chemical properties, then the answer to the second question in the decision tree, "Different physical properties?" is "No."

An important question lies in the properties that differ among polymorphs and whether those properties affect the dosage form performance (*i.e.*, quality or bioavailability). If they do, then from a regulatory standpoint it is appropriate to establish a specification or test (*e.g.*, X-ray powder diffraction or IR) to ensure the proper form is produced. From a production standpoint, it is important to develop a process that reproducibly gives the desired polymorph.

If mixtures of forms cannot be avoided, then quantitative control is needed to ensure that a fixed proportion of forms is obtained. Furthermore, the method of analyzing for the proportion of forms would have to be validated. Also, the proportion of forms would have to remain within stated limits through the retest date of the drug substance and potentially throughout the shelf life of the product—a difficult requirement if the forms interconvert. Thus, the way to avoid a substantial amount of work in this area is to select a single solid form for production. Usually, this would be the most physically stable form when whose bioavailabilities are not significantly different. Selection of the most stable form would, of course, insure that there would be no conversion into other forms.

Powder diffraction is often a useful method to determine the percentages of polymorphs in a mixture; however, as discussed above, the detection limit is variable from case to case and can be as high as 15% or as low as 0.5% or perhaps lower (Matsuda and Tatsumi, 1990; Tanninen and Yliruusi, 1992).

In cases where stability or bioavailability issues exist, the solid form present in the drug product should be investigated, if possible. As discussed above, solid-state NMR appears to be the best method for the study of the drug substance in the dosage form (Bugay, 1993; Saindon *et al.*, 1993). In some cases, solid-state NMR analysis is possible even though tablets contain approximately 95 mg of excipients and 5 mg of drug. There are numerous cases, often involving complex mixtures or low dose

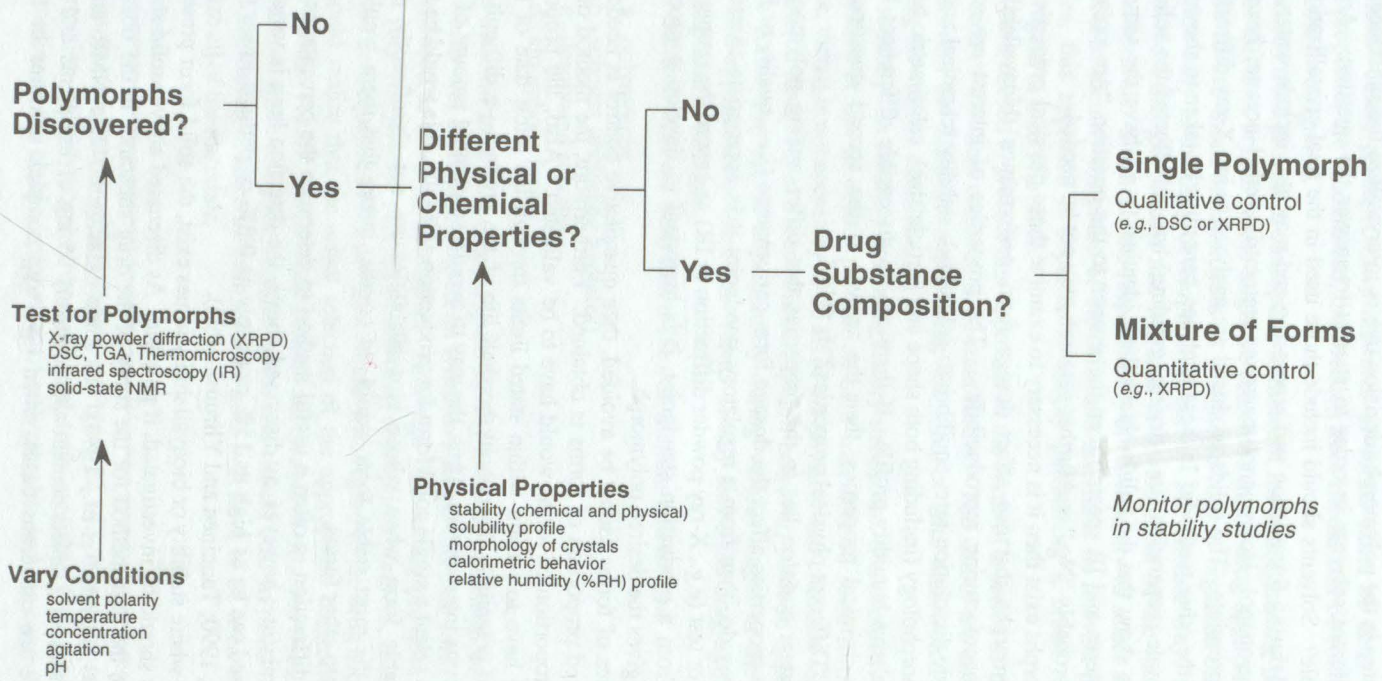

Figure 22.14 Decision tree for polymorphs.

products, where solid-state NMR (and in fact any technique) will not be sensitive enough to identify the polymorph present in the drug product. However, safety and efficacy are, of course, independently controlled by the potency assays and by the physical tests (*e.g.*, dissolution).

B. Solvates (Including Hydrates)

The decision tree for solvates and hydrates (where water is the solvate) is shown in Figure 22.15. It outlines investigations of the formation of solvates, the analytical tests available for solvates, studies of the physical properties of solvates and the controls needed to ensure the integrity of drug substance containing either a single morphic form or a mixture.

The decision tree for solvates is applied after the preliminary crystallizations have been completed. These are essentially the same as in the polymorph decision tree but, in addition, should include solvent-water mixtures in order to maximize the chance for solvate formation. These experiments can be guided by moisture uptake (percent relative humidity) studies. Any solids that indicate a significant change in water content as indicated by the percent relative humidity–moisture profile should also be examined. The resulting solid phases are preferably characterized by a combination of methods—two for phase identity and two to reveal composition and stoichiometry.

With very few exceptions, the structural solvent contained in marketed crystalline drug products is water. It is nevertheless desirable to characterize other solvated crystalline forms of a drug for several reasons: they may be the penultimate form used to crystallize the final product and thus require controlled characterization; they may form if the final crystallization from solvents, especially mixed solvents, is not well controlled; they may be the actual crystallized form of a final product that is desolvated during a final drying step; they may be the form used in recovery for subsequent rework. The relevance of these points will vary from case to case, but for the present discussion we shall treat the subject of solvates in its broadest form.

The physical properties of solvates are often quite different from the anhydrate form. For this reason it is important to characterize the physical properties described in the decision tree. As with polymorphs, a number of methods are useful for the characterization of solvates. Of course, for hydrates the percent relative-humidity profile is particularly important. These methods are listed in the decision tree.

Another important area is the analysis of the material produced after wet granulation of a substance which can form hydrates. We are aware of cases where the bulk drug substance is manufactured and stored as the anhydrate. However, upon wet granulation, there is a conversion (either partial or complete) to a hydrate. Subsequent drying is sometimes not adequate to convert the substance back to the anhydrate, and a hydrate or a mixture of hydrate and anhydrate remains. The formation of a hydrate and its subsequent drying can result in a change in particle size of the drug substance (Himuro *et al.*, 1971).

The manufacturing process of a drug product may include wet granulation or a processing step that will subject the drug substance even to a brief change in temperature and pressure (*e.g.*, milling or compression). In this event, extensive preliminary studies concerning the ability of the drug substance to convert to a new crystal form must be carried out in the laboratory by mimicking these processing steps.

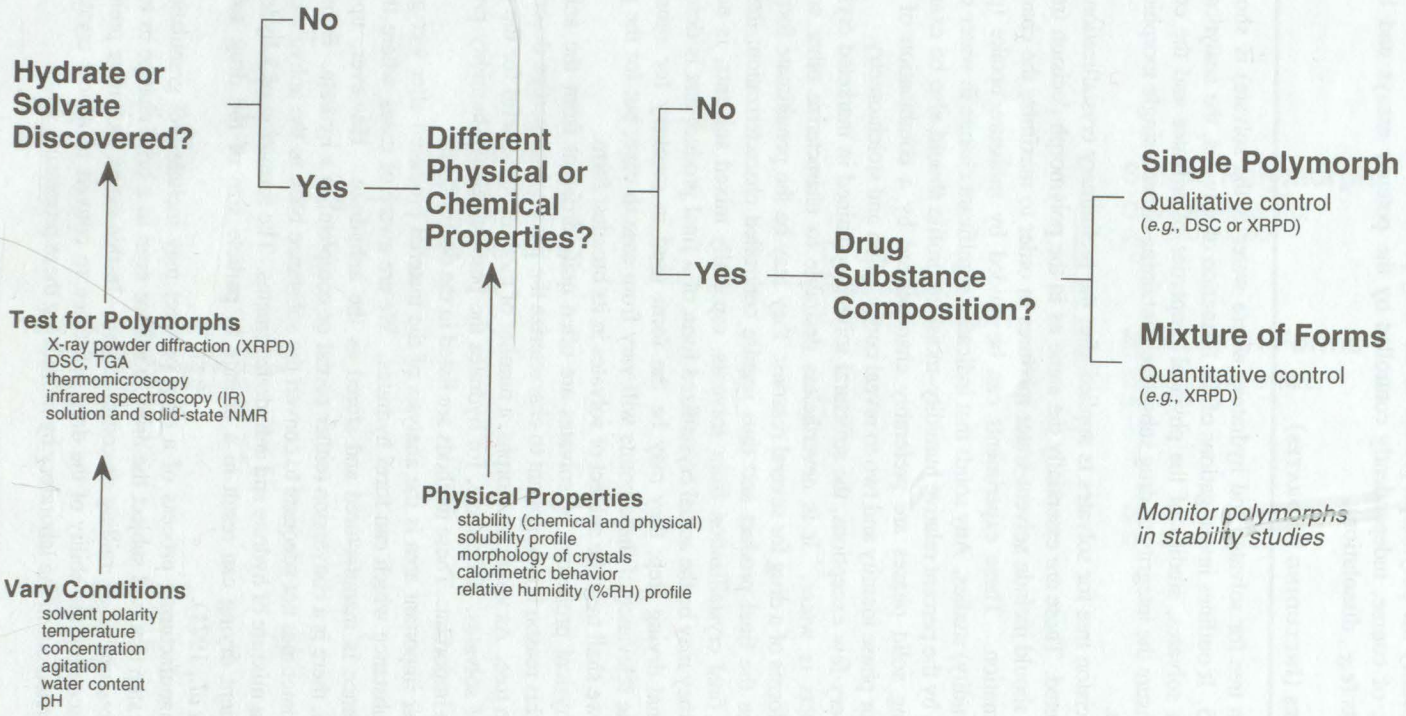

Figure 22.15 Decision tree for solvates (including hydrates).

C. Desolvated Solvates

Desolvated solvates are compounds that crystallize as solvates but undergo desolvation prior to analysis. Often these desolvated solvates retain the structure of the solvate with relatively small changes in the lattice parameters and atomic coordinates, but no longer contain the solvent. In addition, desolvated solvates are apt to be less ordered that their crystalline counterparts. These forms are particularly difficult to characterize properly since analytical studies indicate that they are unsolvated materials (anhydrous crystal forms) when, in fact, they have the structure of the solvated crystal form from which they were derived. Several observations may give clues that one is dealing with a desolvated form:

a. the form can be obtained from only one solvent
b. on heating, the form converts to a structure known to be unsolvated
c. the form has a particularly low density compared to other forms of the same substance

Experiments that help to clarify whether an apparently solvent-free modification is a desolvated form or a true anhydrate include:

a. single-crystal X-ray structure determination in the presence of mother liquor from the crystallization
b. comparison of the X-ray powder diffraction patterns and solid-state NMR spectra of the solvated and desolvated crystal forms
c. determination of the vapor pressure isotherm by varying the vapor pressure of the specific solvent involved

A desolvated form will often take up stoichiometric amounts of the relevant solvent. In addition, crystals of the form directly isolated from the crystallizing medium will show a plateau in their isotherm as the vapor pressure of the solvent is reduced.

Figure 22.16 shows the decision tree used to address regulatory issues involving desolvated solvates. It is similar to the polymorphs decision tree except that the first question involves determining whether a solvate was formed initially and then desolvated, perhaps by "air drying." The remaining questions are identical to the polymorphs decision tree.

D. Amorphous Forms

Amorphous forms are of substantial interest because they usually are much more soluble than their crystalline counterparts. Indeed, there are cases where the amorphous form is the only solid form that has adequate bioavailability. The initial question with this decision tree (Figure 22.17) is similar to the previous ones: Are amorphous forms possible? Amorphous forms can be prepared in different ways, for example, by spray drying or by freeze drying. One can test whether an amorphous form has been produced by using one of the methods listed.

The next question on the decision tree is whether the amorphous forms have different physical properties. The answer to this question will almost certainly be yes. Three differences from crystalline forms may generally be expected for amorphous forms:

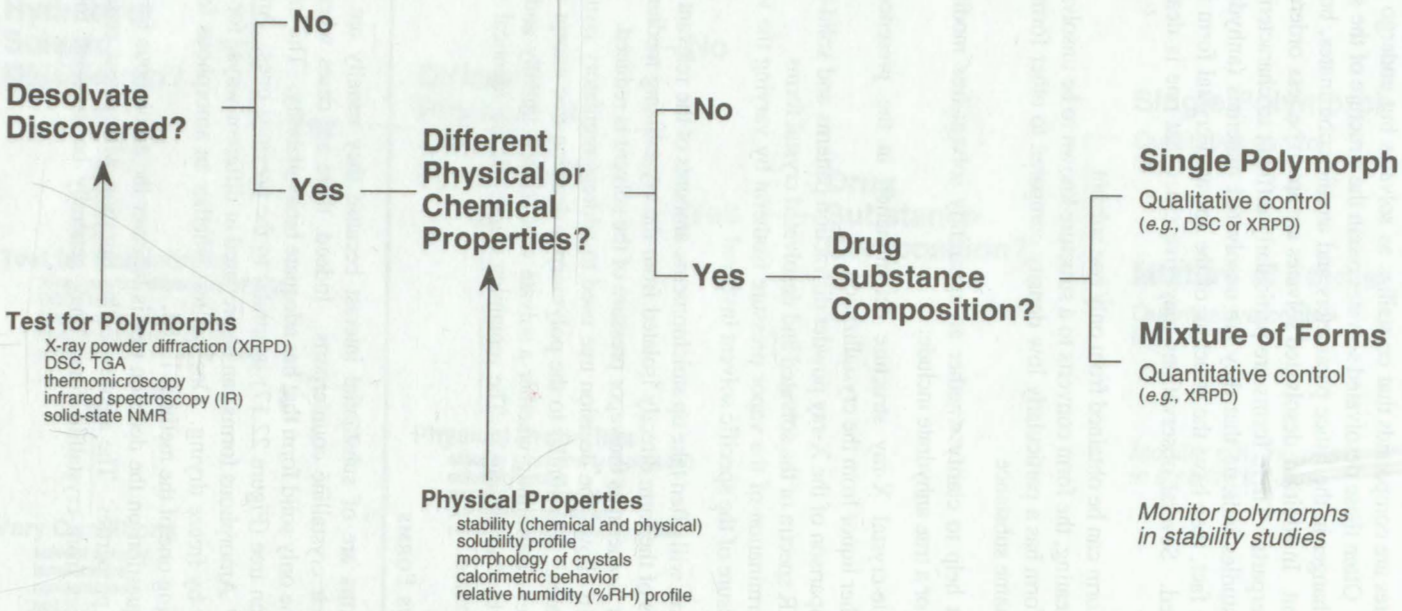

Figure 22.16 Decision tree for desolvates.

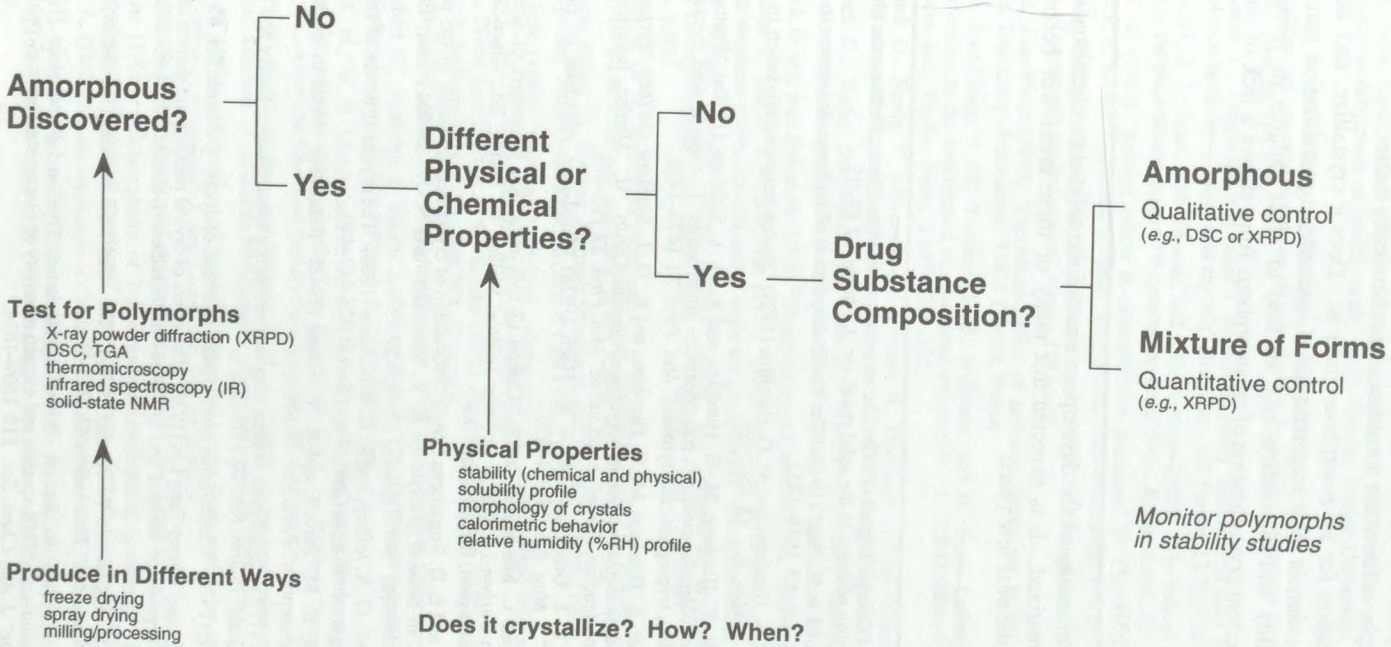

Figure 22.17 Decision tree for amorphous solids.

a. amorphous forms have greater solubility
b. amorphous forms take up water more extensively
c. amorphous forms are sometimes less chemically stable

Another key question for an amorphous form is: Does it crystallize, and how and when? This question is very important since inadvertent crystallization can greatly affect the solubility and dissolution rate, or lead to other failures in formulation. Moreover, inadvertent crystallization of an amorphous from shows a lack of control of the material.

22.11 CONCLUSION

In this last chapter, many of the developing areas of the solid-state chemistry of drugs have been summarized. It is expected that many of these areas will become fully developed over the next few years.

REFERENCES

Ahlneck, Claes and George Zografi (1990) "The molecular basis of moisture effects on the physical and chemical stability of drugs in the solid state" *Int. J. Pharm.* **62** 87–95.

Anchel, Marjorie and A. H. Blatt (1948) "The cyclic dehydration of biphenyl derivatives to fluorenes" *J. Am. Chem. Soc.* **63** 1948–1952.

Andrew, E. R., W. S. Hinshaw, and M. G. Hutchins (1974) "Proton magnetic relaxation in crystalline amino acids" *J. Mag. Res.* **15** 196–200.

Andrew, E. R., W. S. Hinshaw, M. G. Hutchins, and R. O. I. Sjöblom (1976a) "Proton magnetic relaxation and molecular motion in polycrystalline amino acids. I. Aspartic acid, cystine, glycine, histidine, serine, tryptophan, and tyrosine" *Mol. Phys.* **31** 1479–1488.

Andrew, E. R., W. S. Hinshaw, M. G. Hutchins, and R. O. I. Sjöblom (1976b) "Proton magnetic relaxation and molecular motion in polycrystalline amino acids. II. Alanine, isoleucine, leucine, methionine, norleucine, threonine and valine" *Mol. Phys.* **32** 795–806.

Andrew, E. R., T. J. Green, and M. J. R. Hoch (1978) "Solid-state relaxation of biomolecular components" *J. Mag. Res.* **29** 331–339.

Axelson, D. E. and L. Mandelkern (1979) "Carbon-13 spin relaxation parameters of semicrystalline polymers" in *Carbon-13 NMR in Polymer Science*; Wallace M. Pasika, Ed.; American Chemical Society: Washington, DC, Chapter 10.

Belyustin, A. V. and É. D. Rogacheva (1966) "Production of crystallization nuclei in the presence of a seed crystal" in *Growth of Crystals*; A. V. Shubnikov and N. N. Sheftal´, Eds.; Engl. Trans.; Consultants Bureau: New York, NY; Vol. 4, pp 3–5.

Berman, Helen M., G. A. Jeffrey, and R. D. Rosenstein (1968) "The crystal structure of the α'- and β-forms of D-mannitol" *Acta Crystallogr., Sect B* **B24** 442–449.

Bloembergen, N, E. M. Purcell, and R. V. Pound (1948) "Relaxation effects in nuclear magnetic resonance absorption" *Phys. Rev.* **73** 679–712.

Bugay, David E. (1993) "Solid-state nuclear magnetic resonance spectroscopy: theory and pharmaceutical applications" *Pharm. Res.* **10** 317–327.

Byrn, Stephen R. (1976) "Mechanisms of solid-state reactions of drugs" *J. Pharm. Sci.* **65** 1–22.

Byrn, Stephen R., and Chung-Tang Lin (1976) "The effect of crystal packing and defects on desolvation of hydrate crystals of caffeine and L-(–)-1,4-cyclohexadiene-1-alanine" *J. Am. Chem. Soc.* **98** 4004–4005.

Byrn, Stephen R. and Donald W. Kessler (1987) "The solid state reactivity of the crystal forms of hydrocortisone esters" *Tetrahedron* **43** 1335-43.

Byrn, Stephen R., Paul A. Sutton, Brian Tobias, James Frye, and Peter Main (1988) "Crystal structure, solid-state NMR spectra, and oxygen reactivity of five crystal forms of prednisolone *tert*-butylacetate" *J. Am. Chem. Soc.* **110** 1609–1614.

Byrn, Stephen, Ralph Pfeiffer, Michael Ganey, Charles Hoiberg, and Guirag Poochikian (1995) "Pharmaceutical solids: a strategic approach to regulatory considerations" *Pharm. Res.* **12** 945–954.

Cauchon, Nina Sipahimalani (1992) "Solid-state carbon-13 NMR studies of pharmaceuticals and chemical modifications of nucleic acids" Ph.D. Thesis; Purdue University: West Lafayette, IN 47907-1333.

Cholli, A. L., W. M. Ritchey, J. L. Koenig, and W. S. Veeman (1988) "Separation of components in crystalline and amorphous regions of polyethylene by solid state carbon-13 NMR spectroscopy" *Spectr. Lett.* **21** 519–531.

Chow, Kwok Y., Joseph Go, and David J. W. Grant (1986) "Influence of fatty acid additives on the dissolution behavior of adipic acid crystals" *Drug Dev. Ind. Pharm.* **12** 247–264.

Cohen, M. D., Z. Ludmer, J. M. Thomas, and J. O. Williams (1971) "The role of structural imperfections in the photodimerization of 9-cyanoanthracene" *Proc. R. Soc. Lond., Ser. A* **324** 459–468.

Davey, R. J. (1982) "Solvent effects in crystallization processes" in *Current Topics in Materials Science*; E. Kaldis, Ed.; North-Holland: Amsterdam, The Netherlands; Vol. 8, Chapter 6.

Davoll, John, George B. Brown, and Donald W. Visser (1952) "An unusual transformation of isomeric forms of tetraacetyl-D-ribofuranose" *Nature* **170** 64–65.

Desvergne, Jean-Pierre (1973) "Photodimerization of aromatic derivatives in the solid state" Ph.D. Thesis, University of Bordeaux: 33405 Talence, France

Desvergne, Jean-Pierre, J. M. Thomas, J. O. Williams, and H. Bouas-Laurent (1974) "Role of imperfections in the dimerization of substituted anthracenes. I. 1,8-Dichloro-9-methylanthracene" *J. Chem. Soc., Perkin Trans. 2* **1974** 363–368.

Dunitz, Jack D., Emily F. Maverick, and Kenneth N. Trueblood (1988a) "Atomic movements in molecular crystals from diffraction measurements" *Angew. Chem. Int. Ed. Engl.* **27** 880–895.

Dunitz, Jack D., Verner Schomaker, and Kenneth N. Trueblood (1988b) "Interpretation of atomic displacement parameters from diffraction studies of crystals" *J. Phys. Chem.* **92** 856–867.

Dunitz, Jack D. and Joel Bernstein (1995) "Disappearing polymorphs" *Acc. Chem. Res.* **28** 193–200.

Earl, William L. and D. L. VanderHart (1979) "Observations in solid polyethylenes by carbon-13 nuclear magnetic resonance with magic angle sample spinning" *Macromolecules* **12** 762–767.

Enkelmann, Volker, Gerhard Wegner, Kathleen Novak, and Kenneth B. Wagener (1993) "Single-crystal-to-single-crystal photodimerization of cinnamic acid" *J. Amer. Chem. Soc.* **115** 10390–10391.

Fletcher, Hewitt G. Jr., Robert K. Ness, and C. S. Hudson (1951) "The reaction of tribenzoyl-α-D-lyxopyranosyl bromide and methanol" *J. Am. Chem. Soc.* **73** 3698–3699.

Freer, Andrew, Jillian M. Bunyan, Norman Shankland, and David B. Sheen (1993) "Structure of (*S*)-(+)-ibuprofen" *Acta Crystallogr., Section C* **C49** 1378–1380.

Frommer, Jane (1992) "Scanning tunnelling microscopy and atomic force microscopy in organic chemistry" *Angew. Chem. Int. Ed. Engl.* **31** 1298–1328.

Fukushima, Eiichi and Stephen B. W. Roeder (1981) *Experimental Pulse NMR: A Nuts and Bolts Approach*; Addison-Wesley: Reading, MA; Chapter 4.

Fyfe, Colin A. (1983) *Solid State NMR for Chemists*; CFC Press: Guelph, Ontario; pp 36–46.

Galante, Robert N., Anthony J. Visalli and Dahyabhai M. Patel (1979) "Solid-state acetylation of codeine phosphate by aspirin" *J. Pharm. Sci.* **68** 1494–1498.

Garroway, A. N., W. B. Moniz, and H. A. Resing (1979) "Carbon-13 NMR in organic solids: the potential for polymer characterization" in *Carbon-13 NMR in Polymer Science*; Wallace M. Pasika, Ed.; American Chemical Society: Washington, DC, Chapter 4.

Garroway, A. N., W. M. Ritchey, and William B. Moniz (1982) "Some molecular motions in epoxy polymers: a carbon-13 solid-state NMR study" *Macromolecules* **15** 1051–1063.

Gavezzotti, A. (1991) "Generation of possible crystal structures from molecular structure for low-polarity organic compounds" *J. Am. Chem. Soc.* **113** 4622–4629.

Gavezzotti, Angelo (1994) "Are crystal structures predictable?" *Acc. Chem. Res.* **27** 309–314.

Gavezzotti, A. (1996) "Polymorphism of 7-dimethylaminocyclopenta[*c*]coumarin: packing analysis and generation of trial crystal structures" *Acta Crystallogr., Sect. B, Struct. Sci.* **B52** 201–208.

Girifalco, L. A. (1964) *Atomic Migration in Crystals*; Blaisdell: New York, NY.

Grant, David J. W. and Peter York (1986) "A disruption index for quantifying the solid state disorder induced by additives or impurities. II. Evaluation from heat of solution" *Int. J. Pharm.* **28** 103–112.

Griesser, U. J. and A. Burger (1995) "The effect of water vapor pressure on desolvation kinetics of caffeine ⅔-hydrate" *Int. J. Pharm.* **120** 83–93.

Hauffe, Karl (1955) *Reactionen in und an Festen Stoffen*; Springer-Verlag: Berlin, Germany; Chapter 5.

Himuro, Ikuzo, Yoji Tsuda, Keiji Sekiguchi, Isamu Horikoshi, and Motoko Kanke (1971) "Studies on the method of size reduction of medicinal compounds. IV. Solvate formation of chloramphenicol and its application to size reduction" *Chem. Pharm. Bull.* **19** 1034–1040.

Holden, James R., Zuyue Du, and Herman L. Ammon (1993) "Prediction of possible crystal structures from C-, H-, N-, O-, and F-containing organic compounds" *J. Comput. Chem.* **14** 422–437.

Iitaka, Yoichi (1960) "The crystal structure of β-glycine" *Acta Crystallogr.* **13** 35–45.

Iitaka, Yoichi (1961) "The crystal structure of γ-glycine" *Acta Crystallogr.* **14** 1–10.

Imashiro, Fumio, Kiyonori Takegoshi, Sachiko Okazawa, Jun Furukawa, Takehiko Terao, A. Saika, and Asako Kawamori (1983) "NMR study of molecular motions in perisubstituted naphthalenes" *J. Chem. Phys.* **78** 1104–1111.

Jacewicz, Victor W. and John H. C. Nayler (1979) "Can metastable crystal forms disappear?" *J. Appl. Crystallogr.* **12** 396–397.

Johnson, Carroll K. (1976) *ORTEP-II: A FORTRAN Thermal-Ellipsoid Plot Program for Crystal Structure Illustrations*; Oak Ridge National Laboratory: Oak Ridge, TN.

Jones, William, and John O. Williams (1975) "Real space crystallography and defects in molecular crystals" *J. Mater. Sci.* **10** 379–386.

Jost, W. (1960) *Diffusion in Solids, Liquids, and Gases*, Physical Chemistry Monographs; Academic: New York, NY; Vol. 1.

Kaneniwa, Nobuyoshi, Makoto Otsuka, and Tetsuo Hayashi (1985) "Physiochemical characterization of indomethacin polymorphs and the transformation kinetics in ethanol" *Chem. Pharm. Bull.* **33** 3447–3455.

Kararli, Tugrul T., Thomas E. Needham, Clifford J. Seul, and Pat M. Finnegan (1989) "Solid-state interaction of magnesium oxide and ibuprofen to form a salt" *Pharm. Res.* **6** 804–808.

Karfunkel, H. R. and R. J. Gdanitz (1992) "*Ab initio* prediction of possible crystal structures for general organic molecules" *J. Comput. Chem.* **13** 1171–1183.

Kaupp, Gerd (1992a) "Photodimerization of cinnamic acid in the solid state: new insights on application of atomic force microscopy" *Angew. Chem. Int. Ed. Engl.* **31** 592–595.

Kaupp, Gerd (1992b) "Photodimerization of anthracenes in the solid state: new results from atomic force microscopy" *Angew. Chem. Int. Ed. Engl.* **31** 595–598.

Kaupp, Gerd (1992c) "Atomic force microscopy in organic gas/solid reactions: how do the new phases build up?" *Mol. Cryst. Liq. Cryst. Sci. Technol., Sect. A.* **211** 1–15.

Kellens, M., W. Meeussen, and H. Reynaers (1992) "Study of the polymorphism and the crystallization kinetics of tripalmitin: a microscopic approach" *J. Amer. Oil Chem. Soc.* **69** 906–911.

Kessler, Donald W. (1986) "Polymorphs of hydrocortisone-21-esters: their characterization and solid state reactivity" Ph.D. Thesis; Purdue University: West Lafayette, IN 47907-1333.

Kitaigorodskii, A. I. and K. V. Mirskaya (1972) "Prediction of the structure of an organic crystal" *Mater. Res. Bull.* **7** 1271–1280.

Kitamaru, Ryozo, Fumitaka Horii, and Kouichi Murayama (1986) "Phase structure of lamellar crystalline polyethylene by solid-state high-resolution ^{13}C NMR: detection of the crystalline–amorphous interphase" *Macromolecules* **19** 636–643.

Kitamura, M. (1989) "Polymorphism in the crystallization of L-glutamic acid" *J. Cryst. Growth* **96** 541–546.

Kondepudi, Dilip K., Rebecca J. Kaufman, and Nolini Singh (1990) "Chiral symmetry breaking in sodium chlorate crystallization" *Science* **250** 975–976.

Kvick, Åke, W. Michael Canning, Thomas F. Koetzle, and Graheme J. B. Williams (1980) "An experimental study of the influence of temperature on a hydrogen-bonded system: the crystal structure of γ-glycine at 83 K and 298 K by neutron diffraction" *Acta Crystallogr., Sect. B, Struct. Sci.* **B36** 115–120.

Lin, Chung-Tang, Pik-Yen Siew, and Stephen R. Byrn (1978) "Solid-state dehydrochlorination and decarboxylation reactions. II. Reactions of three crystal habits of *p*-aminosalicylic acid hydrochloride and the crystal structure of *p*-aminosalicylic acid hydrochloride" *J. Chem. Soc., Perkin Trans. 2* **1978** 963–968.

Lin, Shan-Yang (1992) "Isolation and solid-state characteristics of a new crystal form of indomethacin" *J. Pharm. Sci.* **81** 572–576.

Lyerla, J. R. (1979) "High resolution carbon-13 NMR studies of bulk polymers" in *Contemporary Topics in Polymer Science*; Mitchel Shen, Ed.; Plenum: New York; Vol. 3, pp 143–213.

Manning, Mark C., Kamlesh Patel, and Ronald T. Borchardt (1989) "Stability of protein pharmaceuticals" *Pharm. Res.* **6** 903–918.

Matsuda, Yoshihisa and Etsuko Tatsumi (1990) "Physicochemical characterization of furosemide modifications" *Int. J. Pharm.* **60** 11–26.

McClure, J. and B. M. Craven (1973) "New investigations of cytosine and its monohydrate" *Acta Crystallogr., Sect. B, Struct. Sci.* **B29** 1234–1238.

McConnell, J. F. (1974) "2-(4-Isobutylphenyl)propionic acid. $C_{13}H_{18}O_2$ Ibuprofen or prufen" *Cryst. Struct. Comm.* **3** 73–75.

Menger, Egbert M., Wiebren S. Veeman, and Engbert de Boer (1982) "Carbon-13 spin-lattice relaxation in solid poly(oxymethylene)" *Macromolecules* **15** 1406–1411.

Molecular Simulations, Inc. (1997) *Cerius*^{2} 9685 Scranton Road, San Diego, CA 92121–3752.

Mullin, J. W. and C. L. Leci (1972) "Desupersaturation of seeded citric acid solutions in a stirred vessel," in *Crystallization from Solution: Nucleation Phenomena in Growing Crystal Systems*, Joseph Estrin, Ed.; AIChE Symposium Series No 121, Vol. 68; American Institute of Chemical Engineers: New York, NY; pp 8–20.

Mullin, J. W. (1993) *Crystallization*; 3rd ed.; Butterworth-Heinemann: Oxford, UK; pp 24–27.

Naito, A., S. Ganapathy, K. Akasaka, and C. A. McDowell (1983) "Spin-relaxation of carbon-13 solid amino acids using the CP-MAS technique" *J. Mag. Reson.* **54** 226–235.

Nass, Kathryn K. (1991) "Process implications of polymorphism in organic compounds" in *Particle Design via Crystallization*; Ramu Ramanarayanan, William Kern, Maurice Larson, and Subhash Sikdar Eds.; American Institute of Chemical Engineers Symposium Series Number 284; American Institute of Chemical Engineers: New York, NY; Vol. 87, pp 72–81.

O'Brien, Matthew, James McCauley, and Edward Cohen (1984) "Indomethacin" in *Analytical Profiles of Drug Substances*; Klaus Florey, Ed.; Academic: New York, NY; Vol. 13, pp 211–238.

Oberholzer, Earl R. and Gerald S. Brenner (1979) "Cefoxitin sodium: solution and solid-state chemical stability studies" *J. Pharm. Sci.* **68** 836–866.

Overney, R. M., L. Howald, J. Frommer, E. Meyer, D. Brodbeck, and H.-J. Güntherodt (1992) "Molecular surface of organic crystals observed by atomic force microscopy" *Ultramicroscopy* **42–44** 983–988.

Paul, Iain C. and David Y. Curtin (1973) "Thermally induced organic reactions in the solid state" *Acc. Chem. Res.* **6** 217–225.

Pazourek, K. (1979) "The effect of pH on the growth of the cytosine monohydrate single crystals" *Czech. J. Phys.* **B29** 222–226.

Perrier, Philippe (1980) Unpublished results; Purdue University: West Lafayette, IN 47907-1336.

Pikal, M. J., A. L. Lukes, and J. E. Lang (1977) "Thermal decomposition of amorphous β-lactam antibacterials" *J. Pharm. Sci.* **66** 1312–1316.

Poliks, Mark D. and Jacob Schaefer (1990) "Microscopic dynamics in chloral polycarbonate by cross-polarization magic-angle spinning carbon-13 NMR" *Macromolecules* **23** 2682–2686.

Power, L. F., K. E. Turner, and F. H. Moore (1976) "The crystal and molecular structure of α-glycine by neutron diffraction—a comparison" *Acta Crystallogr., Sect. B, Struct. Sci.* **B32** 11–16.

Powers, H. E. C. (1971) "Nucleation and the sugar industry" *Z. Zuckerind.* **21** 272–277.

Ramanarayanan, Ramu, William Kern, Maurice Larson, and Subhash Kikdar, Eds. (1991) *Particle Design via Crystallization*, American Institute of Chemical Engineers Symposium Series, No. 284, Vol. 87; American Institute of Chemical Engineers: New York, NY.

Rastogi, R. P., N. B. Singh, and R. P. Singh (1977a) "Organic solid state reactions. II. Kinetics of 8-hydroxyquinoline and maleic anhydride, succinic anhydride, phthalic anhydride, catechol and resorcinol" *Indian J. Chem., Sect. A* **15A** 941–946.

Rastogi, R. P., N. B. Singh, and R. P. Singh (1977b) "Organic solid-state reactions" *J. Solid State Chem.* **20** 191–200.

Rousseau, R. W., K. K. Li, and W. L. McCabe (1976) "The influence of seed crystal size on nucleation rates," in *Analysis and Design of Crystallization Processes*, R. W. Rousseau and M. A. Larson, Eds.; AIChE Symposium Series No 153, Vol. 72; American Institute of Chemical Engineers, New York, NY; pp 48–52.

Saindon, Patricia J., Nina S. Cauchon, Paul A. Sutton, C.-j. Chang, Garnet E. Peck, and Stephen R. Byrn (1993) "Solid-state nuclear magnetic resonace (NMR) spectra of pharmaceutical dosage forms" *Pharm. Res.* **10** 197–203.

Sato, K. and R. Boistelle (1984) "Stability and occurrence of polymorphic modifications of stearic acid in polar and nonpolar solutions" *J. Cryst. Growth* **66** 441–450.

Sato, K., K. Suzuki, M. Okada, and N. Garti (1985) "Solvent effects on kinetics of solution-mediated transition of stearic acid polymorphs" *J. Cryst. Growth* **72** 699–704.

Sato, K. and M. Suzuki (1986) "Solvent crystallization of α, β and γ polymorphs of oleic acid" *J. Am. Oil Chem. Soc.* **63** 1356–1359.

Schaefer, Jacob, E. O. Stejskal, and R. Buchdahl (1977) "Magic-angle carbon-13 NMR analysis of motion in solid glassy polymers" *Macromolecules* **1982** 384–405.

Schaefer, Jacob, M. D. Sefcik, E. O. Stejskal, R. A. McKay, W. Thomas Dixon, and R. E. Cais (1984a) "Molecular motion in glassy polystyrenes" *Macromolecules* **17** 1107–1118.

Schaefer, Jacob, M. D. Sefcik, E. O. Stejskal, and R. A. McKay (1984b) "Carbon-13 $T_{1\rho}$ experiments on solid polymers having tightly spin-coupled protons" *Macromolecules* **17** 1118–1124.

Schilling, Frederic C., Frank A. Bovey, Alan E. Tonelli, Susan Tseng, and Arthur E. Woodward (1984) "Solid-state carbon-13 NMR study of the fold surface of solution-grown 1,4-*trans*-polybutadiene crystals" *Macromolecules* **17** 728–733.

Schmalzried, H. (1968) "Chemical reactions between crystalline solids" in *Reactivity of Solids;* Proceedings of the 6th International Symposium, Schenectady, New York, NY, August 25–30; Wiley-Interscience: New York, NY; pp 551–566.

Schmalzried, Hermann (1981) *Solid-State Reactions*, 2nd ed.; Monographs in Modern Chemistry, Vol 12; Hans F. Ebel, Ed.; Verlag Chemie: New York, NY; Chapter 5.

Simonelli, A. P., S. C. Mehta, and W. I. Higuchi (1970) "Inhibition of sulfathiazole crystal growth by polyvinylpyrrolidone" *J. Pharm. Sci.* **59** 633–638.

Sloan, Gilbert J., John M. Thomas, and John O. Williams (1975) "Basal dislocations in single crystals of anthracene" *Mol. Cyrst. Liq. Cyrst.* **30** 167–174.

Smeyers, Y. G., S. Cuéllare-Rodriguez, E. Galvez-Ruano, and M. S. Arias-Pérez (1985) "Conformational analysis of some α-phenylpropionic acids with anti-inflammatory activity" *J. Pharm. Sci.* **74** 47–49.

Stephenson, Gregory Alan (1994) "Solid-state investigations of selected pharmaceutical compounds" Ph.D. Thesis; Purdue University: West Lafayette, IN 47907-1333.

Sudo, Shogo, Katsutoshi Sato, and Yoshio Harano (1991a) "Solubilities and crystallization behavior of cimetidine polymorphic forms A and B" *J. Chem. Eng. Jpn.* **24** 237–242.

Sudo, Shogo, Katsutoshi Sato, and Yoshio Harano (1991b) "Growth and solvent-mediated phase transition of cimetidine polymorphic forms A and B" *J. Chem. Eng. Jpn.* **24** 628–632.

Sugita, Yoshihisa (1988) "Polymorphism of L-glutamic acid crystals an inhibitory substance for β-transition in beet molasses" *Agric. Biol. Chem.* **52** 3081–3085.

Suzuki, M., T. Ogaki, and K. Sato (1985) "Crystallization and transformation mechanisms of α-, β-, and γ-polymorphs of ultra-pure oleic acid" *J. Am. Oil Chem. Soc.* **62** 1600–1604.

Suzuki, Yoshihisa and Kentaro Hara (1974) "Polymorphism of inosine. III. The equilibrium for the inosine–dimethyl sulfoxide–water system" *Bull. Chem. Soc. Jpn.* **47** 2551–2552.

Tanninen, V. P. and J. Yliruusi (1992) "X-ray powder diffraction profile fitting in quantitative determination of two polymorphs and their powder mixture" *Int. J. Pharm.* **81** 169–177.

Thomas, J. M. (1970) "Reactivity of carbon: some current problems and trends" *Carbon* **8** 413–421.

Thomas, J. M. (1972) "Application of electron microscopy to the study of photochemical reactions in organic solids" *Isr. J. Chem.* **10** 573–580.

Thomas, John M. (1979) "Organic reactions in the solid state: accident and design" *Pure Appl. Chem.* **51** 1065–1082.

Thomas, J. M., and J. O. Williams (1969) "Some electronic and chemical consequences of non-basal dislocations in crystalline anthracene" *Mol. Cryst. Liq. Cryst.* **9** 59–79.

Thomas, J. M., J. O. Williams, and W. Jones (1972) "Electron and optical microscopic studies of photo-induced reactions in aromatic solids" in *Reactivity of Solids*; J. S. Anderson, M. W. Roberts, and F. S. Stone, Eds.; Proceedings of the 7th International Symposium on the Reactivity of Solids, Bristol, July 17–21; Chapman and Hall: London, UK; pp. 515–524.

Tiller, William A. (1991) "Physical defect generation during bulk crystal growth" in *The Science of Crystallization: Macroscopic Phenomena and Defect Generation*; Cambridge: Cambridge, UK; Chapter 7.

Toma, Pascal Henri (1993) "Atomic mobility of selected pharmaceutical compounds" Ph.D. Thesis; Purdue University: West Lafayette, IN 47907-1333.

Tonelli, Alan E., Marian A. Gomez, Hajime Tanaka, Frederic C. Schilling, Madeleine H. Cozine, Andrew J. Lovinger, and Frank A. Bovey (1990) "Solid-state nuclear magnetic resonance, differential scanning calorimetric, and X-ray diffraction studies of polymers" in *Polymer Characterization: Physical Property, Spectroscopy, and Chromatographic Methods*; Clara D. Craver and Theodore Provder, Eds.; Advances in Chemistry Series; American Chemical Society: Washington, DC; Vol. 227, Chapter 24.

Torchia, Dennis A. (1978) "The measurement of proton-enhanced carbon-13 T_1 values by a method which suppresses artifacts" *J. Mag. Res.* **30** 613–616.

Trueblood, K. N. (1985) "Vibrational parameters in crystals: rigid and non-rigid molecules" *J. Mol. Struct.* **130** 103–115.

Usui, F. and J. T. Carstensen (1985) "Interactions in the solid state. I. Interactions of sodium bicarbonate and tartaric acid under compressed conditions" *J. Pharm. Sci.* **74** 1293–1297.

Van Hook, Andrew (1961) *Crystallization: Theory and Practice*; Reinhold: New York, NY; Chapter 1.

Weissbuch, I., L. Addadi, M. Lahav, and L. Leiserowitz (1991) "Molecular recognition at crystal interfaces" *Science* **253** 637–645.

Woodard, Geoffrey D. and Walter C. McCrone (1975) "Unusual crystallization behaviour" *J. Appl. Cryst.* **8** 342.

Wray, Paul E. (1992) "The physics of tablet compaction revisited" *Drug. Dev. Ind. Pharm.* **18** 627–658.

Wright, J. D. (1995) "Impurities and defects" in *Molecular Crystals*, 2nd ed.; Cambridge University: Cambridge, UK; Chapter 4.

Wright, James L., and Jens T. Carstensen (1986) "Interactions in the solid state. II. Interaction of sodium bicarbonate with substituted benzoic acids in the presence of moisture" *J. Pharm. Sci.* **75** 546–551.

Xu, Wei (1997) "Investigation of solid-state stability of selected bioactive compounds" Ph.D. Thesis; Purdue University: West Lafayette, IN 47907-1333.

York, Peter (1992) "Crystal engineering and particle design for the powder compaction process" *Drug Dev. Ind. Pharm.* **18** 677–721.